ProQuest LLC.
789 East Eisenhower Parkway
P.O. Box 1346
Ann Arbor, MI 48106 – 1346

BIOLOGICAL SENSITIZERS OF NEAR UV: GENERATION OF REACTIVE OXYGEN SPECIES AND DAMAGE TO CELLULAR COMPONENTS AND MICROBES

A thesis submitted in partial fulfilment for the requirements of the Nottingham Trent University for the degree of Doctor in Philosophy.

September 2001

ASPASIA HARGREAVES

ABSTRACT

Most of the harmful effects of the near ultraviolet (NUV) radiation (290 – 400 nm) on living organisms appear to be mediated *via* activation of molecular sensitisers. Thus, the potential of L-histidine, L(+)mandelic acid, β–phenylpyruvic acid, *p*-OH-phenylpyruvic acid and L-β–phenyllactic acid to be photolysed by NUV and affect biological systems was investigated. An interest for these compounds was expressed, since they are ubiquitous components of living organisms and, in particular, a part of the metabolic pathway of phenylalanine in humans. On NUV exposure, these endogenous biochemicals are proposed to react with molecular oxygen in aqueous solution to generate a variety of reactive oxygen species (ROS) such as H_2O_2, $^{\cdot}OH$, $O_2^{\cdot-}$ / $HO^{\cdot}$, and $^1O_2$. Chemical assays and the use of selective scavengers aided in the identification of such ROS and have elucidated some possible mechanistic pathways for ROS generation. ROS production on NUV photolysis of L-histidine, L(+)mandelic acid and *p*-OH-phenylpyruvic acid was found to be pH-dependent and maximal in alkaline media, whereas β–phenylpyruvic acid appeared most susceptible to photolysis to produce ROS at near physiological pH (pH 7 – 7.5), an effect that renders it great biological importance. For this reason, the biological effects of photosensitised reactions of β–phenylpyruvic acid were studied in a greater detail than that of other sensitisers.

The NUV photolysis of L-histidine, L(+)mandelic acid, β–phenylpyruvic acid and *p*-OH-phenylpyruvic acid was shown to cause synergistic inactivation of bacteriophage T7, in a dose and pH dependent manner. β–Phenylpyruvic acid was also shown to cause lethality in bacteria, with gram-positive cells being more susceptible than gram-negatives to sensitised NUV inactivation. Subsequently, using HPLC, the cellular concentrations and incorporation of β–phenylpyruvic acid in bacteria were determined.

An assessment of the effect of NUV plus sensitisers (β–phenylpyruvic acid in particular) on individual cellular components such as DNA, lipids and proteins revealed that the photosensitised action of these compounds can cause oxidative damage to all these biomolecules. Thus, the NUV photolysis of β–phenylpyruvic acid was responsible for a variety of DNA damage such as formation of single-strand breaks to pBR322 that subsequently increased its transformation efficiency, DNA damage-induced production of β–galactosidase, and induction of mutations resulting in antibiotic resistance. The NUV photolysis of this compound also resulted in lipid peroxidation of liposomes and bacterial cells and protein damage such as fragmentation of BSA and oxidative modification of *E. coli* proteins.

It is therefore possible that L-histidine, L(+)mandelic acid, β–phenylpyruvic acid, *p*-OH-phenylpyruvic acid and L-β–phenyllactic acid may contribute, in different extends, to some of the effects of solar radiation on health, such as photoageing and ocular damage.

Acknowledgements

There are a number of people who I wish to thank for their help and contribution to this work. First of all, my thanks go to my supervisors Drs. S. I. Ahmad and S. H. Kirk for offering me the opportunity to work on this project. I also wish to thank Prof. M. C. R. Symons FRS for his advice and suggestions on some aspects of this work. I am very grateful to John Butler for allowing me to refer to his work and for useful discussions. Many thanks go to Dr. Luci Mansfield and Kate Holmes for their help and advice on certain experiments, to the technicians of the Microbiology section (Jane Braithwaite, Mike Brice, Pam Horne and Ann MacLoughlan) for their invaluable help and assistance on the experimental work and to Anna Gottlieb and Chris Barnet for all their help. I also wish to thank P. McGreevy and E. Galley of Boots Co. plc for their help in equilibrating the UV sources. Last but not least, I wish to thank the most important person in my life, my husband, Dr. J. S. J. Hargreaves, for his love and support, without whom this work would have never been completed.

TABLE OF CONTENTS

List of Abbreviations

AGE – advanced glycation endproducts

BSA – bovine albumin

DABCO – diazabicyclooctane

DNPH – dinitrophenylhydrazine

DOPA – 3,4-dihydroxyphenylalanine

EPR – electron paramagnetic resonance

GC – gas chromatography

HPLC – high performance liquid chromatography

ISPA – isopropyl alcohol

LB – Luria Bertoni medium

LDL – low density lipoprotein

NA – nutrient agar

NBT – nitro-blue tetrazolium

NUV – near ultraviolet radiation (UVA and UVB)

ONPG – *o*-nitrophenyl-β-D-galactopyranoside

PPA – β–phenylpyruvic acid

ROS – reactive oxygen species

SOD – superoxide dismutase

TBA – thiobarbituric acid

TCA – thrichloroacetic acid

UVR – ultraviolet radiation

List of Tables

List of Figures

CHAPTER 1

INTRODUCTION

1.1 Ultraviolet Radiation

Ultraviolet radiation (UVR) is classified as non-ionising radiation of wavelengths between 200 and 400 nm that occurs naturally in sunlight and is a component of the electromagnetic spectrum (Figure 1.1). The lower wavelength region of ultraviolet light (200-290 nm) is known as UVC or far-UV light. Wavelengths in the range of 290 – 400 nm compose UVA and UVB, which collectively are referred to as near-ultraviolet light (NUV). NUV represents the most energetic component of solar radiation reaching the surface of the earth. UV light, in general, is highly relevant biologically, because living organisms have had to contend with the genotoxic effects of solar UV radiation since the beginning of life on this planet.

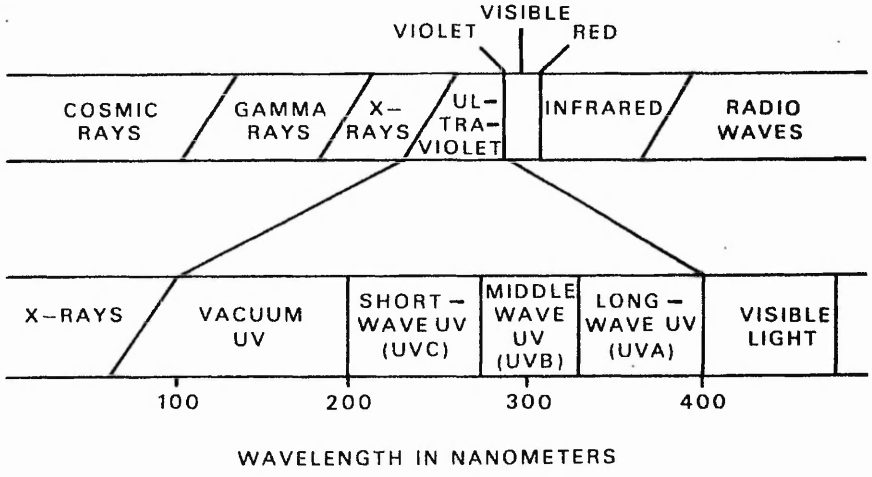

Figure 1.1: Electromagnetic spectrum with expanded scale of ultraviolet radiation (Parrish *et. al.*, 1978).

The importance of UVC, particularly at 254 nm, in causing damage to living systems has been recognised for some time (Li and Hill, 1997; Peak and Peak, 1989; Sage, 1993). There is little melanin protection against lethality of UVC. UVC

radiation is known to exert its cytotoxic action mainly through direct absorption by DNA, with cyclobutane pyrimidine dimers and 6–4 photoproducts being the principal DNA products (Figure 1.2). Because of its lethal effects on biological systems, industry uses UVC to kill microorganisms on equipment and food.

However, UVC is efficiently filtered by the ozone layer of the stratosphere and thus, it does not reach the earth's surface. Short-wave UV radiation (<220 nm) is absorbed by oxygen, which, as a result, splits up and recombines to form ozone (O_3). The ozone, in its turn, filters out UV radiation of longer wavelengths up to about 310 nm.

UVB (290-320 nm) is partially absorbed by the ozone layer, making up only 5% of the UV photons that reach the earth. This small amount of UVB, however, is considered to be the major cause of skin cancer, and animal studies indicate that it is the principal component for squamous cell carcinoma formation (de Gruijl *et. al.*, 1993; Dumaz *et. al.*, 1997; Kress *et. al.*, 1992). UVB is directly absorbed by cellular macromolecules and is known to induce erythemogenic, carcinogenic and photoageing changes on the skin of laboratory animals (de Gruijl *et. al.*, 1993; Flindt-Hansen *et. al.*, 1991). UVB may also produce premutagenic lesions that are not produced by UVC (Sage, 1993).

UVA (320-400 nm), on the other hand, is the most abundant component of solar UV radiation, accounting for approximately 95% of the UV energy reaching the earth's surface at the equator. UVA is the major band emitted by tanning beds and has the reputation of being the 'safe' portion of the UV spectrum. UVA is capable of producing tanning of the skin, but is required in much higher doses to induce biological responses similar to UVB (Tyrrell, 1990). Recent experimental data have made it clear, however, that UVA exposure has significant health risks, although it may not be as dangerous as UVB (de Laat *et. al.*, 1997; Lowe *et. al.*, 1995; Setlow, *et. al.*, 1993). A case-control study showed that the prolonged use of sunbeds and sunlamps is a risk factor for cutaneous malignant melanoma (Walter *et. al.*, 1990). In addition, UVA penetrates much deeper into the skin than any of the other UV components, thus enhancing the carcinogenic effects of UVB. In this way, while 1-10% of UVB can penetrate at an average of 70 μm from the skin's surface through to

the basal layer of the epidermis, 20% of a mid-UVA wavelength (365 nm) can penetrate as far (Bruls *et. al.*, 1984; Tyrrell, 1995). Most important, UVA, which is weakly absorbed by most biomolecules, generates reactive oxygen species (ROS) *via* interaction with intracellular chromophores.

In recent years, increased concern has been expressed over the problem of reduction of the ozone levels in the stratosphere, due to atmospheric pollution. Increasing levels of chlorofluorocarbons and carbon dioxide reach the ozone layer causing ozone depletion. Aside from the poles, the global loss over the past 20 years has been estimated at about 4% a decade (Kelfkens *et. al.*, 1990). As a result, a greater amount of solar radiation can reach the earth. Given the involvement of UVR in the induction of skin cancer, an increased incidence in cancer cases is estimated by the decrease in the ozone layer, although such evidence is not yet available (de Gruijl and Van der Leun, 1994; Kelfkens *et. al.*, 1990). Nevertheless, the popularity of acquiring a tan has resulted in malignant melanoma being the tenth cancer-related cause of death in the USA, and the incidence of melanoma doubling approximately every 10-15 years (Farmer and Naylor, 1996).

1.2 Biological Damage of UVR: Direct Effects

The directly inducible biological damage by UVR is well recognised. UVB radiation leads to the stimulation of the tumour suppressor gene, p53, and to the formation of apoptotic sunburn keratinocytes (Pourzand and Tyrrell, 1999). Further evidence that UVB radiation triggers apoptosis in mammalian cells has come from a recent study, where UVB has been shown to interfere with cytokine signalling and induce apoptosis *via* direct activation of apoptosis related surface receptors (Schwarz, 1998). Additionally, de Laat *et. al.* (1997) have demonstrated that nearly monochromatic 365-nm radiation is carcinogenic in hairless mice, inducing the same type of skin tumours as broad band UVB/UVA sources.

NUV has been shown to cause a variety of changes in biological systems, particularly at the molecular level. Cellular components affected by UV radiation include the plasma membrane, cytoplasmic organelles, proteins, lipids, RNA and DNA (Beer *et. al.*, 1993; Peak and Peak, 1989). Repeated irradiation may lead to an

accumulation of cellular damage, as damage is cumulative with time and exposure (Farmer and Naylor, 1996). If not repaired, damage to DNA can result in various types of cancer in mammalian skin. Also, UV-induced cellular damage is shown to create mutations or cell death in bacteria (Ambler *et. al.*, 1996; Jekler *et. al.*, 1992; Yoshimura *et. al.*, 1996).

In comparison to far-UV, the mechanisms of damage to biological systems by NUV are more complex and variable. Additionally, complex biological systems will be affected according to their molecular composition. Typical UV absorbing features in organic molecules are conjugated bonds. Alternating single and double bonds generally absorb radiation of wavelengths between 200 and 250 nm, and when in a ring between 250 and 300 nm. Protein fractions show absorption at around 280 nm and DNA shows a maximum at around 260 nm. Generally, around their absorption maxima, DNA absorbs 10-20 times as much as an equal weight of protein, although cells have about 50 times more protein than DNA. DNA, therefore, is more susceptible to direct damage by short-band wavelengths, but it is not necessarily the only target.

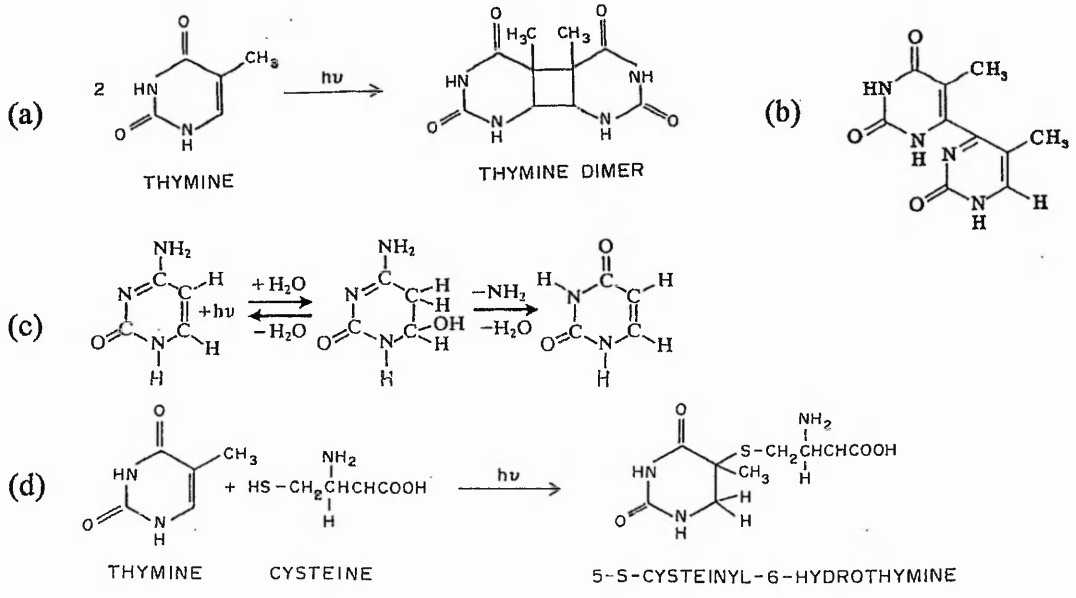

Figure 1.2: Common pyrimidine photoproducts. (a) the thymine dimer as a result of cycloaddition; (b) the (6-4) adduct of thymine; (c) reversible addition of H_2O to cytosine; (d) heteroadduct of thymine on addition of cysteine (5-S-cysteinyl-6-hydrothymine) (adopted from Smith, 1989).

The most photosensitive nucleic acid bases are the pyrimidines. The direct absorption of UVB by DNA can result in the formation of four pyrimidine photoproducts (Figure 1.2). The major products are two types of dipyrimidine lesions: cyclobutane pyrimidine dimers and pyrimidine-pyrimidone (6-4) adducts (Cadet *et. al.*, 1992; Rosenstein and Mitchell, 1986). Cyclobutane-type dimers are formed when two thymine molecules, for example, are linked to each other between their respective C5 and C6 atoms, forming a cyclobutane ring. The two other pyrimidine photoproducts are those, which are formed through addition of water to the 5,6 double bond (hydration products), and those resulting from addition of an amino acid or a purine to the 5,6 double bond (heteroadducts).

1.3 Indirect Effects of UVR: Damage *via* Photosensitisers

The biological effects of NUV are enhanced in the presence of photosensitisers. Indirect sensitised reactions of NUV are strongly dependent on oxygen and involve the generation of reactive oxygen species (ROS). Since oxygen in its ground state does not absorb NUV radiation, it is evident that the energy present in photons of 290 – 400 nm is not directly transferred to the oxygen molecule, but rather a chromophore is involved which activates ground state oxygen to generate ROS. The sensitiser may be restored to its previous form at the end of the reaction, or it may itself undergo a chemical change. Photosensitisers are generally divided into two categories; those produced synthetically (e.g. drugs) and those that are naturally occurring in biological systems.

1.3.1 Synthetic Sensitisers of NUV

Any drug capable of absorbing light may induce phototoxic effects, provided that the excitation energy is not dissipated as heat. Such well-know organic and inorganic compounds include H_2O_2 (Hartman and Eisenstark, 1978; Rosen *et. al.*, 1996), phenols, thiophenes as well as dyes such as methylene blue derivatives, xanthene dyes (e. g. rose bengal), acridine dyes, azur blue and erythrosin. Other synthetic sensitisers include drugs like tetracycline, furosemide (a carboxylic acid derivative that acts as a diuretic drug) (Vargas *et. al.*, 1998), derivatives employed in photodynamic therapy such as phthalocyanins, and sulphonamide-derived oral

antidiabetics and diuretics (Selvaag *et. al.*, 1997). To the list, drugs that have given rise to photoallergic or phototoxic reactions such as amiodarone, afloqualone, chlorpromazine, griseofulvin, psoralens, and quinolones can be added (Paillous and Fery-Forgues, 1994).

1.3.2 Naturally Occurring Sensitisers of NUV

Sensitisers of natural origin are also known as endogenous photosensitisers. Biological compounds that act as sensitisers of NUV are usually molecules with three (e.g. riboflavin) or four rings (e.g. porphyrins, chlorins) (Figure 1.3). Other biologically relevant molecules that are known to produce ROS on NUV photolysis are flavins, pterins, metalloporphyrins, kynurenic acid, retinoids, rhodamines, quinones, angelicins, (Redmond and Gamlin, 1999), thiouracils and thiouridines, and the reduced forms of the nicotinamide coenzymes NADH and NADPH (Burchuladze and Fraikin, 1991; Cunningham *et. al.*, 1985).

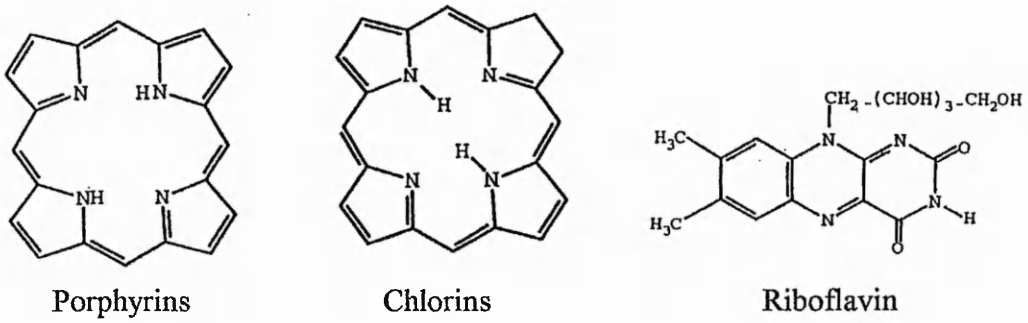

Figure 1.3: Chemical structure of some natural photosensitisers (taken from Kohen *et. al.*, 1995).

Other recently identified sensitisers include advanced glycation endproducts (AGE). AGE are covalently cross-linked, high molecular weight aggregates which are formed on reaction of sugars with proteins. These aggregates have complex aromatic structures, absorb light in the UVA region of the spectrum, and have been proven capable of generating singlet oxygen, hydrogen peroxide, hydroxyl radicals and superoxide anions upon photolysis by NUV (Linetsky *et. al.*, 1996; Linetsky and Ortwerth, 1997; Masaki *et. al.*, 1997; Ortwerth *et. al.*, 1997). Additionally, some aromatic amino acids are known to act as sensitisers of NUV. It has been

demonstrated that NUV photolysis of phenylalanine, tryptophan and tyrosine induce synergistic inactivation of phage T7 (Craggs *et. al.*, 1994).

1.3.3 Reactive Oxygen Species

ROS are highly reactive species associated with the oxygen atom, and have stronger reactivity with other molecules than molecular oxygen. ROS usually indicate the chemically reactive free radicals and all the other species that behave like free radicals. These free radicals are atoms or groups of atoms that possess one or more unpaired electrons. Some of the most biologically important ROS are the following four: hydroxyl radical ($^{\cdot}OH$), superoxide anion ($O_2^{\cdot-}$), hydrogen peroxide (H_2O_2) and singlet oxygen ($^1O_2$). Other biologically important free radicals include those associated with membrane lipids [lipid hydroperoxide (ROOH), lipid peroxyl radical ($ROO^{\cdot}$) and lipid alkoxyl radical ($RO^{\cdot}$)]; nitric oxide (NO) (a reactive nitrogen species); thioyl radical ($RS^{\cdot}$), and carbon radicals ($R_3C^{\cdot}$). Once generated, ROS can readily react with any macromolecule in the immediate environment, causing DNA damage, DNA-protein cross-links, protein cross-linking (e.g. collagen and elastin), oxidative inactivation of certain enzymes, the functional impairment of organelles and cells (fibroblasts, melanocytes, keratinocytes, and Langerhans cells) and peroxidation of membrane lipids (Carbonare and Pathak, 1992; de Gruijl, 1997; Santanam *et. al.*, 1998). To prevent these types of cellular damage that can lead to oxidative stress, cells contain a range of ROS quenchers, each specific for a certain type of ROS.

1.3.3.1 Hydroxyl Radical

The hydroxyl radical is a highly reactive non-specific oxidant. This radical reacts with extremely high rate-constants with almost every type of molecule found in living cells: sugars, phospholipids, amino acids, nucleotides and organic acids. Due to its high reactivity, $^{\cdot}OH$ has a very short half-life and its diffusion distance is exceedingly short. Thus, $^{\cdot}OH$ can undergo oxidative processes only at the sites of its formation. The $^{\cdot}OH$ is not enzymatically inactivated and can only be detoxified by direct free radical scavengers. One of the ways cells manage to cope with $^{\cdot}OH$ toxicity is by producing melatonin. Melatonin is proven to be a good biological scavenger of $^{\cdot}OH$ (Reiter *et. al.*, 1998).

Because of its high reactivity, the ·OH is difficult to detect in solution. A variety of methods have been developed, however, to detect ·OH. These involve techniques such as electron paramangetic resonance (EPR) and spin trapping. Additionally, there is a range of ·OH scavengers that assist in the understanding of the role of ·OH in biological damage. Such known scavengers are ascorbic acid, mannitol, isopropyl alcohol, and benzoate. Hydrobenzoic acids and their esters are also known to protect cell from ·OH-mediated damage, as estimated by EPR-spin trapping (Masaki *et. al.*, 1997).

1.3.3.2 Hydrogen Peroxide

Hydrogen preoxide (H_2O_2) is known to be both a reactive oxygen species and a photosensitiser (Ahmad, 1981; Hartman and Eisenstark, 1978; Rosen *et. al.*, 1996). There are several enzymes in the cell that produce H_2O_2. These include glycollate oxidase, D-amino acid oxidase and urate oxidase. The damaging nature of H_2O_2 is mainly due to the metal-ion dependent formation of ·OH (Fenton reaction). Thus, in the presence of trace amounts of iron or copper salts, the following reactions are possible:

$$Fe^{2+} + H_2O_2 \rightarrow Fe^{3+} + {\cdot}OH + OH^-$$
$$Cu^{+} + H_2O_2 \rightarrow Cu^{2+} + {\cdot}OH + OH^-$$

Additionally, in the presence of superoxide and a metal catalyst (Fe^{3+} or Cu^{2+}) the Haber-Weiss reaction can take place:

$$O_2^{\cdot-} + H_2O_2 \rightarrow O_2 + {\cdot}OH + OH^-$$

·OH production by H_2O_2 will depend on the location of transition metal complexes. Thus, the binding of copper or iron to DNA and proteins can lead to site specific damage when these systems are exposed to H_2O_2. Unlike ·OH, H_2O_2 has a rather long half-life and, because it is uncharged, it can pass through cell membranes. H_2O_2, therefore, can undergo reactions at locations other than those of its production (i.e. when encountering metal complexes).

In order to prevent H_2O_2 mediated oxygen toxicity, cellular systems are equipped with catalase, glutathione reductase and glutathione peroxidase. These enzymes are important participants in the cellular redox system, and their function is to specifically quench and eventually protect reduced glutathione and protein thiol groups from oxidation. Catalase decomposes H_2O_2 to yield water and molecular oxygen.

1.3.3.3 Superoxide Anion

Superoxide ($O_2^{\cdot-}$) is the one electron reduced form of molecular oxygen (Figure 1.4). $O_2^{\cdot-}$ is generated during the normal metabolic activity of the cell that involves systems such as xanthine and NAD(P)H oxidases, flavoproteins and iron/sulphur complexes. Also, $O_2^{\cdot-}$ is the by-product of oxygen-utilising systems. For example, the slow autoxidation of ferrous hemoglobin to the ferric form, by oxygen, leads to $O_2^{\cdot-}$ formation (Hogg, 1998). Finally, several photosensitisers are known to generate $O_2^{\cdot-}$ upon photolysis (Craggs *et. al.*, 1994; Cunningham *et. al.*,1985; Menon *et. al.*, 1992).

$O_2^{\cdot-}$ in aqueous solutions can act as a base. When $O_2^{\cdot-}$ accepts a proton, it forms the hydroperoxyl radical ($HO_2^{\cdot}$). Hence, the presence of $O_2^{\cdot-}$ in solution is strongly pH dependent. As well as acting as a base, $O_2^{\cdot-}$ is a reducing agent. For example, it reduces Fe^{3+} of the haem protein cytochrome c to Fe^{2+} and the yellow dye nitro-blue tetrazolium (NBT) to formazan blue (Halliwell and Gutteridge, 1999). $O_2^{\cdot-}$ can also reduce the thymine hydroperoxyl radical and react with nitric oxide to form peroxynitrite (Koppenol *et. al.*, 1992).

$O_2^{\cdot-}$ in aqueous solutions is also a weak oxidising agent and can oxidise ascorbic acid and compounds containing the thiol group. Generally, $O_2^{\cdot-}$ is an unstable free radical and, unless it is intercepted by another molecule, it undergoes dismutation in aqueous solutions to generate H_2O_2:

$$O_2^{\cdot-} + O_2^{\cdot-} + 2H^+ \rightarrow H_2O_2 + O_2$$

This reaction does not happen fast enough, as the cells contain an enzyme, superoxide dismutase (SOD), that specifically catalyses the reaction, increasing the rate constant by four orders of magnitude. The discovery of SOD indicated that $O_2^{\cdot-}$ formation is a major factor in oxygen toxicity and that SOD constitutes an essential defence against it (McCord and Fridovich, 1968). The involvement of $O_2^{\cdot-}$ in oxidative DNA damage was demonstrated using *Escherichia coli* mutants that lack SOD (Keyer *et. al.*, 1995). In this study, it was shown that $O_2^{\cdot-}$ promotes DNA damage by increasing the amount of free iron that is available to catalyse hydroxyl radical production. Elevated $O_2^{\cdot-}$ concentrations in the cell can reductively leach iron from the iron-sulfur clusters of dehydratases such as aconitase and fumarase, and the iron storage protein ferritin.

$O_2^{\cdot-}$ not only contributes to H_2O_2 formation, but being able to reduce Fe^{3+} to Fe^{2+} ($Fe^{3+} + O_2^{\cdot-} \rightarrow O_2 + Fe^{2+}$) it can enhance the occurrence of Fenton reaction, and consequently, the production of $^{\cdot}OH$. By quenching $O_2^{\cdot-}$, SOD prevents redox cycling of the metal ion, and in combination with catalase/glutathione peroxidase, protects the cell against oxidative stress.

Until recently, there has been little hard evidence for biological damage due to direct reactions of $O_2^{\cdot-}$. In the past few years however, targets damaged specifically by $O_2^{\cdot-}$ have been identified. Certain iron-sulphur cluster-containing enzymes are known to be directly inactivated by $O_2^{\cdot-}$. These include the TCA cycle enzyme aconitase and the enzyme dihydroxyacid dehydratase that is involved in branched-chain amino acid synthesis in *Escherichia coli* (Flint and Allen, 1996; Gardner, 1997). It is also believed that the protonated form of superoxide radical, the perhydroxy radical (hydroperoxide) might be involved in superoxide-mediated oxidation reactions leading to lipid peroxidation (Aikens and Dix, 1991).

1.3.3.4 Singlet Oxygen

Sensitised UV photolysis often generates singlet oxygen (eg. the photolysis of hematoporphyrin, riboflavin and methylene blue) (Fernandez *et. al.*, 1997; Ito *et. al.*, 1993). Singlet oxygen is a highly reactive, short-lived intermediate which can oxidise

a variety of biological molecules. Singlet oxygen can exist in two forms (Weldon *et. al.*, 1999). The lowest excited electronic state of molecular oxygen ($^1\Delta_gO_2$) has an energy of ~94 kJ/mol above the ground state, is a common intermediate in many solution-phase photosystems and is the most well-known form of singlet oxygen (Figure 1.4). The second excited state of molecular oxygen ($^1\Sigma_g{}^+O_2$) is also a singlet (Figure 1.4). It is ~63 kJ/mol higher in energy than the singlet delta state and is best known as an intermediate in many gas-phase photosystems. Even though $^1\Sigma_g{}^+O_2$ itself may not react with a substrate in aqueous solution, it decays to yield $^1\Delta_gO_2$ that does react with organic substrates (e.g. proteins and lipids). Both forms of singlet oxygen have a great oxidising ability, and here they are referred to as simply $^1O_2$.

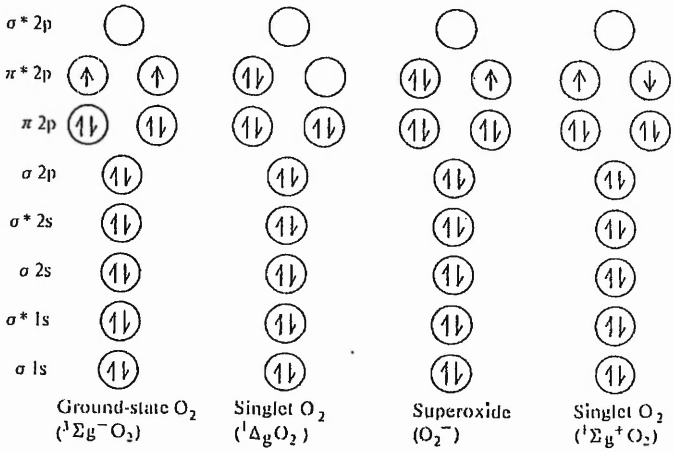

Figure 1.4: The oxygen molecule at its ground state, as a singlet, and superoxide radical (adopted from Halliwell and Gutteridge, 1999).

Several model biochemical systems have been shown to produce $^1O_2$. These systems include the peroxidase-catalysed oxidation of halide ions, the peroxidase-catalysed oxidation of indole-3-acetic acid, the lipoxygenase-catalysed oxidation of unsaturated long chain fatty acids and the bleomycin-catalysed decomposition of hydroperoxides. Additionally to these systems, eosinophil cells were shown to generate $^1O_2$, indicating that $^1O_2$ may play a significant role as intermediate in some biological processes (Kanofsky, 1989).

$^1O_2$ can interact with other molecules in essentially two ways: it can either combine chemically with them, or it can transfer its excitation energy to them,

returning to the ground state while the molecule enters an excited state. In this way, $^1O_2$ is known to attack conjugated double bonds, often giving endoperoxides. $^1O_2$ is toxic to cells and has been shown to promote bacterial killing (Dahl *et. al.*, 1987; Dahl *et. al.*, 1989; Pellieux *et. al.*, 2000). The cell's molecular defence towards $^1O_2$ involves antioxidants like α-tocopherol and carotenoids (Dahl *et. al.*, 1989; Palozza and Krinsky, 1992). Other compounds known to quench $^1O_2$ include 1,4-diazabicyclooctane (DABCO) and the azide ion (Fernandez *et. al.*, 1997; Kohen *et. al.*, 1995).

1.3.4 Type I and Type II Photodynamic Reactions

Type I or radical reactions are one-electron oxidation reactions. These reactions involve the direct interaction of the sensitiser with the substrate through electron transfer. Generally, the sensitiser absorbs photons until it reaches a state of sufficient energy to release an electron into the solution. Solvated electrons can be generated in this manner under low light intensities and can undergo further reactions. Indole derivatives in neutral pH, for example, can release electrons in solution from their first excited singlet state. A sensitiser on its triplet excitation state can also abstract an electron from a substrate (hydrogen or charge transfer), giving semireduced sensitiser and semioxidised substrate. These free radical products are very reactive and can react with oxygen to give a ground state sensitiser molecule and $O_2^{\cdot-}$ (or its conjugate acid $HO_2^{\cdot}$):

$$^3Sen + Sub \rightarrow Sen^{\cdot-} + Sub^{\cdot+}$$

$$Sen^{\cdot-} + O_2 \rightarrow {}^0Sen + O_2^{\cdot-}$$

and

$$^3Sen + Sub \rightarrow Sen^{\cdot} + Sub^{\cdot}$$

$$Sen^{\cdot} + O_2 \rightarrow {}^0Sen + HO_2^{\cdot}$$

In a recent study, the photosensitisers riboflavin, menadione and benzophenone were shown to undergo type I photosensitisation in the presence of UVA and cause oxidative modification of DNA bases (Douki and Cadet, 1999).

Photosensitised reactions that involve energy transfer are known as Type II or oxygen reactions. In such reactions, the triplet state sensitiser can transfer its energy to a ground state substrate yielding ground state sensitiser and substrate triplet, or react with another triplet to form one excited singlet and one singlet ground state molecule. The formation of $^1O_2$ is a type II reaction involving energy transfer.

Whether a given sensitiser-substrate system will react *via* the type I or type II reaction mechanism depends on the nature of the sensitiser, the substrate, and experimental conditions such as pH and O_2 concentrations. In this way, the aromatic amino acids tryptophan and tyrosine undergo type I photosensitisation, whereas rose bengal and porphyrins are almost exclusively type II photosensitisers (Fernandez *et. al.*, 1997; Kohen *et. al.*, 1995).

1.3.5 DNA Damage

DNA damage induced by photosensitisation may result via a type I reaction mechanism where the sensitiser reacts directly with the DNA producing free bases, nucleosides or short oligonucleotides (Douki and Cadet, 1999), or via a type II reaction where O_2, and subsequently ROS, are involved. ROS, and in particular ·OH radicals, are known to cause all types of oxidative modification to DNA including sugar lesions, single-strand breaks, modification to purine and pyrimidine bases, DNA-DNA intrastrand adducts, and abasic sites (Cadet *et. al.*, 1999; Dizaroglu, 1993).

The ·OH radical is efficiently involved in the abstraction of a hydrogen atom from various sites of deoxyribose with the exception of the C2' (Breen and Murphy, 1995). Usually, the formation of C3', C4' and C5'-centered radicals leads to DNA strand breaks, whereas ·OH-mediated oxidation of C1' gives rise to 2-D-deoxyribonolactone.

In addition, the UVA-sensitised formation of ·OH has been shown to induce DNA strand breaks. In one study, pyridone 1 was used as a specific source of ·OH radicals (Adam *et. al.*, 1999) and ·OH scavengers were used to investigate the role of ·OH in oxidative DNA damage (Oroskar *et. al.*, 1996). In both cases, ·OH-mediated

single- and double-strand breaks resulted in the relaxation and linearisation of supercoiled pBR322 DNA.

Furthermore, ·OH reacts in a multiplicity of ways with all four DNA bases giving ring saturation and ring fragmentation products. Thus, ·OH adds to the C5-C6 double bond of pyrimidines giving rise to pyrimidine radicals. The C5 position of pyrimidines with the highest electron density is the preferred site of attack by ·OH. An equal volume of oxidising and reducing products are known to be formed. The initially produced pyrimidine radicals are converted into the corresponding peroxyl radicals upon fast reaction with oxygen, and are further reduced by $O_2^{\cdot-}$ to relatively stable hydroperoxides. Thus, the products of ·OH-mediated oxidation of thymine are *cis* and *trans* thymine glycols with dihydrothymine formed as an intermediate (Evans *et. al.*, 1993) (Figure 1.5). The presence of thymine glycol products during DNA synthesis appears to block DNA replication (Clark and Beardsley, 1987). Abstraction by ·OH of a hydrogen atom from the methyl group of thymine can also take place, even though less frequently.

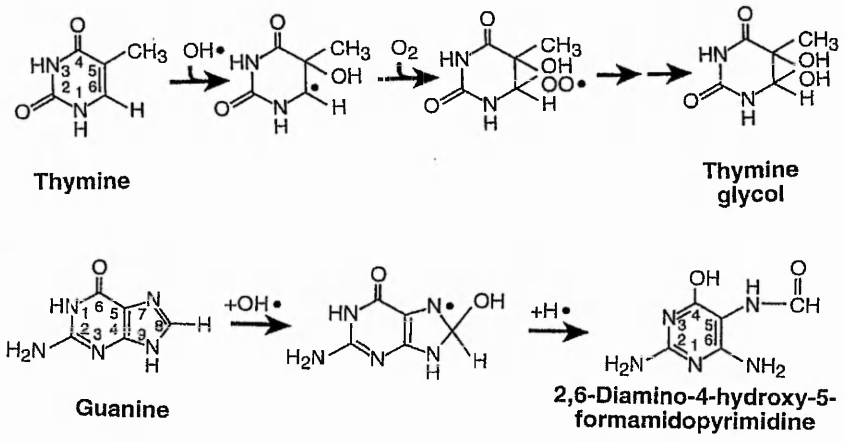

Figure 1.5: Formation of thymine glycol and FapyGua by ·OH attack at thymine and guanine residues respectively (adopted from Friedberg *et. al.*, 1995).

Of the reactions of ·OH with the purines, those of guanine are the most common. The guanine base exhibits the lowest ionisation potential among nucleic acid components, and is therefore the most susceptible DNA target for oxidation reactions mediated by ·OH. Thus, ·OH can add on to guanine residues at C4, C5 and

C8 positions to give hydroxyguanine radicals. In this way, addition of ·OH to C8 of guanine produces a radical that can be reduced to 8-hydroxy-7,8-dihydroguanine, oxidised to 8-hydroxyguanine or undergo ring opening followed by one electron reduction and protonation to give 2,6-diamino-4-hydroxy-5-formamidopyrimidine (FapyGua) (Figure 1.5). The 8-hydroxyguanine derivative of guanine is known to be a mispairing lesion during DNA replication that causes G → T and A → C substitutions (Cheng *et. al.*, 1992).

The major oxidation product of guanine is 8-oxo-7,8-dihydro-2'-deoxyguanosine (8-oxodGuo). This modified guanine nucleotide can be mutagenic by base pairing with either cytosine or adenine (Pavlov *et. al.*, 1994). Induction of 8-oxodGuo is most efficient, in terms of biologically relevant dose-responses, upon sensitisation reactions involving the longer wavelengths of UVA irradiation (Douki *et. al.*, 1999; Zhang *et. al.*, 1997). In a study involving formation of 8-oxodGuo by H_2O_2 alone or in the presence of NUV, H_2O_2 was shown to increase formation of 8-oxodGuo in cultured cells, but the synergistic generation of 8-oxodGuo was much higher (Rosen *et. al.*, 1996). The induction of 8-oxodGuo in the DNA of cells exposed to H_2O_2 and UVA or UVB may involve formation of other ROS like $^1O_2$ and $O_2^{\cdot-}$. However, reactions of guanine reducing radicals with $O_2^{\cdot-}$ can lead to an increasing yield of FapyGua at the expense of 8-oxodGuo (Douki and Cadet, 1999).

Singlet oxygen is also able to produce strand breakage and modify DNA bases, and is known to be extremely reactive towards guanine components (Ravanat and Cadet 1995; Cadet *et. al.*, 2000). In studies involving UVA-induced photosensitisation of riboflavin, sequence-specific DNA cleavage of calf thymus DNA was observed. The specific cleavage sites were found to be guanine residues (Ito *et. al.*, 1993). Similar observations were made from the photosensitisation reactions of methylene blue during which $^1O_2$ was shown to cause single-strand breaks in supercoiled plasmid DNA, exclusively at guanine residues (Stary and Sarasin, 2000). The major oxidation product from $^1O_2$-mediated DNA damage is 8-oxodGuo. $^1O_2$ was also shown to be involved in the inhibition of polymerase II-dependent RNA synthesis (Arai *et. al.*, 1997). This may reflect $^1O_2$-mediated DNA strand breaks that can block transcriptional elongation.

1.3.5.1 DNA Repair

DNA modification by oxidation can lead to mutagenesis and cell death. If not removed from DNA before replication, oxidised bases may lead to mutations by inducing misreading of the base itself and possibly the adjacent bases. Similarly, ring-fragmented bases and abasic sites are thought to block DNA replication by blocking DNA polymerase (Evans *et. al.*, 1993). DNA damage triggers a wide range of cellular responses such as an alteration in gene expression, a delay in cell-cycle progression, activation of programmed cell death, and the stimulation of DNA repair (Wang, 1998).

Cells are equipped with a range of repair enzymes that recognise and remove DNA lesions. Thus, UVA-mediated oxidised damage to guanine is mostly repaired *via* a base excision repair pathway and specifically recognised by the formamidopyrimidine glycosylase (Fpg) in *Escherichia coli* and the Ogg1 protein in eukaryotes (Girard and Boiteux, 1997; Le Page *et. al.*, 1998; Shennan *et. al.*, 1996). In the same way, thymine glycols are removed by thymine glycol DNA glycosylase. These initial enzymatic events during base excision repair result in the removal of the modified moieties as free bases, creating sites of base loss [apurinic or apyrimidinic (AP) sites]. To complete base excision repair, a second class of base excision enzymes, AP endonucleases, recognise and remove these sites (Friedberg *et. al.*, 1995).

The repair of helix-distorting damage, such as pirimidine dimers and pyrimidine (6-4) pyrimidone photoproducts induced by UV light are enzymatically removed from the DNA as intact nucleotides in a process known as nucleotide excision repair. The recognition and incision steps of human nucleotide excision repair use fifteen to eighteen polypeptides, whereas *E. coli* requires only three proteins, namely the UvrABC endonucleases, to obtain a similar result (Shennan *et. al.*, 1996; Van Houten, 1990). However, this repair mechanism presents similarities between prokaryotic and eukaryotic organisms in the use of a distortion-recognition factor, a strand separating helicase to open the double strand, and participation of structure-specific endonucleases (Batty and Wood, 2000). The incision function of the endonucleases is followed by exonuclease action to remove the DNA fragment

containing the lesion. Recently, the human replication protein A was reported to interact specifically with damaged double-stranded DNA and to participate in multiple steps of nucleotide excision repair including the damage recognition step (Lao *et. al.*, 2000). The specificity of binding to DNA varied with the type of damage with a 60-fold preference for a pyrimidine (6-4) pyrimidone photoproduct.

Two other types of DNA repair include mismatch repair and recombinational repair (Hoeijmakers, 2001). Mismatched DNA bases can occur from errors in replication or from miscoding properties of damaged bases. In these cases, the mismatched base is located and removed by a similar mechanism to the nucleotide excision repair. Single- and double-strand breaks are repaired by the RecBC nuclease and the Rec A protein in *E. coli*, which is also involved in homologous and site-specific recombination of damaged DNA (Friedberg *et. al.*, 1995; Moustacchi, 2000).

Besides the repair mechanisms mentioned above, prokaryotes are equipped with a set of physiological responses to DNA damage termed SOS responses. A variety of lesions to DNA, induced by UV radiation, ionising radiation or chemicals, can trigger an SOS response, which often results in the temporary blockage of the normal DNA replication process or in other changes that can enhance cell survival. Thus, SOS-regulated responses include induction of DNA polymerase II production and activation of the RecA protein (Friedberg *et. al.*, 1995; Quillardet and Hofnung, 1985). The SOS process leading to production of the RecA protein is under the direction of the *recA* and *lexA* genes (Figure 1.6). DNA damage may cause distortion of the DNA helix leading to the presence of single-stranded DNA, which activates the protease function of the RecA protein. The activated RecA protein catalyses the cleavage of the LexA repressor protein, which is the repressor of the SOS gene. The SOS process is terminated when repair to the damaged DNA ends RecA protease function.

A large set of genes (e.g. *uvrA*, *uvrB*, *recN*, *ruv* and a number of damage-inducible genes) are activated in the SOS response to optimise cell survival, but at the cost of mutagenesis, because the SOS system is more error prone than any other repair system (Kohen *et. al.*, 1995).

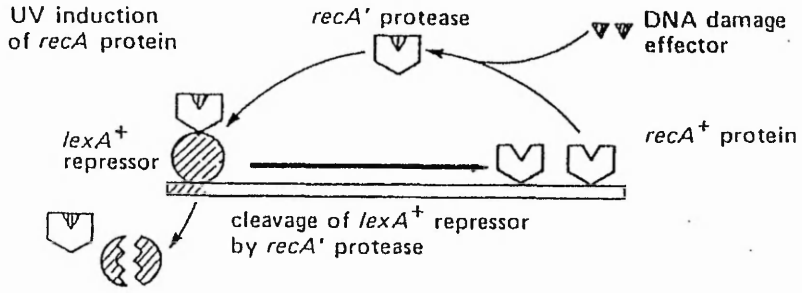

Figure 1.6: Regulation of the recA gene *in vivo*. The broad arrow represents increased transcription of the recA gene (Kohen *et. al.*, 1995).

In humans, several types of DNA lesions, such as the cyclobutane pyrimidine dimmers, are removed more rapidly from transcribed DNA strands than from other regions of DNA (Hanawalt, *et. al.*, 1992). This preferential repair of active genes (transcription-coupled repair) is deficient in Cockayne's syndrome, which is characterised by developmental abnormalities and UV-sensitivity (Hansson, 1992; Hoeijmakers, 2000).

1.3.6 DNA-Protein Cross-Links

NUV sensitised formation of ·OH and $^1O_2$ is known to cause covalent cross-linking between DNA and proteins. DNA-protein cross-links may be formed by combination of a DNA radical and a protein radical, by addition of a DNA radical to an aromatic amino acid, or by addition of a protein radical to a DNA base. Thus, protein cross-links involving thymine and tyrosine have been identified (Nackerdien *et. al.*, 1991). In this case, a ·OH-generated allyl radical of thymine adds to C3 of tyrosine and oxidation of the adduct radical is followed. In T7 phage, DNA-protein cross-links are believed to cause its inactivation by preventing DNA injection into the host cell during infection (Hartman *et. al.*, 1979).

1.3.7 Protein Damage

Protein damage by ROS is often complex and irreversible, and frequently leads to protein unfolding and denaturation. Functional proteins may be highly sensitive to ROS attack because relatively small regions of the entire macromolecule,

e.g. the activity centre or an enzyme, control their biological properties. Additionally, photosensitised reactions can result in changes of the protein's properties such as the absorption spectrum, molecular weight, electrophoretic pattern, solubility, and heat sensitivity. Modification of proteins is often initiated by interactions of $^{\cdot}OH$ with the main chain α-CH- groups, the hydrocarbon side chains, and the functional groups of amino acid residues (Stadtman, 1995). Thus, $^{\cdot}OH$ can cause amino acid oxidation, decarboxylation, deamination, polypeptide-chain scission and crosslinking.

Oxidised proteins may result in protein radicals, which can cause further damage to normal proteins and other biomolecules. Radical attack on proteins results in the formation of protein hydroperoxides and catechols, which are species of moderate stability and can react further with ROS (Dean *et. al.*, 1993). Often, radical damage to proteins is site specific and involves transition metals. Sulphur-containing side chains are particularly vulnerable to oxidation, whereas the aromatic amino acids are the most susceptible to oxidative modification by all forms of ROS. Most of the oxidising pathways lead to carbonyl-containing products such as aldehydes and ketones. Such protein carbonyl contents are often used as an index of molecular oxidative modifications, and can be measured using the 2,4-dinitrophenylhydrazine assay (Levine *et. al.*, 1994).

Histidine is one of the most important target amino acids for $^1O_2$, and is often used to monitor $^1O_2$ in solution. Histidine residues can oxidise to asparagine, aspartic acid and 2-oxo-histidine residues. Methionine undergoes photooxygenation and can react with $^1O_2$ to give sulphoxides, whereas reaction of tryptophan with $^1O_2$ generates *N*-formylkynurenine, which can also act as photosensitiser (Kohen *et. al.*, 1995). Upon $^{\cdot}OH$ attack, phenylalanine residues are converted to their 2-, 3-, and 4-hydroxy-phenylalanine derivatives (Stadtman, 1995). Also, $^{\cdot}OH$ addition to tyrosine residues results in production of 3,4-dihydroxyphenylalanine (DOPA), which has reducing properties, and in tyrosine-tyrosine cross-links (Gieseg *et. al.*, 1993). The susceptibility of the other amino acids to irreparable damage depends upon the conformation of the domain in which they are found (Rauk *et. al.*, 1997). However, the subsequent events after photosensitisation may not be confined to the initial sites because excitation energy and electrons can migrate within a molecule.

Photooxidation and covalent cross-linking of the peptide chain involving the amino acids histidine, tryptophan, tyrosine, methionine, lysine and cysteine has been observed (Verweij and Steveninck, 1982). Histidine was found to be most reactive with -SH groups, whereas cysteine-cysteine cross-links showed involvement of S–S bond formation. Ortwerth and Olesen (1994) also showed that protein-bound chromophores can act as sensitisers of UVA and can cause protein damage and cross-linking. In their study, UVA irradiation of human lens proteins resulted in damage to histidine, cysteine and methionine residues that was attributed to tryptophan acting as photosensitiser. Histidine and tryptophan destruction was observed throughout the UVA spectrum employed with 80% damage to tryptophan residues at 290 nm. A possible mechanism for the production of cross-links has been suggested (Spikes *et. al.*, 1999). According to this, ROS produced by light-excited photosensitisers may interact with amino acid residues prone to photooxidation such as histidine, tryptophan and tyrosine in one protein molecule to give radicals that, in turn, react with normal or photo-altered residues in another protein molecule. The capability of some proteins to be cross-linked can be altered by changing their conformation. Thus, those amino acid residues involved must be exposed and have the proper orientation in the molecule to permit cross-linking.

Furthermore, a study by Carbonare and Pathak (1992) showed that the NUV-photosensitised generation of $^1O_2$ and $O_2^{\cdot-}$ can result in the structural and functional alteration of cutaneous proteins such as collagen and elastin. In the presence of riboflavin or haematoporphyrin, irradiated collagen exhibited increased insolubility, increased molecular weight, and gel-like precipitation as indicators of formation of intermolecular cross-links. More recent studies showed that UVA-sensitised production of ROS can result in extensive accumulation of abnormal elastin (Kawaguchi *et. al.*, 1997) and in stimulation of collagenase production that leads to excessive collagen degredation (Kawaguchi *et. al.*, 1996; Petersen *et. al.*, 1995). Exposure of plasma proteins to UVA and 8-methoxypsoralen also resulted in protein oxidation, cross-linking and fragmentation as revealed by electrophoresis (Reinheckel *et. al.*, 1999).

The susceptibility of proteins to $^1O_2$-mediated damage was further supported by studies that demonstrated the high reactivity of membrane proteins with $^1O_2$. In a study involving nine Leukemia cell lines with different protein content, it was shown that an increase in the protein content of the cell resulted in higher protection against $^1O_2$-mediated membrane damage during photosensitisation by photofrin, a haematoporfirin derivative used in photodynamic therapy (Schafer and Buettner, 1999). Also, Kanofsky (1991) has shown membrane proteins to react with about 80% of the $^1O_2$ produced in cell membranes. These results indicate that cellular proteins are key targets for $^1O_2$ attack. Such physical quenching may offer some protection against cell damage by preventing lipid peroxidation.

1.3.8 Lipid Peroxidation

Membrane lipids are, in general, the first targets for the attack by ROS as these species are frequently generated in association with membranes. Saturated lipids are not a target for ROS, while unsaturated lipids can be easily oxidised. Lipid peroxidation is the oxidative deterioration of polyunsaturated lipids (i.e. lipids that contain more than two carbon-carbon double covalent bonds). ROS can readily attack polyunsaturated fatty acids (e.g. linoleic acid, arachidonic acid), phospholipids and cholesterol. In polyunsaturated lipids a $-CH_2-$ group separates the adjacent double bonds. The initiation step of lipid peroxidation involves the abstraction of a hydrogen atom from the $-CH_2-$ group by $^{\cdot}OH$. The resulting carbon radical tends to be stabilised by a molecular rearrangement to form a conjugate diene that lacks the middle $-CH_2-$ group. Conjugated dienes readily react with molecular oxygen to generate lipid peroxy radicals. Peroxy radicals are capable of abstracting hydrogen atoms from other lipid molecules, propagating the lipid peroxidation reaction. The peroxy radical combines with the hydrogen atom to give lipid hydroperoxide (Figure 1.7).

$^1O_2$, on the other hand, can react directly with carbon-carbon double bonds by an *ene* reaction to give hydroperoxides. This direct addition of $^1O_2$ to unsaturated lipids can rapidly cause peroxidation and does not involve a chain reaction. If no free redox-active metal is available, hydroperoxides can accumulate and eventually be

enzymatically removed from the cell. In the presence of transition metals, however, hydroperoxides react to give peroxy and alkoxy radicals that can undergo further reactions. Lipid peroxidation induced by $^1O_2$ appears to be a function of the lipid content of the cell. Increasing the unsaturation of membrane lipids results in an increase of hydroperoxide formation (Schafer and Buettner, 1999). The damaging effect of $^1O_2$ is enhanced in lipid membranes as it has a longer half-life in such condensed media (Fukuzawa, 2000; Paillous and Fery-Forgues, 1994).

Damage to polyunsaturated fatty acids tends to reduce membrane fluidity, which is known to be essential for the proper functioning of biological membranes. As a result, membrane leakage can occur, and eventually cell lysis (Beer *et. al.*, 1993). In addition, ROS-mediated lipid peroxidation of membranes can cause intracellular Ca^{2+} increases that may lead to activation of endonucleases. The measurement of cytokine secretion, malondialdehyde production and extracellular leakage of lactate dehydrogenase have been used as indicators of lipid peroxidation (Morliere *et. al.*, 1991; Tebbe *et. al.*, 1997).

Lipid peroxidation not only threatens the integrity and function of membranes, but also produces a variety of toxic products. Thus, from the reactions of peroxy radicals, lipid hydroperoxide, cyclic peroxide and cyclic endoperoxide can emerge (Figure 1.7). These compounds can undergo polymerisation, or fragmentation to form aldehydes and ketones, of which malondialdehyde and *trans*-4-hydroxy-2-nonenal are produced in high yields. Malondialdehyde and *trans*-4-hydroxy-2-nonenal are known to react *via* a Michael addition with nucleophilic side-chains of proteins resulting in protein cross-linking (Selverstone Valentine *et. al.*, 1998; Toyokuni, 1999). Also, malondialdehyde and *trans*-4-hydroxy-2-nonenal are known to react with deoxyguanosine, the former forming adducts detected by mass spectrometry (Chaudhary *et. al.*, 1994), and the later forming 1,*N*-etheno-deoxyguanosine (Sodum and Chung, 1988). Thus, lipid peroxidation can damage membrane proteins and DNA as well as other lipids.

The oxidation products of the peroxidation of unsaturated lipids and their respective yields depend on whether $^{\cdot}OH$ or $^1O_2$ reactions are involved (Paillous and Fery-Forgues, 1994). The $^1O_2$-mediated peroxidation of linoleic acid, for example, can produce equal amounts of 9-, 10-, 12-, and 13-hydroperoxides. Abstraction of

hydrogen by ·OH, on the other hand, yields almost exclusively 9- and 13-hydroperoxide products.

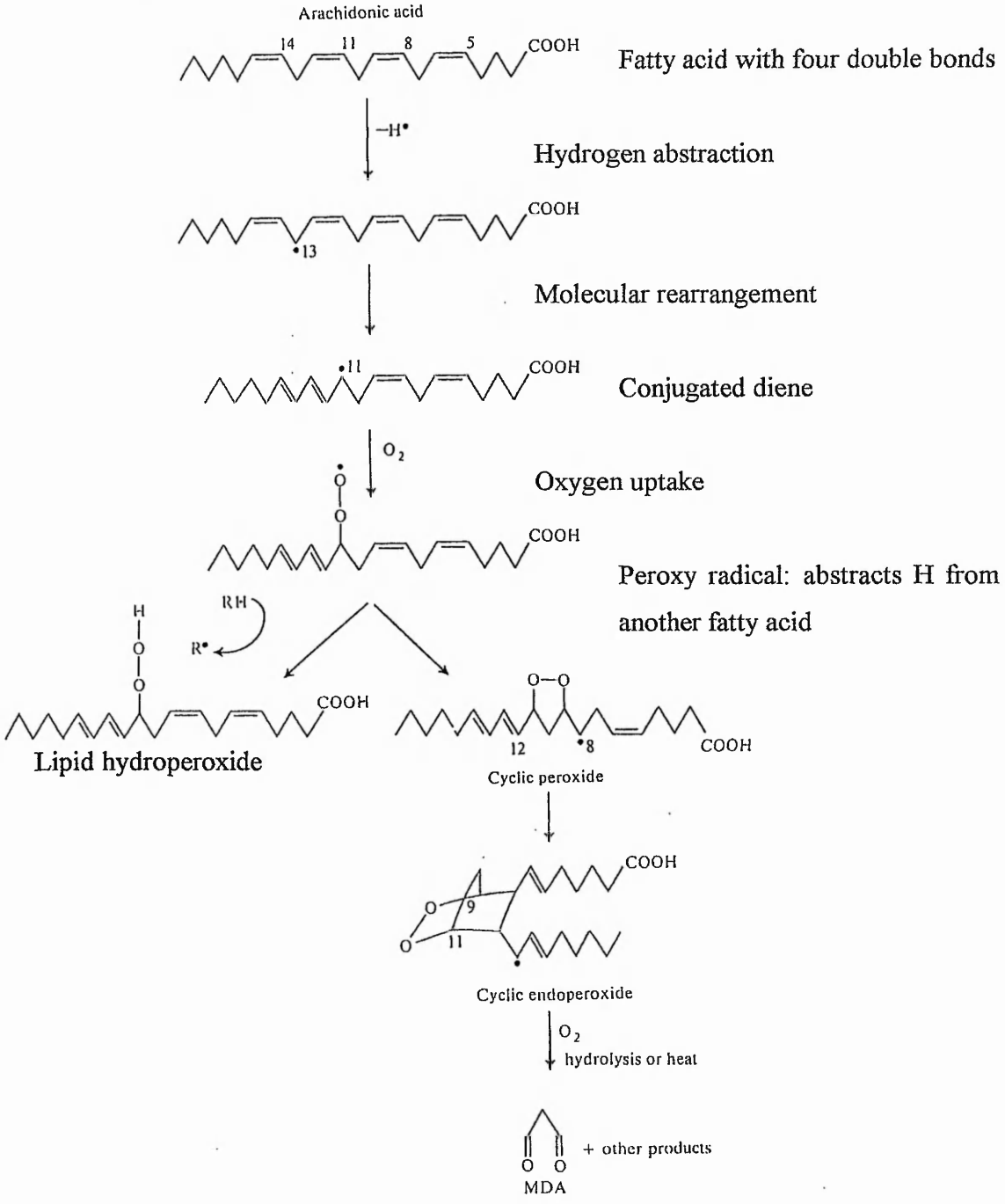

Figure 1.7: Schematic representation of initiation, propagation and termination products of lipid peroxidation of arachidonic acid. Initial abstraction of H at C-13 is shown, although H can also be abstracted at C-7 or C-10, giving different peroxidation end products (taken from Halliwell and Gutteridge, 1999).

$O_2^{\cdot-}$ does not readily cross biological membranes. However, the protonated form of $O_2^{\cdot-}$, the hydroperoxide radical ($HO_2^{\cdot}$), is more reactive and it appears to be capable of abstracting a hydrogen atom from some fatty acids, such as linoleic acid (Aikens and Dix, 1991). Furthermore, being uncharged, $HO_2^{\cdot}$ like H_2O_2 can cross membranes easily.

Antioxidants prevent initiation or break the chain of oxidation reactions involved in lipid peroxidation. They can either directly react with the oxygen radical, bind free metal ions, terminate the propagation reaction by interacting with the lipid peroxy and alkoxy radicals, and convert peroxides to non-radical products such as alcohols. Thus, water-soluble antioxidants (e.g. ascorbic acid, glutathione) and lipid-soluble antioxidants (e.g. α-tocopherol, β-carotene, ubiquinol) react differently with different oxidants. It was shown that UVA-induced lipid peroxidation in cultured human keratinocytes was inhibited by ascorbic acid in a concentration-dependent manner (Tebbe *et. al.*, 1997). The major antioxidant action of α-tocopherol in biological membranes is to react with lipid peroxy and alkoxy radicals, donating a hydrogen atom and so terminating the chain reaction of peroxidation. In turn, α-tocopherol can be regenerated by ascorbic acid (Frei *et. al.*, 1992).

Peroxidation can equally be induced by UVA and UVB radiation (Morliere *et. al.*, 1995). Unlike DNA damage and mutagenicity where a strong increase in the effect of wavelengths below 320 nm has been observed, the biological effectiveness for lipid peroxidation induced by UVB is extremely low compared to that of UVA. In an earlier study, an increase in the number of conjugate diene double bonds, which are indicators of lipid peroxidation, was observed after both UVB and UVA irradiation (Punnonen *et. al.*, 1991).

1.4 NUV and Health Risks

Many photosensitised reactions are particularly important in the photochemical alterations of biomolecules. Often, however, the accumulation of molecules that can act as natural photosensitisers can have health implications. Thus, porphyrins that accumulate in the skin of porphyric patients suffering from impaired

heme biosynthesis or metabolism are responsible for the phototoxic response of areas of skin exposed to UVA and visible radiation. Also, genetic or acquired impairment of tryptophan metabolism can lead to exaggerated production of kynurenic acid, which is responsible for actino-reticulosis disease, as a result of a strong phototoxic response (Chalmers and Lawson, 1982).

1.4.1 Photoageing

Dermatoheliosis, the ageing of the skin is a well-documented result of exposure to sunlight. Photoaged skin is characterised by altered pigmentation, loss of elasticity and formation of wrinkles. Photoaged skin also displays prominent alterations in the cellular component and the extracellular matrix of the connective tissue with an accumulation of abnormal elastin fibres in the deep dermis, and a severe loss of collagen, the major structural protein of the connective tissue. The agents of these changes are UV-generated ROS that deplete and damage non-enzymatic and enzymatic antioxidant defence systems of the skin. As well as causing permanent genetic changes (Le Page *et. al.*, 1998; Stary and Sarasin, 2000), ROS activate cytoplasmic signal transduction pathways in resident fibroblasts that are related to growth, differentiation and connective tissue degradation (Kawaguchi *et. al.*, 1996; Petersen *et. al.*, 1995). In a study where ROS were produced by a xanthin and xanthin oxidase system, they were shown to increased mRNA expression of elastin in cultured human dermal fibroblasts. Addition of catalase essentially prevented the ROS-induced alteration is elastin mRNA levels, suggesting that ROS produced in the dermis may contribute to elastin deposition observed in photoaged skin (Kawaguchi *et. al.*, 1997). In addition, ROS were found to contribute to structural and functional alterations of collagen leading to formation of protein cross-links (Carbonare and Pathak, 1992; Kawaguchi *et. al.*, 1996). Cross-linked collagen is invariably poorly soluble, resistant to pepsin digestion and loses its contractile property. In general, ageing tissue shows a progressive accumulation of products derived from the oxidative modification of protein and protein-associated carbonyls as a result of ROS reactions (Berlett and Stadtman, 1997).

Studies of the involvement of ROS in photoageing have identified a number of ROS with a possible role in the UVA-induced generation of photoaged skin. Yasui

and Sakurai (2000) reported the *in vivo* detection and imaging of the generation of $O_2^{\cdot-}$ and $^1O_2$ in the skin of mice following UVA irradiation. In a study by Carbonare and Pathak (1992) $O_2^{\cdot-}$ and $^1O_2$ that were generated on photosensitised reactions of psoralens, riboflavin and hematoporphyrin were shown to induce the denaturation of collagen and other skin proteins and the formation of cross-links. Moreover, treatment of skin with a source of $^{\cdot}OH$ produced skin changes such as dermal thickness and sunburn cells that quantitatively resembled those produced by UVB, suggesting a possible role of $^{\cdot}OH$ in ROS mediated photoageing (Ibbotson *et. al.*, 1999). In a different report, the time/dose dependent generation of common deletion (a mutation in the mitochondrial DNA that is increased in photoaged skin) was attributed to the generation of $^1O_2$ during UVA irradiation of normal human fibroblasts (Berneburg *et. al.*, 1999). The common deletion was diminished when irradiating in the presence of $^1O_2$ quenchers and increased when enhancing $^1O_2$ half-life in D_2O. These studies indicate the possible contribution of these ROS *in vivo* to the alterations in collage and photoageing of exposed skin. Thus, the UVA induced generation of these species within human skin appears to be of critical importance. A decrease in the overall ROS load by sunscreens or other protective agents may represent promising strategies to prevent or minimise ROS induced photoageing.

Finally, of particular interest is the identification of the actual endogenous chromophores in the skin that may contribute to the generation of ROS on UVA irradiation and subsequently the UVA-induced skin photodamage. Recently, the UVA-induced photoreactivity of two light-absorbing epidermal photoreceptors, namely *trans*-urocanic acid and eumelanin, was studied in order to understand the role these chromophores may play in photoageing (Simon, 2000). Also, a group of enzymes known as matrix metaloproteinases that are found in the skin were shown to induce photoageing by their involvement in the degradation of collagen. All-*trans* retinoic acid was shown to inhibit the UV induction of matrix metaloproteinases, and thus protecting against UV-induced collagen destruction and reducing the effects of photoageing (Fisher *et. al.*, 1999).

1.4.2 Photocarcinogenesis

Skin cancers associated with exposure to UV radiation are predominant in light-skinned populations that have high sun sensitivity. Increased exposure to sunlight increases the risk of developing skin cancer. There are two major categories of skin cancer, non-melanoma skin cancers and cutaneous melanomas. Non-melanoma skin cancers include basal cell carcinoma and squamous cell carcinoma, both resulting from the malignant transformation of keratinocytes.

Basal cell carcinoma is the predominant form of skin cancer and has no unique precursor lesion. This type of tumour occurs more frequently on the trunk and is associated with sunburns that occurred in childhood (de Gruijl, 1997).

Squamous cell carcinoma has the most straightforward relationship to sun exposure. The risk increases with life-long accumulated exposure and has been associated with chronic occupational exposure. The precursor lesions of squamous cell carcinoma are actinic keratoses, premalignant lesions of epidermal cells (Farmer and Naylor, 1996; de Gruijl, 1997). If squamous cell carcinoma is neglected, it could metastasise.

The role of UVB radiation in inducing non-melanoma skin carcinogenesis has been attributed in part to mutations on the *p53* tumour suppressor gene (Dumaz *et. al.*, 1997). The dysfunctional protein of *p53* fails to repress the carcinogenic progression. The majority of the mutations on analysed mouse tumours were found at dipyrimidine sites and were C→T transitions. Such mutations were found in *p53* in a majority of squamous cell carcinomas and basal cell carcinomas, as well as in actinic keratoses (Dumaz *et. al.*, 1997; Ziegler *et. al.*, 1994). Thus, these mutations occur at a very early stage of the development of squamous cell carcinoma. It has been suggested that inactivation of DNA repair pathways which lead to an increased mutation rate and chromosomal instability may be the first step in carcinogenesis (Schmutte, 1999).

Cutaneous melanoma results from the malignant transformation of melanocytes. Cutaneous melanoma is the rarest type of skin tumour and the most

aggressive. These tumours can rapidly metastasise and account for most of the skin cancer related mortality. Cutaneous melanoma frequently occurs at anatomical locations that are not the most heavily sun-exposed. This type of cancer results from intermittent overexposure and from high levels of ambient UV radiation during childhood (de Gruijl, 1997). An additional risk factor for cutaneous melanoma is the presence of pigmented lesions on the skin like freckles or moles, known as melanocytic nevi. At least some nevi may be precursor lesions for melanoma (Farmer and Naylor, 1996). Exposure to UVA may play an important role in cutaneous melanoma formation. In an animal model, exposure to UVA alone has been shown to induce melanocytic hyperplasia, a precursor to melanoma (Ley, 1997).

The risk of all types of skin cancer is dramatically increased for patients with the heritable disorders *Xeroderma pigmentosum* and Farconi's anemia. Patients of the former lack a proper nucleotide excision repair mechanism by which UVB-induced adducts can be removed from genomic DNA, whereas patients of the later are sensitive to DNA cross linking agents but have no defect in DNA repair (Hansson, 1992). Also, people who have had skin tumours run a substantially increased risk of subsequent occurrences of skin cancer.

1.4.2.1 UVR Induced Carcinogenesis and Apoptosis

Apoptosis or programmed cell death is characterised by cell shrinkage, membrane blebbing, chromatin condensation and DNA fragmentation. Studies on the effect of NUV on apoptosis of fibroblast and lymphoma cells show that UVA induces immediate and delayed apoptosis, whereas UVB induces delayed apoptosis (Pourzand *et. al.*, 1997; Pourzand and Tyrrell, 1999). It has been recently reported that over-expression of the *bcl-2* protein suppresses apoptosis in cells that have undergone oxidative stress (Pourzand *et. al.*, 1997). Also, over-expression of *bcl-2* is quite common in basal cell carcinoma and cutaneous malignant melanoma (Morales-Ducret et. al, 1995). Disregulation of the apoptotic mechanism in skin can therefore lead to skin cancer.

The most common type of damage from UV radiation to the skin is sunburn. Sunburn cells are an example of apoptosis, and this self-destructive disintegration process can eliminate pre-cancerous cells.

1.4.3 Atherosclerosis

Atherosclerosis is primarily a disease of the endothelium, caused by high plasma cholesterol levels. A critical mechanism of atherosclerosis is the ROS-mediated oxidation of low-density lipoprotein (LDL). The lipid component of LDL is oxidised by a ROS-mediated chain reaction forming lipid hydroperoxides and other lipid peroxidation products (Esterbauer and Ramos, 1996). It has been demonstrated that nitric oxide and its substrate L-arginine have antiatherogenic properties and inhibit LDL oxidation (Hogg, 1998). High concentrations of cholesterol, however, have been shown to elevate endothelial formation of $O_2^{\cdot-}$ in atherogenic arteries (Ohara *et. al.*, 1993). Consequently, elevation of $O_2^{\cdot-}$ impairs endothelial-dependent relaxation. In addition, reactions between nitric oxide and $O_2^{\cdot-}$ generate a powerful oxidant, peroxynitrite, which is able to initiate lipid peroxidation and oxidatively modify LDL (Hogg, 1998). Thus, $O_2^{\cdot-}$ seems to play a key role in enhancing oxidative stress in endothelium and, as a consequence, in atherosclerosis.

1.4.4 Ocular Damage

Ocular damage from UV exposure includes damage to the cornea, lens, iris, and associated epithelial and conjunctival tissues. The most common acute ocular effect on the cornea after exposure to UV is photokeratitis, the result of increased production of pro-inflammatory cytokines. Other ocular effects on the cornea that result from chronic UV exposure are climatic droplet keratopathy (a degeneration of the fibrous layer of the cornea with the accumulation of droplet-shaped deposits), pinguecula (a raised opaque mass adjacent to the cornea), pterygium (an outgrowth of the conjuctiva), and squamous cell carcinoma of the cornea and conjunctiva (de Gruijl, 1997; Longstreth *et. al.*, 1998). Additionally, malignant melanoma of the uveal tract is the most commonly occurring primary ocular malignancy, and cataract is the major type of damage to the lens associated with UV exposure. Animal studies

show that cataract can be induced by chronic UVA (Zigman *et. al.*, 1991) and UVB exposure (Jose and Pitts, 1985).

Cataract is characterised by a gradual loss in the transparency of the lens. Cataract formation can be partially attributed to an increased presence of covalently cross-linked, high molecular weight aggregates, which produce increased light scattering. These aggregates appear with time as yellow and then brown protein-bound pigments primarily localised in the lens nucleus. The most common of these aggregates are advanced glycation endproducts (AGE). AGE are generated from the reaction of lens proteins with L-threose, the major oxidation product of glucose and ascorbic acid. The common feature of these protein chromophores is that they absorb mainly in the UVA region of the spectrum and are believed to generate ROS (Linetsky *et. al.*, 1996; Linetsky and Ortwerth, 1997; Masaki *et. al.*, 1997; Ortwerth *et. al.*, 1997). As a result, extensive photolytic damage can occur to amino acid residues, especially those containing -SH groups (Linetsky *et. al.*, 1996).

1.4.5 Immunosuppression

It is believed that the decreased immune responses observed after UV irradiation serve to prevent excessive inflammation and damage to the skin that has been exposed to the sun. The immunosuppressive effects of UVR exposure may result in failure of the body to reject UVR-induced tumours. Immune suppression can occur locally or systemically, depending on the dose of UVR and the type of immune response. The role of UVB in immunosuppression is well established. UVB exposure is known to impair the induction of contact hypersensitivity to cutaneous antigens and induce antigen specific tolerance. Thus, UVB-induced immunosuppression is responsible for contact and delayed-type hypersensitivity reactions against virus-infected cells and microorganisms (Garssen *et. al.*, 1998).

Urocanic acid and DNA have been identified as the major chromophores in UV-induced systemic immunosuppression. The *in vitro* action spectrum for mixed epidermal cell lymphocyte reaction showed that the UVB-induced suppression of immune responses is associated with UVB-induced DNA damage and the formation of thymine dimers. DNA damage was therefore shown to be the trigger for the

production of cytokines that modulate immune responses (Hurks *et. al.*, 1997). In addition, urocanic acid isomerisation from *trans* to *cis* urocanic acid was shown to act as a mediator for some of the systemic suppressive effects of UVB, altering cell-membrane components and consequently affecting internal cell signal-transduction pathways (de Fabo and Noonan, 1983). It was also found that *cis*-urocanic acid might exert its immunosuppressive action by binding to histamine receptors on skin cells (Noonan and de Fabo, 1992). Moreover, UVB irradiation and *cis*-urocanic acid were shown to diminish the number of Langerhans cells in the epidermis and disturb the proper priming of T cells, often leading to the generation of suppressor T cells (Longstreth *et. al.*, 1998). Such immunosuppressive effects are of particular interest in phototherapy. In a study using psoriatic patients, it was observed that the functional ability of epidermal cells to prevent herpes simplex virus was suppressed during UVB plus psoralens irradiation (Jones *et. al.*, 1996). Also, most subjects undergoing phototherapy exhibited a dose-dependent suppressed natural killer cell activity and a decrease in cytokine production during or after irradiation.

ROS are also associated with all inflammatory disorders (i.e. abnormalities of the immune response that can lead to tissue degeneration). Inflammation includes the recruitment of neutrophills and monocytes to the lesion. However, the effect of UVA in ROS generation and immunossupression is not yet as clear. It has been reported that $O_2^{\cdot-}$ is involved in intracellular pathways that lead to the recruitment of inflammatory cells and inflammatory mediators such as cytokines (Schwartz *et. al.*, 1995). Also, the involvement of ROS in the UVA-induced secretion of pro-inflammatory cytokines in human keratinocytes was demonstrated by the protective effect of ascorbic acid (Tebbe *et. al.*, 1997). In addition, studies of immune responses involving mice carrying the *xeroderma pigmentosum* gene showed that UVA plus psoralen irradiation treatment induced stronger and more prominent histological changes such as epidermal necrosis, cell infiltration and sunburn cell formation in the deficient compared to the wild type mice. Although contact hypersensitiviy was induced equally in all mice, UVA mediated local and systemic immunosuppression reactions were greatly enhanced in the XPA gene deficient mice (Miyauchi-Hashimoto *et. al.*, 1996). These results suggested a possibility that enhanced immunosuppression might be involved in the development of skin cancers in *xeroderma pigmentosum* individuals.

1.4.6 Neurodegenerative Diseases

The role of ROS in Alzheimer's and Parkinson's diseases has been recently considered. Oxidative stress has been implicated as one of the most important contributors to neuronal degeneration of melanised neurones in Parkinson disease. One of the causes of nigral cell death is believed to be ROS-mediated lipid peroxidation (Yoritaka *et. al.*, 1996). In this study, it was shown that the amount of *trans*-4-hydroxy-2-nonenal-modified protein was 50 times more in nigral neurones of Parkinson patients than in the control subjects.

Similarly, oxidative stress may contribute to neuronal loss in Alzheimer's disease. It is believed that ROS may be involved in the production, aggregation and toxicity of β-amyloid, which is thought to contribute to neuronal damage in Alzheimer's disease (Nixon and Cataldo, 1994). A comparative study involving brain tissue from Alzheimer's patients and healthy subjects showed increased levels of protein carbonyls and oxidised products of DNA bases, strengthening the possibility that oxidative damage may play a role in the pathogenesis of Alzheimer's disease (Lyras *et. al.*, 1997).

1.5 Antioxidant Defence Mechanisms

The skin possesses an elaborate antioxidant defence system to deal with UVR-induced oxidative stress. Such endogenous antioxidants are generally divided in two categories: enzymatic and non-enzymatic. Some of the more commonly known enzymatic antioxidants include superoxide dismutase, catalase and glutatheone peroxidase. Non-enzymatic antioxidants include α-tocopherol, glutathione, melatonin, ubiquinol, ubiquinone, ascorbic acid and carotenoids. To date, there is sufficient evidence of the protective effect of these antioxidants against the harmful effect of UVR and also of the effect of UVR on antioxidant status. Studies that examined the rate of synthesis and degradation of a number of endogenous antioxidants in response to UVR reported a decrease in the activities of catalase and SOD and the concentrations of α-tocopherol, ascorbic acid and glutathione in mice skin after a single exposure (Shindo *et. al.*, 1993). In contrast, chronic repeated

exposures to UVR or UVA resulted in an increase or recovery of antioxidant activity and concentration (Okada *et. al.*, 1994; Shindo and Hashimoto 1997). These results suggested that the antioxidant status of the skin depends on the rates of both synthesis and degradation of each compound, and that the recovery observed is due to an increased rate of synthesis after irradiation.

Another important issue in the antioxidant defence of the skin against the effects of UVR is how the antioxidant status of the dermis and epidermis compare. Experimental data on the dermis and epidermis of hairless mice indicated that the activity of enzymatic antioxidants was 50-85 % higher, and non-enzymatic antioxidant levels were 24-95 % higher, in the epidermis than the dermis (Shindo *et. al.*, 1993). An examination of the antioxidant status after UV irradiation revealed a dramatic decrease in all antioxidants in both the dermis and epidermis. For some of these antioxidants, this decrease was more severe in the epidermis, suggesting that UVR is more damaging to this skin layer. This would also explain the finding of a higher amount of antioxidants in the epidermis, and emphasise the importance of antioxidants as a natural defence against solar radiation.

In addition, of particular interest is the role of genetic polymorphism in antioxidant status and the way this affects susceptibility of individuals to oxidative stress. Studies of the incidence of breast cancer in women, showed that the antioxidant status of the individual plays an important role in the risk factor for developing the disease. Endogenous antioxidants including the polymorphic MnSOD can act to reduce the load of oxidative stress that is believed to play a role in breast cancer. Studies showed that women with a defect in MnSOD genotype had a four-fold increase in breast cancer risk. Risk was most pronounced among women below the median consumption of dietary ascorbic acid and α-tocopherol (Ambrosone *et. al.*, 1999). Thus, genetic variability in enzymes that result in increased production of ROS and those that protect the cell from oxidative stress can have an impact for risk of the disease.

1.6 Aims

Based on the understanding that the deleterious effects of UVA are mediated by ROS whose formation is photosensitised by endogenous chromophores, an investigation was undertaken to identify a number of biologically relevant compounds as potential sensitisers of UVA. The compounds chosen were L-histidine L(+)mandelic acid, β–phenylpyruvic acid, *p*-OH-phenylpyruvic acid and L-β–phenyllactic acid. Their choice was based on the structural similarity to phenylalanine, tryptophan and tyrosine all of which have been shown in the past to undergo photosensitised reactions in the presence of UVA radiation and generate ROS (Craggs *et. al.*, 1994; McCormick *et. al.*, 1976; Ortwerth and Olesen, 1994). In addition, similarly to the above-mentioned amino acids, the compounds of interest are ubiquitous components of living cells. In this project, a detailed analysis of the potential of these substances to act as photosensitisers and affect biological systems will be carried out.

A. UV Absorption

The absorption properties of these compounds will be investigated with an emphasis on their ability to absorb radiation in the UVA and UVB wavebands. The absorption patterns of the different compounds will be compared in an attempt to identify possible functional groups responsible for photosensitised reactions. Following this, a possible correlation between absorption spectra and photosensitisation reactions will be explored. In this way, the ability of the compounds that exhibit the highest photosensitising potential to cause biological damage will be determined and compared to their absorption spectra. Such a comparison will lead to the better evaluation of the photosensitising properties of these potential sensitisers.

B. Photosensitised Reactions and ROS Generation

The ability of the compounds of interest to undergo photolysis to generate ROS will be investigated using two chemical assays. The reduction of nitro-blue

tetrazolium will be used as an indication of $O_2^{\cdot-}$ formation, and the reactivity of deoxyribose with $^{\cdot}OH$ will be used for the determination of the latter. Enzymatic and non-enzymatic scavengers that are known to have high affinity for certain ROS will be included in the assays in an attempt to confirm the generation of these and other ROS that may act as intermediates in their formation. Such studies could direct us to possible mechanistic pathways of ROS generation. The pH dependence of ROS production will be also investigated by varying the pH of the solution.

C. Synergistic Inactivation of Bacteriophage T7

After establishing the photosensitised potential of these compounds, their effects on biological systems will be investigated. Bacteriophage T7 will be used due to the simplicity of its composition. Given that the phage only contains DNA and proteins, and the well-established damaging effect of UVB to these components (Rosenstein and Mitchell, 1987; Zheng and Kligman, 1993), any synergistic inactivation would be attributed to the effect of UVA plus photosensitisers. By establishing that the compounds used as photosensitisers are not toxic to the phage, the synergistic effect could be attributed to the action of ROS. To support this argument further ROS scavengers will be included in the irradiated phage suspensions.

D. Photosensitised Lethality in Bacteria

Bacteria are a much more complex system to study the effects of photolysis than viruses as they contain DNA, proteins and lipids, and also a DNA repair system and antioxidant defences. However, they are often a good system for the study of the target molecules for ROS oxidation *in vivo*. Bacterial cells will be used in this study to investigate the possible incorporation or uptake of the sensitiser by the cell, and therefore determine the location of ROS generation in relation to cellular targets. There will be three different approaches to this aim. First, the use of a DNA repair deficient strain, together with the wild type, would give an indication of any damage possibly caused to the genome by ROS in addition to that inflicted on UV absorption. This would be evident if ROS generation takes place near the DNA. Second, the use of a gram-positive and a gram-negative species and any differences in the

susceptibility of the two to sensitised treatment would be indicative of the effect of photosensitised reactions on the cell membrane, and whether it acts as a target or a protective barrier. Finally, further evidence on the incorporation of the sensitiser in the cell will be achieved by HPLC analysis of the endogenous levels of the compound before and after treatment in both gram-positive and gram-negative species.

E. Photosensitised Damage to Individual Cellular Components

Further investigation of the role of the photolysis of the sensitisers studied to cause damage to cellular components will involve studies of the individual component in question. The reason for such an approach will be to determine the extent of damage induced under the experimental conditions employed, and also to identify specific types of damage. This, in turn, would enable us to indirectly identify the involvement of particular types of ROS and thus provide supportive evidence for their generation on UVA photolysis. Thus, pBR322 will be used as a model system to observe possible strand-break formation as the change of supercoiled to open circular ratio, and as a possible indication for the involvement of $^{\cdot}OH$ (Cadet *et. al.*, 1999; Oroscar *et. al.*, 1995). Also, the mutagenic potential of the sensitisers will be investigated with a particular interest in the role of base oxidation as the premutagenic modification. The use of a transversion mutator strain of *E. coli* that is deficient in repairing 8-oxodGuo or the misincorporation of this modified base during DNA replication would elucidate a possible role for $^1O_2$ in DNA damage as this ROS modifies selectively guanine residues (Ravanat and Cadet 1995; Stary and Sarasin, 2000). In addition, the effect of ROS generated on photosensitised reactions in the initiation and propagation of lipid peroxidation will be studied using liposomes as a model system. The selection of such a system is on the basis that it carries an opposite charge to that of the photosensitiser ensuring strong interaction and formation of ROS near potential lipid targets. Moreover liposomes do not contain any of the antioxidants that are normally present in cells or other potential targets (e.g. proteins) which would lead to an underestimation of ROS involved in the peroxidation process. Generally, the use of liposomes, in combination to using selective scavengers, could elucidate the involvement of $^1O_2$ and $^{\cdot}OH$ in lipid peroxidation. Finally, for a more detailed study on photosensitised damage to proteins, BSA will be used as a model system to pinpoint the involvement of ROS in

protein oxidation, and protein extracts will be used in an attempt to observe selective oxidation of certain proteins.

F. Biological Relevance of Sensitisers Identified

In order to determine the biological relevance of the compounds identified in this study as photosensitisers on UVA, an evaluation will be included where the same concentration of NADH will be used. The biological effects of the sensitisers studied will be compared to that of NADH, an established endogenous chromophore (Burchuladze and Fraikin, 1991; Cunningham *et. al.*, 1985). In addition, the results of all of the above studies will be used to evaluate the photosensitising potential of each of these compounds in terms of their biological effect, and a comparison of the different biochemicals to each other will lead us to an understanding of their biological significance.

CHAPTER TWO

MATERIALS AND METHODS

2.1 Microorganisms and Growth Media

2.1.1 Bacterial Strains, Plasmids and Bacteriophages

MICROORGANISMS	REPAIR CHARACTERISTICS	OTHER CHARACTERISTICS
Bacteriophage T7		
Escherichia coli strains:		
B	wild	best host for phage T7
KL16	wild	
SA162	*uvrA* mutant (nucleotide excision repair)	
SA191	$lacO^c$	constitutive for β-galactosidase
$mutT^+$	wild	Str^r, *leuB6*, qsr'^-
$mutT^-$	*MutT* mutant (nucleoside triphosphatase activity)	Str^r A•T→ C•G transversions
PQ37	*uvrA* mutant; *rfa* mutant (lipopolysaccharide production)	*sfiA*::Mud(Ap *lac) cts*, *galE*, *galY*
JA221 (pBR322)		Amp^r, Tet^r
Enterococcus faecalis	wild	
Staphylococcus aureus	wild	

Table 2.1: A list of the microorganisms involved in this study. The genes involved in DNA repair and other critical genotypic markers are shown.

The microorganisms employed in these experiments were obtained from the Nottingham Trent University culture collection unless otherwise stated. Together

with their critical genotypic markers, they are listed in Table 2.1. They were bacteriophage T7, *Escherichia coli* B, *Escherichia coli* KL16, *Escherichia coli* SA162, *Escherichia coli* SA191, *Escherichia coli* PQ37, *Escherichia coli mutT*$^+$ and *mutT*$^-$ (obtained from the *E. coli* Genetic Stock Centre, Yale University, CT, USA), *Escherichia coli* JA221 containing pBR322, *Enterococcus faecalis* and *Staphylococcus aureus*.

Long-term storage of bacteria was in 15% glycerol at -20°C. To 0.85 ml of bacterial culture, 0.15 ml sterile glycerol was added with vortex mixing to ensure the equal dispersal of glycerol. For every-day use, bacteria were kept on agar slants and plates made with the required media and antibiotics as indicated in section 2.1.2. Bacteriophage T7 lysates were prepared as detailed in section 2.5.1. A few drops of chloroform were added to the lysates to keep the phage suspensions free from bacterial contamination. Bacterial cultures on plates and slants, and the bacteriophage T7 lysates, were stored at 4°C.

2.1.2 Growth Media

All growth media, buffers and glassware used for microbial work were sterilised by autoclaving at 121°C for 15 min. Trypton soya agar (TSA), trypton soya broth (TSB), nutrient agar (NA) and nutrient broth (NB) were obtained from Oxoid, Unipath Ltd, UK and prepared according to the manufacturer's instructions. Luria Bertoni (LB) medium was prepared by dissolving 5 g of yeast extract, 10 g of trypton (both supplied by Oxoid) and 5 g of sodium chloride (Sigma Chemical Co., Poole, UK) in 1 L distilled water. For LB agar, 1.5% agar bacteriological (Oxoid) was added.

NA and NB were used for growth of *E. coli* strains B, KL16, SA191 and SA162. NA and NB supplemented with streptomycin (50 μg ml^{-1}) were used for growth of *E. coli mutT*$^+$ and *mutT*$^-$. LB broth and agar containing ampicillin (50 μg ml^{-1}) and tetracyclin (20 μg ml^{-1}) were used for growth of *E. coli* JA221. LB medium was also used for growth of *E. coli* PQ37. *E. faecalis* and *S. aureus* were cultured on TSA and in TSB media.

2.1.3 Stock Antibiotics

Antibiotics were purchased from Sigma. For all preparations distilled water was used. Stock antibiotics were sterilised by filtration and stored in aliquots at-20°C.

Ampicillin – 20 mg ml^{-1} of the sodium salt of ampicillin in water.
Tetracycline – 5 mg ml^{-1} tetracycline hydrochloride in ethanol/water (50% v/v).
Streptomycin – 20 mg ml^{-1} in water.
Rifampicin – 100 mg ml^{-1} in methanol.
Chloramphenicol – 20 mg ml^{-1} in ethanol.

2.2 Irradiation Conditions

The UV source employed was a Philips R-UVA solarium lamp (HP3148/A). It consisted of a horizontal planar array of eight TL09 lamps of 40 W each (Philips Electronics, Croydon). The average irradiance of the system at a distance of 12 cm was 6.03 x 10^{-3} W cm^{-2} UVA (98.8 %) and 7.07 x 10^{-5} W cm^{-2} UVB (1.2 %) [Figure 2.1 (b)]. The UVB present in the UV source was eliminated when required, using a sheet of Mylar plastic 36 μm thick (from the Department of Dermatology, Leiden University, Holland).

UVB irradiation was performed using a Philips TL01 narrow-band (311 nm) UVB lamp with an average output at a distance of 12 cm of 1.13 x 10^{-3} W cm^{-2} UVB and 1.08 x 10^{-4} W cm^{-2} UVA [Figure 2.1 (a)].

UVC irradiation was performed using a TJV 15 W germicidal lamp emitting at a distance of 12 cm 0.3 x 10^{-3} W cm^{-2}.

Radiometry was performed using a Glen Spectral radiometer, model 1680B. The determination of the spectral output of the R-UVA and TL01 sources and the calibration of the radiometer were performed by Boots, Co. plc. The energy dose applied to a given sample was calculated from the relationship:

Measured irradiance (W m^{-2}) = dose (J m^{-2}) / exposure time (seconds)

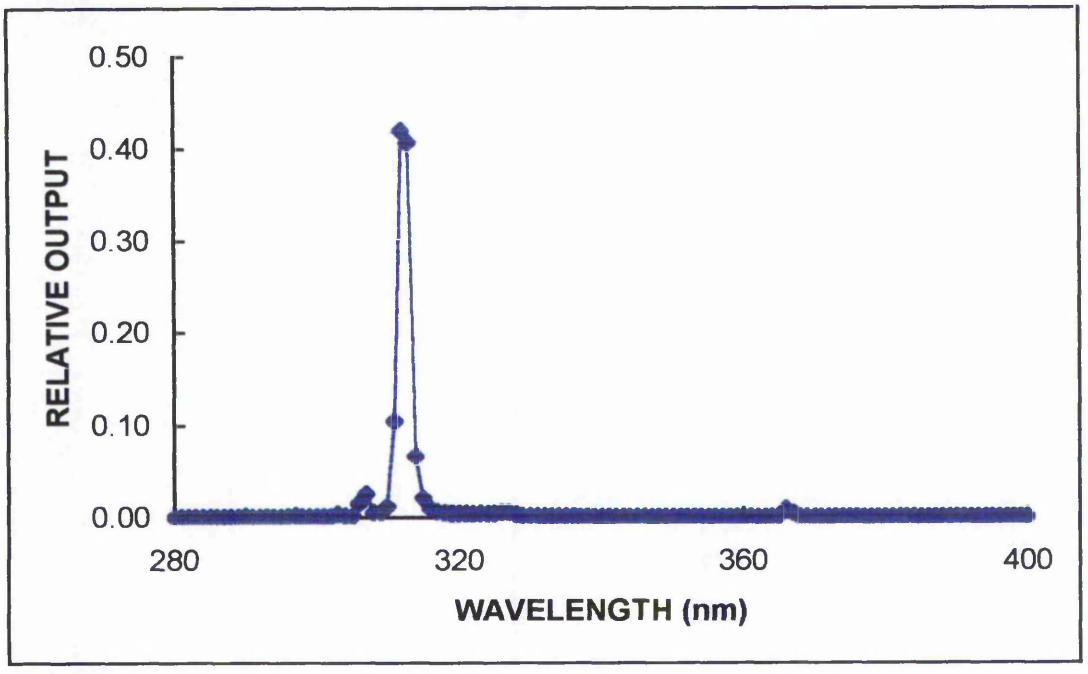

(a) TL01

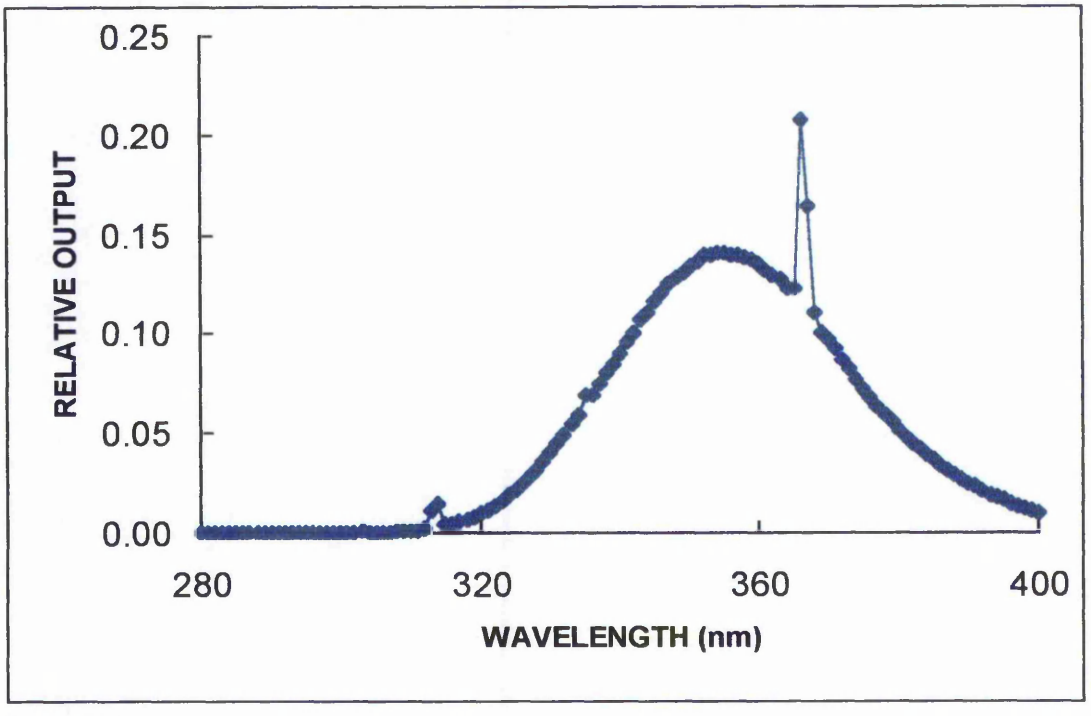

(b) R-UVA

Figure 2.1: The relative spectral output of (a) Philips TL01 and (b) R-UVA lamps, determined at 1 nm intervals using a Glen Spectral radiometer (model 1680B).

2.3 NBT Assay

2.3.1 Reagents

Nitro-blue tetrazolium (NBT), superoxide dismutase (SOD), catalase (bovine liver, thymol free), 1,4-diazabicyclo[2.2.2]octane (DABCO), β–carotene, L(+)mandelic acid, β–phenylpyruvic acid, *p*-OH-phenylpyruvic acid, and L-β–phenyllactic acid were purchased from Sigma Chemical Co., Poole, UK. L-histidine, sodium benzoate, sodium azide, K_2HPO_4 and KH_2PO_4, were purchased from BDH Ltd., Poole, UK. Mannitol was purchased from Fisher Scientific, UK. Distilled water was used for all experiments. All chemicals were of analytical reagent grade. The concentrations given for reagents are the final concentrations used.

2.3.2. Assay Conditions

Reaction mixtures (10 ml final volume) were prepared in uncovered glass Petri dishes (90 mm in diameter) by adding to 0.05 M K_2HPO_4/KH_2PO_4 buffer of appropriate pH (6.5-9) 1 mM of the sensitiser [L-histidine, L(+)mandelic acid, β–phenylpyruvic acid, *p*-OH-phenylpyruvic acid, or L-β–phenyllactic acid], NBT (20 μM), and when required, scavengers at concentrations given in Table 2.2. In experiments in which heat denatured catalase was used, native enzyme in solution was pre-treated by boiling for 10 min. Mixtures were irradiated under the NUV, UVB or UVC lamps, and 1 ml samples were removed at appropriate intervals (5 min). Controls included non-irradiated samples that were incubated in the dark for time equivalent to the irradiation period and reaction mixtures without the sensitiser. A_{560} values of all the samples were determined spectrophotometrically using a Cecil 1000 series spectrophotometer (Cecil Instruments Ltd, UK) and were plotted against the equivalent energy dose (calculated as described in section 2.2).

The sensitisers used in this assay and throughout this study are referred to as their acid form (e.g. L(+)mandelic acid) for consistency. At a given pH however, the compounds are expected to reach equilibrium between their acid and base form with the equilibrium shifting to the base form (e.g. L(+)mandelate) with increased

alkalinity. Generally, solutions of the sensitisers (x10) were freshly prepared by dissolving each compound in 0.05 M phosphate buffer (K_2HPO_4/KH_2PO_4) of appropriate pH. Subsequently senitisers were diluted in the reaction mixtures to give a final concentration of 1 mM, unless otherwise stated.

SCAVENGER	CONCENTR. USED	ROS SCAVENGED	pH	RATE CONSTANT OF REACTION ($M^{-1} s^{-1}$)
Mannitol	100 mM	$^{\cdot}OH$	7	[a]2.7×10^9
Sodium Benzoate	10 mM	$^{\cdot}OH$	3	[a]4.3×10^9
Isopropyl Alcohol	100 mM	$^{\cdot}OH$	7	[a]1.5×10^9
DABCO	10 mM	$^1O_2$	–	[b]2.4×10^7
β–Carotene	50 μM	$^1O_2$	–	[b]1.5×10^{10}
Sodium Azide	20 mM	$^1O_2$	–	[c]$3 \times 10^8 - 1.5 \times 10^9$
Superoxide Dismutase	2550 units ml^{-1}	$O^{\cdot-}_2$	7	[d]2.3×10^9
Catalase	1400 units ml^{-1}	H_2O_2	–	[a]$1.7 - 2.6 \times 10^7$

Table 2.2: Scavengers used in sensitised reactions of NUV. The final concentration of the chemical in solution, the ROS that is selectively quenched and the rate constant of this reaction are listed ([a]Halliwell and Gutteridge, 1999; [b]Kohen *et. al.*, 1995; [c]Fernandez *et. al.*, 1997; [d]Klug *et. al.*, 1972).

2.4 Deoxyribose Assay for $^{\cdot}OH$

2.4.1 Reagents

Deoxyribose, trichloroacetic acid (TCA), ferric chloride, EDTA (dipotassium salt), sodium hydroxide and hydrogen peroxide were purchased from BDH, $FeSO_4$ from Analytical Supplies Ltd., Derby, UK, thiobarbituric acid (TBA) from Aldrich Chemical Co. Ltd., Poole, UK and NADH (enzymatically reduced) from Sigma.

2.4.2 Assay Conditions

The method of Halliwell and Gutteridge (1981) was used with minor modifications. Briefly, to 0.5 ml of TBA (1% w/v in 0.1 N NaOH) and 0.5 ml of TCA (2.8 mg ml^{-1}) was added 0.8 ml samples of a freshly made reaction mixture containing 10 mM deoxyribose, 0.1 mM iron (III)-EDTA, 0.8 mM $FeSO_4$ and 1% (v/v) H_2O_2. Samples were boiled for 15 minutes and A_{532} subsequently read. The complete reaction mixture minus H_2O_2 was used as a blank. When determining the production of $^{\cdot}OH$ by the system under study, $FeSO_4$ and H_2O_2 were replaced by the sensitiser (L-histidine, L(+)mandelic acid, β–phenylpyruvic acid, *p*-OH-phenylpyruvic acid, L-β–phenyllactic acid or NADH at 1 mM final concentration) plus NUV. Irradiation of the mixtures was carried out before adding TBA and TCA. In this case, the complete mixture treated with NUV irradiation but without added sensitiser was used as a blank.

2.5 Growth, Titration and NUV Irradiation of Bacteriophage T7

2.5.1 Growth and Titration of Phage T7

The method of Craggs *et. al.*, (1994) was adopted. High titre phage was prepared by adding a drop of phage lysate (of approximately 10^7 pfu ml^{-1}) to 0.5 ml of an overnight culture of *Escherichia coli* B placed in a sterile glass test tube. The mixture was incubated for 20 min at 37°C to allow for infection. After the designated period, 4 ml soft NA (0.5% w/v agar) were added to the infected *E, coli* culture, and the mixture was overlaid on the surface of a NA plate and allowed to set. On setting, the plate was incubated at 37°C overnight. The following day, the top soft agar layer was removed using a sterilised spatula, placed in a centrifuged tube, and centrifuged at 12,000 g for 10 min. The supernatant, or phage lysate, was collected and titrated as follows. Serial dilutions (10^{-2} – 10^{-6}) of the lysate were performed in 0.05 M K_2HPO_4/KH_2PO_4 buffer, pH7. 0.1 ml of each dilution was mixed with 0.5 ml of *E. coli* B and incubated for 20 min at 37°C. 4 ml of soft NA were added to the infected bacterial culture and the mixture was used to overlay NA plates (this was done in duplicates for each dilution). The plates were incubated at 37°C for 4 hours (or until

clearly visible plaques were formed) and the number of plaques was counted for the determination of pfu ml^{-1}.

2.5.2 Irradiation of Phage T7

Phage suspensions were prepared by adding 0.1 ml of phage T7 lysate (of approximately 10^7 pfu ml^{-1}) to 0.05 M phosphate buffer of appropriate pH. Sensitisers (1 mM) and scavengers (at concentrations given in Table 2.2) or 0.5 mg ml^{-1} BSA (bovine albumin – fraction V powder, 98 %, electrophoresis grade, supplied by Sigma) were added as required. The suspensions (10 ml final volume) were irradiated in uncovered glass Petri dishes (90 mm in diameter) under the NUV lamp. The Petri dishes were rested on ice packs to avoid a rise in temperature in the suspension. Non-irradiated controls were incubated in the dark for time equivalent to the irradiation period. At constant time intervals (5 min), 0.1 ml samples were removed and used undiluted or after performing serial dilutions in phosphate buffer (10^{-2} – 10^{-4}). 0.1 ml of each dilution or the undiluted samples was mixed with 0.5 ml of an overnight culture of *Escherichia coli* B in glass test tubes. The mixtures were incubated at 37°C for 20 minutes. Following that, 4 ml of soft NA (0.5% agar) were added to each tube, and the mixtures were overlaid on the surface of pre-labelled NA plates. On setting, the plates were incubated at 37°C for four hours (or until visible plaques were formed), and the number of plaque forming units (pfu) was determined. The phage T7 survival rates (%) were subsequently calculated by comparison to the control plates at time 0, and the results were plotted against the energy doses applied to obtain kill curves.

2.6 Irradiation of Bacterial Cultures in the Presence of Sensitisers

A 10-ml culture of the bacterial strain of interest was grown by a 1 in 20 inoculation using an overnight culture. The fresh culture was grown by shaking (200 rpm min^{-1}) for 2 hours at 37°C. The bacterial cells were harvested by centrifugation (20 min at 2,000 g) and re-suspended in 10 ml 0.05 M phosphate buffer, pH 7. The suspension was irradiated with appropriate doses of NUV (or UVB alone) in the presence of 1 mM sensitiser when required. Non-irradiated controls were incubated

in the dark for time equivalent to the irradiation period. At appropriate time intervals, 0.1 ml samples were removed and serial dilutions were performed in phosphate buffer. 0.1 ml of the appropriate dilutions was spread on recovery agar plates. After incubation at 37°C for up to 48 hours, colony (viable) counts were performed and the cell survival rates (%) were subsequently calculated by comparison to control plates at time 0. These values were used to plot survival curves against the energy dose applied.

2.7 HPLC for the Determination of Endogenous Concentrations of β–Phenylpyruvic Acid in *E. coli* KL16 and *E. faecalis*

2.7.1 Reagents and Apparatus for HPLC

Benzene, ethyl acetate, hydrochloric acid, methanol, tetrahydrofuran, ammonium chloride, and sodium chloride were purchased from Sigma. 4-hydrazino-2-stilbazole dihydrochloride was purchased from Tokyo Kasei Ind. Co., Tokyo, Japan. Deionised distilled water was used for all experiments. All chemicals were of analytical-reagent grade.

The liquid chromatograph (Beckman Instruments Inc., Berkeley, CA, USA) was fitted with a fluorescence detector (Perkin-Elmer LS-1), and a cut-off filter cutting out light of wavelengths shorter than 430 nm was used. The column was μBondapak Phenyl (particle size 10μm; 300 x 3.9 mm; Waters Assoc. Milford, MA, USA). The column temperature was ambient (25°C). The mobile phase was a mixture of 0.1 M hydrochloric acid, tetrahydrofuran and water (10:24:64, v/v; pH 2), and the flow-rate was 1 ml min^{-1}. After every analysis, the column was washed with aqueous methanol (1:1 v/v) at a flow rate of 1 ml min^{-1} for 10 minutes. All solutions were de-gassed before using.

2.7.2 Extraction of β–Phenylpyruvic Acid from *E. coli* and *E. faecalis* and Derivatisation

100-ml cultures of *E. coli* KL16 and *E. faecalis* were freshly grown by a 1 in 20 inoculation using an overnight culture of each organism. The fresh cultures were grown by shaking (200 rpm min^{-1}) for 2 hours at 37°C, in the presence and absence of 1 mM β–phenylpyruvic acid. The bacterial cells were harvested by centrifugation (10 min at 18,000 g), washed twice in phosphate buffer at pH 7, and the total cell counts were estimated by performing serial dilutions in phosphate buffer and spreading 0.1 ml of appropriate dilutions on recovery agar plates. The suspensions were centrifuged as above, and the bacterial pellets were re-suspended in 1 ml water. The cell suspensions were placed on ice and were sonicated (at 6 microns amplitude, for 3 x 30 sec with 30-sec intervals, using an MSE Soniprep 150). The cell debris was removed by centrifugation (5 min at 11,600 g) using a bench microcentrifuge (MSE MicroCentaur, Sanyo, Sussex, UK).

Following that, the samples were treated as described by the method of Hirata *et. al.* (1981). Briefly, 1 ml of cell extract was transferred in a 10-ml glass centrifuge tube, and 0.2 ml of water followed by 1 ml of a mixture of benzene and ethyl acetate (1:1 v/v) were added to it. The mixture was shaken for 3 min and centrifuged (1 min at 2,000 g). The organic layer was discarded, then the aqueous layer was acidified with 0.15 ml of concentrated hydrochloric acid, to pH 1 or lower, followed by addition of 0.5 g of sodium chloride. The mixture was extracted twice with 1-ml portions of ethyl acetate by shaking and centrifugation as before. The extracts were combined and concentrated to dryness *in vacuo* at room temperature. To the residue, 1 ml of water, 0.5 ml of 0.5 M ammonium chloride solution (pH 4, adjusted with 0.1 m hydrochloric acid) and 0.5 ml of 1.2 mM 4′-hydrazino-2 stilbazole dihydrochloride solution in methanol (freshly prepared) were added. The mixture was warmed at 50°C for 10 min in the dark to develop fluorescence and cooled in ice water. Within 2 hours, a 50-µl aliquot of the reaction mixture was applied to the chromatograph. The amount of β-phenylpyruvic acid was calibrated by replacing the 1-ml sample with 1 ml of a β-phenylpyruvic acid standard solution. The peak area at the retention time of 13 min was used for the quantitation. A standard curve was performed for each experiment by applying the

extraction and derivatisation method to standards of known concentrations of β-phenylpyruvic acid. The specificity of the method was tested by replacing the standard β-phenylpyruvic acid solutions with standard solutions of aromatic compounds similar to β-phenylpyruvic acid (tyrosine, phenylalanine and *p*-OH-phenylpyruvic acid.

2.8 Isolation and Irradiation of pBR322

2.8.1 Buffers and Reagents

Agarose, blue/orange x 6 loading dye, and λDNA pre-digested with Hind III marker were supplied by Promega Corporation, UK. Ethidium bromide and Trizma base (tris[hydroxymethyl]aminomethane, electrophoresis grade) were obtained from Sigma. Glacial acetic acid was supplied by BDH.

TE: 10 mM Tris base, pH 8 (adjusted with HCl), 1 mM EDTA, pH8

TAE (x 50): 242 g Tris base, 57.1 ml glacial acetic acid, 100 ml 0.5 M EDTA, pH 8 in 1 L water.

2.8.2 Isolation of pBR322 DNA

A single colony of *E. coli* JA221 was used to inoculate a starter culture of 10 ml LB medium containing the appropriate selective antibiotics (Section 2.1.2). The culture was incubated overnight at 37°C. 1 ml of the overnight culture was added to 100 ml selective LB medium, and the culture was left to grow at 37°C with shaking (300 rpm) to an A_{600} of 1.5. 20 mg chloramphenicol was then added, and the culture was incubated overnight with shaking at 37°C. The bacterial cells were harvested by centrifugation (6,000 g for 15 min), and plasmid DNA was isolated using a QIAfilter Plasmid Maxi kit (QIAGEN Ltd., UK) as described in the supplied handbook. The DNA that was obtained from the preparation was dissolved in 0.5 ml TE buffer and stored at -20°C.

2.8.3 Irradiation of pBR322 DNA Preparation and Electrophoresis

Samples of total volume of 40 μl were placed in wells of a 96-well plate. Each sample was composed of 25 μl of the DNA preparation (157 μg ml^{-1}) and 15 μl of phosphate buffer (0.05 M final concentration) at pH 7.5. Where required, some of the buffer was replaced with an aliquote of 10 mM solution of β-phenylpyruvic acid, L(+)mandelic acid or L-histidine to give the required final concentration (1 – 8 mM). The plate was placed on ice to avoid evaporation and irradiated with a total energy of 11.88 x 10^4 J m^{-2}. Non-irradiated controls were incubated in the dark.

At 10 min time intervals, 8 μl aliquots (containing 0.8 μg DNA) were removed from each well, mixed with 2μl of loading dye and loaded on an eight-well agarose gel (1% w/v in TAE buffer containing 0.5 μg ml^{-1} ethidium bromide). 5μg of λDNA pre-digested with Hind III marker that was heated at 65°C for 10 min and then placed on ice was included in the gel. Electrophoretic separation of the products (relaxed and supercoiled forms) was performed in 1x TAE buffer containing 0.5 μg ml^{-1} ethidium bromide using a Bio-Rad horizontal mini gel electrophoresis system and with 60 V (200 Bio-Rad power supply) for 1 hour. The fluorescence arising from the UV excitation of the ethidium bromide was detected, and the gels were imaged and quantified using quanti-scan (Qscan) software. Generally, the density of each DNA band was determined, and the resulting peak areas were used to calculate the % open circular DNA. This was done by taking the ratio of open circular to supercoiled plus open circular DNA, then multiplying by 100.

2.9 Transformation of *E. coli mutT*$^+$ and *mutT*$^-$ Strains with pBR322

2.9.1 Preparation of Competent Cells for Transformation

30 ml LB medium were inoculated with 0.5 ml of overnight cultures, grown from single colonies of *E. coli mutT*$^+$ and *mutT*$^-$. The cultures were incubated at 37°C with shaking (200 rpm) for two hours, then placed on ice for 20 min. The cells were recovered by centrifugation (20 min at 1,000 g) and the pellets were re-suspended in 10 ml ice-cold $CaCl_2$ (0.1 M). The suspensions were centrifuged as above, and the

cells were re-suspended in 1 ml ice-cold $CaCl_2$ (0.1 M). The suspensions were left on ice for 1 hour. After that period the cells were competent and ready to be transformed.

2.9.2 Preparation of pBR322 and Transformation

Plasmid DNA was diluted to 5 ng μl^{-1} in phosphate buffer at pH 7. Samples (40 µl) were irradiated in a 96-well plate with a total energy of 11.88×10^4 J m^{-2}. The irradiated 96-well plate was kept on ice to avoid overheating. To appropriate samples, β–phenylpyruvic acid (4 mM final concentration) was added prior to irradiation. Non-irradiated controls with and without β–phenylpyruvic acid were incubated in the dark.

25 ng pBR322 DNA (5 µl of the irradiated DNA suspensions) were added to 0.2 ml of competent cells. The cells were left on ice for 30 min, heat-shocked for 3 min at 42°C and returned to the ice for another 30 min. To the cell suspension, 0.8 ml of LB medium were added and the cells were incubated for 1 hour at 37°C. From each sample, 0.1 ml were spread on recovery plates (LB agar supplemented with 50 µg ml^{-1} streptomycin) and 0.1 ml was spread in duplicate on selective media (LB agar containing 50 µg ml^{-1} ampicillin and/ or 20 µg ml^{-1} tetracycline). After incubation of all the plates at 37°C for 24 hours, the number of transformed colonies was counted. The transformation efficiency of each sample was calculated by dividing the average number of transformed colonies in the duplicate plates with the average number of transformed colonies in the control plates where untreated plasmid was used. The resulting values express the factor of additional transformation efficiency resulting from each treatment over that given by using untreated DNA.

2.10 Assay for β–Galactosidase

The method of Quillardet and Hofnung (1985) was adopted. A 30 ml overnight culture of *E. coli* PQ37 (tester strain) was divided into 5 ml samples. Appropriate samples were treated with NUV alone (11.88×10^4 J m^{-2}) or in the presence of 1 mM sensitiser. 10 ml LB medium was added to each sample followed

by incubation at 37°C for one hour to allow for protein synthesis. The cultures were centrifuged (2,000 g for 20 min) and the pellets re-suspended in 10 ml phosphate buffer at pH 7. A few drops of toluene (Sigma) were added to each culture with shaking. Three minutes later, the β–galactosidase assay was initiated by the addition of 1 ml of 12 mg ml^{-1} *o*-nitrophenyl-β-D-galactopyranoside (ONPG) (Sigma). The reaction was terminated 5 minutes later by addition of 2 ml Na_2CO_3 (1 M). The cell debris was removed by centrifugation (2 min at 11,600 g), and the absorbance at 420 nm was determined using phosphate buffer as the blank. *E. coli* SA191 that is constitutive for β–galactosidase was used as a positive control. The positive control (6 ml overnight culture), was given the same treatment as the *E. coli* PQ37 samples, including incubation in fresh media, centrifugation and re-suspension in phosphate buffer prior assaying.

2.11 Mutagenesis and Rifampicin Resistance in *E. coli*

30-ml cultures of *E. coli* KL16 or *E. coli mutT*⁻ were grown by a 1 in 20 inoculation using overnight cultures. The fresh cultures were grown with shaking (200 rpm) for 2 hours at 37°C. The bacterial cells were harvested by centrifugation (12,000 g for 10 min) and re-suspended in 10 ml phosphate buffer of the required pH. The appropriate suspensions were irradiated with suitable doses of NUV in the presence of 1 mM sensitiser when required. All cell suspensions were centrifuged as above and the pellets re-suspended in 1 ml phosphate buffer of appropriate pH. From each sample, 0.1 ml were removed and diluted in phosphate buffer. 0.1 ml of each dilution was spread on recovery agar plates for the determination of total counts. The plates were incubated at 37°C for up to 48 hours, and the number of cfu was counted. From the remaining samples, 0.1 ml were spread on each of six NA plates, containging100 μg ml^{-1} rifampicin. The plates were incubated at 37°C for up to 48 hours, after which the number of resistant colonies was counted. The frequency of mutation was calculated by dividing the total cell population (cfu) with the number of mutant colonies. The factor of increase in mutation frequency was calculated by dividing the mutation frequency values of treated samples with the values of the spontaneous mutation frequency of the control.

2.12 Assay for the Detection of Lipid Hydroperoxide

2.12.1 Preparation of Bacterial Samples

10-ml cultures of *E. coli* KL16 and *E. faecalis* were grown by a 1 in 20 inoculation using an overnight culture of each organism. The fresh cultures were grown by shaking (200 rpm) for 2 hours at 37°C. The total cell counts were estimated by removing 0.1 ml from each culture, performing serial dilutions in phosphate buffer and spreading 0.1 ml of each dilution on appropriate recovery agar plates (section 2.1.2). The bacterial cells were then harvested by centrifugation (20 min at 2,000 g), and the pellets were re-suspended in 1 ml phosphate buffer, pH 7. The suspensions were irradiated with NUV (11.88×10^4 J m^{-2}) in the presence or absence of 1 mM β-phenylpyruvic acid followed by sonication (at 6 microns amplitude for 3 x 30 sec with 30-sec intervals using an MSE Soniprep 150) on ice.

2.12.2 Extraction and Assay of Lipid Hydroperoxide

The lipid hydroperoxide was extracted from the sonicated samples into chloroform by the method described in the Lipid Hydroperoxide Assay Kit supplied by Cayman Chemical company, MI, USA. This extraction included a deproteination step and ensured the elimination of nearly all the interfering substances from the samples. The assay performed by this kit measured the hydroperoxides that directly utilise the redox reactions with ferrous ions. The resulting ferric ions were detected spectrophotometrically using thiocyanate ion as the chromogen and measuring absorbance at 500 nm. Quantitative determination of the amount of lipid hydroperoxide present in each sample was achieved by including in the assay a series of standard dilutions of the lipid hydroperoxide solution provided to obtain a standard curve.

2.12.3 Measurement of Lipid Hydroperoxide from Irradiated Liposomes

Positively charged liposome (supplied by Sigma) that contained 63 μmoles L-α-phosphatidylcholine (egg yolk), 18 μmoles stearylamine and 9 μmoles cholesterol

was dissolved in 5 ml ethanol. 0.1 ml of this suspension (1.8 μmoles liposome) was added to 0.9 ml of phosphate buffer, pH 7. The suspensions were irradiated with NUV (11.88 x 10^4 J m^{-2}) in the presence of 1 mM β-phenylpyruvic acid or 1 mM NADH when appropriate, and lipid hydroperoxides were extracted and assayed as described in 2.12.2. Untreated samples and samples incubated in the dark with added β-phenylpyruvic acid were used as controls. Mannitol (100 mM) and isopropyl alcohol (ISPA, 100 mM) were also included in addition to β-phenylpyruvic acid and NUV as required.

2.13 Western Blotting for Detection of Oxidatively Modified Proteins

2.13.1 Buffers and Reagents

Reagents were prepared in distilled water, unless stated otherwise. 2-mercaptoethanol, 2,4-dinitrophenylhydrazine, trifluoroacetic acid, glycine, sodium dodecylsulphate (SDS, electrophoresis grade), dimethyl formamide (DMF), 30% acrylamide: bisacrylamide, TEMED, ammonium persulfate, deoxycholic acid (sodium salt), bicinchoninic acid (4,4′-dicarboxy-2,2′-biquinoline, disodium), BSA (bovine albumin – fraction V powder, 98 %, electrophoresis grade), SDS-PAGE markers (30 – 200 kDa) and the monoclonal Anti-Dinitrophenyl – IgE (alkaline phosphatase conjugate) antibody were purchased from Sigma. Sucrose was obtained from Fisher Scientific, and glycerol from BDH.

Sample treatment buffer: 0.75% Tris base, 5% (v/v) 2-mercaptoethanol, 5% sucrose from a 10% stock solution, pH adjusted to 6.8 using concentrated HCl, stored at 4°C.

BSA standard working reagent: This was prepared by the addition of 50 parts reagent A to 1 part reagent B and stored at room temperature.

Reagent A: 1% (w/v) bicinchoninic acid (sodium salt), 2% (w/v) sodium carbonate, 0.16% (w/v) sodium hydroxide, 0.9% (w/v) sodium hydrogen carbonate, pH 11.25.

Reagent B: 4% (w/v) copper sulphate.

Upper gel: 3.5 ml distilled water, 5 ml stacking gel buffer, 1.5 ml acrylamide, 20µl TEMED, 0.5 ammonium persulfate.

Lower gel: 0.85 ml distilled water, 8.75 ml separating gel buffer, 7 ml acrylamide, 25 µl TEMED, 0.875 ammonium persulfate.

Stacking gel buffer (double strength): 0.25 M Tris-HCl, pH 6.8, 0.02% w/v SDS, stored at room temperature.

Separating gel buffer (double strength): 0.75 M Tris-HCl, pH 8.8, 0.2% w/v SDS, stored at room temperature.

Electrode buffer: 0.025 M Tris base, 0.192 M glycine, 0.1 % w/v SDS, pH 8.3 adjusted with concentrated HCl, stored at room temperature.

Coomassie staining solution: 25% v/v ethanol, 10% v/v acetic acid, 0.02% w/v coomassie blue R-250, stored at room temperature.

Destaining solution: 10% v/v methanol, 10% v/v acetic acid, stored at room temperature.

Electroblotting buffer: 20 mM Tris base/150 mM glysine, pH 8 adjusted with concentrated HCl, stored at room temperature.

TBS (x 10): 50 mM Tris base/200 mM NaCl, pH 7.4 adjusted with concentrated HCl, stored at room temperature.

TBS/Tween: 1 ml Tween 20 per litre of TBS (x 1).

Substrate buffer: 0.75 M Tris base, pH 9.5, stored at 4°C.

2.13.2 Preparation of Whole-Cell Bacterial Protein Extracts

50 ml NB media were inoculated (1 in 10) using an overnight culture of *E. coli* KL16. The culture was grown at 37°C with shaking (200 rpm) for three hours. The culture was aliquot and the cells were harvested by centrifugation at 18,000 g for 10 minutes. The cell pellets were washed in 10 ml phosphate buffer, pH7 and the cells were re-centrifuged (18,000 g for 10 min). Each pellet was then weighed in an eppendorf tube. Sample treatment buffer (1.8 ml per 100 mg of wet weight of cells) was added to each sample followed by vortex mixing. 20% SDS (0.2 ml per 100 mg of wet weight of cells) was added to the mixture and vortex mixed. The samples were heated at 90°C for 10 minutes, cooled and centrifuged at 11,600 g for 5 minutes in a microcentrifuge. The supernatant that contained the protein extract was divided into

aliquots (0.5 ml). Some of the aliquots were placed in a six-well plate and treated with NUV alone (11.88×10^4 J m^{-2}) or in the presence of 1 mM β-phenylpyruvic acid. After irradiation, the protein concentrations of each of these samples and of aliquots used as non-irradiated controls were estimated as described in section 2.13.3, and the samples were stored at –20°C.

2.13.3 Bicinhoninic Acid Protein Assay

Bacterial protein extracts were assayed along a range of 0 – 1 mg ml^{-1} BSA standard protein solutions by diluting 20 µl of protein sample to 1 ml with distilled water in an eppendorf tube. 150 µl of 0.1% (w/v) sodium deoxycholate was added to each tube. Following a 5 minute incubation at room temperature, protein was precipitated by the addition of 144 µl of 50% (w/v) TCA and each tube was thoroughly vortex mixed. Tubes were centrifuged (11,600 g for 15 min) and the supernatant was removed. The pellets were washed in 1 ml distilled water, 150 µl deoxicholate and 72 µl TCA, vortex mixed and centrifuged (11,600 g for 15 min). Protein was re-dissolved in 50 µl of 0.1 M sodium hydroxide containing 5% (w/v) SDS. Following the addition of 1 ml BSA standard working reagent, each tube was thoroughly mixed and incubated at 60°C for 30 minutes. The absorbance of the samples was read at 562 nm and the values for the BSA samples were used to prepare a standard curve that was then used for the estimation of the protein concentration of the cell extracts.

2.13.4 Sample Derivatization

The method of Levine *et. al.* (1994) was adopted. This method is based on the reaction of the carbonyl groups with 2,4-dinitrophenylhydrazine. To a known volume of protein extract, an equal volume of 12% SDS was added with mixing, followed by addition of two volumes of 2,4-dinitrophenylhydrazine solution (20 mM 2,4-dinitrophenylhydrazine in 10% (v/v) trifluoroacetic acid). After mixing, the samples were allowed to stand for 30 minutes at room temperature. The mixtures were neutralised by adding 1.5 sample volumes of 2 M Tris base/ 30% glycerol. The neutralised solution turns from yellow to orange.

2.13.5 SDS-Polyacrylamide Gel Electrophoresis, Electroblotting and Immunostaining

Samples containing 10 μg of protein (either BSA or *E. coli* protein extracts) were applied to two 12% acrylamide gels. The gels were run for 45 minutes at 50 V (PowerPack 300, BioRad, UK) in electrode buffer.

After electrophoresis, one gel was stained with Coomassie blue, and the other that contained pre-stained molecular weight markers was incubated in electroblotting buffer for 20 minutes. After that time, the gel was placed on top of a nitrocellulose membrane, and between 18 sheets of chromatography paper (3 MM Chr chromatography paper, Watman International, Ltd., UK) all cut to the size of the gel and pre-soaked in electroblotting buffer. The 'sandwich' was placed between the graphite electrode plates of a transfer unit (Trans-Blot SD semi-dry transfer cell, BioRad, UK), where 150 mA constant current was applied for one hour (200/2.0 PowerPack, BioRad, UK). After electroblotting, the membrane was incubated twice in 40 ml TBS containing 3% w/v BSA for 20 minutes with shaking at room temperature. The membrane was transferred in fresh TBS containing 3% BSA and 8 μl monoclonal Anti-Dinitrophenyl – IgE (alkaline phosphatase conjugate) antibody solution (1:5000 dilution) and was incubated overnight at 4°C with shaking. Following that, the membrane was washed three times in TBS/Tween 20 for 20 minutes with shaking, rinsed in distilled water and developed in 20 ml substrate buffer containing 33 μl BCPI (50 mg ml^{-1} in DMF) and 44 μl NBT (75 mg ml^{-1} in DMF). Overdeveloping was prevented by replacing the substrate buffer with distilled water. The membrane was then allowed to dry and stored in the dark.

CHAPTER THREE

SENSITISATION REACTIONS AND PRODUCTION OF ROS IN SOLUTION

3.1 Introduction

Numerous studies support the hypothesis for the involvement of endogenous sensitiser molecules in the induction of oxidative stress (Carbonare and Pathak, 1992; Cunningham *et. al.*, 1985; Ley, 1997; Ortwerth and Olesen 1994). Compounds including the aromatic amino acids phenylalanine, tryptophan and tyrosine have been shown to produce a variety of ROS on NUV photolysis (Craggs *et. al.*, 1994; Kohen *et. al.*, 1995; Ortwerth and Olesen, 1994). These ROS, in turn, cause a variety of cellular changes including damage to DNA and protein, and lipid peroxidation.

The reaction mechanisms of the UV photolysis of phenylalanine, tryptophan and tyrosine are quite complex and have not been worked out in detail. In general, UV exposure of aqueous phenylalanine leads to absorption by the benzyl radical ($C_6H_5CH_2^{\cdot}$). Photolysis of aqueous tryptophan is attributed to the absorption of the indole ring (Figure 3.1), whereas photolysis of tryrosine involves the disruption of the phenolic OH bond (Figure 3.2) that gives a phenoxyl-type aromatic free radical (Smith, 1989). The stable reaction products reported from the UV photolysis of tryptophan include among others N-formylkynurenine. This oxidation product of tryptophan can act as a photosensitiser of longer wavelength UVA radiation (Kohen *et. al.*, 1995; Smith, 1989) and has been implicated in the ageing of the ocular lens (Ortwerth and Olesen, 1994). Photolysis of tyrosine (which is also known to be produced on UV photolysis of phenylalanine) gives among other products, dihydroxyphenylalanine (DOPA) the precursor of melanin (Gieseg *et. al.*, 1993; Smith, 1989).

Based on the biological importance of the photolysis of phenylalanine, tyrosine and tryptophan, a number of organic compounds, that have either a similar structure or are part of the metabolic pathway of these amino acids in humans, were screened as potential photosensitisers. Thus, L-histidine (Paretzoglou, *et. al.*, 1998), L(+)mandelic acid, β–phenylpyruvic acid, *p*-OH-phenylpyruvic acid and L-

β–phenyllactic acid (Figures 3.1 and 3.2) were selected for this study. On NUV photolysis, these compounds are proposed to react with molecular oxygen in aqueous solution to generate H_2O_2, $^{\cdot}OH$, $O_2^{\cdot-}$ / $HO^{\cdot}$, and $^1O_2$.

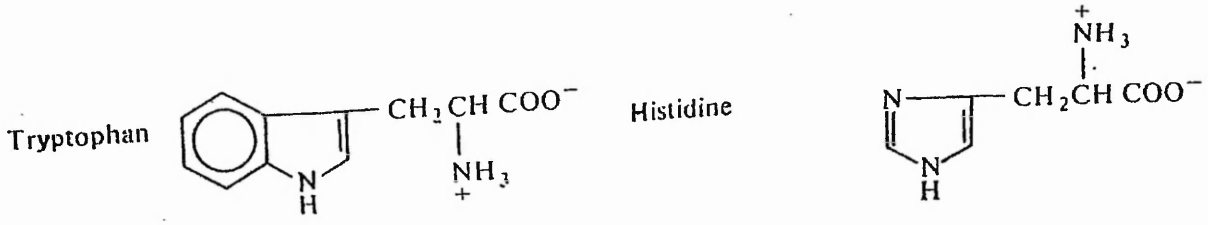

Figure 3.1: The structure of the amino acids tryptophan and histidine.

L-histidine, L(+)mandelic acid, β–phenylpyruvic acid, *p*-OH-phenylpyruvic acid and L-β–phenyllactic acid are ubiquitous components of living organisms. L-histidine is a major building block of most proteins and is frequently found within the active sites of enzymes. This amino acid contains an indole ring within its side chain, as does tryptophan (Figure 3.1). The latter has been shown to be reactive to NUV exposure and produce $O_2^{\cdot-}$ *via* H_2O_2 (Ahmad, 1981; Craggs *et. al.*, 1994). It is likely that L-histidine may be photolysed in a similar way.

The current study is also of interest because β–phenylpyruvic acid, *p*-OH-phenylpyruvic acid, L-β–phenyllactic acid and to a lesser extent L(+)mandelic acid occur in humans as metabolites of phenylalanine and have been identified as regular excretion products in uncontrolled phenylketonuria (Figure 3.2) (Blau, 1970; Chalmers and Lawson, 1982; Hill *et. al.*, 1972). According to the later study, the observed ranges for β–phenylpyruvic acid, L-β–phenyllactic acid and L(+)mandelic acid for untreated patients were 226 –1910 mg g^{-1}, 164 – 1965 mg g^{-1} and 15 – 71 mg g^{-1} creatine respectively. During normal metabolism, phenylalanine is converted to tyrosine and then *p*-OH-phenylpyruvic acid. When this metabolic pathway is blocked, as in the case of phenylketonuria, an alternative pathway takes place (Figure 3.2).

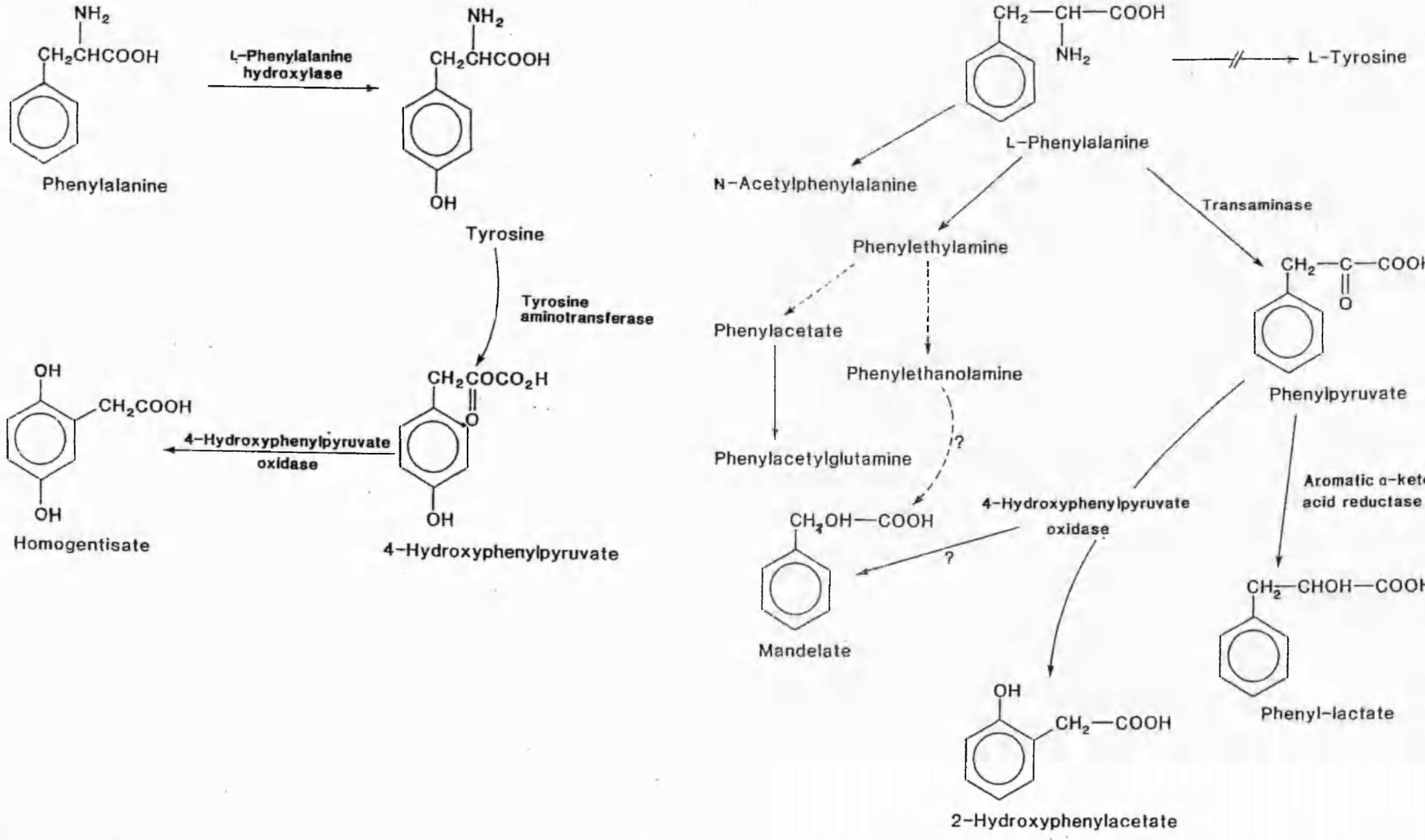

Figure 3.2: Metabolism of L-phenylalanine in normal individuals (left) and those suffering from phenylketonuria (right) where the activity of phenylalanine hydroxylase is absent (modified from Chalmers and Lawson, 1982).

In normal individuals, OH-phenylpyruvic acid is a product of tyrosine metabolism and a metabolite of 3,4-dihydroxy-phenylalanine (DOPA), a precursor of melanin. Phenylpyruvic acid is also a metabolite of phenylalanine and plays an important role in catabolic reactions of endogenous amino acids in the cell. Studies showed phenylpyruvic acid to be located on the cell membrane of rat hepatocytes and from there to participate in the intracellular protein degradation (Kadowaki *et. al.*, 1992). The role of phenylpyruvic acid in proteolysis is to increase transamination reactions by triggering the release of insulin (Malaisse *et. al.*, 1983). Although all these studies were performed in rats, a similar situation is believed to occur in human cells. Also, even though liver cells are expected to have higher concentrations of this compound than the cells of the skin, the presence of phenylpyruvic acid in skin may contribute to the hazardous effects of UVR. In addition, both β–phenylpyruvic acid and *p*-OH-phenylpyruvic acid are normal brain constituents (Chalmers and Lawson, 1982). L(+)mandelic acid is produced and excreted in trace amounts in urine (1-15 μM) but elevated amounts are found after exposure to styrene or ingestion of urinary antibacterial drugs (e.g. methenamine mandelate) of which L(+)mandelic acid is often a major component (Chalmers and Lawson, 1982; Roesel *et. al.*, 1980).

3.2 Aims

This chapter will focus on the chemistry of the compounds proposed as sensitisers in this study. Their absorption spectra will be determined, with an interest in their ability to absorb UVA and UVB radiation. A comparison of the absorption pattern of each compound will lead towards the identification of possible functional groups that may participate in photodynamic reactions. Following this, the use of two chemical assays will provide information on the ability of these compounds to undergo photolysis and generate ROS. Thus, the reduction of nitro-blue tetrazolium by $O_2^{\cdot -}$ (Figure 3.5) will be used as evidence for the production of this ROS, and the reactivity of deoxyribose with $^{\cdot}OH$ will be used for the determination of the later. The photosensitised potential of these compounds will, subsequently, be compared to that of NADH, an established endogenous chromophore (Burchuladze and Fraikin, 1991; Cunningham *et. al.*, 1985). The addition of enzymatic and non-enzymatic scavengers that are known to have high affinity for certain ROS will help to confirm the

generation of these and other ROS that may be formed as intermediate species. The use of such scavenging systems may also prove useful in the quantitative determination of some of these ROS. Finally, varying the pH of the solution will help to investigate the pH dependence of ROS formation.

Following this, the action spectra of the compounds that exhibit the highest photosensitising potential will be determined and compared to their absorption spectra. Such a comparison will lead to the better evaluation of the ptotosensitising properties of these biochemicals. Finally, an attempt will be made to identify from these studies the possible mechanisms of photolysis of these compounds and ROS generation.

3.3 UV Absorption Spectra of L-Histidine, L(+)Mandelic Acid, β–Phenylpyruvic Acid, *p*-OH-Phenylpyruvic Acid and L-β–Phenyllactic Acid

Chemical reactions on NUV photolysis of any sensitiser molecule depend on the absorption spectrum of the molecule. In Figure 3.3, the absorption spectra of L-histidine, L(+)mandelic acid, β–phenylpyruvic acid, *p*-OH-phenylpyruvic acid and L-β–phenyllactic acid (as measured by a Beckman DU-7 spectrophotometer, Beckman, USA) are shown. The scans were performed for 10 mM solution of the sensitiser in phosphate buffer at pH 7, 8, and 9 using the appropriate pH buffer as the background. Changing the pH did not affect the absorption spectra.

It can be seen from Figure 3.3 that all five compounds show some absorption in the UVB region. The aromatic ring, which is a common feature in the five compounds, may be responsible for the peak observed at 260 nm (March, 1985).

From the literature, the absorption maximum for histidine is 211 nm (Smith, 1989). The peak for L-histidine is quite flat between 260 – 400 nm, with increased absorption at 260 nm. The sensitiser absorbs light mostly in the UVB region, but there is some absorption in the UVA region. As can be seen from Figure 3.1 and Figure 3.3 (a), L-histidine possesses an entirely different structure and profile from the other sensitisers. In this case there is some low residual absorbance in the region

of interest, which could possibly be ascribed to n-π* transitions associated with the nitrogen moieties (Figure 3.4). However, histidine has been reported to undergo decomposition by UV radiation in this spectral region, and form products that can photolyse further. Such reactions may be initiated by the weak light absorption in the long-wavelength tail of the amino acid spectra (Smith, 1989).

The absorption spectra of L(+)mandelic acid and L-β–phenyllactic acid are quite similar, reflecting the similarity between their structures (Figure 3.2). They absorb light mostly between 260 – 280 nm with a sharp drop after 280 nm.

Compared to L(+)mandelic acid [Figure 3.3 (b)] and L-β–phenyllactic acid [Figure 3.3 (e)], β–phenylpyruvic acid [Figure 3.3 (c)] and *p*-OH-phenylpyruvic acid [Figure 3.3 (d)] have a broader absorption spectrum. In the case of β–phenylpyruvic acid, a solder originates at 390 nm and after a plateau at around 330 nm and one at 285 nm, there is a pick at 260 nm. A solder for *p*-OH-phenylpyruvic acid originates at around 385 nm and peaks at 280 nm. The similarity in the absorption spectra of these compounds corresponds to their similar structures (Figure 3.2). Both compounds have a ketone carbonyl group in their structure, which seems to be the key feature absorbing in the NUV region. L(+)mandelic acid and L-β–phenyllactic acid that do not contain this type of carbonyl group are inactive in this region of the spectrum. In fact, the L-β–phenyllactic acid molecule is very similar to that of β–phenylpyruvic acid with the only difference being that in the latter case there is a ketonic carbonyl group *β* to the carboxylic acid group as opposed to an alcohol, and it can therefore be considered a partially hyrdogenated derivative of β–phenylpyruvic acid. Comparison of their spectra clearly demonstrates the above suggestion of the importance of the ketone group.

In the literature, the n-π* spectral transitions which would be expected for the C=O functionality have been reported to be relatively weak and to occur in the region of interest to this study (Banwell, 1983). Although there are other functional groups in the sensitisers which are expected to absorb UV light, such as the aromatic rings, in general the types of transition involved occur at higher energies than those applied in this study (e.g. the $\pi - \pi^*$ transitions of the aromatic ring have been reported to occur

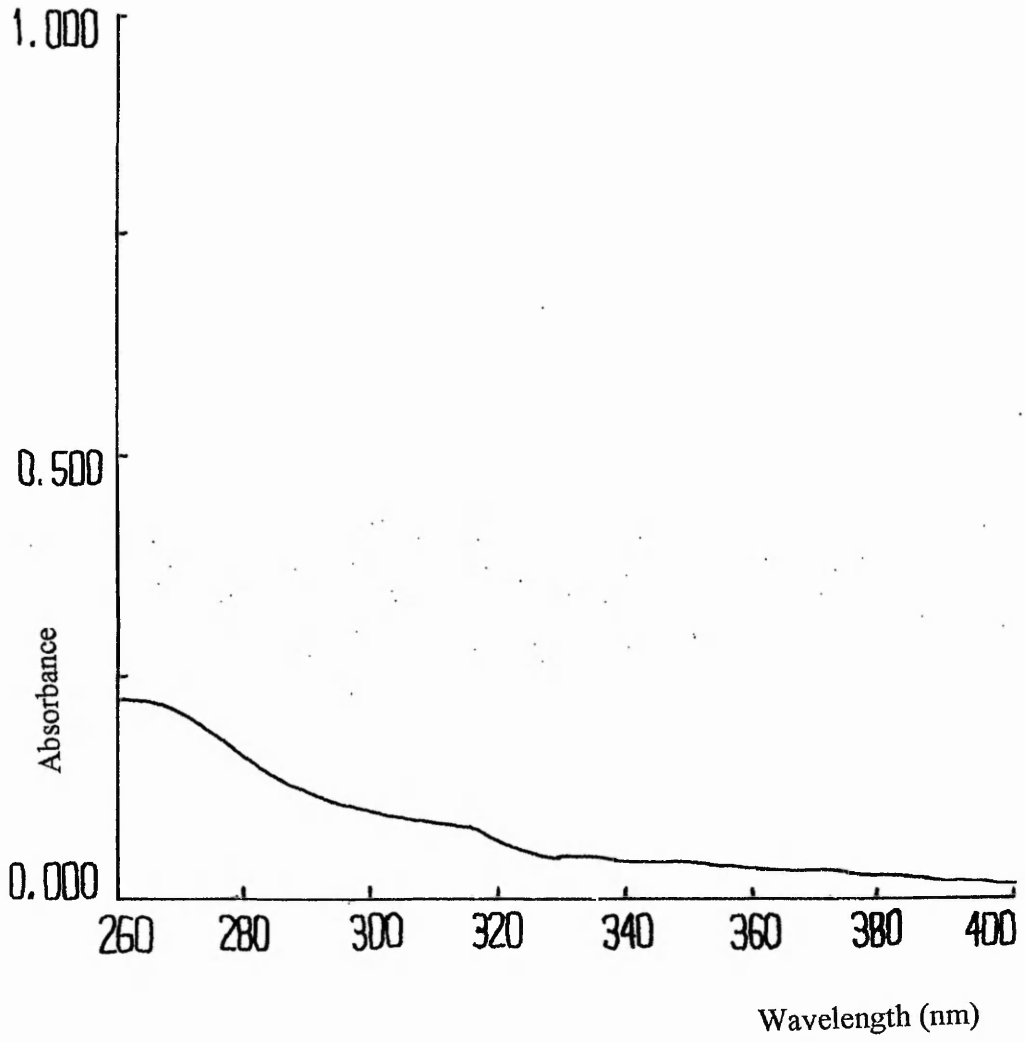

Figure 3.3 (a): Absorption spectrum of a 10 mM aqueous solution of L-histidine in phosphate buffer, pH 7.

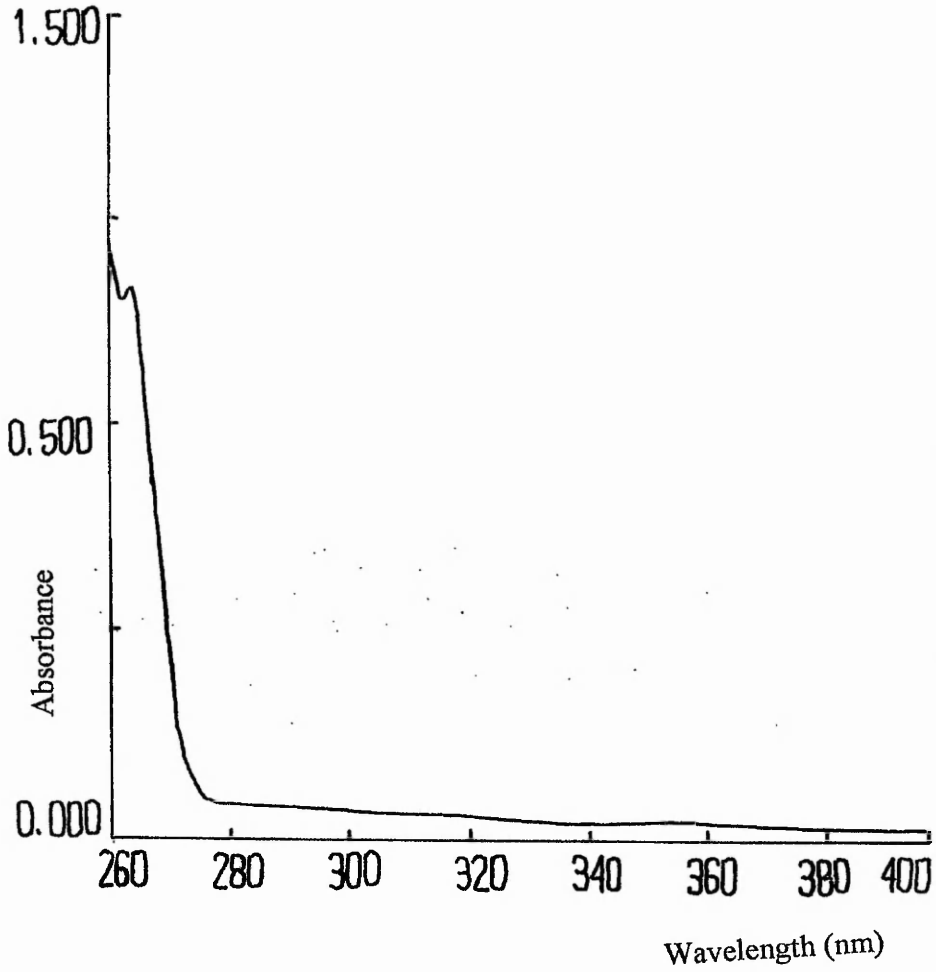

Figure 3.3 (b): Absorption spectrum of a 10 mM aqueous solution of L(+)mandelic acid in phosphate buffer, pH 7.

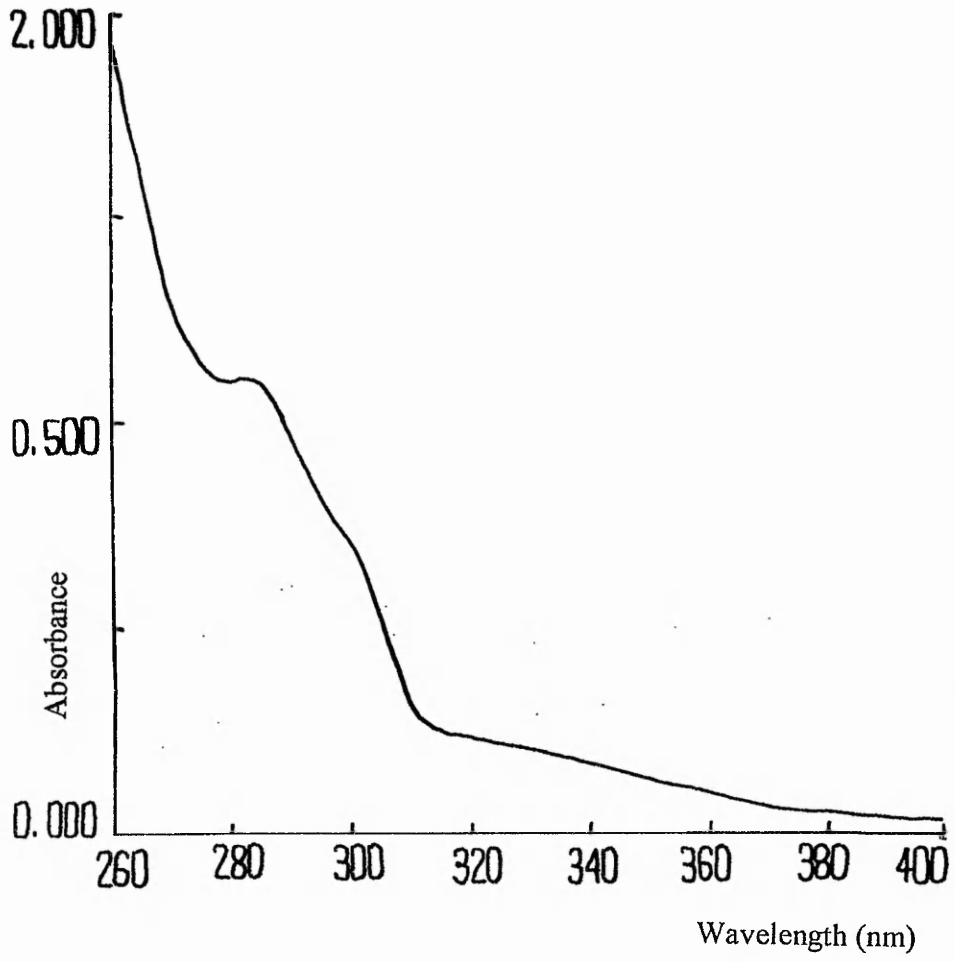

Figure 3.3 (c): Absorption spectrum of a 10mM aqueous solution of β–phenylpyruvic acid in phosphate buffer, pH 7.

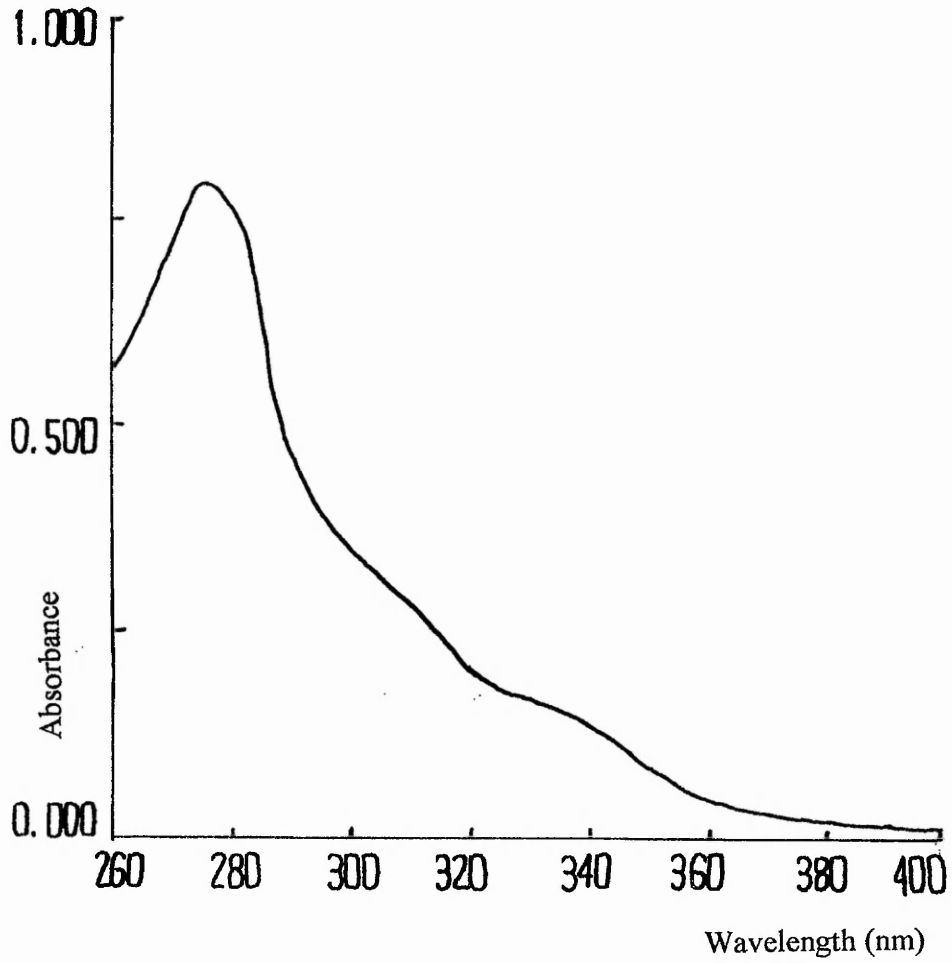

Figure 3.3 (d): Absorption spectrum of a 10 mM aqueous solution of *p*-OH-phenylpyruvic acid in phosphate buffer, pH 7.

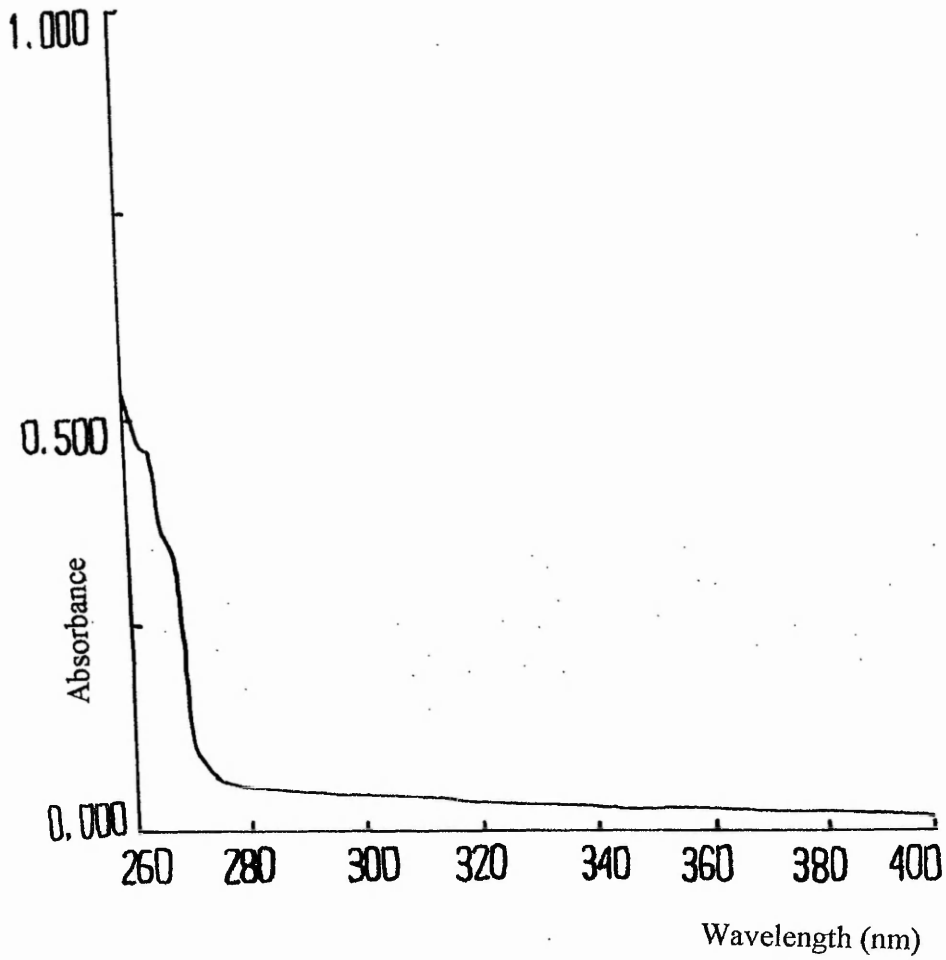

Figure 3.3 (e): Absorption spectrum of a 10 mM aqueous solution of L-β–phenyllactic acid in phosphate buffer, pH 7.

in the region 180 – 220 nm and are, of course, dependent upon the presence / nature of substituents) (Figure 3.4). The lack of influence of pH on the spectra is not surprising, since the functional groups of interest are not expected to be protonated / deprotonated under these conditions.

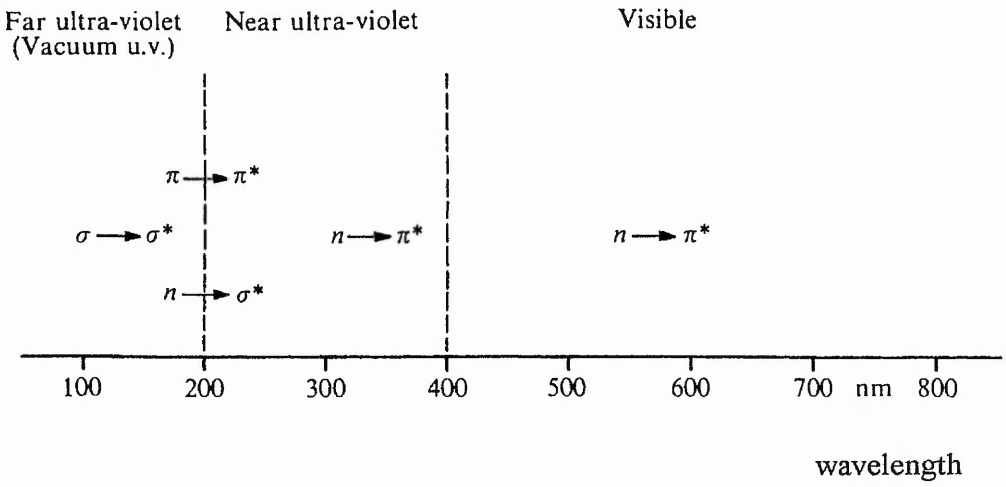

Figure 3.4: The regions of the electronic spectrum and the type of transition which occurs in each (Banwell, 1983).

3.4 NBT Assay

The reduction of the yellow dye nitro-blue tetrazolium (NBT) to formazan blue has been used in the past as a means of detection for the generation of $O_2^{\cdot-}$ in solution (Carbonare and Pathak, 1992; Menon *et. al.*, 1992). $O_2^{\cdot-}$ reacts with NBT with a rate constant of 6 x 10^4 M^{-1} s^{-1} at pH 7-11 (Figure 3.5). In order to probe the possible production of $O_2^{\cdot-}$ by photolysis, NBT reduction was conducted with the various sensitisers at different pH values as detailed in section 2.3.2.

The NUV photolysis of L-histidine, L(+)mandelic acid, β–phenylpyruvic acid, *p*-OH-phenylpyruvic acid and L-β–phenyllactic acid apparently resulted in generation of blue colour as an indicator of $O_2^{\cdot-}$. The reduction of NBT and subsequent formation of blue colour was estimated by measuring the absorbance at 560 nm as described in the literature (Halliwell and Gutteridge, 1999; Menon *et. al.*, 1992).

Irradiation of the NBT mixture without sensitiser, or incubation of NBT with sensitiser but without NUV, showed no increase in A_{560}, confirming that the generation of NBT reducing species occurs only when these compounds are photolysed by NUV light (Figure 3.6). The lack of reactivity of all the sensitisers in the absence of NUV also indicates that there is no contribution of the pure compound to the A_{560}, i.e. that the compounds themselves do not behave as reductants.

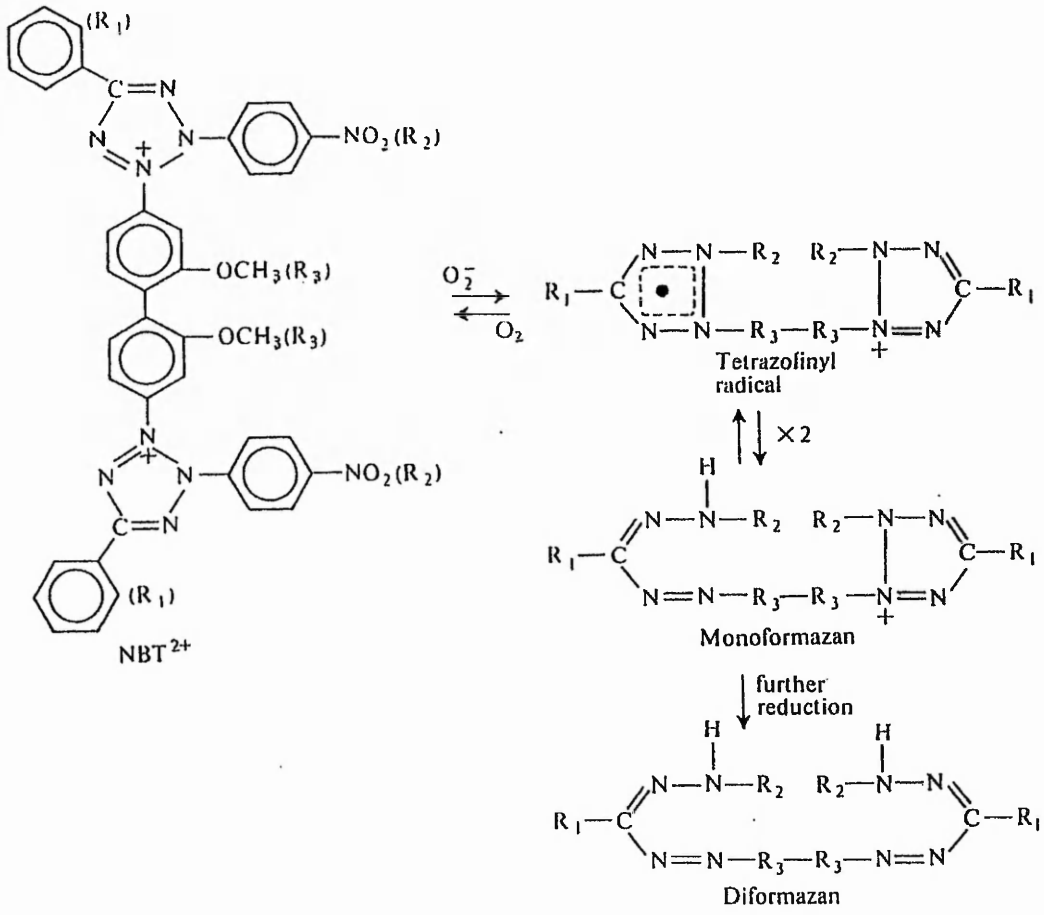

Figure 3.5: Reduction of NBT^{2+} by $O_2^{\cdot-}$ (Halliwell and Gutteridge, 1999).

It can be seen from Figure 3.6 that all the sensitisers react with NBT to different extents. L(+)mandelic acid [Figure 3.6 (b)] seems to be the most reactive of the compounds (maximum A_{560} of 0.21), followed by β–phenylpyruvic acid (A_{560} = 0.17) [Figure 3.6 (d)] and *p*-OH-phenylpyruvic acid (A_{560} = 0.16) [Figure 3.6 (c)]. At the same energy dose, L-histidine [Figure 3.6 (a)] has a smaller effect in the NBT reaction (A_{560} = 0.14) and L-β–phenyllactic acid is almost non-reactive (A_{560} = 0.06)

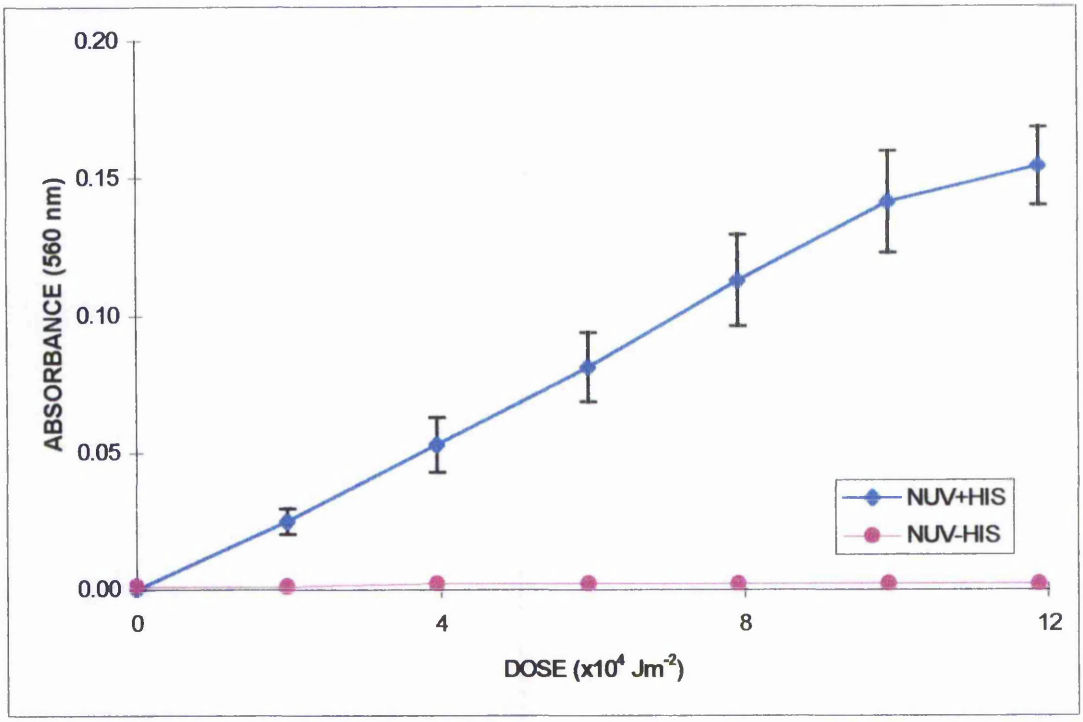

Figure 3.6 (a): The effect of L-histidine and NUV on the NBT reaction. 1 mM L-histidine solution in phosphate buffer, pH 9, was irradiated with varying doses of NUV (◆). The points represent the mean ± the standard error of the mean of 10 observations. (●) represent irradiation of the NBT reaction mixture without the sensitiser.

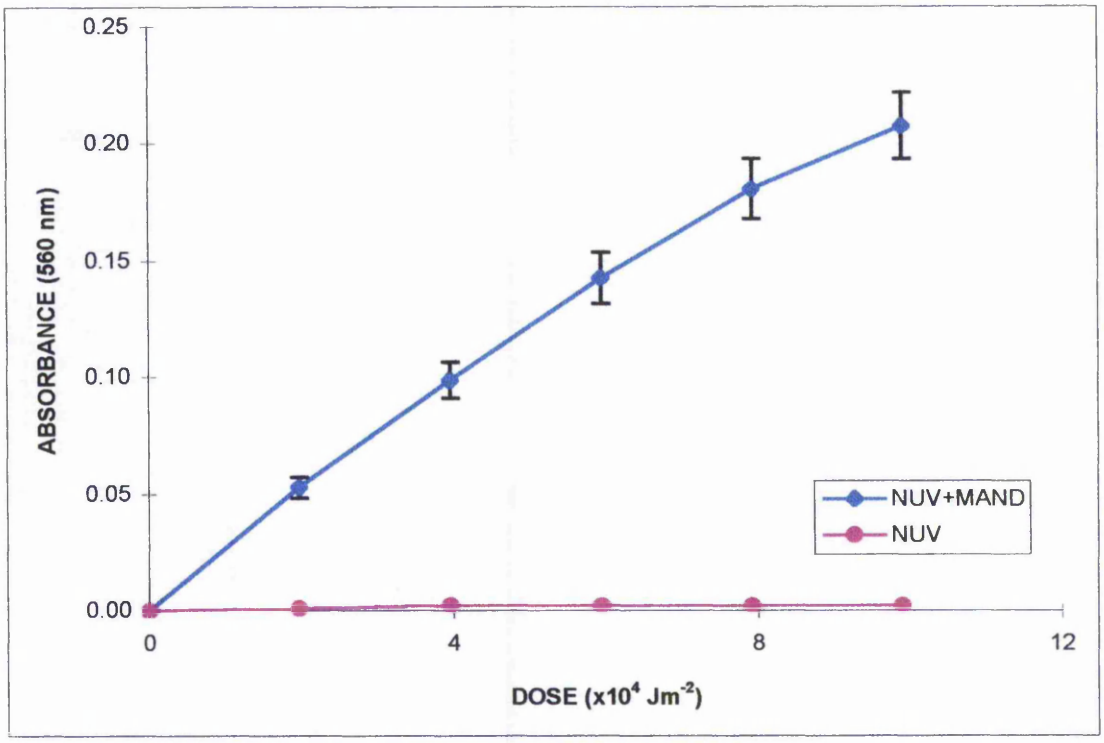

Figure 3.6 (b): The effect of L(+)mandelic acid and NUV on the NBT reaction. 1 mM L(+)mandelic acid solution in phosphate buffer, pH 9, was irradiated with varying doses of NUV (◆). The points represent the mean ± the standard error of the mean of 10 observations. (●) represent irradiation of the NBT reaction mixture without the sensitizer.

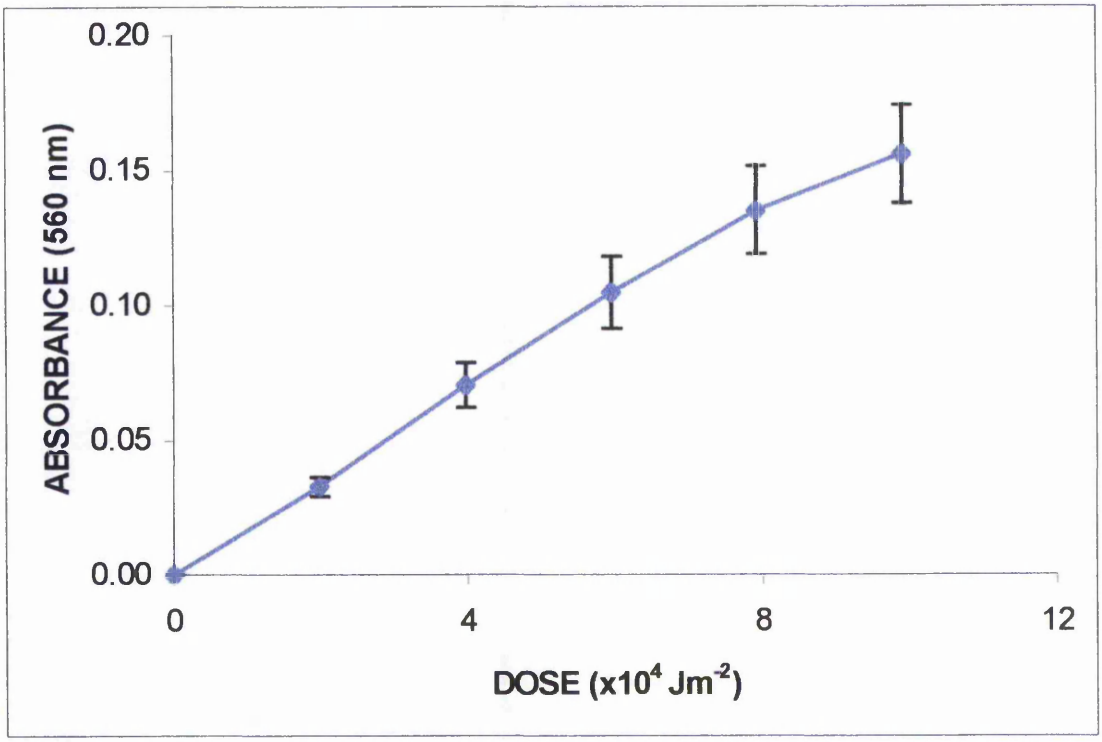

Figure 3.6 (c): The effect of *p*-OH-phenylpyruvic acid and NUV on the NBT reaction. 1 mM *p*-OH-phenylpyruvic acid solution in phosphate buffer, pH 9, was irradiated with varying doses of NUV (◆). The points represent the mean ± the standard error of the mean of 8 observations.

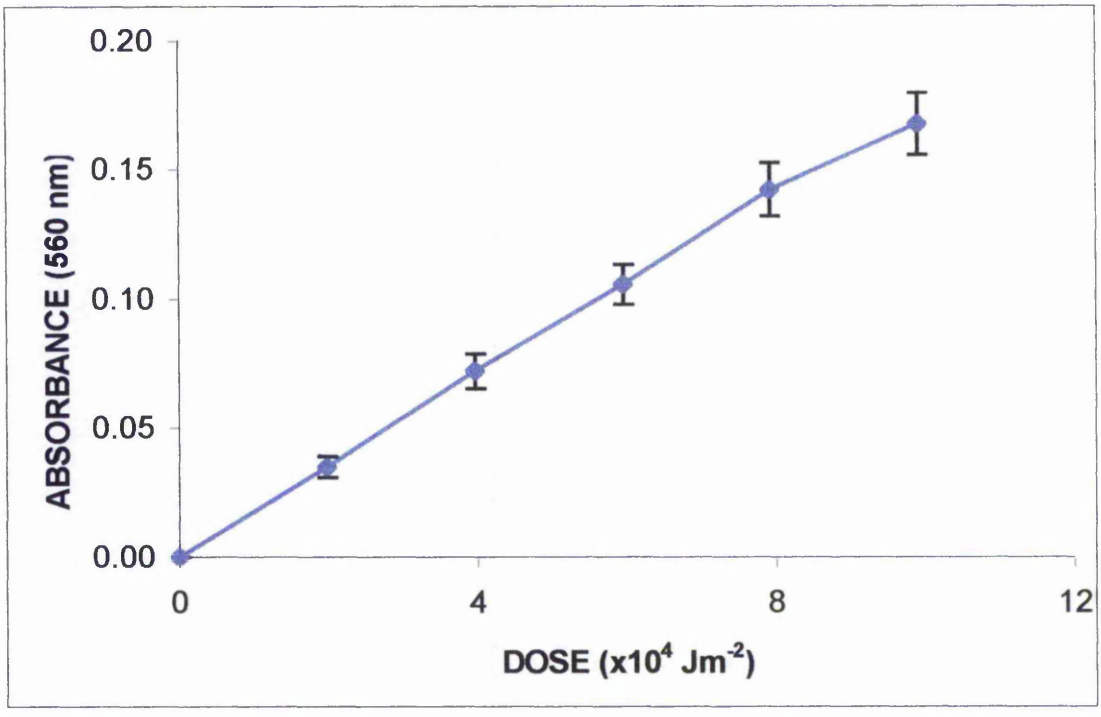

Figure 3.6 (d): The effect of β–phenylpyruvic acid and NUV on the NBT reaction. 1 mM β–phenylpyruvic acid solution in phosphate buffer, pH 7, was irradiated with varying doses of NUV (◆). The points represent the mean ± the standard error of the mean of 8 observations.

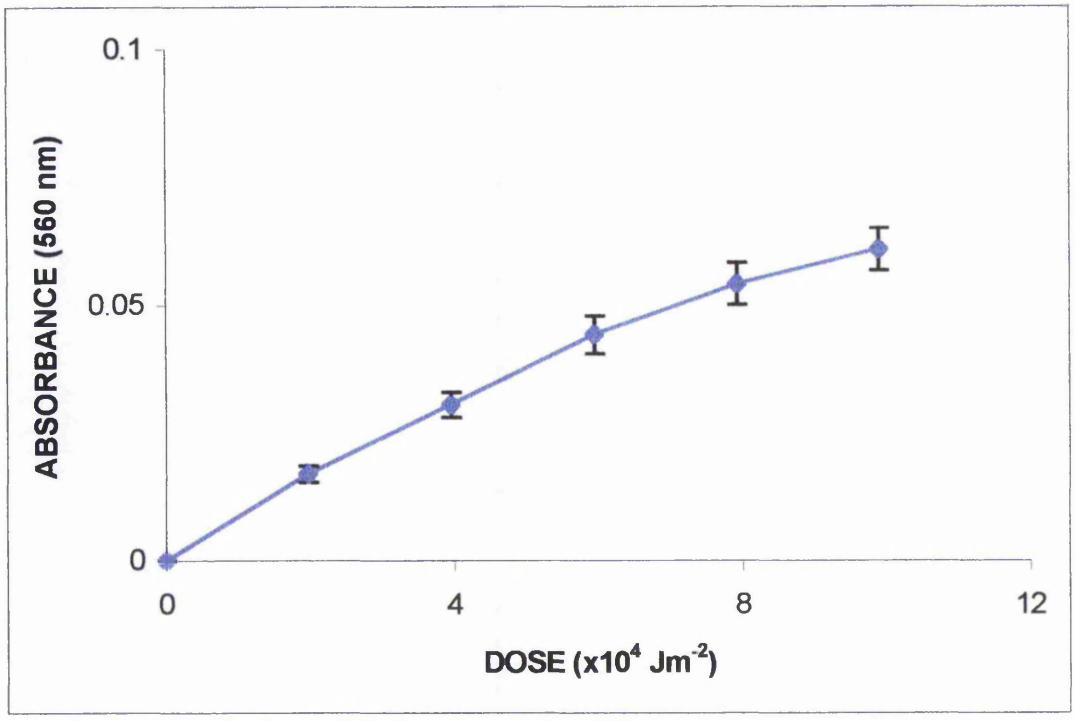

Figure 3.6 (e): The effect of L-β–phenyllactic acid and NUV on the NBT reaction. 1 mM L-β–phenyllactic acid solution in phosphate buffer, pH 9, was irradiated with varying doses of NUV (◆). The points represent the mean ± the standard error of the mean of 4 observations.

[Figure 3.6 (e)]. Except for L(+)mandelic acid, the performance of these compounds in the NBT assay relates to their absorption in the NUV region. In other words, the order of intensity of the absorbance of the sensitisers in the 260 – 400 nm spectral region is generally the same as the order of their reactivity as observed in the NBT reaction. For example, the absorbance values of the pure compounds at 330 nm are $A_{330} = 0.03$ for L(+)mandelic acid [Figure 3.3 (b)], $A_{330} = 0.21$ for β–phenylpyruvic acid [Figure 3.3 (c)], $A_{330} = 0.17$ for *p*-OH-phenylpyruvic acid [Figure 3.3 (d)], $A_{330} = 0.05$ for L-histidine [Figure 3.3 (a)], and $A_{330} = 0.03$ for L-β–phenyllactic acid [Figure 3.3 (e)]. This observation is not surprising because, as stated previously, a relationship is to be expected between the ability of a compound to absorb UV radiation and its efficacy as a sensitiser. An exception is L(+)mandelic acid, which will be discussed later. Experiments also confirmed that the production of NBT reducing species is proportional to the irradiation energy in the dose ranges employed.

3.4.1 pH Dependence of NBT Reduction

To determine the pH effect on NBT reducing species production, the NBT reaction was carried out at a range of pH values from 6.5 to 9 using an equal energy exposure (7.92×10^4 J m^{-2}). It can be seen from Figure 3.7 that the generation of NBT reducing species upon photolysis of L-histidine, L(+)mandelic acid and *p*-OH-phenylpyruvic acid increases with the pH of the reaction mixture. Photolysis of L-histidine [Figure 3.7 (a)] resulted in very low reduction at pH below 7.5, with similar effects observed at pH 6.5 and 7 (A_{560} of 0.01-0.02). NBT reduction occurs in an approximately linear function with the pH above 7 with maximum at pH 9 (A_{560} of 0.12). Photolysis of L(+)mandelic acid [Figure 3.7 (b)] had the greatest effect in the NBT reaction compared to other sensitisers, with high reduction even at low pH (A_{560} of 0.08 at pH 6.5). A plateau started to form after pH 8 with maximum at pH 9 of A_{560}=0.19. In comparison, photolysis of *p*-OH-phenylpyruvic acid [Figure 3.7 (c)] had a greater effect than L-histidine but less than L(+)mandelic acid in NBT reduction. Compared to L-histidine, this compound did not show as steep an increase in A_{560}, but had a higher value at pH 6.5 (A_{560} of 0.04). A steep increase however, can be observed at pH 9 with a maximum of A_{560}=0.14. From these results, it can be concluded that the pH plays an important role in the photolysis of these compounds.

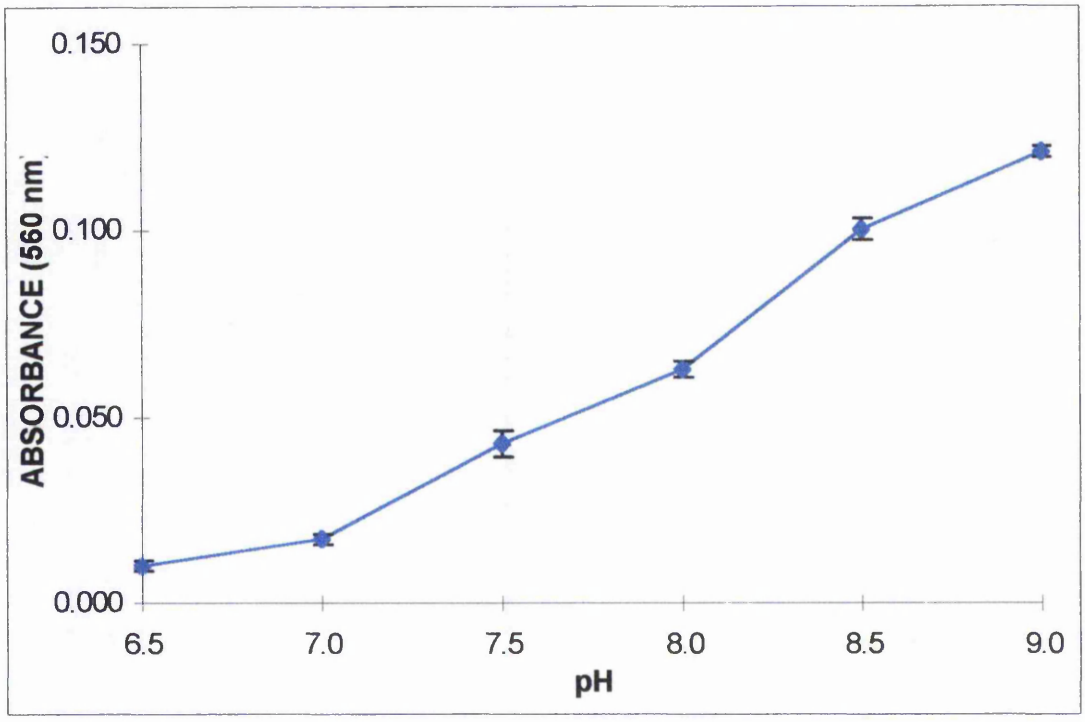

Figure 3.7 (a): pH effect on NBT reduction from the NUV photolysis of L-histidine. Reaction mixtures containing 1 mM L-histidine in phosphate buffer at varying pHs were irradiated (7.92×10^4 J m^{-2}) and the absorbance at A_{560} was determined. Values represent the mean $\pm$ the standard error of the mean of 3 observations.

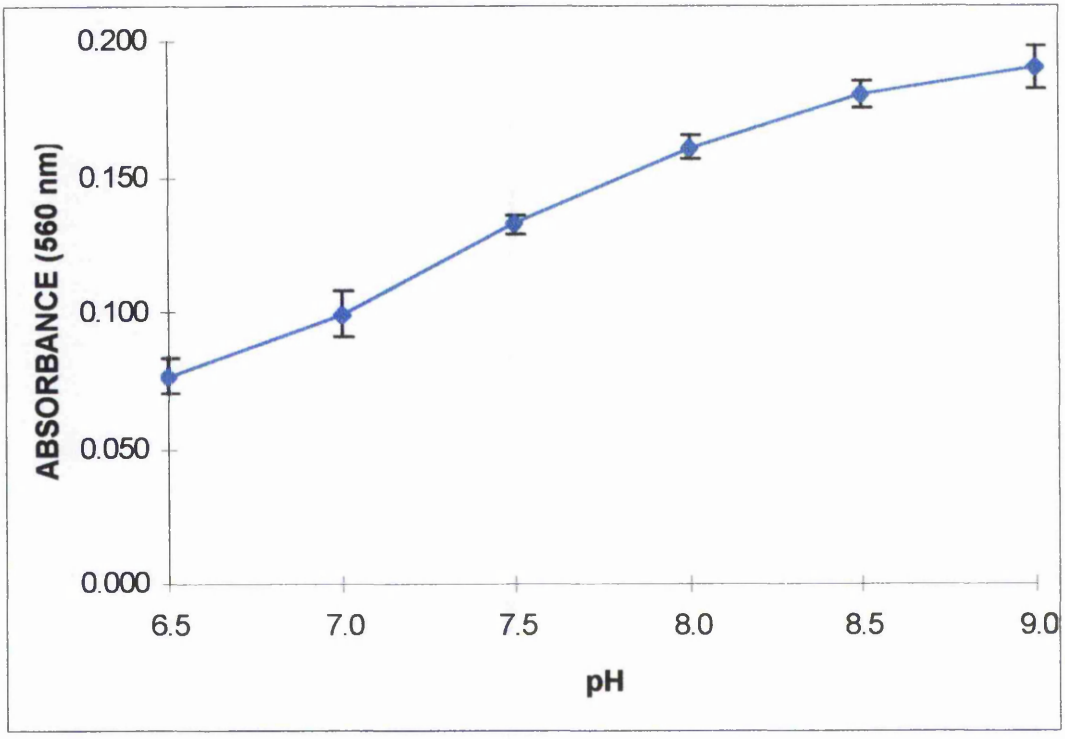

Figure 3.7 (b): pH effect on NBT reduction from the NUV photolysis of L(+)mandelic acid. Reaction mixtures containing 1 mM L(+)mandelic acid in phosphate buffer at varying pHs were irradiated (7.92×10^4 J m^{-2}) and the absorbance at A_{560} was determined. Values represent the mean $\pm$ the standard error of the mean of 4 observations.

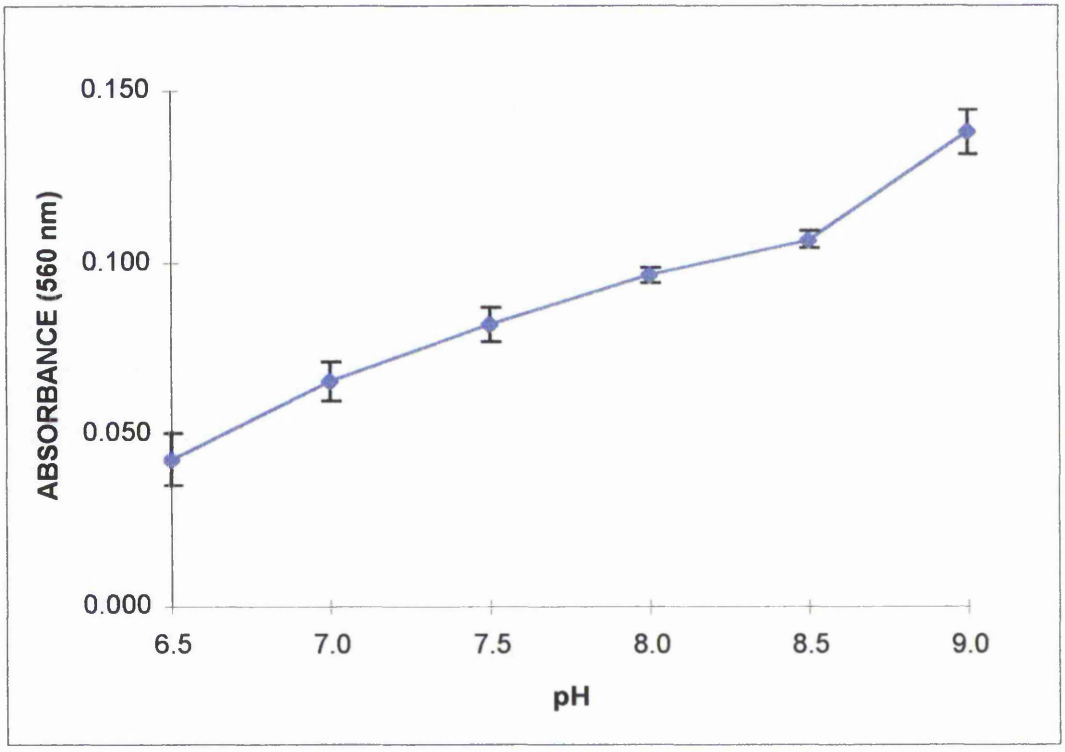

Figure 3.7 (c): pH effect on NBT reduction from the NUV photolysis of p-OH-phenylpyruvic acid. Reaction mixtures containing 1 mM p-OH-phenylpyruvic acid in phosphate buffer at varying pHs were irradiated (7.92×10^4 J m^{-2}) and the absorbance at A_{560} was determined. Values represent the mean $\pm$ the standard error of the mean of 4 observations.

SENSITISER (pH dependent)	A_{560} ($x10^3$) ± SEM (no. obs)					
	pH 6.5	pH 7	pH 7.5	pH 8	pH 8.5	pH 9
L-histidine	10 ± 1 (3)	17 ± 1 (3)	43 ± 4 (3)	63 ± 2 (3)	100 ± 3 (3)	121 ± 1 (3)
L(+)mandelic acid	77 ± 4 (3)	99 ± 4 (4)	132 ± 2 (3)	161 ± 2 (4)	180 ± 3 (3)	190 ± 4 (4)
p-OH-phenyl-pyruvic acid	43 ± 7 (2)	65 ± 6 (3)	78 ± 6 (5)	96 ± 2 (2)	107 ± 3 (2)	135 ± 16 (7)
SENSITISER (weak pH dependence)	**PH 6.5**	**pH 7**	**pH 7.5**	**pH 8**	**PH 8.5**	**pH 9**
β-phenylpyruvic acid	114 ± 1 (2)	180±10 (5)	183 ± 7 (4)	178 ± 9 (3)	187 ± 2 (2)	193 ± 6 (2)
L-β-phenyllactic acid	29 ± 2 (3)	31 ± 1 (3)	45 ± 6 (3)	47 ± 10 (3)	52 ± 7 (3)	53 ± 6 (5)

Table 3.1: NBT assay results of sensitisers plus NUV irradiation (7.92 x 10^4 J m^{-2}). NBT reduction is represented as increase in absorbance readings at 560 nm. Values express the average absorbance reading (x 10^3) for each pH ± standard error of the mean for the number of observations given in parenthesis.

On the other hand, NUV photolysis of β–phenylpyruvic acid and L-β–phenyllactic acid is rather independent of the pH of the medium exhibiting weak pH dependence, and a similar reduction in NBT is observed in the range of pH tested. These results are summarised in Table 3.1.

The fact that photolysis of L-histidine, L(+)mandelic acid and *p*-OH-phenylpyruvic acid is maximal at high pH indicates that biological effects are likely to be localised where the pH is high. The presence of L-histidine, for example, on enzyme active sites may result in protein damage if the enzyme is exposed to NUV. The high level of β–phenylpyruvic acid photolysis at near physiological pH (pH 7 – 7.5) renders this compound of great biological importance, because even at low concentrations, it can be photolysed at high rate at these pH values.

The influence of pH on the reduction of NBT can be attributed to a number of possible effects such as a pH effect on either the sensitiser molecule, the NBT or diformazan molecule, or the reducing species (e.g. $O_2^{\cdot-}$). As mentioned in section 3.2, pH does not influence the absorption spectra of the sensitisers within the region of interest (260-400 nm). Also, the mechanism of NBT reduction by $O_2^{\cdot-}$ is not expected to be pH dependent, as shown in Figure 3.5. This, and the pH independence of the photolysis of β–phenylpyruvic acid and L-β–phenyllactic acid, indicates that the pH does not affect NBT reduction or diformazan formation directly. The formation of $O_2^{\cdot-}$, however, can be anticipated to be pH dependent since the inter-conversion between $O_2^{\cdot-}$ and hydroperoxide radicals can occur on addition of a proton:

$$O_2^{\cdot-} + H^+ \leftrightarrow HO_2^{\cdot}$$

Taking the pKa of $O_2^{\cdot-}$ to be 4.8 as reported in the literature (Halliwell and Gutteridge, 1999), the pH dependence of the ratio of $O_2^{\cdot-}$ to $HO_2^{\cdot}$ can be calculated by application of the Henderson – Hasselbach equation:

$$pH = pKa + \log_{10} [O_2^{\cdot-}] / [HO_2^{\cdot}]$$

At the pH values of interest, the ratios are 50 for pH 6.5, 501 for pH 7.5, 5,012 for pH 8.5 and 15,849 for pH 9. Therefore, assuming that $O_2^{\cdot-}$ was solely responsible for the reduction of NBT (as has been claimed in the literature e.g. Halliwell and Gutteridge, 1999) and all other parameters remaining constant, a 300-fold difference in A_{560} between pH 6.5 and 9 would be expected. This is definitely not the case (Table 3.1). A likely explanation for the observations reported here is that since $HO_2^{\cdot}$ itself is a strong reductant – even stronger than $O_2^{\cdot-}$, it may possibly also reduce NBT, minimising the pH effect on A_{560}. The high reactivity of $HO_2^{\cdot}$, however, may render it less specific, so that it would react with other species in solution as efficiently. However, the observation that the photolysis of β–phenylpyruvic acid and L-β–phenyllactic acid are not pH dependent indicates that the reduction of NBT is not uniquely specific for $O_2^{\cdot-}$/ $HO_2^{\cdot}$, and that non-pH dependent reducing species are also produced. In this context, it is interesting to note that others have also suggested that

the reduction of NBT is not uniquely specific to $O_2^{\cdot-}$, but other species (e.g. the excited state of the sensitiser) may mediate NBT reduction (Menon *et. al.*, 1992). An important question therefore arises as to what is the contribution of $O_2^{\cdot-}$ to the NBT results.

3.4.2 Confirmation of NBT Reduction by $O_2^{\cdot-}$ Using Superoxide Dismutase

To corroborate the generation of $O_2^{\cdot-}$, photolysis was carried out in the presence and absence of SOD. The use of SOD in the assay would result in formation of H_2O_2 (dismutation product). The dismutation reaction operates between pH 4.8 and 9.5, with a rate constant of 2.3×10^9 M^{-1} sec^{-1} at pH 7 and 25°C (Klug *et. al.*, 1972). The rate constant is not affected significantly by pH change. Also, SOD inactivation by H_2O_2 is very slow, with a half-life for SOD of 27 min at pH 9.6 in the presence of 1.28×10^{-4} M H_2O_2 (Hodgson and Fridovich, 1975). Thus, the concentration of SOD and the experimental parameters involved were such that enzyme activity would remain high throughout the experiments.

NBT ASSAY - Slope [Δ A ($J\ m^{-2}$)$^{-1}$] ($x10^3$)				
SENSITISER	-SOD		+SOD	
	pH 7	pH 9	pH 7	pH 9
L-histidine*	2.9 ± 0.1 (2)	13.4 ± 1.8 (4)	1.4 ± 0.1 (2)	5.2 ± 0.5 (4)
L(+)mandelic acid	12.5 ± 1.9 (3)	26.0 ± 1.9 (5)	7.3 ± 0.6 (3)	13.7 ± 1.0 (5)
β-phenylpyruvic acid	14.5 ± 0.9 (2)		10.0 ± 0.5 (2)	
L-β-phenyllactic acid		6.2 ± 0.5 (4)		3.9 ± 0.1 (4)

Table 3.2: The effect of SOD on the NBT reaction. Mixtures containing 1 mM of the sensitiser alone or supplemented with 0.5 mg ml^{-1} SOD at pH 7 (pH 7.5 for *) and 9 were subjected to various doses of NUV, and the slopes of change of absorbance with NUV dose ± standard error of the mean are illustrated for the number of observations given in parenthesis.

Results show that the reduction of NBT is significantly decreased in the presence of SOD for all the sensitisers and pH values employed in the experiments

(Table 3.2). On addition of SOD to the reaction mixture, NUV photolysis of *p*-OH-phenylpyruvic acid resulted in the formation of a brown product that interfered with the detection of the blue formazan. The use of SOD was, therefore, not appropriate for this sensitiser. However, the formation of a product on addition of SOD in the presence of NUV is an indication of the possible decomposition of *p*-OH-phenylpyruvic acid by NUV.

If the decrease in the amount of NBT reduced corresponds to the amount of $O_2^{\cdot-}$ generated, the concentration of $O_2^{\cdot-}$ can be calculated using the molecular extinction coefficient for reduced NBT of 7500 at 560 nm (Menon *et. al.*, 1992) from the following formula: $\Delta A = \varepsilon \times \Delta C \times L$ where ΔA is the absorbance change, ε the molecular extinction coefficient, ΔC the concentration change and L the path length of the cuvette (1 cm). Thus, using the data from Table 3.2, the concentration of $O_2^{\cdot-}$ generated on photolysis of the sensitisers was estimated as shown in Table 3.3.

APPARENT CONCENTRATION OF SUPEROXIDE (μM)				
SENSITISER	-SOD		+SOD	
	pH 7	pH 9	pH 7	pH 9
L-histidine*	0.39	1.79	0.19	0.69
L(+)mandelic acid	1.67	3.47	0.97	1.83
β-phenylpyruvic acid	1.93		1.33	
L-β-phenyllactic acid		0.83		0.52

Table 3.3: Generation of $O_2^{\cdot-}$ in the NBT reaction. Values represent the estimated concentration of $O_2^{\cdot-}$ that was produced on NUV photolysis of 1 mM of the sensitiser at pH 7 (pH 7.5 for *) and 9 in the presence and absence of SOD.

From Table 3.3, several conclusions can be drawn. In all cases and at different pH values, it can be seen that the addition of SOD reduced the reduction of NBT, confirming, to differing extents, the production of $O_2^{\cdot-}$ on photolysis of all the sensitisers investigated. However, despite the fact that the enzyme is in sufficient excess to quench the reaction, the inhibition of NBT reduction is incomplete, confirming that the assay is non-specific towards $O_2^{\cdot-}$ and that additional reducing

species are produced. Although it is difficult to make a definite assignment, the mechanism in Figure 3.5 implies that any species which is capable of transferring electrons to the NBT^{2+} cation will cause reaction. In this context, it is particularly interesting to note that it has been reported that the photolysis of L-histidine in the wavelength range employed here is capable of producing solvated electrons (Smith, 1989). Therefore, at least in the case of L-histidine, one possibility for additional NBT reduction is directly by electrons from solution. From Table 3.3, it is also evident that there is an influence of pH on the effect of the addition of SOD.

In summary, and in agreement with the earlier suggestion, NBT reduction on addition of SOD, in excess, indicates that the reduction of NBT is not exclusively due to reaction with $O_2^{\cdot-}$, but that other species may be involved. Indeed, the sensitiser in the excited state may react directly with the NBT^{2+} cation *via* a type I photosensitised reaction (see section 1.3.4), or decomposition leading to the production of solvated electrons may occur. In the case of L(+)mandelic acid which does not absorb light extensively in the NUV region, the photolytic effect can not be explained by this mechanism.

3.4.3 Waveband Dependence of NBT Reduction

UV photosensitisation of the compounds tested depends greatly on their absorption spectra. Here, an attempt was made to determine the action spectra of the compounds that exhibit the highest photosensitising potential, namely L(+)mandelic acid and β–phenylpyruvic acid. It is of interest to determine whether the absorption pattern of these biochemicals reflects the intensity of their photolysis and subsequently the generation of ROS. Experiments showed that the amount of NBT reduced after irradiation indeed depends on the wavelengths involved. Figures 3.8 (a) and (b) show the effects of UVA, UVB and UVC on L(+)mandelic acid and β–phenylpyruvic acid photolysis respectively. UVA exposure was achieved by placing a sheet of Mylar plastic between the NUV source and the irradiated solution (section 2.2).

Figure 3.8 shows that when these compounds are irradiated by NUV, they similarly reduce NBT, and this reflects the degree of their photolysis. In Figure 3.8 (a), L(+)mandelic acid is shown to exhibit the highest effect on NBT reduction in the UVC waveband. However, equal energy exposures by UVA or UVB result in the same amount of NBT reduction. Comparing these results to the absorption spectrum of L(+)mandelic acid some correlation can be observed. The enhanced reduction of NBT on UVC irradiation reflects the high peak of L(+)mandelic acid in this waveband [Figure 3.3 (b)]. Although very little, the absorption of L(+)mandelic acid in the UVA and UVB wavebands is very similar and, according to the results in Figure 3.8 (a), it amounts to equal levels of photolysis. It can be concluded that in both wavebands, the photosensitised potential of L(+)mandelic acid is much higher than that expected form the levels of light absorption. In general, the action spectrum of L(+)mandelic acid corresponds to its absorption spectrum.

From Figure 3.8 (b), it can be observed that β–phenylpyruvic acid is most effective in reducing NBT in the UVC waveband. However, the effect of β–phenylpyruvic acid is about half that of L(+)mandelic acid. Comparing this result to the absorption spectrum of β–phenylpyruvic acid [Figure 3.3 (c)] a higher rate of reduction would be expected, since the absorption of β–phenylpyruvic acid in the UVC band is much higher than that of L(+)mandelic acid. It seems that the absorption in the UVC by this compound does not result effectively in photolysis and, subsequently, ROS generation. The extent of photolysis in the UVB region is also lower than that predicted by the absorption spectrum of β–phenylpyruvic acid, and is, again, half that of L(+)mandelic acid. In contrast, UVA seems to be the primary wavelength range to induce a photosensitised reaction. Even though β–phenylpyruvic acid absorbs less in the UVA than in the UVB region, this absorption of photons is sufficient to induce an enhanced photolytic effect. In general, the action spectrum of β–phenylpyruvic acid does not correspond to its absorption spectrum, in the sense that UVA results in enhanced photolysis. This, however, is in agreement with the knowledge that UVA is the primer waveband to induce photosensitised reactions and not UVB or UVC. In addition, the increased reduction of NBT observed for L(+)mandelic acid when irradiated by UVC may reflect a direct reduction by energy transfer of this compound rather than by involvement of ROS.

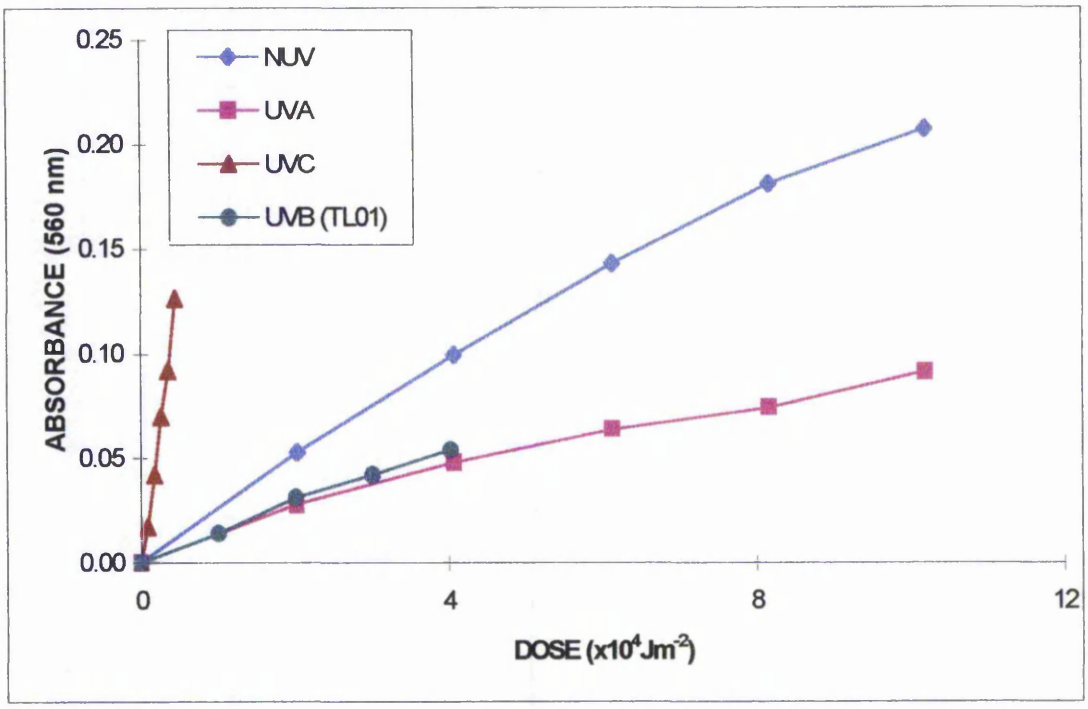

Figure 3.8 (a): Wavelength dependent photolysis of L(+)mandelic acid. NBT reaction mixtures at pH 9 supplemented with 1 mM L(+)mandelic acid were irradiated with NUV (◆), UVA (■), UVC (▲) and UVB (TL01) (●). The data given are representative of several experiments.

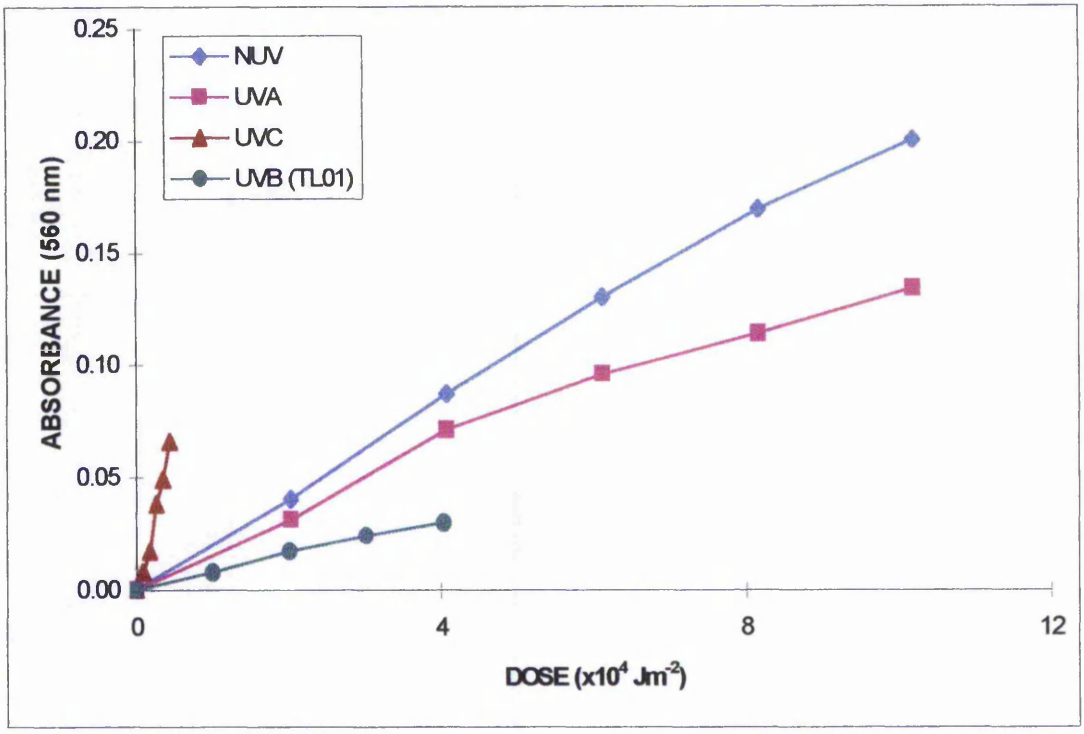

Figure 3.8 (b): Wavelength dependent photolysis of β–phenylpyruvic acid. NBT reaction mixtures at pH 7 supplemented with 1 mM β–phenylpyruvic acid were irradiated with NUV (◆), UVA (■), UVC (▲) and UVB (TL01) (●). The data given are representative of several experiments.

By cutting out the 1.2 % of UVB using a filter in the NUV source, and thus separating the three wavebands, the action spectrum of these compounds was determined. Although this was not as accurate as if experiments were performed using narrow-band irradiation, some interesting conclusions were drawn. A comparison between absorption and action spectra can lead to the better evaluation of the ptotosensitising properties of these biochemicals.

3.5 Generation of H_2O_2 and $^1O_2$ as Intermediates of $O_2^{\cdot-}$ Formation

In order to understand the mechanism of the formation of $O_2^{\cdot-}$, the need to determine whether it is generated directly upon irradiation of the sensitisers tested, or indirectly *via* other ROS, becomes evident. Thus, experiments were carried out where a specific H_2O_2 scavenger (catalase) and $^1O_2$ scavengers (β–carotene, DABCO, or sodium azide) were added in the NBT reaction mixture (Table 2.2).

Catalase enzymatically converts H_2O_2 to water and molecular oxygen. To ensure that the results reflect the scavenging properties of this enzyme for H_2O_2 and are not due to its proteinacious nature, experiments were repeated using heat denatured enzyme. The results are summarised in Tables 3.4 and 3.5.

Results show that addition of catalase in the NBT reaction mixture produced a quenching effect at pH 9 for L-histidine, L(+)mandelic acid and *p*-OH-phenylpyruvic acid (Table 3.4) and at pH 7 for β–phenylpyruvic acid (Table 3.5). This indicates that H_2O_2 is generated on photolysis of these sensitisers. The greater effect of catalase at pH 9 indicates that H_2O_2 is preferentially produced at high pH values. A possible reaction mechanism, which would give H_2O_2 and relate to the production of $O_2^{\cdot-}$ is as follows:

$$O_2^{\cdot-} + H^+ \leftrightarrow O_2H^{\cdot} + H^{\cdot} \rightarrow H_2O_2$$

where $H^{\cdot}$ is abstracted from a substrate. However, the pH dependence of H_2O_2 generation implies that it is not produced consecutively from $O_2^{\cdot-}$ as more protons are

potentially be lethal. Phage T7 DNA contains only about 10% non-coding sequences (Dunn and Studier, 1983), so the inactivation curve can be interpreted on the basis of a one-hit principle: each DNA lesion causes inactivation. Since T7 does not have the capacity to repair damage to DNA and protein, it depends on the repair machinery of the host. However, any damage to the protein part of the phage may impair the ability to inject the DNA into the host. Thus, whereas DNA lesions may be repaired by the DNA-repair systems of the host, protein damage that occurs before DNA injection can not be corrected. It can, therefore, be relatively easy to calculate the extent of damage in T7 phage in comparison to a complex system (i.e. bacterial). The inactivation effect is measured by the reduced plaque-forming ability of the phage.

Previous studies of the inactivation of phage T7 by NUV and H_2O_2 have revealed that these agents can induce synergistic effect i.e. the combined action of non-lethal concentrations of H_2O_2 and NUV is greater than the value obtained by the individual agent (Ahmad, 1981; Hartman *et. al.*, 1979). Ahmad (1981) showed that photolysis of H_2O_2 generates $O_2^{\cdot-}$ and this may be responsible for phage inactivation. Hartman *et. al.* (1979) demonstrated the importance in the relationship between phage inactivation and DNA-protein interaction. It was shown in their studies that single-strand DNA breaks did not account for phage inactivation, but DNA-protein cross-links prevent normal injection of phage DNA. The influence of phage proteins in UV induced DNA damage is also supported by a more recent study, which demonstrated that the presence of DNA-bound phage proteins causes significant alterations to the DNA structure. On UV irradiation, such alterations result in increased base dimerisation and photoproduct formation of T7 phage DNA (Fekete *et. al.*, 1999).

4.2.2 Phage T7 Inactivation by Sensitisers of NUV

In order to determine the effect the photolysis of L-histidine, L(+)mandelic acid, β–phenylpyruvic acid and *p*-OH-phenylpyruvic acid may have on a biological system, experiments were performed using suspensions of bacteriophage T7 in phosphate buffer (as described in section 2.5.2). Exposure of phage T7 to NUV (9.9 x 10^4 Jm^{-2}) in the absence of sensitiser resulted in 88 % inactivation at pH 9 and 73 % inactivation at pH 7 (Figure 4.1 and Table 4.1). The reduction in phage survival by

NUV alone at both pH values is not surprising, as it is likely that certain amino acid side chains of coat and tail proteins will themselves act as NUV sensitisers. It is known, for example, that the amino acids tryptophan, tyrosine, and phenylalanine generate ROS on NUV photolysis in a pH-dependent manner (Graggs *et. al.*, 1994; Kohen *et. al.*, 1995). The presence of protein-bound histidine should also be considered as L-histidine is proposed to act as sensitiser of NUV generating ROS most effectively in alkaline media (Paretzoglou *et. al.*, 1998). ROS produced on NUV photolysis of these amino acids would target both the protein coat and DNA genome of the phage leading to inactivation.

Phage T7 treated with any of the sensitisers involved in this study alone showed no inactivation, demonstrating that none of these compounds display any toxicity to the phage by itself at the concentrations employed.

A combined treatment with the sensitiser and NUV, on the other hand, greatly enhanced the inactivation showing a synergistic effect (Figures 4.2 - 4.9 and Table 4.1). This synergy implies that in addition to the damaging effect of NUV alone, products of sensitised photolysis contribute to phage inactivation, the effect being greater at pH 9 than pH 7 or 7.5 for the pH dependent sensitisers. The pH dependence of the phage inactivation attributed to the NUV photolysis of L-histidine, L(+)mandelic acid and *p*-OH-phenylpyruvic acid exhibits the same pattern observed for these compounds in the NBT assay. This reflects the pH dependent formation of ROS like $O_2^{\cdot-}$, and possibly other photoproducts, which are responsible for the inactivation of the phage particles.

It can be seen from Figures 4.1 - 4.8, that, when 1 mM of sensitiser was included in the irradiated T7 phage suspension, phage lethality increases compared to that caused by NUV alone. Thus, NUV (9.9×10^4 Jm^{-2}) plus L-histidine or L(+)mandelic acid appear to have a similar damaging effect on phage viability, the values for phage inactivation by L-histidine being approximately 98 % and 89 % at pH 9 and pH 7.5 respectively, and by L(+)mandelic acid around 99 % at pH 9 and 87 % at pH 7 (Table 4.1). *p*-OH-Phenylpyruvic acid, however, induced a three log inactivation (99.7 %) when photolysed by the same dose of NUV at pH 9 (Figure 4.6

and Table 4.1). Also, photolysis of β–phenylpyruvic acid caused about 98 % inactivation at pH7 (Figure 4.8).

From these results, it is apparent that even though the error bars overlap in some cases, the general order of photosensitised lethality is: β–phenylpyruvic acid > *p*-OH-phenylpyruvic acid > L-histidine > L(+)mandelic acid, at pH 7 / 7.5, and *p*-OH-phenylpyruvic acid > L(+)mandelic acid > L-histidine at pH 9. Comparing this pattern to that observed for the NBT assay in Chapter 3 (Table 3.1), there is a correlation between the results from the NBT assay and the T7 inactivation, except for the L(+)mandelic acid results. However, as discussed in the previous chapter, it appears that a complex may be forming between the L(+)mandelic acid and the NBT molecules that is responsible for the photolysis observed, giving rise to unexpectedly high assay results.

In addition, even though the NBT assay has been used in the past as $O_2^{\cdot-}$ specific (Carbonare and Pathak, 1992; Menon *et. al.*, 1992), the results presented in the previous chapter demonstrate that this assay is not totally specific. Although, therefore, it would be tempting to assumed that $O_2^{\cdot-}$ is indeed the primary ROS responsible for phage inactivation, this conclusion must be viewed with caution and further evidence would be necessary to make a definite assignment. However, some support for the hypothesis that photosensitised generation of $O_2^{\cdot-}$ may be responsible for T7 phage inactivation can be found in the literature (Ahmad, 1981; Craggs *et. al.*, 1994; Paretzoglou *et. al.*, 1998).

% INACTIVATION OF PHAGE T7 ± SEM (no. obs.)		
SENSITISER	pH 7 / 7.5	pH 9
NUV alone	73.0 ± 1.5 (15)	88.1 ± 0.8 (10)
L-Histidine	88.7 ± 0.9 (3)	97.5 ± 0.6 (5)
L(+)Mandelic acid	86.7 ± 1.9 (6)	98.5 ± 0.4 (4)
p-OH-Phenylpyruvic acid	89.8 ± 2.1 (4)	99.7 ± <0.1 (3)
β–Phenylpyruvic acid	98.3 ± 0.4 (8)	
NADH		93.8 ± 1.9 (3)

Table 4.1: The effect of NUV alone or in addition to the appropriate sensitiser in the survival of bacteriophage T7. Values represent the % inactivation achieved after irradiation (9.9×10^4 Jm^{-2}) of a phage suspension in the desired pH ± the standard error of the mean for the number of observations given in parenthesis.

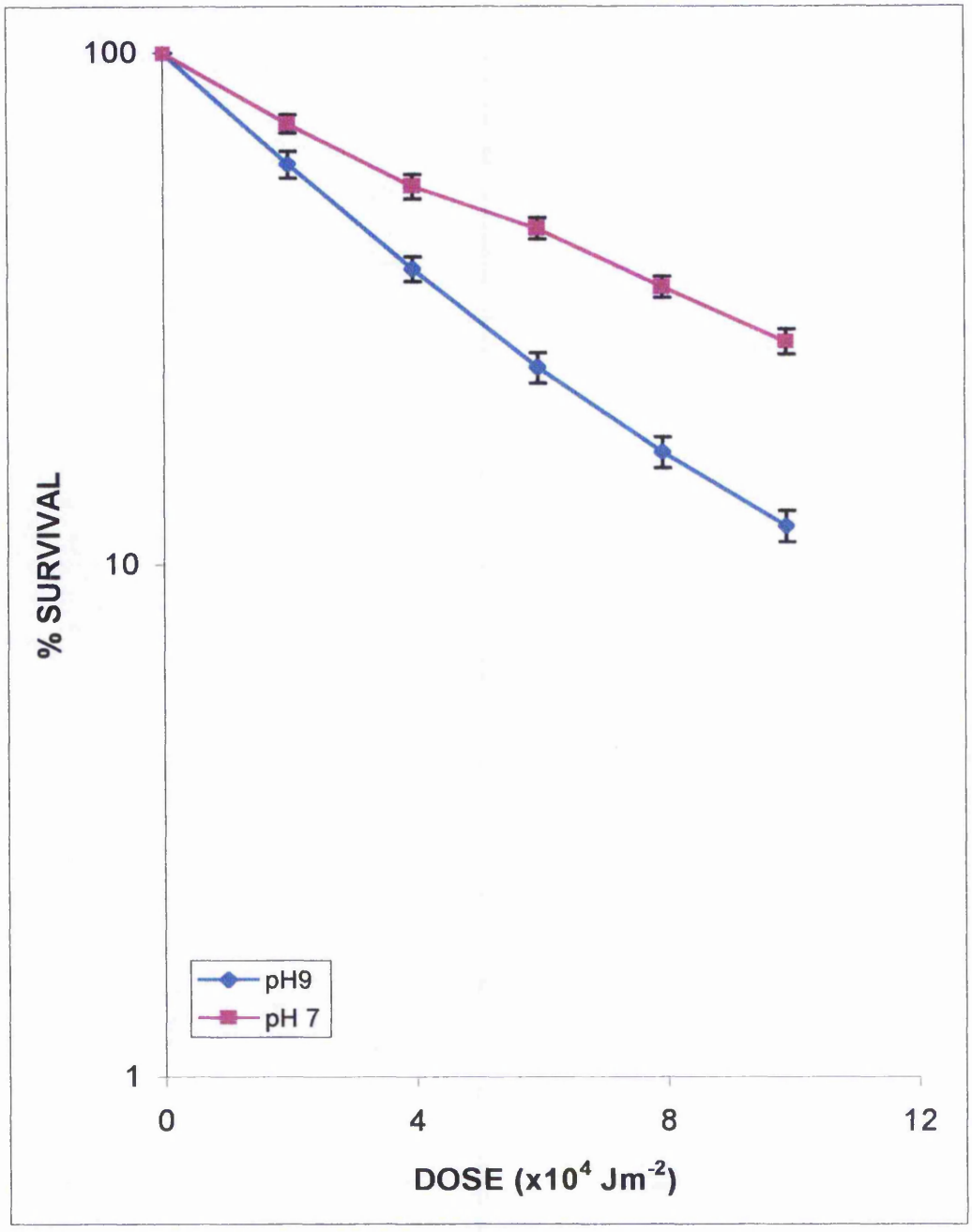

Figure 4.1: NUV-induced inactivation of phage T7. Phage suspensions in phosphate buffer at pH 7 (■) and 9 (◆) were irradiated with varying doses of NUV. The points represent the mean ± the standard error of the mean of 15 and 10 observations respectively.

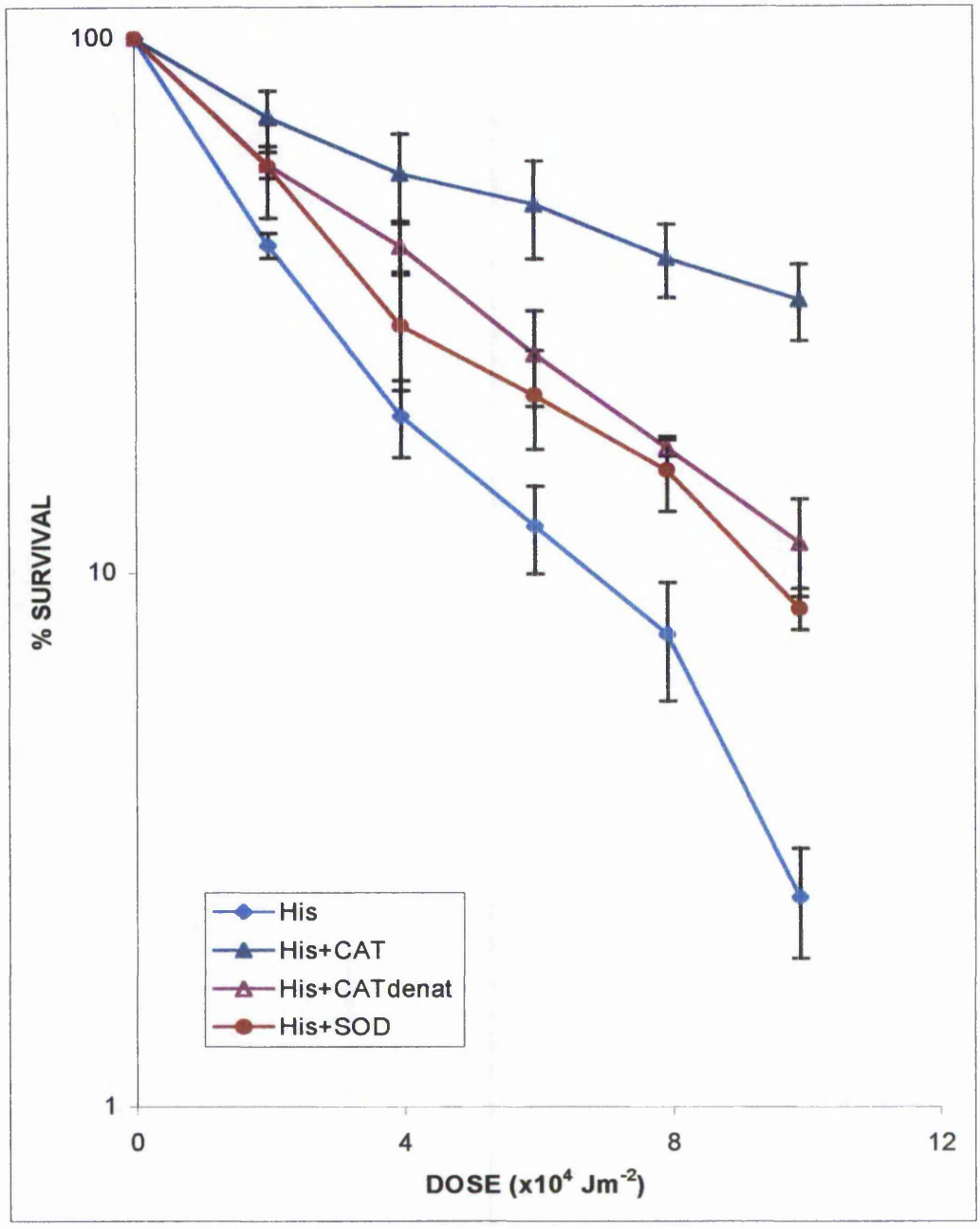

Figure 4.2: L-histidine plus NUV-induced inactivation of phage T7 at pH9. Phage suspensions incubated with 1 mM L-histidine alone (◆), (n=5) or with L-histidine plus SOD (●), (n=2), catalase (▲), (n=3), denatured catalase (△), (n=3) and were irradiated with varying doses of NUV. Each point represents the mean ± the standard error of the mean.

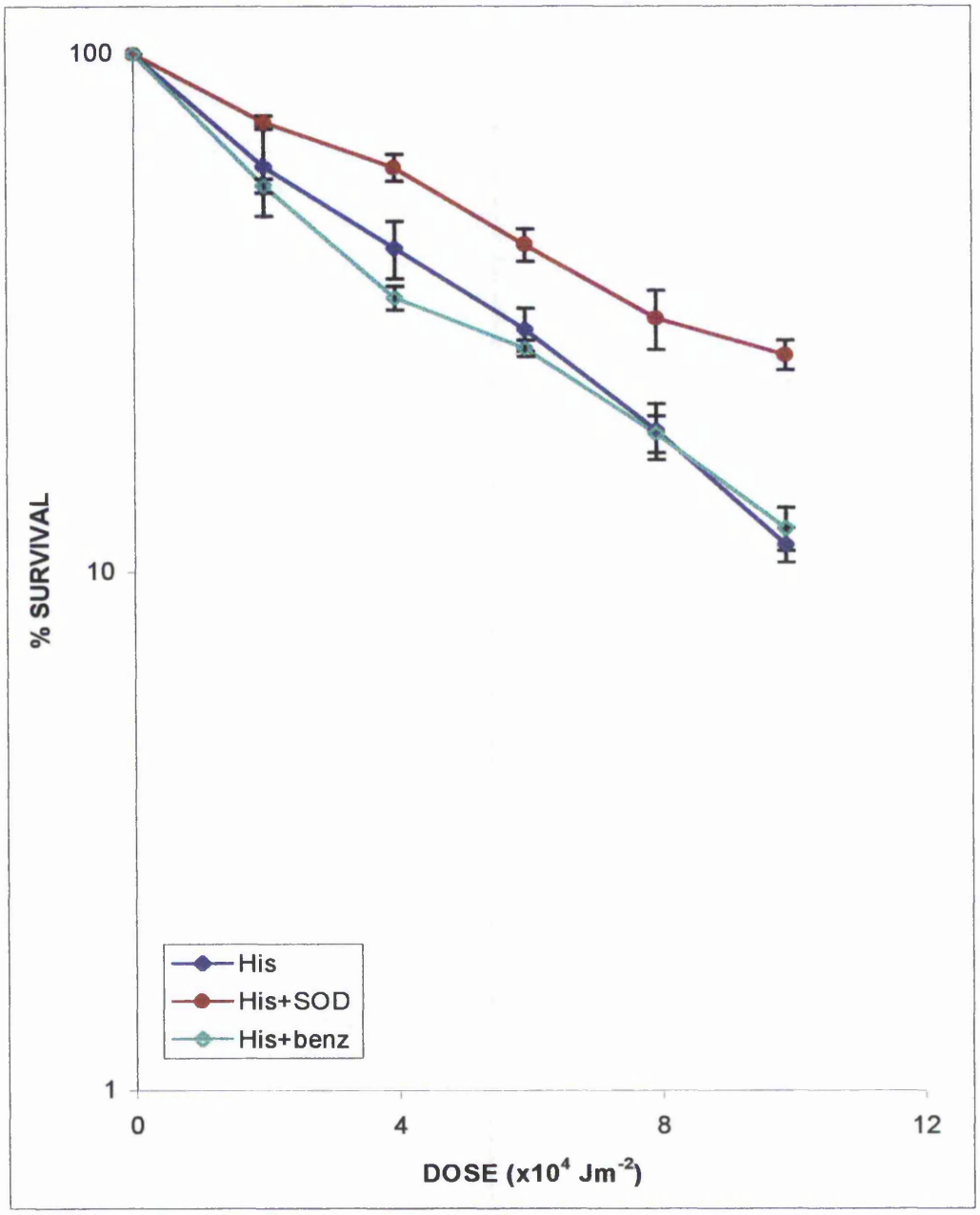

Figure 4.3: L-histidine plus NUV-induced inactivation of phage T7 at pH 7.5. Phage suspensions incubated with 1 mM L-histidine alone (◆), (n=3) or with L-histidine plus SOD (●), (n=2), Na-benzoate (✧), (n=2) and were irradiated with varying doses of NUV. Each point represents the mean ± the standard error of the mean.

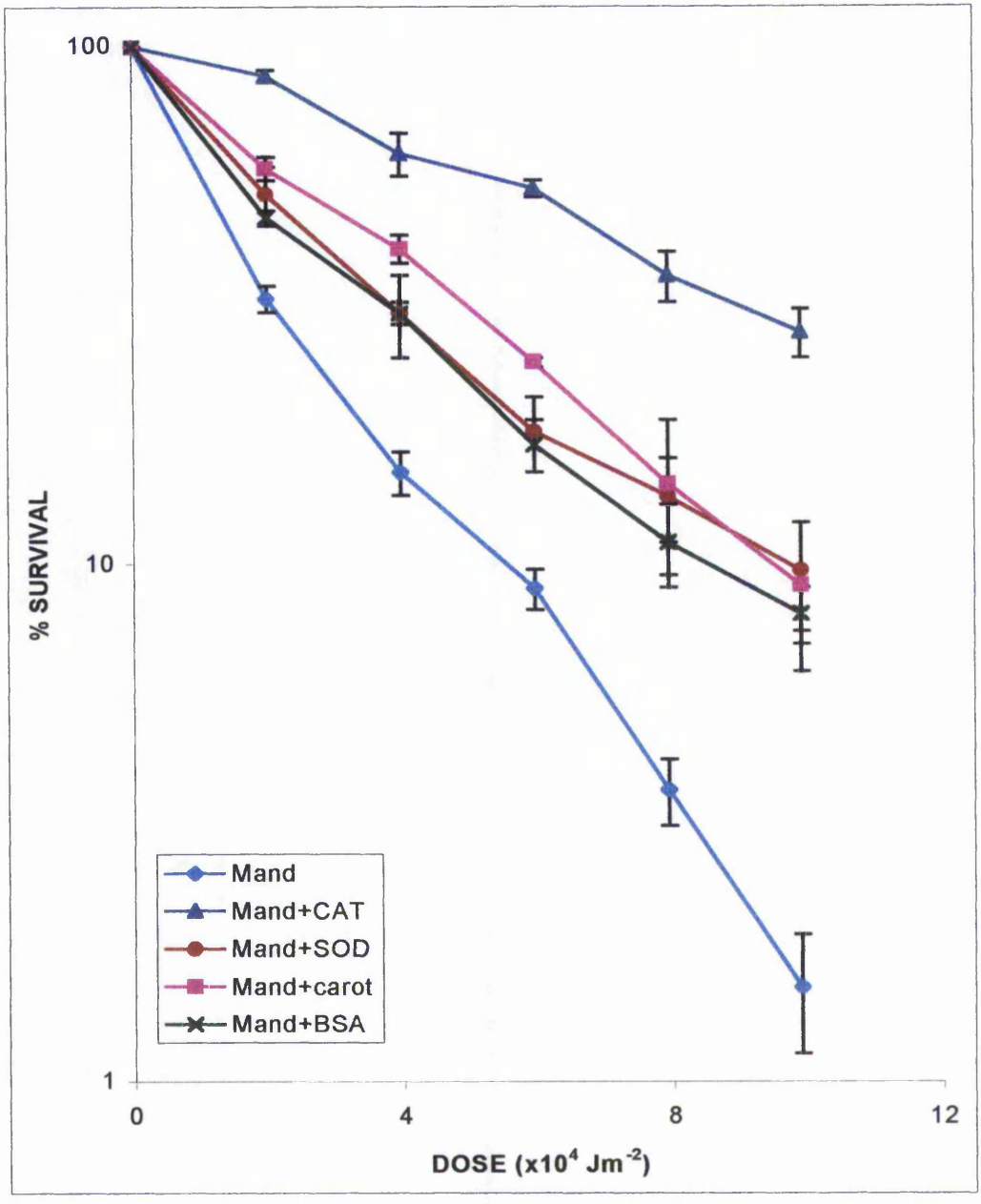

Figure 4.4: L(+)mandelic acid plus NUV-induced inactivation of phage T7 at pH9. Phage suspensions incubated with 1 mM L(+)mandelic acid alone (◆), (n=4) or with L(+)mandelic acid plus SOD (●), (n=2), catalase (▲), (n=2), BSA (×), (n=2), carotene (■), (n=2) and were irradiated with varying doses of NUV. Each point represents the mean ± the standard error of the mean.

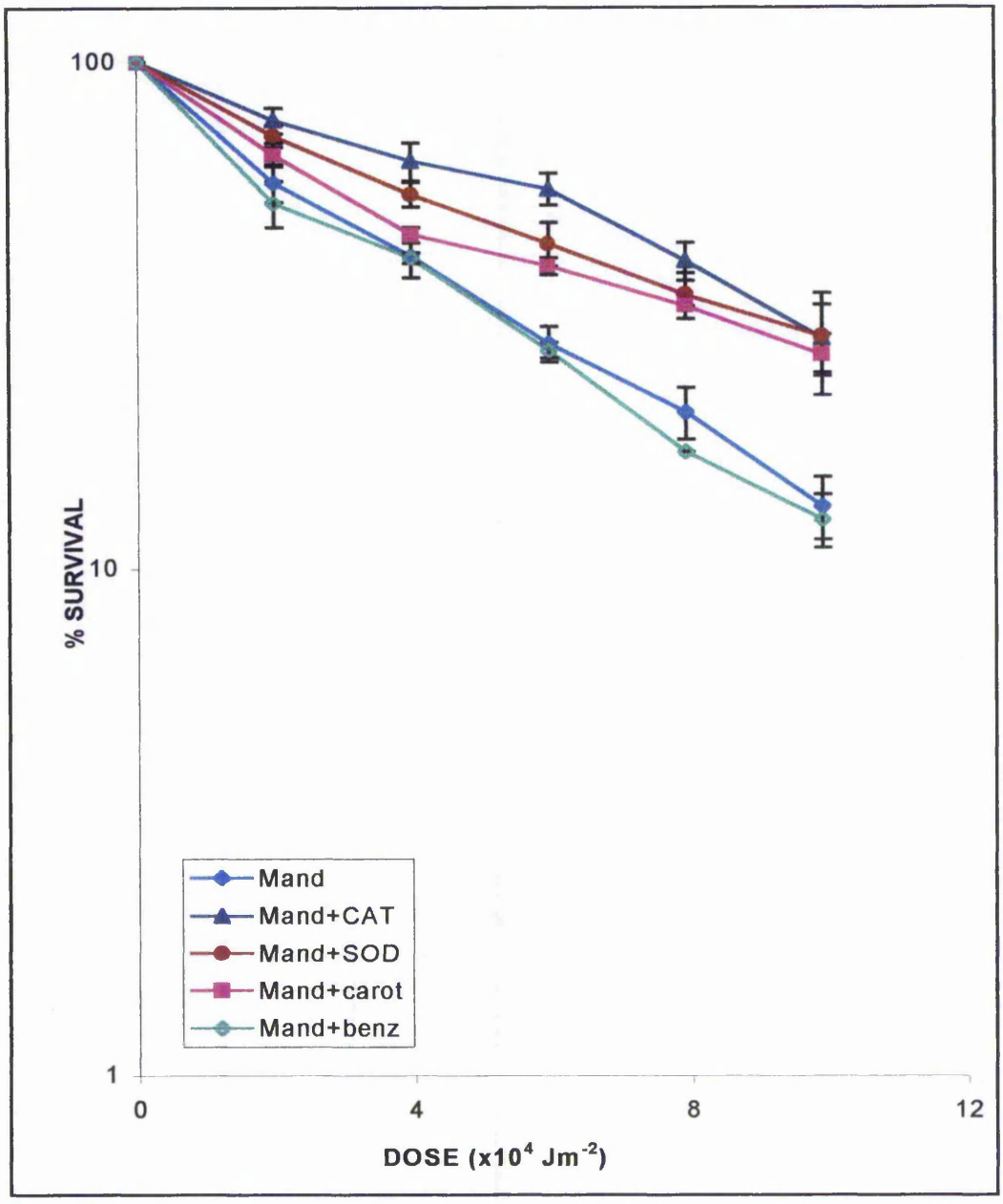

Figure 4.5: L(+)mandelic acid plus NUV-induced inactivation of phage T7 at pH7. Phage suspensions incubated with 1 mM L(+)mandelic acid alone (◆), (n=6) or with L(+)mandelic acid plus SOD (●), (n=4), catalase (▲), (n=2), carotene (■), (n=2), Na-benzoate (◇), (n=2) and were irradiated with varying doses of NUV. Each point represents the mean ± the standard error of the mean.

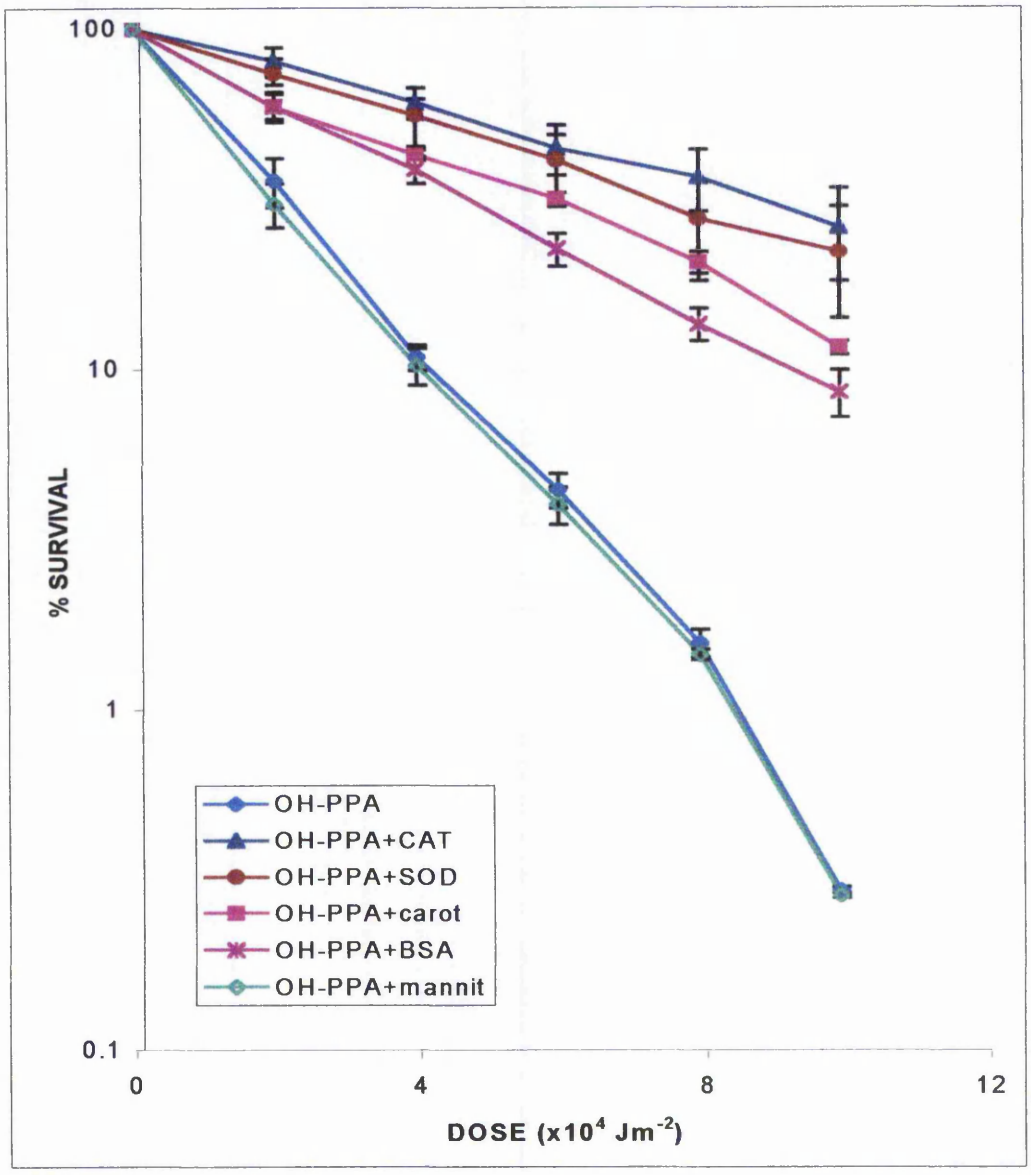

Figure 4.6: *p*-OH-phenylpyruvic acid (OH-PPA) plus NUV-induced inactivation of phage T7 at pH9. Phage suspensions incubated with 1 mM *p*-OH-phenylpyruvic acid alone (◆), (n=3) or with *p*-OH-phenylpyruvic acid plus SOD (●), (n=2), catalase (▲), (n=2), BSA (×), (n=2), carotene (■), (n=2), mannitol (✧), (n=2) and were irradiated with varying doses of NUV. Each point represents the mean ± the standard error of the mean.

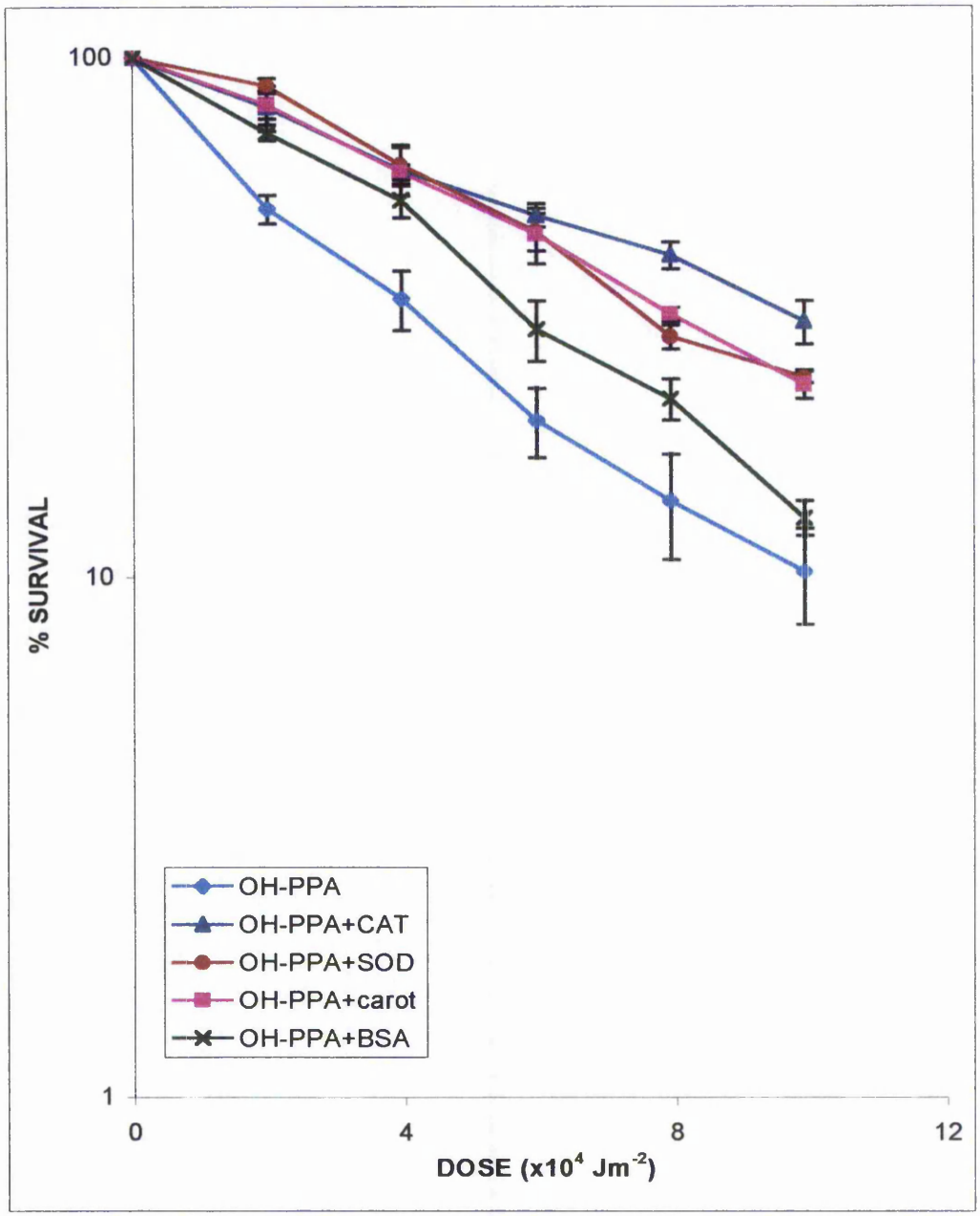

Figure 4.7: *p*-OH-phenylpyruvic acid (OH-PPA) plus NUV-induced inactivation of phage T7 at pH7.5. Phage suspensions incubated with 1 mM *p*-OH-phenylpyruvic acid alone (◆), (n=4) or with *p*-OH-phenylpyruvic acid plus SOD (●), (n=3), catalase (▲), (n=2), BSA (×), (n=2), carotene (■), (n=2) and were irradiated with varying doses of NUV. Each point represents the mean ± the standard error of the mean.

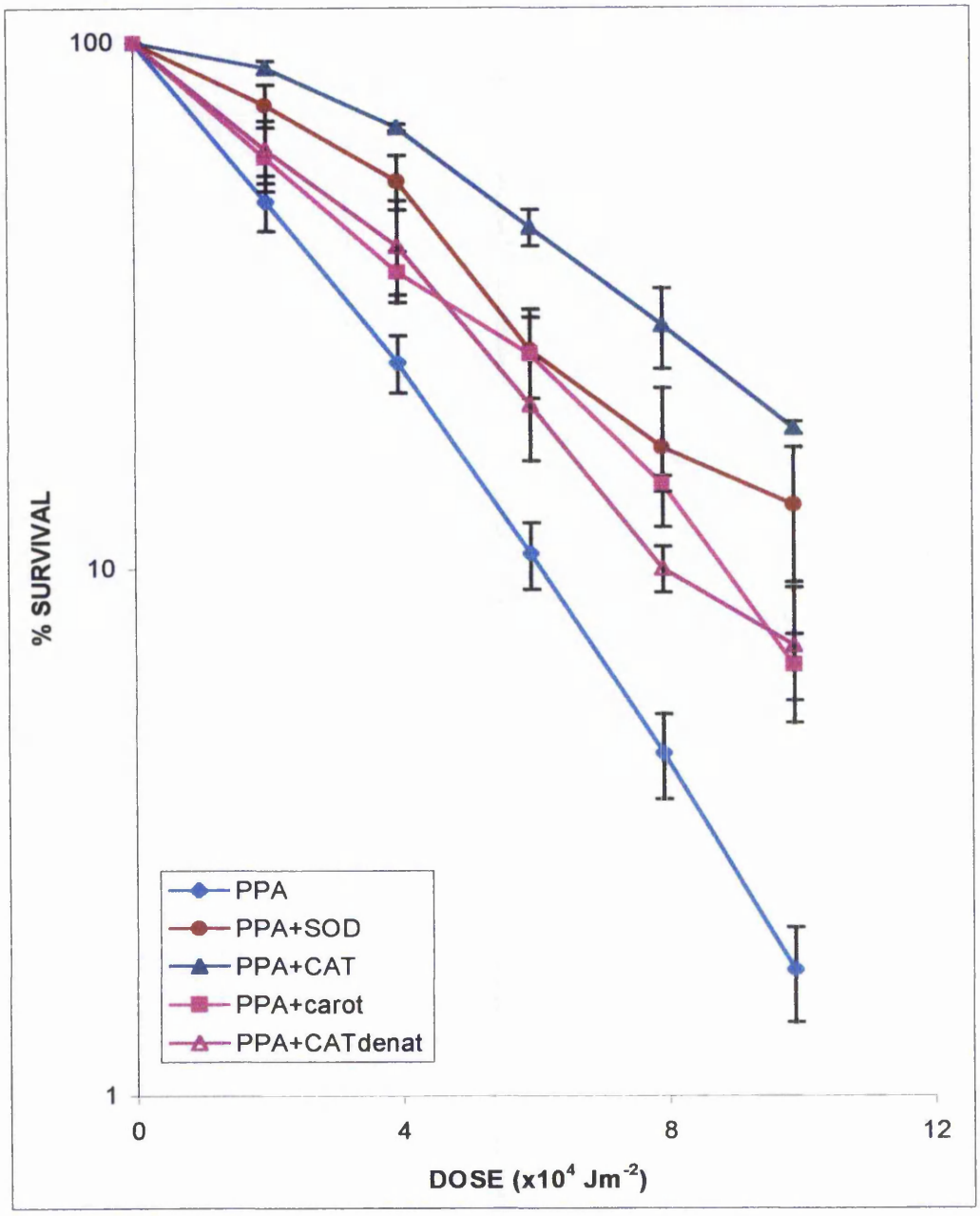

Figure 4.8: β–Phenylpyruvic acid (PPA) plus NUV-induced inactivation of phage T7 at pH7. Phage suspensions incubated with 1 mM β–phenylpyruvic acid alone (◆), (n=8) or with β–phenylpyruvic acid plus SOD (●), (n=2), catalase (▲), (n=2), denatured catalase (△), (n=2), carotene (■), (n=2) and were irradiated with varying doses of NUV. Each point represents the mean ± the standard error of the mean.

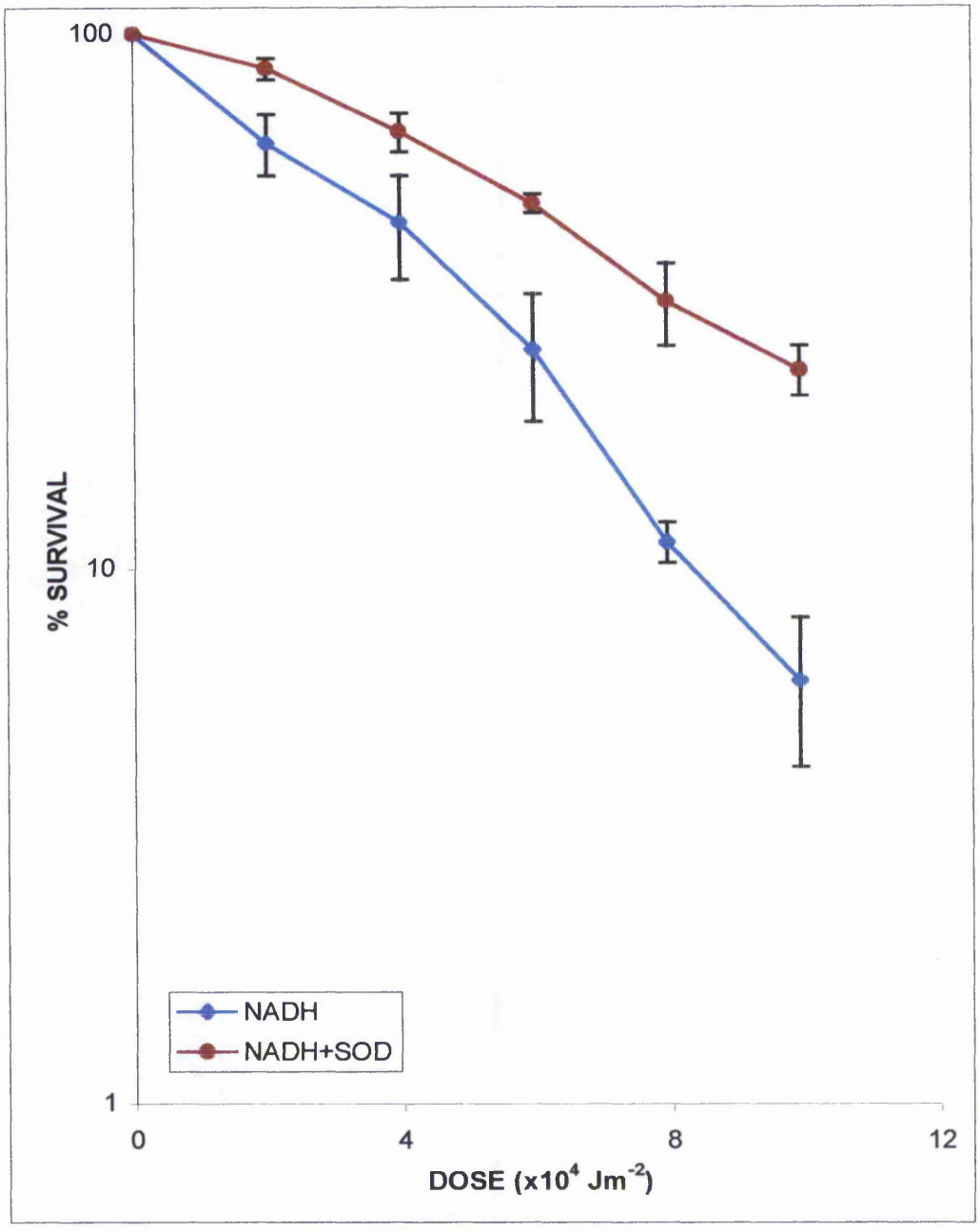

Figure 4.9: NADH plus NUV-induced inactivation of phage T7 at pH9. Phage suspensions incubated with 1 mM NADH alone (◆), or with NADH plus SOD (●), and were irradiated with varying doses of NUV. The points represent the mean ± the standard error of the mean of 3 and 2 observations respectively.

4.2.3 Evidence for the Involvement of ROS in Phage Inactivation

Since exposure to the sensitiser alone did not result in phage lethality and treatment with NUV alone inactivated only a small percentage of the phage particles, the enhanced synergistic effect observed must be due to the photosensitised action of the sensitisers. In Chapter 3, it was concluded that the NUV photolysis of the sensitisers under
investigation results in the generation of a variety of ROS such as H_2O_2, $O_2^{\cdot-}$, $^1O_2$ and $^{\cdot}OH$. It is believed that these products of photolysis may be responsible for phage inactivation. In order to examine this possibility, scavenging experiments were undertaken, in an attempt to identify the particular ROS involved in phage lethality.

From Figures 4.2, 4.4-4.8, it is evident that addition of catalase in the irradiated phage suspension resulted in significant protection from sensitised inactivation at all pH values (7, 7.5 and 9). The protective effect observed by catalase indicates that H_2O_2 is one of the ROS generated on photolysis of the sensitisers tested, as expected from the results in Chapter 3. It can also be said that H_2O_2 production may be largely responsible for phage inactivation. The main reason for this is the strong possibility that any H_2O_2 in the phage environment may lead to further production of $O_2^{\cdot-}$ and $^{\cdot}OH$. Indeed, as has been previously reported, H_2O_2 generated on NUV photolysis of the sensitisers can be photolysed further to give $O_2^{\cdot-}$, preferentially at high pH (Ahmad, 1981; Hartman *et. al.*, 1979). $O_2^{\cdot-}$ produced on NUV photolysis of H_2O_2 at pH 9 may be partially and indirectly responsible for the increased inactivation observed at this pH. The presence of an additional amount of $O_2^{\cdot-}$ at pH 9 is expected since there is a pH dependence of $O_2^{\cdot-}$ production as discussed in Chapter 3. This can be observed especially for *p*-OH-phenylpyruvic acid (Figure 4.6) and L(+)mandelic acid photolysis (Figure 4.4). In addition, H_2O_2 may generate $^{\cdot}OH$ by a Fenton-like reaction in the presence of transition metal ions (Fe^{2+} and Cu^{+}) (see section 1.3.3.2), traces of which may be part of the phage particles. By scavenging the H_2O_2 that is generated on NUV photolysis of the sensitiser using catalase, the amount of $^{\cdot}OH$ and $O_2^{\cdot-}$ is also reduced, explaining the highly protective effect observed on addition of this scavenger in the phage suspension (Figures 4.2, 4,4-4.8). Moreover, H_2O_2 has a longer half-life than the majority of ROS and, therefore, more chance to be removed by catalase before it can react.

Another explanation for the good scavenging ability of catalase in the phage experiments may be that the enzyme also reacts with any $^1O_2$ present. In a recent study, it was shown that catalase can be oxidised by $^1O_2$ resulting in a shift in the electrophoretic mobility of the enzyme (Lledias and Hansberg, 2000). The oxidation of catalase was probably due to heme modification and was specific for $^1O_2$ as light alone had no effect. However, it was stated in this study that all the catalases tested remained active after $^1O_2$ oxidation. Therefore, if $^1O_2$ is also responsible for the inactivation observed and catalase quenches this ROS, then the protection observed on addition of this enzyme would be higher than that given from the reaction with H_2O_2 alone.

A comparison of the protective effect of catalase for different sensitisation reactions on T7 indicates that this is greater for L-histidine (Figure 4.2), L(+)mandelic acid (Figures 4.4 and 4.5) and *p*-OH-phenylpyruvic acid (Figures 4.6 and 4.7), all showing inactivation reduced to around 70 %. The presence of catalase on NUV photolysis of β–phenylpyruvic acid, on the other hand, reduced the phage kill to about 82 %. Generally, the protective effect of catalase was much higher at pH 9. This result is in agreement with the results of catalase added in the NBT assay (Table 3.4), further supporting the conclusion that H_2O_2 is more reactive as a reducing agent at high pH values where it undergoes photolysis to give $O_2^{\cdot-}$.

The scavenging effect on addition of SOD with any of the sensitisers to the irradiated phage suspension provides additional support to the conclusion obtained from the NBT assay (discussed in Chapter 3), where $O_2^{\cdot-}$ / $HO_2^{\cdot}$ was shown to be a major product in the NUV photolysis of the sensitisers under investigation. The results in this chapter also support the generation of $O_2^{\cdot-}$ when L-histidine (Figures 4.2 and 4.3), L(+)mandelic acid (Figures 4.4 and 4.5) or β–phenylpyruvic acid (Figure 4.8) are irradiated with NUV. Thus, in the presence of SOD, phage inactivation was reduced to about 74 % and 92 % on photolysis of L-histidine at pH 7.5 and 9 respectively and 71 % and 90 % on photolysis of L(+)mandelic acid at pH 7 and 9 respectively. The protective effect of SOD on phage viability in the presence of β–phenylpyruvic acid and NUV (Figure 4.8), on the other hand, allowed to about 87

% inactivation. This, however, seems greater than the equivalent result from the NBT assay for this compound (Table 3.2).

Furthermore, SOD results showed photolysis of *p*-OH-phenylpyruvic acid (Figures 4.6 and 4.7) to generate a significant amount of $O_2^{\cdot-}$, this being greater at pH 9 than at pH 7.5 (T7 inactivation was reduced to around 76 % and 78 % at pH 7.5 and 9 respectively). This observation could not be made using the NBT assay, since in the presence of NUV, a mixture of NBT, SOD and *p*-OH-phenylpyruvic acid resulted in the formation of a brown product that interfered with the detection of the blue formazan.

A question arises at to whether the protective effect observed in the phage assay by SOD or catalase was due to the enzymatic properties of these scavengers and not due to their proteinaceous nature. The use of 0.5 mg ml^{-1} BSA and denatured catalase in the experiments (Figures 4.2, 4.4, 4.6, 4.7 and 4.8), and their inability to prevent T7 inactivation to the same extent as catalase, show that the effect of the latter is indeed due to its enzymatic properties. In the case of SOD, however, there is little difference between the result of this enzyme and the quenching observed for BSA or denatured catalase. A small protection from inactivation using catalase or SOD must be attributed to their proteinaceous nature and the extent of such protection would be equal to that observed by BSA and denatured catalase. This effect may be due to non-specific competitive quenching and reflects competition between phage particles and protein, rather than specific scavenging. The inability of SOD to protect the phage in the same extent as catalase, may reflect a lack of involvement of $O_2^{\cdot-}$ in the inactivation of the phage particles. The case may be that most of the lethality observed in the bacteriophage is due to ROS like $^{\cdot}OH$ and $^1O_2$. $^{\cdot}OH$, in particular, is very reactive species and is known to readily react with all nucleobases causing DNA modification and DNA-protein cross-links (Cadet *et. al.*, 2000; Nackerdien *et. al.*, 1991).

When mannitol was included in the irradiated T7 suspension in the presence of *p*-OH-phenylpyruvic acid at pH 9, it had no protective effect (Figure 4.6). The same was observed for sodium benzoate in the presence of NUV plus L-histidine (Figure 4.3) and L(+)mandelic acid (Figure 4.5) at pH 7.5 and 7 respectively. Both mannitol

and sodium benzoate have high affinity for ·OH and react with rate constants of 2.7 x 10^9 M^{-1} s^{-1} and 4.3 x 10^9 M^{-1} s^{-1} respectively (Halliwell and Gutteridge, 1999). The inability of these ·OH scavengers to prevent phage inactivation reflects the very short half-life and high reactivity of ·OH, as well as the possibility that the generation of ·OH from H_2O_2 is highly localised. H_2O_2 could be long enough lived to reach key targets such as the phage genome before generating the more harmful ·OH in a Fenton-like reaction. It is also important to note that ·OH is a minor product of the photolysis of these sensitisers compared to $O_2^{\cdot-}$, as indicated by the low levels detected by the deoxyribose assay (Table 3.6).

Exposure of the phage to sodium azide and DABCO induced inactivation that interfered with the experiment. Incubation of a phage suspension with these scavengers in the absence of NUV or sensitiser caused phage inactivation in a time and concentration dependent manner indicating toxicity to the phage particles that was independent of photolysis. Thus, the use of these $^1O_2$ scavengers was inappropriate in this system. However, when β–carotene was added to the irradiated phage suspension in addition to the sensitiser, it showed a protective effect on phage viability at pH 7, 7.5 and 9 (Figures 4.4-4.8). Although β–carotene is a well-known $^1O_2$ quencher (Beutner *et. al.*, 2000; Kohen *et. al.*, 1995; Menon, 1992; Palozza and Krinsky, 1992) the protective effect observed in the phage experiments may be partially due to this scavenger acting as a filter of NUV as it exhibits some absorption in the NUV region (A_{330} = 0.184 at 50 mM concentration) (Figure 4.10). Thus, even though the protective effect of β–carotene on phage inactivation apparently supports the generation of $^1O_2$ upon photolysis of L(+)mandelic acid (Figures 4.4 and 4.5), *p*-OH-phenylpyruvic acid (Figures 4.6 and 4.7) and β–phenylpyruvic acid (Figure 4.8), further experiments on the accurate detection of $^1O_2$ in the irradiated phage suspension (e.g. using a chemical trap or spectroscopy) would be required to confirm this conclusion.

The T7 inactivation attributed to ROS produced on photolysis of β–phenylpyruvic acid is greater than that observed for the other sensitisers at a similar pH (Figures 4.3 and 4.5). This observation is in agreement with the results obtained in the NBT assay, where β–phenylpyruvic acid was clearly shown to act as the best

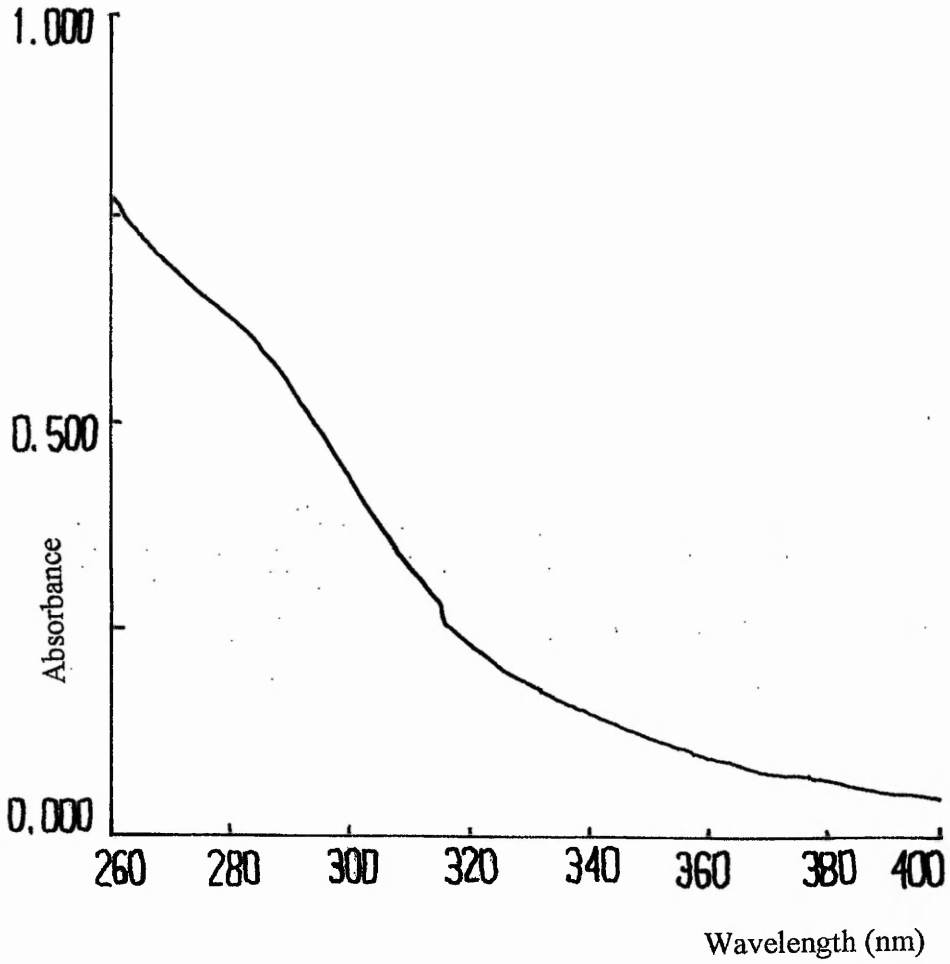

Figure 4.10: Absorption spectrum of a 50 mM aqueous suspension of β–carotene in phosphate buffer, pH 7.

photosensitiser at pH 7 and 7.5 (Table 3.1), and reflects the high absorption profile of this compound in the NUV region of interest [Figure 3.3 (c)]. Therefore, the high potential of β–phenylpyruvic acid to cause phage inactivation when photolysed comes as additional support to the conclusion that at near physiological pH values, which are more common in a natural biological environment, the NUV photolysis of even small concentrations of β–phenylpyruvic acid may be more biologically relevant than that of other sensitisers.

Finally, the synergistic effect of NUV plus L-histidine, L(+)mandelic acid, *p*-OH-phenylpyruvic acid or β–phenylpyruvic acid on T7 phage viability was compared to that of the photolysis of NADH (Figure 4.9 and Table 4.1). From this, the ability of NADH to act as a photosensitiser and cause phage inactivation becomes evident. Also, the protective effect of SOD indicates that $O_2^{\cdot-}$ is generated when NADH is treated with NUV, as previously reported (Cunningham *et. al.*, 1985; Burchuladze and Fraikin, 1991), and that this radical is indirectly responsible for phage inactivation. However, the photolysis of L-histidine (Figure 4.2), L(+)mandelic acid (Figure 4.4), and *p*-OH-phenylpyruvic acid (Figure 4.6) at pH 9 and β–phenylpyruvic acid at pH 7 (Figure 4.8) resulted in greater reduction of phage viability compared to that of NADH at pH 9 indicating that these compounds are potentially more important as photosensitisers.

The difference between NADH and the photosensitisers proposed in this study may be in the sequence of ROS generation. Thus, whereas NADH in the presence of NUV was shown to initially generate $O_2^{\cdot-}$ and through dismutation, Heber-Weiss and Fenton reactions $^1O_2$, H_2O_2 and $^{\cdot}OH$ (Burchuladze and Fraikin, 1991), the NUV photolysis of the sensitisers in this study was proposed to result in direct production of $^1O_2$, H_2O_2 and $^{\cdot}OH$ (section 3.7). $O_2^{\cdot-}$ is of relatively low reactivity and does not react directly with nucleotides and amino acids (Cadet *et. al.*, 1992; Halliwell and Gutteridge, 1999). This may be reflected in the lower level of phage T7 inactivation observed for NADH at pH 9 compared to that of the other sensitisers (Table 4.1).

The overall conclusion that can be drawn from the results for photosensitised T7 inactivation is that phage viability is reduced in a logarithmic manner related to the

NUV dose applied. Since some inactivation is always present and addition of ROS scavengers does not result in total protection, it can be concluded that NUV is also absorbed by the protein and DNA molecules of the phage, causing direct, irreversible damage. This is especially the case for the UVB component of the radiation source (1.2 %) as such wavelengths are more readily absorbed by these biomolecules (Beer *et. al.*, 1993; Peak and Peak, 1989; Pourzand and Tyrrell, 1999). The fact that this damage is greater at pH 9 can be attributed to pH dependent photosensitisation of the small amount of endogenous sensitisers that are present in the phage proteins, i.e. the amino acids tryptophan, tyrosine, phenylalanine and histidine (Graggs *et. al.*, 1994; Kohen *et. al.*, 1995; Paretzoglou *et. al.*, 1998).

4.3 Photosensitised Lethality in Bacteria

4.3.1 Introduction

The photodynamic action of various compounds has been tested in the past in an attempt to discover alternative methods for the treatment of bacterial infections (Ceburkov and Gollnick, 2000; Martinez and Chignell, 1998; Oroskar *et. al.*, 1995). Thus, photodynamic antimicrobial chemotherapy, involving photosensitisers and visible or UV light has been proposed as a treatment of locally occurring infections, such as periodontal diseases, infected wounds and skin conditions. In this way, some of the best photosensitisers, namely porphyrins and phthalocyanines have been proven to show low toxicity to host cells and are now in common usage in photodydamic therapy, whereas a combination of UVA and psoralens form the basis of photochemotherapy (Ceburkov and Gollnick, 2000).

Studies, however, have shown that gram-negative bacteria are resistant to such treatments (e.g. Dahl *et. al.*, 1989; Padula *et. al.*, 1996). Resistance is mainly due to the properties of the outer membrane of gram-negative bacteria, absent from the gram-positive cells. The cell wall of gram-negative bacteria contains a lipopolysaccharide coat that offers some protection from the toxic effects of exogenous agents. This is accomplished by the outer membrane functioning as a structural barrier against the penetration of hydrophobic or high molecular weight compounds into the cell, and by preventing the binding of these compounds to the

cytoplasmic membrane. In addition, the unsaturated fatty acids and proteins of the outer membrane are known to react with $^1O_2$ and other ROS, thus forming a chemical trap for these radicals. Gram-positive bacteria, on the other hand, have thin cell membranes, which are porous to photosensitisers making them more susceptible to the photolytic action of these agents.

Studies of the sensitivity of bacteria to $^1O_2$ showed that the concentration of $^1O_2$ required to effectively kill bacteria (the gram-negative *Salmonella typhimurium* and *E. coli*) was found to be several orders of magnitude lower than that of H_2O_2 needed to achieve the same effect (Dahl *et. al.*, 1987). It was also found that the outer cell wall of gram-negative cells initially protects from extracellular $^1O_2$, although it may also serve as a source of secondary reaction products, which increase the rate of killing (Dahl *et. al.*, 1987; Dahl *et. al.*, 1989). $^1O_2$ is known to react with cell membranes causing lipid peroxidation, a process that can result in membrane leakage and, eventually, cell lysis (Schafer and Buettner, 1999). Additionally, gram-positive strains (of *Staphylococcus aureus* and *Sarcina lutea*) that contained high levels of carotenoids were found to be more resistant to lethality than non-pigmented mutant strains of the same organisms, indicating that lethality was due to $^1O_2$ (Dahl *et. al.*, 1989).

4.3.2 The Synergistic Effect of NUV plus β–Phenylpyruvic Acid or L(+)Mandelic Acid on Bacterial Cells

Using the NBT assay, β–phenylpyruvic acid was shown to undergo photolysis in the presence of NUV [Figure 3.6(d)] and indirect evidence collected indicated that ROS including H_2O_2, $O_2^{\cdot-}$, $^1O_2$ and $^{\cdot}OH$ were generated at pH 7. In addition, when exposed to NUV (9.9×10^4 Jm^{-2}) β–phenylpyruvic acid can cause T7 inactivation by two logs at this pH (Figure 4.8). Thus, the question arises as to whether NUV plus β–phenylpyruvic acid can have a similar synergistic effect on a bacterial system. Therefore, the susceptibilities of three bacterial species (*E. coli*, *S. aureus* and *E. faecalis*) to NUV in the presence and absence of β–phenylpyruvic acid at pH 7 were examined.

Experiments were carried out by the *in vitro* exposure of *E. coli* cultures to NUV in the presence and absence of the sensitiser, as described in section 2.6. The selection of two strains of *E. coli*, KL16 and SA162 was on the basis of their genetic make up. *E. coli* KL16 is the wild type, whereas *E. coli* SA162 is a DNA-repair mutant strain (*uvrA*) deficient in excision endonuclease enzymes that are involved in repairing UV induced DNA damage (Van Houten, 1990). A comparison on the effect of treatment between the two strains may give an insight in the factors affecting cell survival.

Data presented in Figure 4.11 demonstrates the effect of NUV in the presence and absence of β–phenylpyruvic acid on the two strains of *E. coli*, KL16 and SA162. *E. coli*, KL16 was found to be fairly resistant to treatment by NUV alone (49 % cell death was observed when exposed to 11.88×10^4 Jm^{-2}). The synergistic action showed little additional inactivation, with the effect being greater at higher energy exposures. *E. coli* SA162 on the other hand, was found to be more susceptible to NUV irradiation (NUV alone causing 97 % inactivation), and this effect was enhanced in the presence of β–phenylpyruvic acid.

From the results shown in Figure 4.11, the following observations can be made: treatment with NUV alone resulted in some inactivation of *E. coli* KL16 cells but in considerably higher lethality of *E. coli* SA162. In both cases, cell death is independent of photolysis and does not involve the photosensitised generation of ROS. Thus, it must be the direct absorption of the irradiation energy that leads to inactivation. Since the cell components that can absorb NUV radiation and subsequently be modified to such extent that would be lethal to the cell are the DNA and proteins, it is these two types of biomolecules that must be affected. Also, since both strains of bacteria receive an equal energy dose, a similar degree of inactivation would be expected. This is not the case, however. With both strains being *E. coli*, they would contain roughly the same amount of protein and DNA. The only difference between the two strains is that, as mentioned above, *E. coli* SA162 is a DNA repair mutant strain. It can, therefore, be argued that the lethality of NUV lies in inducing DNA damage, and that the increased cell death observed for *E. coli* SA162 would be a result of the inability of this organism to repair this damage. The

wild type *E. coli*, on the other hand, has functional DNA repair mechanisms and can therefore survive a fair amount of DNA damage. This would explain why there is only 49 % cell death observed for *E. coli* KL16 when irradiated with NUV (11.88 x 10^4 Jm^{-2}) compared to 97 % lethality observed for *E. coli* SA162 when exposed to the same energy dose.

It is known that DNA can absorb in the UVB region of the spectrum, and that such an energy exposure is capable of causing DNA base dimerisation and photoproduct formation (Cadet *et. al.*, 1992; Kohen *et. al.*, 1995). If not repaired (as it may well be the case for *E. coli* SA162), these types of damages can be lethal. Whereas the UVB present (1.2 %) in the UV source employed in the experiments may be responsible for direct DNA damage, the UVA component (98.8 %) of the NUV lamp may be responsible for indirect DNA damage *via* photosensitisation reactions as has been previously reported (Cadet *et. al.*, 1999; Dizaroglu, 1993).

Treating the two cultures with NUV plus β–phenylpyruvic acid resulted in 59 % lethality for *E. coli* KL16 and 99.4 % lethality for *E. coli* SA162 when exposed to 11.88 x 10^4 Jm^{-2} (Figure 4.11). The additional effect observed in the presence of β–phenylpyruvic acid can be attributed to cellular damage caused by ROS. From the literature, it appears unlikely that any effect attributed to ROS like $^{\cdot}OH$, $^1O_2$ and $O_2^{\cdot-}$ is due to DNA damage, unless their generation takes place on or near the DNA (Halliwell and Gutteridge, 1999). For this to happen, the sensitiser must penetrate the cell and bind to the DNA. This is less likely to happen in gram-negative cells that have a protective outer cell membrane.

Thus, the majority of ROS generated outside the cell will be unable to react with key targets and cause inactivation. In addition, $O_2^{\cdot-}$ does not readily cross biological membranes due to both being negatively charged. The protonated form of $O_2^{\cdot-}$ ($HO_2^{\cdot}$), however, like H_2O_2 are uncharged and can, therefore, cross membranes easily (Aikens and Dix, 1991). Also, given its relatively long half-life, H_2O_2 can, after its formation outside the cell, cross the cell membrane and react to give $O_2^{\cdot-}$ and $^{\cdot}OH$ that can damage the bacterial genome. Furthermore, the presence of $^1O_2$ and $^{\cdot}OH$ in the immediate cell environment may initiate lipid peroxidation causing irreparable

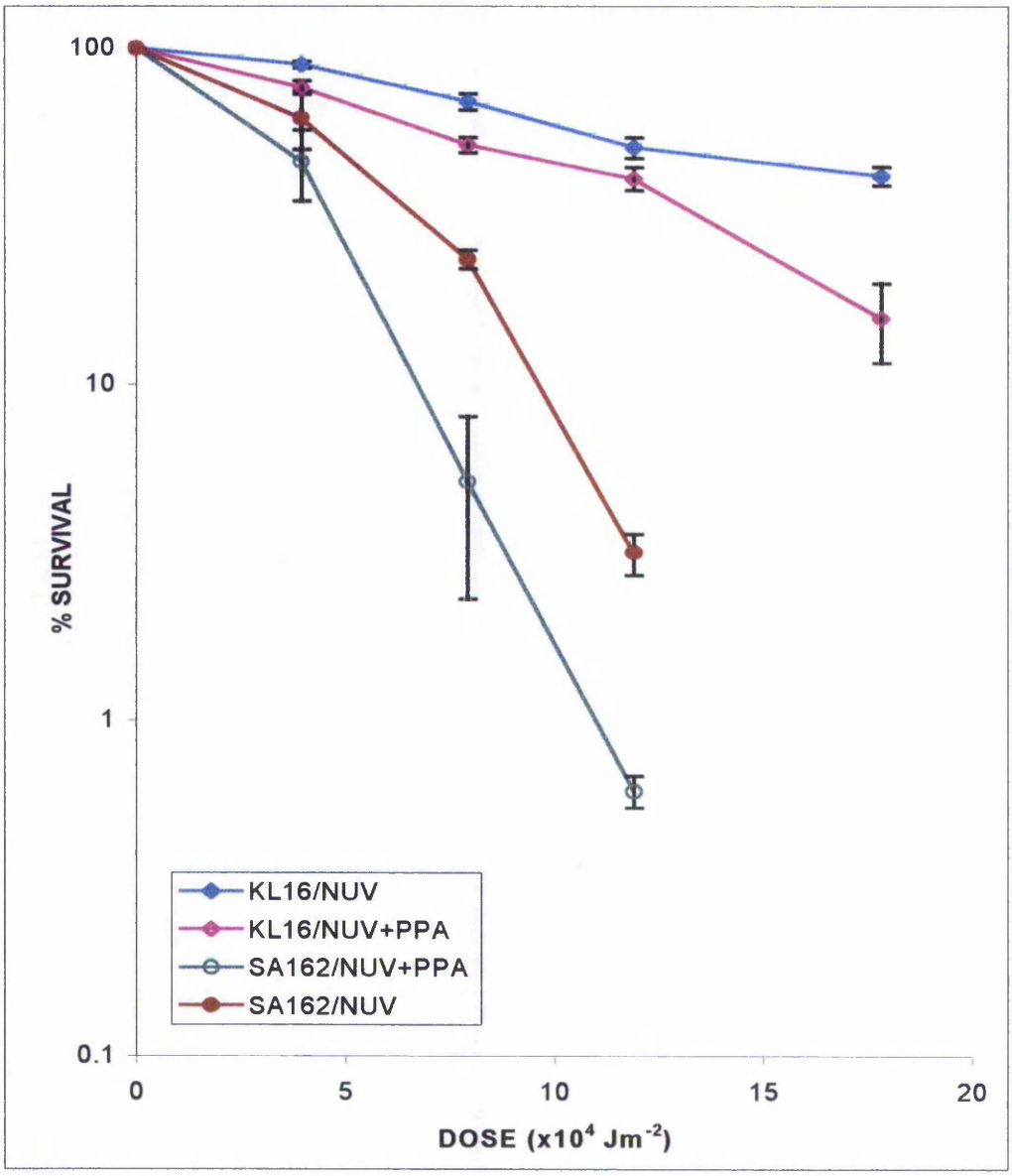

Figure 4.11: The effect of NUV ± β–phenylpuruvic acid (PPA) on *E. coli* survival. *E. coli* KL16 (wild type) was irradiated with NUV alone (◆), (n=10), or NUV plus 1 mM β–phenylpuruvic acid (✧), (n=6). The % survival was compared to *E. coli* SA162 (DNA repair deficient) treated with NUV alone (●), (n=2) or in the presence of 1 mM β–phenylpuruvic acid (o), (n=2). Each point represents the mean ± the standard error of the mean.

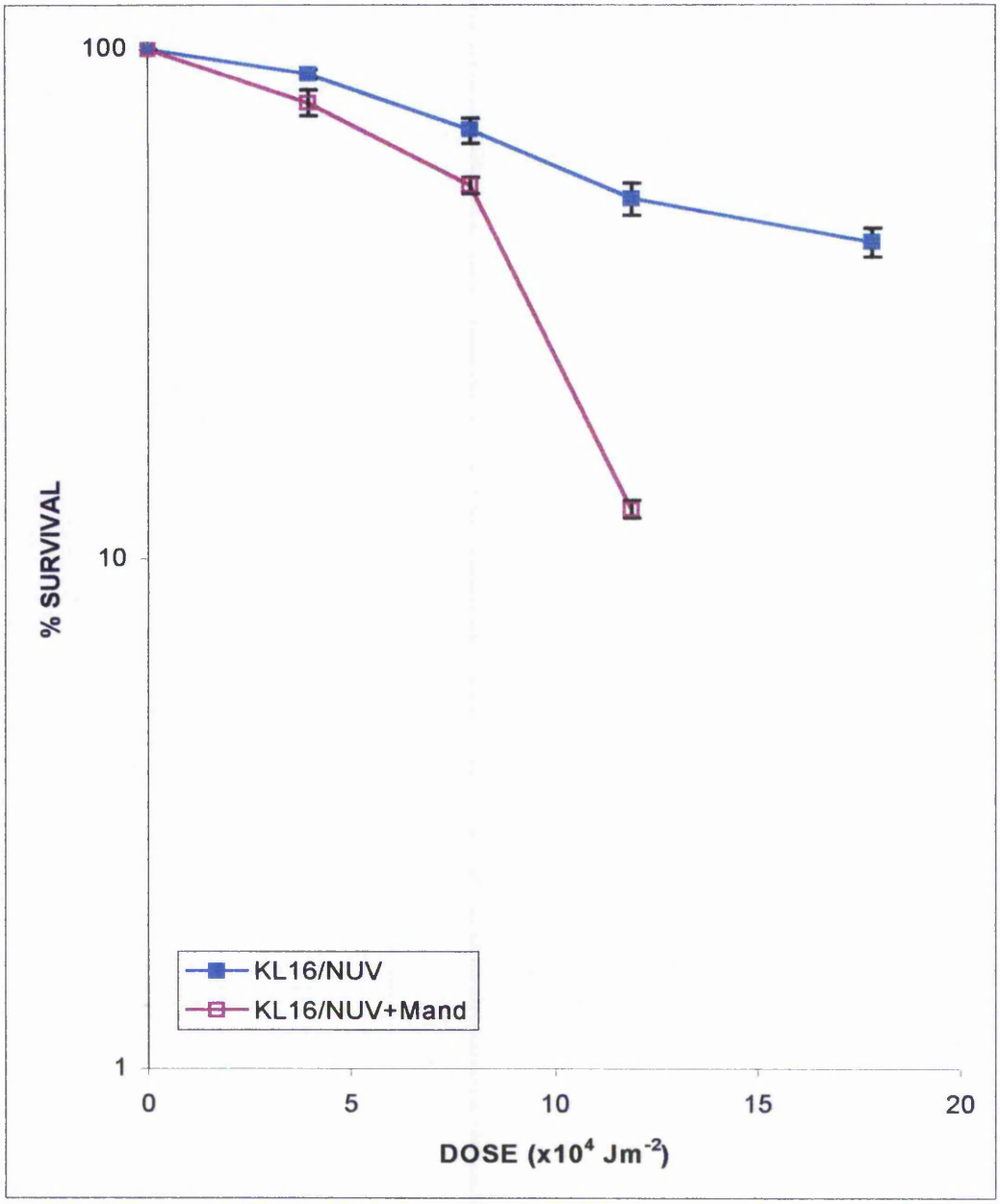

Figure 4.12: The effect of NUV ± L(+)mandelic acid on the survival of *E. coli* KL16. *E. coli* KL16 was irradiated with NUV alone (■), (n=10), or NUV plus 1 mM L(+)mandelic acid (□), (n=2). Each point represents the mean ± the standard error of the mean.

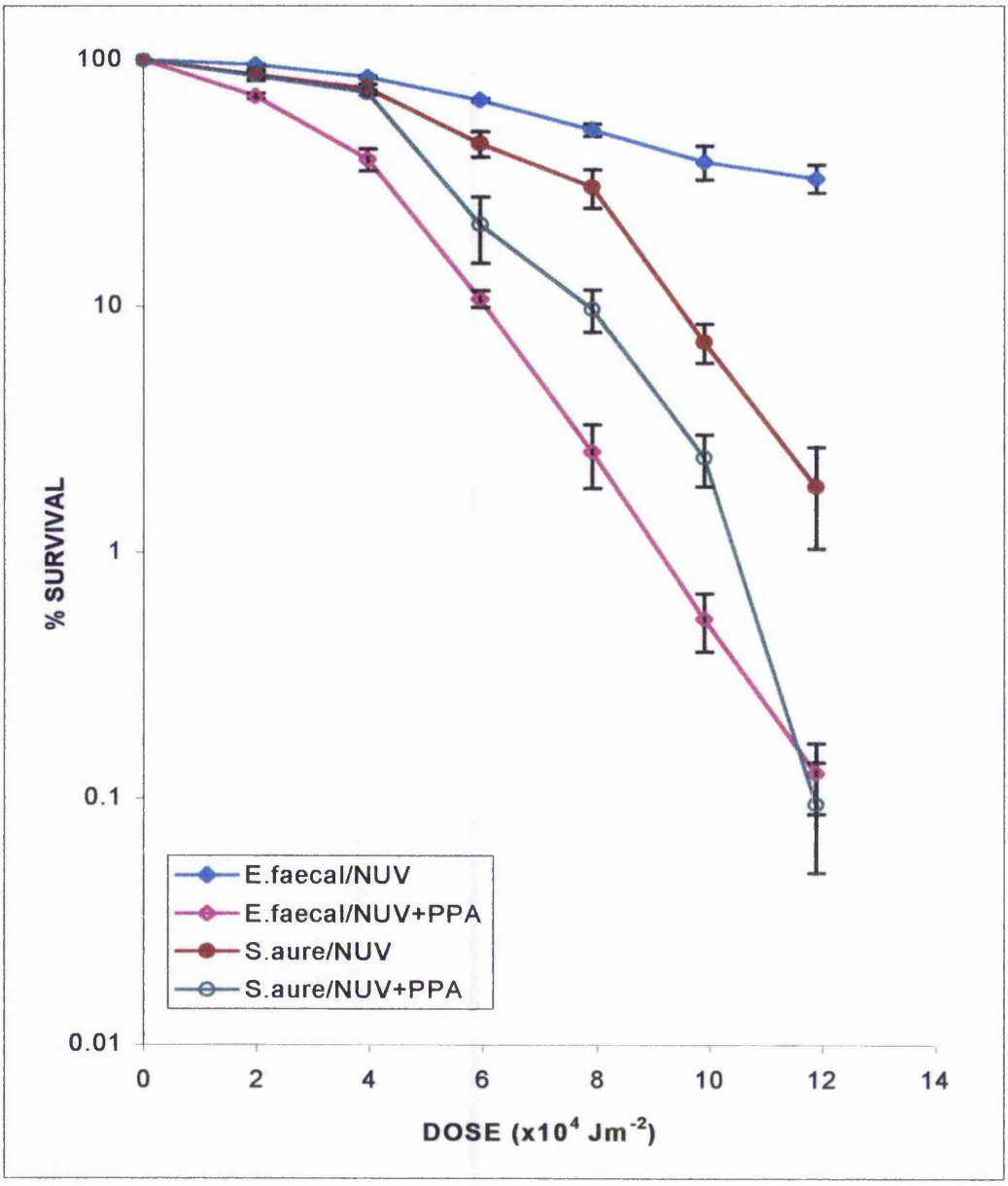

Figure 4.13: The effects of NUV ± β–phenylpuruvic acid (PPA) on *E. faecalis* and *S. aureus* survival. *E. faecalis* was irradiated with NUV alone (◆), (n=4), and NUV plus 1 mM β–phenylpuruvic acid (◇), (n=3). The % survival was compared to *S. aureus* treated with NUV alone (●), (n=3) or in the presence of 1 mM β–phenylpuruvic acid (o), (n=3). Each point represents the mean ± the standard error of the mean.

damage to the cell membrane resulting in membrane leakage and eventually cell lysis. Since $O_2^{\cdot-}$, H_2O_2, $^{\cdot}OH$ and $^1O_2$ are generated by β–phenylpyruvic acid in the presence of NUV (Table 3.4 and Figure 4.8), this may well be the case in the experiments involving *E. coli* cells.

When β–phenylpyruvic acid was replaced with L(+)mandelic acid in the *E. coli* KL16 suspension, similar results were observed (Figure 4.12). NUV photolysis of L(+)mandelic acid resulted to the same amount of cell death as noted for β–phenylpyruvic acid for exposures up to 7.92×10^4 Jm^{-2}, but at a higher NUV dose (11.88×10^4 Jm^{-2}) increased lethality was observed (about 88 % inactivation). As seen in Chapter 3, the photolysis of L(+)mandelic acid generated a greater apparent concentration of both $O_2^{\cdot-}$ (Table 3.3) and $^{\cdot}OH$ (Table 3.6) than the other sensitisers at pH 9, probably by a mechanism other than direct photolysis of the compound. The case may be that in the experiments involving *E. coli* cells, even though they were carried out at pH 7, a significant amount of ROS was present. The bacterial cells seemed able to withstand a fair amount of stress, but at high NUV doses / ROS concentrations, the cellular damage occurring becomes irreversible.

Treatment of the *E. coli* KL16 culture by L(+)mandelic acid alone (in the dark) did not affect cell survival, indicating that this compound does not display any toxicity to this organism. In Chapter 3, it was suggested that since L(+)mandelic acid does not exhibit a strong absorption in the NUV spectrum, the photosensitised effects observed may be due to the formation of a complex, yet to be defined, that on NUV absorption can generate ROS. Since a synergistic action between L(+)mandelic acid and NUV is evident in the inactivation of *E. coli* KL16, a similar mechanism of action, i.e. the formation of a complex between this compound and a cell component that renders L(+)mandelic acid with photosensitiser properties, may be in operation. However, the only evidence for this argument is the lethality observed, therefore, further work is necessary to elucidate the mode of action of L(+)mandelic acid.

Exposure of the gram-positive bacteria *E. faecalis* and *S. aureus* (both wild type) to NUV (11.88×10^4 Jm^{-2}) in the presence of β–phenylpyruvic acid resulted in 99.9 % cell death for both species (Figure 4.13). This synergistic effect was much

greater than that observed for the gram-negative *E. coli* cells (Figure 4.11). Incubation of the bacteria with 1 mM β–phenylpyruvic acid alone did not affect cell survival, indicating that this compound is not toxic to the cells and acts only in a synergistic way.

From Figure 4.13, it can also be noted that NUV alone caused a higher degree of cell death to the two gram-positive species compared to the *E. coli* KL16 cells exposed to the same energy dose (Figure 4.11). Thus, exposure of *E. faecalis* to NUV alone resulted in 67 % inactivation compared to 49 % inactivation observed for *E. coli* KL16 when treated with the same NUV dose. Since gram-negative bacteria have an extra outer membrane compared to the gram-positive ones, it may be possible that this membrane acts as a filter of NUV (i.e. membrane components absorb some of the NUV) causing less irradiation to reach the bacterial genome. Although absorption of NUV by the phospholipid membrane would result in lipid peroxidation, this effect may not be as lethal to the cell as a higher UV exposure to the DNA. The lack of a double phospholipid membrane may explain why the gram-positive *E. faecalis* is more susceptible to NUV than *E. coli* KL16.

In addition, compared to *E. faecalis*, *S. aureus* showed increased sensitivity to NUV treatment (with 98.2% lethality observed). Apparently, exposure to a NUV dosage higher than 4×10^4 J m^{-2} is able to cause irreversible inactivation of this organism. This finding is supported by the literature, where *S. aureus* was found to be sensitive to UV radiation. Thus, in a study by Jekler *et. al.* (1992) for example, UVB radiation was found to have an antimicrobial effect primarily on *S. aureus*. Also, from their studies, Yoshimura *et. al.* (1996) concluded that since *S. aureus* is often associated with the condition atopic dermatitis, and given its high sensitivity to NUV, phototherapy provides one of the most effective ways of treatment.

The increased lethality of *S. aureus* and *E. faecalis* attributed to the photolysis of β–phenylpyruvic acid indicates that the sensitiser may either easily enter gram-positive cells or bind to them, and then undergo photolysis. Indeed, other photosensitisers (e.g. haematoporphyrin, phycocyanin) have been reported to attach firmly to the membrane of gram-positive but not of gram-negative bacteria although

the exact location of binding has not been determined (Padula *et. al.*, 1996). This binding is believed to be essential for the photosensitised action of the sensitiser, as the incorporation of the sensitiser into the cells is much more important than the production of ROS.

Furthermore, as described earlier, several studies of the toxicity of bacteria to $^1O_2$ showed that gram-positive cells are more susceptible to damage induced by this ROS (Dahl *et. al.*, 1987; Dahl *et. al.*, 1989; Pellieux *et. al.*, 2000). In the later study, experiments that involved *E. coli* and *S. aureus* showed that the gram-positive *S. aureus* was 10 times more susceptible to inactivation than the gram-negative *E. coli*, although no explanation was given for this difference. Since a similar result can be observed in Figures 4.11 and 4.12, it can be suggested that the photosensitised action of β–phenylpyruvic acid on bacterial cells may be due to the generation of $^1O_2$. The production of $^1O_2$ on NUV photolysis of β–phenylpyruvic acid is supported by the protective effect of β–carotene on phage T7 inactivation (Figure 4.8). However, unlike other studies (Dahl *et. al.*, 1987; Dahl *et. al.*, 1989) where toxicity to bacteria was by pure $^1O_2$ (a physical separation between sensitiser and substrate prevented non-$^1O_2$ reactions from occurring), during the NUV photolysis of β–phenylpyruvic acid in this study, various ROS such as $^{\cdot}OH$, $O_2^{\cdot-}$, and $^1O_2$ are produced simultaneously and it is therefore difficult to assess the role of each species unambiguously in the resulting biological effects.

An additional observation from results on the photosensitised lethality of bacterial cells is that the amount of cellular damage inflicted on the bacterial cultures is greater than that expressed as cell death. After a 30-min irradiation, and incubation of the bacterial cells for up to 48 hours (section 2.6), it was noticed that they take longer to grow and form smaller colonies compared to non-irradiated controls. This observation may suggest that many types of cellular damage (e.g. damage to DNA) may be repairable and thus not lethal to the cell, or that some types of damage to cell components are not lethal ones (e.g. lipid peroxidation can be terminated by endogenous antioxidants or the resulting hydroperoxides can be removed from the cell). In both cases, cell division would be postponed until the cell is functional.

4.4 Determination of Endogenous Concentrations of β–Phenylpyruvic Acid in *E. coli* KL16 and *E. faecalis* Using High Performance Liquid Chromatography (HPLC)

The importance of ROS generation by photosensitisation on inducing a biological effect would depend on the cellular concentration of the sensitiser. Since most ROS have very short half-lives, only those generated on, or near, cellular targets would have a damaging effect. Thus, the incorporation of the sensitiser into the cell is much more important than the production of ROS. It is, therefore, of interest to determine the location of a photosensitiser in relation to the cell (inside or outside the cell membrane), in order to evaluate and explain its photodynamic action on bacteria.

After demonstrating the potential of β–phenylpyruvic acid to act as a sensitiser of NUV generating a variety of ROS and causing phage T7 inactivation and bacterial cell death at pH 7, its biological importance was further investigated by determining its intracellular concentrations in two bacterial species. Thus, the presence of endogenous levels of β–phenylpyruvic acid in *E. coli* KL16 and *E. faecalis* and the uptake of the sensitiser by these bacteria were investigated using HPLC (section 2.7). The results are summarised in Table 4.2.

The specificity of the method used towards β–phenylpyruvic acid was tested by incorporating aromatic compounds with similar structures to this biochemical. Thus, injecting 100 nM of tyrosine, phenylalanine or *p*-OH-phenylpyruvic acid into the column gave no peak, whereas addition of 50 nM of these compounds to a 50 nM standard solution of β–phenylpyruvic acid resulted in a peak with the same peak area as that of 50 nM of β–phenylpyruvic acid alone.

Extracts of approximately 1 x 10^8 *E. coli* KL16 and 6 x 10^8 *E. faecalis* cells were used for the preparation of the samples injected into the HPLC column as described in section 2.7.2. It can be seen in Table 4.1 that both *E. coli* KL16 and *E. faecalis* contain small amounts of β–phenylpyruvic acid naturally (27.4 and 28.4 nmoles per 1 x 10^8 cells respectively). After a 30-min incubation of the cells in 1 mM β–phenylpyruvic acid however, both the *E. coli* and *E. faecalis* samples showed

increased endogenous levels of the sensitiser. All the β–phenylpyruvic acid treated *E. coli* KL16 and *E. faecalis* samples gave higher peaks than those of the untreated cells (Table 4.2).

β–PHENYLPYRUVIC ACID STANDARD SOLUTIONS (nM)	PEAK AREA	BACTERIAL SAMPLE	PEAK AREA	CONCENTRATION OF PPA / 1 x 10^8 CELLS (nmoles)
0	0.000			
10	10.126	*E. coli* KL16	20.164	27.4
20	20.835	*E. coli* KL16 + PPA	29.547	45.0
40	27.414	*E. coli* KL16 + PPA	23.027	32.8
60	45.203	*E. faecalis*	20.696	28.4
80	44.154	*E. faecalis* + PPA	31.470	48.6
100	56.360	*E. faecalis* + PPA	33.454	52.4

Table 4.2: HPLC analysis of β–phenylpyruvic acid concentrations in *E. coli* KL16 and *E. faecalis*. A series of β–phenylpyruvic acid standard solutions of known concentrations were used for the determination of a standard curve. The fourth column represents the readings for a number of *E. coli* KL16 and *E. faecalis* samples, some pre-treated with 1 mM β–phenylpyruvic acid (PPA) as described in section 2.7.

From the equation of the trendline of the standard curve, the concentrations of β–phenylpyruvic acid in the bacterial samples were calculated. The results are shown in the last column of Table 4.2. From this, the β–phenylpyruvic acid-treated *E. coli* cells show an average 11.5 nmoles increase in endogenous β–phenylpyruvic acid over the untreated culture. The average increase of β–phenylpyruvic acid in the treated *E. faecalis* cells was 22.1 nmoles over the untreated control. This is almost double the concentration detected in the untreated sample and twice as much an increase as that observed in the *E. coli* samples. Thus, *E. faecalis* can incorporate β–phenylpyruvic acid faster and more efficiently than *E. coli* over the same time period. The difference in the uptake of the sensitiser by the two bacteria probably lies in the different structure of their cell membranes. The HPLC results support further the conclusions of section 4.3.2 that the ability of β–phenylpyruvic acid to enter and remain in the

gram-positive *E. faecalis* or bind firmly to its cell membrane makes the cells more susceptible to sensitised NUV damage.

However, it is possible that the photodynamic action of β–phenylpyruvic acid and its lethality towards cells may be due to binding to the cell membrane rather than entering the cell. Even though gram-positive cells have a more porous membrane than the gram-negative ones, β–phenylpyruvic acid is expected to carry a negative charge that would lead to localisation of this compound on the outer surface of the membrane - because the sensitiser is ionic (and hence water soluble) it has a low affinity for the hydrophobic, lipid part of the membrane. However, although water soluble, β–phenylpyruvic acid also has a hydrophobic group (the phenyl ring) which could preferentially locate in the inner, hydrophobic part of the membrane. Therefore, the suggestion is that the hydrophilic, ionic group of β–phenylpyruvic acid (the carboxylate) remains on the outer region of the cell membrane, whilst the phenyl group penetrates further to the inner part of the membrane. The carbonyl group, which is believed to be the chromophore as described in Chapter 3 (and therefore the locus of ROS generation) is located mid-way between the carboxylate and phenyl groups on the molecule. The fact that both the gram-positive *E. faecalis* and the gram-negative *E. coli* contained elevated amounts of β–phenylpyruvic acid after incubation in the presence of this compound, indicates that this binding occurs in both species, but it is found to a greater extent in the gram-positive cells.

Therefore, it is possible to explain the differing susceptibility of the gram-positive and gram-negative species on the basis of the known differences in membrane structure. In the gram-negative case, there is a double phospholipid membrane (the plasma and outer membranes) and so it is likely that the sensitiser would preferentially locate in the outer membrane, where ROS generation would have less of an impact on the survival of the cell. In summary, it is probable that attachment of β–phenylpyruvic acid to the outer membrane of gram-negative cells would prevent this sensitiser from moving further through the cell wall to regions where it would have a greater damaging effect. It has been reported that other sensitisers (e.g. phycocyanin, haematoporphyrin and its derivative, photofrin) exhibit differences in their binding to the membranes of gram-positive and gram-negative

bacteria (Padula *et. al.*, 1996). Compared to these biomolecules, β–phenylpyruvic acid is much smaller in size and therefore it could be expected to incorporate into the cell more easily. In the case of gram-positive bacteria, it may be possible that due to its small size, β–phenylpyruvic acid could diffuse through the outer peptidoglycan layer of the gram-positive cell wall and become incorporated into the plasma membrane. Then on NUV photolysis, ROS generated at this location could target cell components. In conclusion, the difference between the gram-positive and negative species may be due to the fact that there is a double phospholipid membrane in the latter case, and that the outer of these membranes acts as a trap leading to the preferential location of the sensitiser in an area where its effects will be less lethal. In the case of gram-positive species no such barrier is available.

Among the ROS generated on the photolysis of β–phenylpyruvic acid, $^1O_2$ is believed to play an important role in the inactivation of bacteriophage T7 and possibly the bacteria cells. The virucidal and bactericidal action of $^1O_2$ has been previously reported (Dahl *et. al.*, 1987; Dahl *et. al.*, 1989; Pellieux *et. al.*, 2000). Also, it has been demonstrated that $^1O_2$ would be highly localised in the hydrophobic region of a membrane, irrespectively of its generation site, because of its higher solubility in the inner hydrophobic region with low polarity (Fukuzawa, 2000). The attachment of β–phenylpyruvic acid on the cell membrane would ensure the generation of $^1O_2$ in a region where it could react with membrane proteins and lipids causing lipid peroxidation. As mentioned earlier, lipid peroxidation may lead to membrane leakage and cell death.

It can, therefore, be concluded that the additional synergistic effect observed when β–phenylpyruvic acid was included in the irradiated cultures (Figures 4.11 and 4.13) may be mainly due to membrane damage rather than damage to the bacterial genome, since ROS generated on the photolysis of this compound would be expected to be highly localised in this area.

It is unlikely that bacteria such as *E. coli* and *E. faecalis* would encounter the concentrations of β–phenylpyruvic acid used in this study in their natural environment. However, HPLC results indicated that β–phenylpyruvic acid could bind

to these bacteria. This finding provides an explanation to the effects the photolysis of this sensitiser had on these bacterial species as observed in section 4.3. Given that β–phenylpyruvic acid is a natural metabolite in humans (thus non-toxic), its use in photodynamic therapy for treatment of bacterial infections may be of consideration.

It would be interesting to carry out further experiments to examine the concentrations of β–phenylpyruvic acid in human cells, and also the potential of these cells to uptake β–phenylpyruvic acid. Skin fibroblasts and keratinocytes would be of particular interest as these types of cells are most highly exposed to solar UV radiation. Such studies would be important especially in cases of phenylketonuria where the presence of elevated concentrations of β–phenylpyruvic acid would be expected.

4.5 Conclusion

The efficiencies of a variety of sensitisers to cause, upon NUV photolysis, irreversible cellular damage to living systems were demonstrated in this chapter. The photolysis of β–phenylpyruvic acid was of particular interest as this sensitiser was shown to produce a comparatively large effect at pH 7, probably reflective of the pH independence of this photolysis. Thus, NUV plus β–phenylpyruvic acid were shown to produce 98 % inactivation of bacteriophage T7 at pH 7, probably by generation of $^1O_2$ and H_2O_2 and subsequently $O_2^{\cdot-}$ and $^{\cdot}OH$. These ROS may target both the protein coat and DNA genome of the phage T7 leading to inactivation. L(+)Mandelic acid and L-histidine produced similar effects at pH 9, whereas *p*-OH-phenylpyruvic acid caused the highest level of inactivation (99.7 %) at this pH. The results of β–phenylpyruvic acid and *p*-OH-phenylpyruvic acid on reducing phage survival may reflect the high absorption of these compounds in the NUV region.

The NUV photolysis of β–phenylpyruvic acid also proved effective in causing lethality to all the bacterial species tested. *E. coli* mutants with a DNA repair deficiency (excision repair) were shown to be more susceptible to damage, indicating that DNA is an important target of photosensitisation leading to cell death. However,

any damage to the DNA may be attributed mostly to the effect of NUV alone, as the DNA can directly absorb some of this irradiation (particularly in the UVB spectrum).

The contribution of photolysis generated ROS in cell inactivation would be mostly due to damage caused in the cell membrane, since the production of ROS would be expected to be highly localised in this area. In addition, gram-positive bacteria were found to be more prone to synergistic inactivation, possibly because of the less complicated structure of their cell membranes. It is suggested that β–phenylpyruvic acid could readily bind to the cell membrane and as a result, on NUV photolysis, ROS would be generated very near to potential cellular targets such as membrane proteins and lipids. This suggestion was supported further by the HPLC results, where the concentration of β–phenylpyruvic acid after UV exposure was indeed shown to be greater in the gram-positive *E. faecalis*.

CHAPTER FIVE

AN INVESTIGATION OF THE EFFECTS OF NUV PLUS SENSITISERS ON DNA, LIPIDS AND PROTEINS

5.1 Introduction

The study of the biological sensitisers undertaken in this work involves an assessment of the ability of the photolytic products of these compounds (H_2O_2, $^{\cdot}OH$, $O_2^{\cdot-}$ / $HO_2^{\cdot}$ and $^1O_2$) to cause molecular damage to DNA, proteins and lipids. In the previous chapter, an attempt was made to identify possible targets of attack for ROS generated on photosensitisation of the compounds of interest that resulted in the inactivation of viruses and bacteria. In this chapter, the examination of the *in vitro* effects of the NUV photolysis of L-histidine, L(+)mandelic acid, *p*-OH-phenylpyruvic acid and β–phenylpyruvic acid on major cellular components, namely DNA, lipids and proteins is undertaken.

DNA is the most important cellular constituent as it is the key element of life. Damage to DNA can lead to mutations or cell death and is one of the major precursors of carcinogenesis in eukaryotes (Schmutte, 1999). Photosensitised modification to proteins may result to DNA-protein cross-links, and formation of aggregates and protein radicals (Dean *et. al.*, 1993; Nackerdien *et. al.*, 1991). Lipids are also an essential component of the cell, as they are the major constituents of cell membranes on which the homeostasis of the cell depends, and their oxidative damage may result in lipid peroxidation, membrane leakage and, eventually, cell lysis (Beer *et. al.*, 1993).

The experiments described in this chapter first focus on the NUV photolysis of β–phenylpyruvic acid, since the potency of this biochemical to generate ROS at near physiological pH (e.g. pH 7.5) has been demonstrated in the previous chapters and most of the cellular components to be studied normally function at this pH. Of particular interest is the genotoxicity of β–phenylpyruvic acid and its ability to cause mutations in bacteria.

In addition, emphasis is given to the type of molecular damage that can be caused by the various sensitisers. This would depend on the nature and the quantity of ROS that are generated on photolysis of a particular sensitiser. In this way the study of photolysis-induced damage to biological components may also give some more information on the ROS involved, as certain types of molecular damage are known to be initiated by a particular kind of ROS. $^{\cdot}OH$ radicals, are known to cause all types of oxidative modification to DNA including sugar lesions, single-strand breaks, and modification to purine and pyrimidine bases (Cadet *et. al.*, 1999; Dizaroglu, 1993). $^1O_2$, on the other hand, whereas also able in producing strand breaks and modifying DNA bases, it has a higher affinity for the guanine residue (Ito *et. al.*, 1993; Stary and Sarasin, 2000). In addition, both $^{\cdot}OH$ and $^1O_2$ are known to participate in the initiation and propagation of lipid peroxidation, whereas H_2O_2 and $O_2^{\cdot-}$ are less reactive and unable to initiate the peroxidation reaction.

5.2 Aims

Further investigation of the role of the photolysis of the sensitisers studied to cause damage to cellular components will involve studies of the individual component in question. The reason for such an approach will be to determine the extent of damage induced under the experimental conditions employed, and also to identify specific types of damage. This, in turn, would enable us to indirectly identify the involvement of particular types of ROS and thus provide supportive evidence for their generation on UVA photolysis. The results of these studies will then be used to evaluate the photosensitising potential of each of the compounds identified as photosensitisers in terms of their biological effect. A comparison of the different compounds to each other and to NADH will lead us to an understanding of their biological significance.

For studying sensitised DNA damage, the pBR322 plasmid DNA was chosen. This plasmid is a common tool for the *in vitro* study of oxidative damage to DNA as single and double strand brakes can be easily identified by agarose gel electrophoresis (Burchuladze and Fraikin 1991; Martinez and Chignell, 1998; Oroskar *et. al.*, 1995; Repanovici *et. al.*, 1997). It will, therefore, be used here as a model system to observe possible strand-break formation as the change of supercoiled to open circular ratio,

and as a possible indication for the involvement of ·OH (Cadet *et. al.*, 1999; Oroscar *et. al.*, 1995). The photosensitised damage to the plasmid will be further investigated by looking at changes of its transformation efficiency. Studies of types of DNA damage other than strand breaking will include an investigation of the mutagenic potential of the sensitisers with a particular interest in the role of base oxidation as the premutagenic modification. Thus, the use of a transversion mutator strain of *E. coli* that is deficient in repairing 8-oxodGuo, or the misincorporation of this modified base during DNA replication, would elucidate a possible role for $^1O_2$ in DNA damage as this ROS modifies selectively guanine residues (Ravanat and Cadet 1995; Stary and Sarasin, 2000). Another tool to study DNA damage *in vivo* will be the triggering of an SOS response in an excision repair deficient strain of *E. coli*.

Moreover, the effect of ROS generated on photosensitised reactions in the initiation and propagation of lipid peroxidation will be studied using liposomes as a model system. The selection of such a system is on the basis that it carries an opposite charge to that of the photosensitiser ensuring strong interaction and formation of ROS near potential lipid targets. Moreover liposomes do not contain any of the antioxidants that are normally present in cells or other potential targets (e.g. proteins) which would lead to an underestimation of ROS involved in the peroxidation process. Generally, the use of liposomes, in combination to using selective scavengers, could elucidate the involvement of $^1O_2$ and ·OH in lipid peroxidation. Following this, the occurrence of lipid peroxidation reactions in bacteria will be investigated with an interest in possible differences between gram-positive and gram-negative species.

Finally, for a more detailed study on photosensitised damage to proteins, BSA will be used as a model system to pinpoint the involvement of ROS in protein oxidation, and protein extracts will be used in an attempt to observe selective oxidation of certain proteins.

5.3 Determination of Photosensitised DNA Damage

In the previous chapters, it was shown that β–phenylpyruvic acid, L(+)mandelic acid and L-histidine can act as sensitisers of NUV, generating a variety of ROS when photolysed and causing DNA and / or protein damage leading to inactivation of bacteriophage T7. Treating bacteria with β–phenylpyruvic acid and L(+)mandelic acid also caused inactivation, but owing to the complexity of a bacterial cell it is quite difficult to determine whether cell death was due to damage to the cell membrane or the DNA. In this chapter, the ability of these compounds to induce DNA damage under cell-free conditions is therefore evaluated.

Recent studies have shown that UVA irradiation of pBR322 in the presence of photosensitisers (namely aminomethyl-trimethyl-psoralen, fluoroquinolone and naphthyridine antibacterials) can result in single-strand breaks (Martinez and Chignell, 1998; Oroskar *et. al.*, 1995). *In vitro* experiments were thus carried out in this study using plasmid DNA to examine the possible occurrence of single-strand breaks mediated by the photosensitisers under investigation.

5.3.1 Quantitative Determination of Plasmid pBR322

Plasmid pBR322 was prepared as described in section 2.8.2. The concentration of the DNA preparation was determined by measuring the absorbance of the sample at 280 and 260 nm to estimate the amount of protein and nucleic acid respectively (Maniatis *et. al.*, 1982). Thus, 10 µl of the DNA preparation was diluted to 1 ml in a 1-ml quartz cuvette. Readings of A_{260} = 0.0314 and A_{280} = 0.0261 gave a ratio of A_{260}/ A_{280} = 1.2. The amount of DNA present in the sample was calculated as 50 x A_{260} x dilution factor = 50 x 0.0314 x 100 = 157 µg ml^{-1}.

5.3.2 Induction of Photocleavage to pBR322 DNA

Damage to plasmid pBR322 by NUV alone or in the presence of sensitisers at pH 7.5 was measured as described in section 2.8.3. Experiments were conducted to evaluate the dose and concentration dependence of damage to the plasmid. Control

experiments involved incubation of the plasmid in the dark in the presence or absence of the sensitiser for a period equivalent to the irradiation time. Single-strand breaks and nicking of the DNA were scored by monitoring the relaxation of the fast-migrating supercoiled fraction of the plasmid following agarose gel electrophoresis (Figure 5.1).

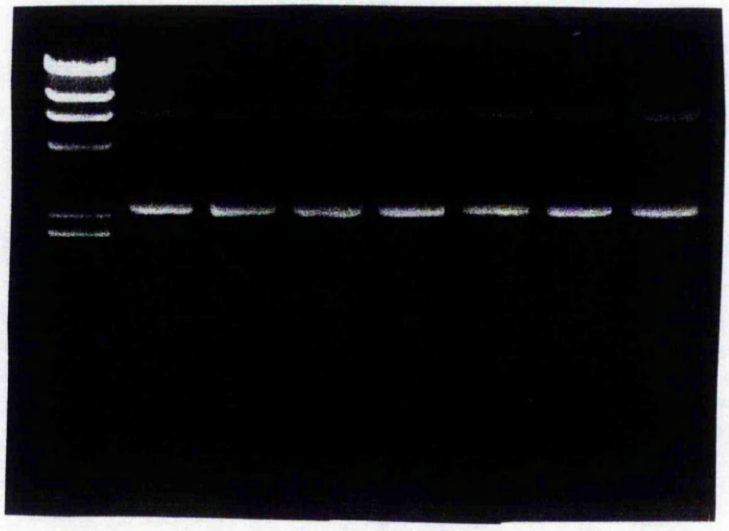

Figure 5.1: Agarose gel electrophoresis of pBR322 DNA. This is a representative result showing the effect of NUV in the presence and absence of 4 mM β–phenylpuruvic acid on the plasmid. Showing from left to right λ DNA/Hind III marker (lane 1), pBR322 untreated control (lane 2), pBR322 treated with 3.96×10^4 Jm^{-2}, 7.92×10^4 Jm^{-2} and 11.88×10^4 Jm^{-2} in the absence of β–phenylpuruvic acid (lanes 3, 5 and 7 respectively) and in the presence of the sensitiser (lanes 4, 6 and 8 respectively). The upper pBR322 band is the open circular form and the lower band the supercoild form.

In Figure 5.2 (a) the ability of photolysed β–phenylpyruvic acid (4 mM) to induce cleavage of the plasmid DNA is demonstrated. The non-irradiated control (first bar of data) shows that, initially, 75 % of the sample DNA was in the supercoiled form whereas the remaining 25 % was open-circular. NUV irradiation alone of the plasmid resulted in a small increase in relaxed DNA with time (by about 1-2% every 10 minutes). This is also evident in Figure 5.2 (b). Addition of 4 mM β–phenylpyruvic acid showed a further increase in the amount of relaxed DNA, and that was proportional to the time of exposure. On the other hand, when the plasmid was treated with NUV and 1 mM β–phenylpyruvic acid [Figure 5.2 (b)] there was no easily observable cleavage additional to that achieved by NUV alone, indicating that a higher than 1 mM concentration of this sensitiser is required to achieve apparent synergistic cleavage to the plasmid.

Statistical analysis of the data in Figure 5.2 (a), using the Paired T test for parametric distributions, showed that, compared to the untreated samples, the effect of NUV alone on inducing strand breaks is significant only after 30 minutes of exposure ($P = 0.02$), whereas a significant synergistic effect is observed after 20 minutes of exposure ($P = 0.01$ and 0.02 for the 20 and 30 minute samples respectively). The synergistic effect on inducing cleavage of the plasmid after 20 minutes of exposure in the presence of 4 mM β–phenylpyruvic acid was significantly greater not only compared to the untreated controls but also compared to the effect of NUV alone ($P = 0.013$).

Further investigation on the concentration effect of NUV plus β–phenylpyruvic acid in inducing single-strand breaks showed an increase in the percentage of open-circular DNA, compared to the non-irradiated controls, at all the concentrations employed in the experiments, with the effect being greater at 8 mM [Figure 5.3 (a)]. Although NUV alone produced a similar result to that observed on addition of 1 mM β–phenylpyruvic acid as shown in Figure 5.2 (b), on exposure to the same energy dose (11.88×10^4 J m^{-2}), there is an additional synergistic effect in the presence of 4 and 8 mM β–phenylpyruvic acid [Figures 5.2 (a) and 5.3 (a)].

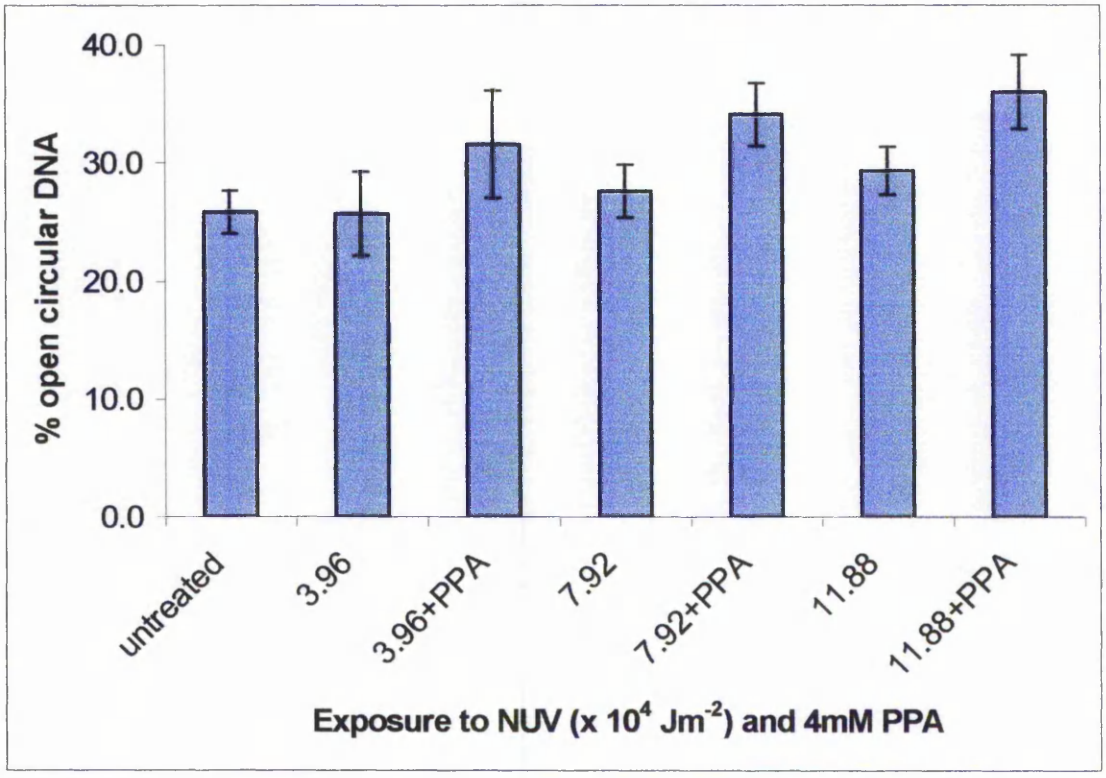

Figure 5.2 (a): Cleavage of pBR322 DNA in the presence of various doses of NUV and 4 mM β–phenylpuruvic acid (PPA). Each bar represents the percentage of open-circular plasmid DNA present in 0.8 μg of DNA sample after exposure to NUV alone or in the presence of β–phenylpuruvic acid. The first bar is the untreated control. The values given are the average ± the standard error of the mean for 3 observations.

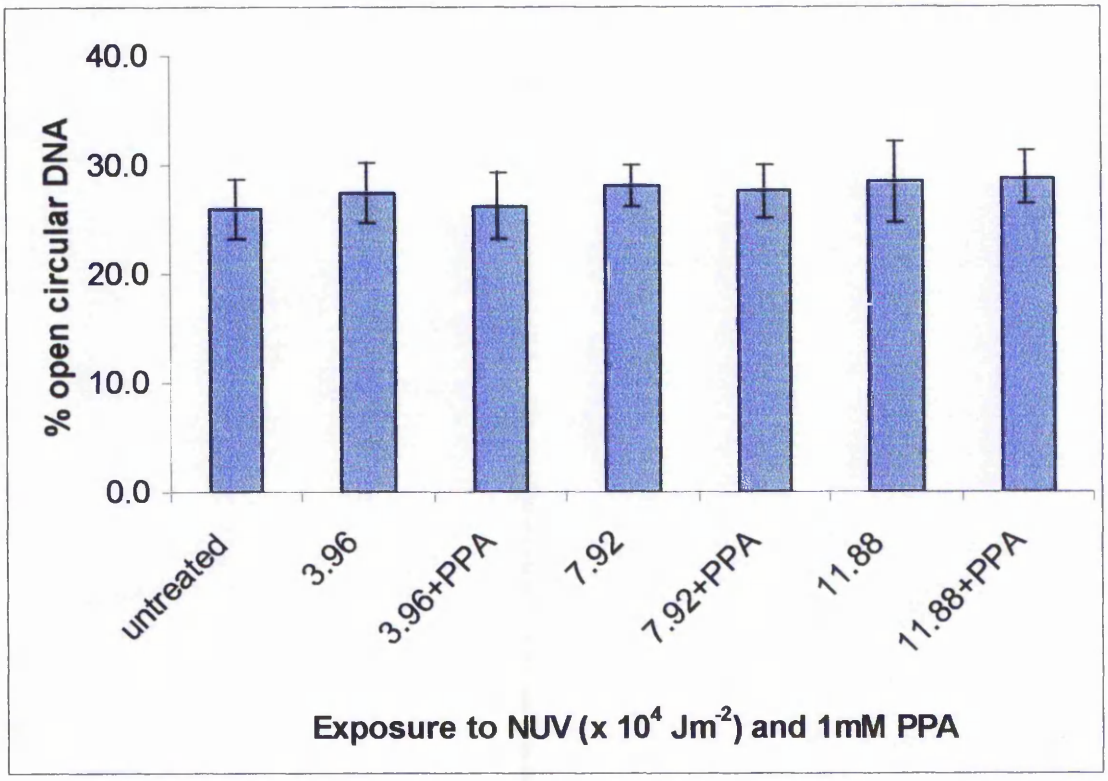

Figure 5.2 (b): Cleavage of pBR322 DNA in the presence of various doses of NUV and 1 mM β–phenylpuruvic acid (PPA). Each bar represents the percentage of open-circular plasmid DNA present in 0.8 μg of DNA sample after exposure to NUV alone or in the presence of β–phenylpuruvic acid. The first bar is the untreated control. The values given are the average ± the standard error of the mean for 2 observations.

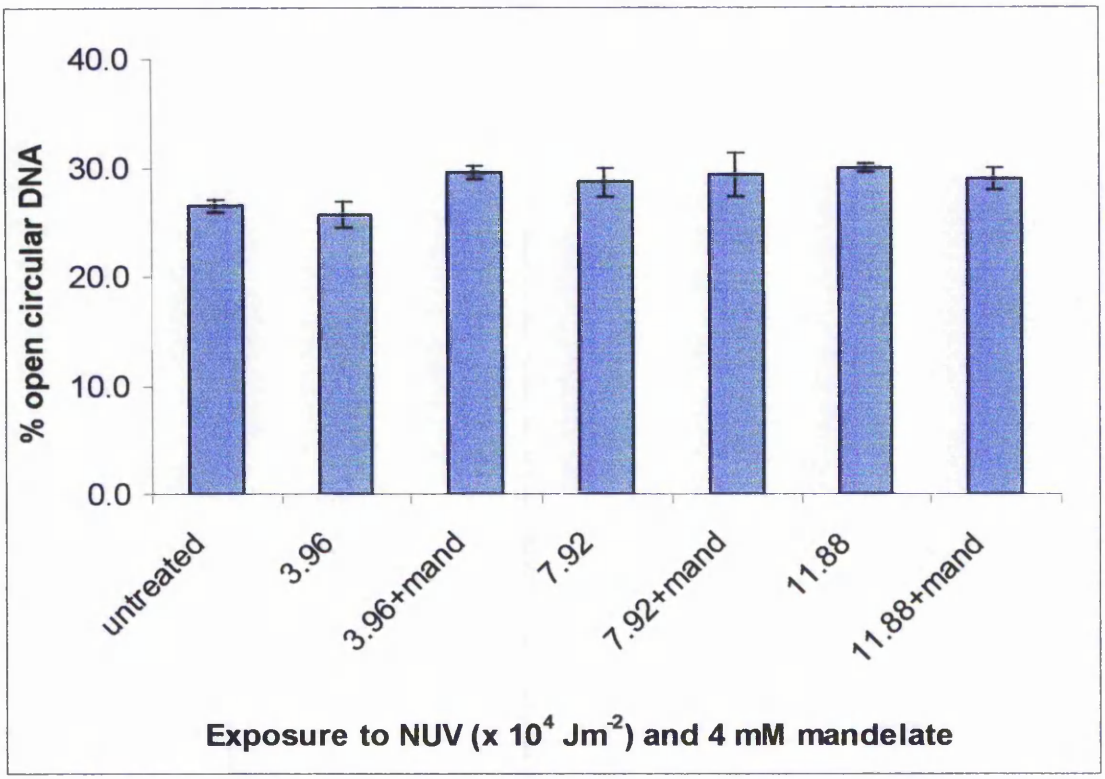

Figure 5.2 (c): Cleavage of pBR322 DNA in the presence of various doses of NUV and 4 mM L(+)mandelic acid. Each bar represents the percentage of open-circular plasmid DNA present in 0.8 μg of DNA sample after exposure to NUV alone or in the presence of L(+)mandelic acid. The first bar is the untreated control. The values given are the average ± the standard error of the mean for 3 observations.

Treatment of the plasmid with 4 mM β–phenylpyruvic acid in the dark [last bar of data in Figure 5.3 (a)] also resulted in an increase in the percentage of open-circular DNA compared to the untreated control (first bar of data). However, the synergistic effect was greater than that of β–phenylpyruvic acid alone even at lower concentrations [Figure 5.3 (a)].

At the pH used in these experiments (pH 7.5), both the plasmid DNA and β–phenylpyruvic acid are negatively charged, making it unlikely that there is any ionic interaction between the sensitiser and the DNA. However, since it is the phosphate groups in the DNA molecule that carry the negative charge, interactions of the sensitiser with other parts of the molecule prior irradiation can not be excluded. It may be possible, therefore, that other types of DNA damage such as monoadducts and cross-links may arise from the DNA / β–phenylpyruvic acid interaction, in addition to single-strand breaks and nicking of DNA that would result in open-circular plasmid.

Compared to β–phenylpyruvic acid, L(+)mandelic acid showed a lesser effect in inducing single-strand breaks to the plasmid. It can be seen in Figure 5.2 (c) that, on inclusion of 4 mM L(+)mandelic acid in the irradiated pBR322 solution, there was significant increase in the percentage of open-circular DNA compared to both the untreated control ($P = 0.037$ as determined by the Paired T test) and NUV alone ($P = 0.035$), especially at lower energy doses (3.96×10^4 J m^{-2}). NUV alone had an effect only after 20 minutes of exposure where it resulted to about 2% increase in the relaxation of the plasmid over the untreated control as the energy dose doubled. This is consistent with the observation made from Figures 5.2 (a) and (b).

The photosensitised effect of L(+)mandelic acid is concentration dependent as shown in Figure 5.3 (b). Incorporation in the reaction mixture of 8 mM L(+)mandelic acid caused more DNA strand breaking than lower concentrations. However, the same concentration of β–phenylpyruvic acid is more effective in inducing photocleavage of the plasmid. This may reflect the low absorption of NUV light by L(+)mandelic acid compared to β–phenylpyruvic acid [Figure 3.3 (b) and (c)] and the pH dependence of the photosensitised action of the former. Incubation of the plasmid with L(+)mandelic acid in the dark [last bar in Figure 5.3 (b)] did not result in additional

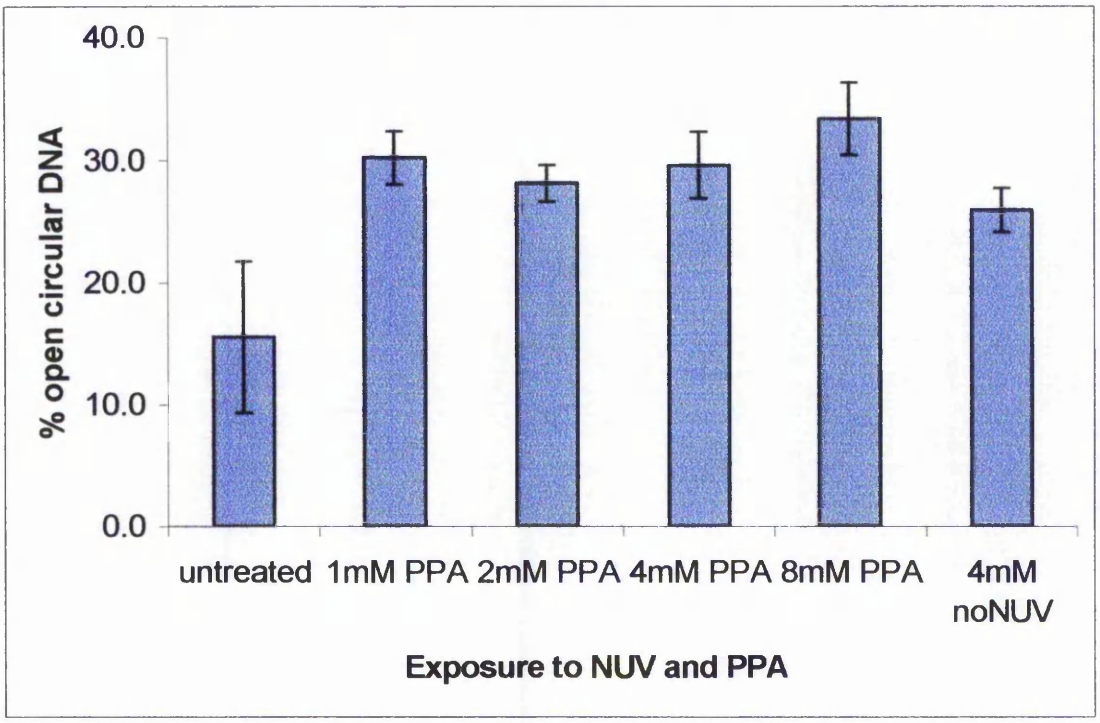

Figure 5.3 (a): The concentration effect on cleavage of pBR322 DNA in the presence of NUV plus various concentrations of β–phenylpuruvic acid (PPA). Each bar represents the percentage of open-circular plasmid DNA present in 0.8 μg of DNA sample after irradiation with 11.88 x 10^4 J m^{-2} in the presence of the sensitiser. An untreated DNA sample and one incubated with the sensitiser alone were included as controls (first and last bar respectively). The values given are the average ± the standard error of the mean for 2 observations.

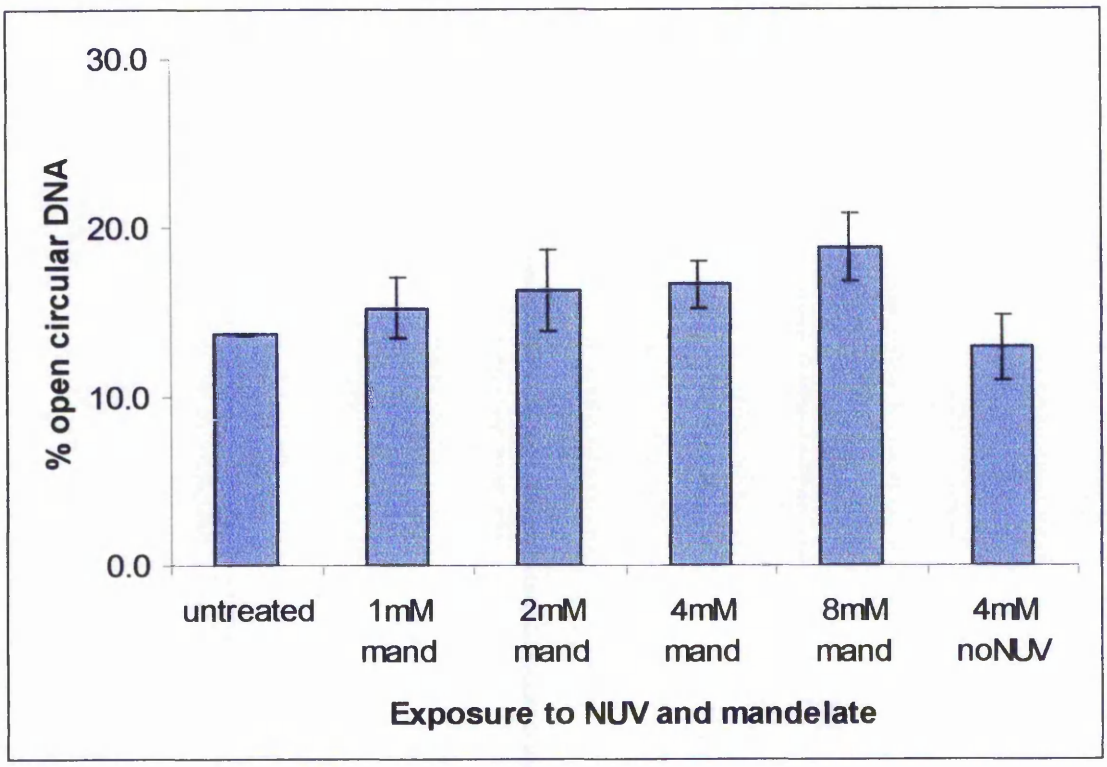

Figure 5.3 (b): The concentration effect on cleavage of pBR322 DNA in the presence of NUV plus various concentrations of L(+)mandelic acid. Each bar represents the percentage of open-circular plasmid DNA present in 0.8 μg of DNA sample after irradiation with 11.88 x 10^4 J m^{-2} in the presence of the sensitiser. An untreated DNA sample and one incubated with the sensitiser alone were included as controls (first and last bars respectively). The values given are the average ± the standard error of the mean for 2 observations.

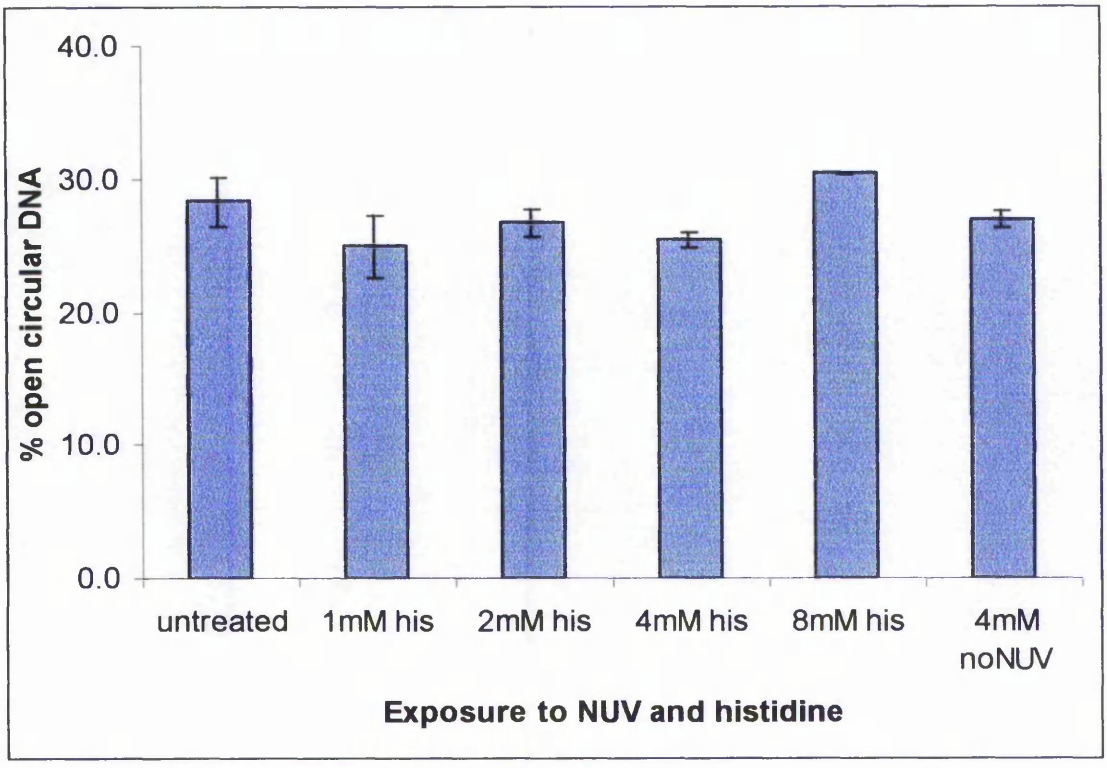

Figure 5.3 (c): The concentration effect on cleavage of pBR322 DNA in the presence of NUV plus various concentrations of L-histidine. Each bar represents the percentage of open-circular plasmid DNA present in 0.8 μg of DNA sample after irradiation with 11.88×10^4 J m^{-2} in the presence of the sensitiser. An untreated DNA sample and one incubated with the sensitiser alone were included as controls (first and last bars respectively). The values given are the average ± the standard error of the mean for 2 observations.

strand breaking to that present in the untreated control (first bar), indicating that any increase in the open-circular form of the plasmid in the presence of L(+)mandelic acid is due to a synergistic effect.

Finally, the ability of L-histidine to induce strand breaks to the plasmid was studied, and the results are shown in Figure 5.3 (c). Compared to the controls, L-histidine does not seem to cause any photocleavage to the irradiated plasmid at pH 7.5, except at 8 mM concentration. Even at this concentration, the increase in the open-circular DNA contributed to L-histidine plus NUV is only about 2% compared to the non-irradiated controls. This effect is not much greater that that of NUV alone observed on similar experiments (Figures 5.2). The reduced effect of L-histidine to induce single-strand breaks to the plasmid compared to β–phenylpyruvic acid and L(+)mandelic acid follows the pattern of the extend of the NUV photolyis of these compounds as determined by the NBT assay (Table 3.1). According to these results, the photolysis of L-histidine at pH 7.5 was shown to be a three-fold and a four-fold less effective than that of β–phenylpyruvic acid and L(+)mandelic acid respectively at this pH.

Reactive oxygen species generated on the photolysis of β–phenylpyruvic acid and L(+)mandelic acid are believed to be responsible for the damage to the DNA observed in Figures 5.2 and 5.3. It is generally believed that $^1O_2$ oxidises exclusively the guanine base which exhibits the lowest ionisation potential among nucleobases and the sugar moiety, whereas $^{\cdot}OH$ react readily with all nucleobases (Cadet *et. al.*, 2000; Ito *et. al.*, 1993). In comparison, $O_2^{\cdot -}$ is virtually non-reactive towards DNA, although it also oxidises the guanine residue but with lower affinity than $^1O_2$ (Douki and Cadet, 1999). Single strand breaking is therefore generally attributed to $^{\cdot}OH$ radicals (Cadet *et. al.*, 1999). It was previously shown that $^{\cdot}OH$ may be responsible for the single-strand breaks formed on pBR322 on the UVA photolysis of psoralens (Oroskar *et. al.*, 1995). Since both β–phenylpyruvic acid and L(+)mandelic acid were shown to generate $^{\cdot}OH$ in the presence of NUV (Table 3.6), this may also be the case in this study. The generally low yield of single strand breaks in supercoiled plasmid DNA in these experiments may reflect the low contribution of $^{\cdot}OH$ to the overall photosensitised oxidation of the plasmid.

In addition, the direct involvement of the sensitiser in inducing DNA damage can not be ruled out. The sensitiser molecules may be subjected near the surface of the DNA to ionic strength and electric field effects that would influence their reactivity towards the DNA components. Thus, the senstiser in the excitation state may also cause DNA strand breaks, along with formation of monoadducts and cross-links. On the other hand, other radicals derived from DNA may escape into the suspension after initial strand breaking and quench the triplet sensitiser molecule or the ·OH generated upon photolysis.

Further experiments would be required to clarify the role played by the photoproducts of β–phenylpyruvic acid and L(+)mandelic acid in single-strand break formation and other types of DNA damage. It would also be interesting to investigate the pathways that lead to generation of strand breaks, as they may be different from those that lead to monoadduct formation and cross-links.

Although reactions in chromosomal DNA may not be the same as those in plasmid DNA, damage to DNA is almost certainly involved in photocarcinogenesis and photomutagenicity, and this study with pBR322 predicts that β–phenylpyruvic acid may be the most photogenotoxic of the sensitisers tested in this study. This conclusion is consistent with the data on phage T7 inactivation shown in Figure 4.8 and bacterial killing in Figures 4.11 and 4.13.

5.3.3 Transformation of *E. coli mutT*$^{+}$ and *mutT*$^{-}$ Strains with pBR322 Treated with NUV and β–Phenylpyruvic Acid

Further studies of the photosensitisation of pBR322 plasmid with β–phenylpyruvic acid involved transformation experiments using *E. coli* cells. The *E. coli* strains employed were the wild type *mutT*$^{+}$ and the A•T → C•G transversions mutator *mutT*$^{-}$ (described in Table 2.1). Certain events like the misincorporation of guanine opposite adenine during replication are not corrected in *E. coli mutT*$^{-}$. This strain is also defective in repairing 8-oxodeoxyguanosine (8-oxo-dGuo) lesions (Pavlov *et. al.*, 1994). Furthermore, 8-oxo-dGuo, which is the major oxidation product of guanine, is capable of base pairing with either cytosine or adenine. Thus,

the incorporation of 8-oxodGuo opposite template adenine in *mutT*$^-$ cells can go undetected. In the previous section, the NUV photolysis of β–phenylpyruvic acid lead to the generation of single strand breaks to plasmid DNA. Using the *mutT*$^-$ strain, it may be possible to study the photosensitised effect of β–phenylpyruvic acid in inducing DNA damage to produce 8-oxo-dGuo.

INCREASE IN TRANSFORMATION				
pBR322 DNA	*E. coli mutT*$^+$		*E. coli mutT*$^-$	
	TC	AMP + TC	TC	AMP + TC
β–PPA alone	0.6 ± 0.2 (5)	0.9 ± 0.3 (6)	1.1 ± 0.2 (6)	0.8 ± 0.2 (6)
NUV alone	1.2 ± 0.4 (6)	1.1 ± 0.5 (4)	1.4 ± 0.2 (6)	1.9 ± 0.5 (6)
NUV + β–PPA	3.8 ± 0.9 (5)	6.2 ± 1.5 (4)	4.3 ± 1.5 (5)	4.5 ± 1.8 (4)
Sheered	1.8 ± 0.5 (3)	0.6 ± 0.2 (3)	1.7 ± 0.2 (3)	2.9 ± 0.8 (3)

Table 5.1: The effect of β–phenylpyruvic acid (β–PPA) plus NUV on the transformation efficiency of pBR322. Transformants were selected in the presence of tetracycline (TC) and ampicillin (AMP). Values represent the average factor of increase in the transformation efficiency for different treatments of pBR322 DNA over that observed using untreated plasmid. A sample of mechanically sheered DNA was also included as a control. For each average, the standard error of the mean and the number of observations (in parenthesis) are shown.

In section 4.3.2, it was found that cells deficient in DNA repair (*E. coli* SA162) were more susceptible to inactivation by β–phenylpyruvic acid plus NUV treatment. This finding led to the conclusion that non-repaired DNA damage may be responsible for cell death. Therefore, if wild type (*mutT*$^+$) and repair deficient (*mutT*$^-$) *E. coli* cells were transformed with plasmid treated with NUV plus β–phenylpyruvic acid, and since plasmid DNA would be expected to survive only if repaired by the cellular enzymatic machinery, the survival of the cells grown on selective media would be related to the extent of damage to the plasmid. This hypothesis was tested by the *in vitro* exposure of pBR322 DNA to NUV in the presence and absence of β–phenylpyruvic acid followed by transformation of competent cells as described in section 2.9.2. Only transformants that carry a

functional plasmid would carry antibiotic resistance and thus be able to grow in selective media.

The results from transformation experiments using pBR322 are summarised in Table 5.1. The transformation efficiency was expected to drop as the plasmid was subjected to oxidative damage (Padula *et. al.*, 1996). If the plasmid remained intact and no damage took place, the transformation efficiency of each sample should remain the same as of the untreated control. However, Table 5.1 shows a small increase in the transformation efficiency when the plasmid was treated with PPA alone or NUV alone, and a considerable increase when the plasmid was exposed to both NUV and β–phenylpyruvic acid. The probability value (P) for the synergistic effect observed was less than 0.02 compared to β–phenylpyruvic acid alone and less than 0.04 compared to NUV alone as determined by the Mann-Whitney test for non-parametric distributions. To test whether the increase in transformants was due to the relaxation of the plasmid, a sample where the DNA was sheared by pipetting up and down (5 times with a 5-50 µl adjustable pipette set at 40 µl) was included. Indeed, the transformation efficiency was increased using this sample ($P < 0.04$), but not as much as when the plasmid was treated with β–phenylpyruvic acid and irradiated.

The small increase in transformation efficiency, on exposure of the plasmid to β–phenylpyruvic acid in the dark, suggests a possible interaction between the DNA components and the sensitiser that resulted in the relaxation of the plasmid. This is in agreement with the observation in section 5.3.2 where treatment of pBR322 with β–phenylpyruvic acid alone resulted in strand breaking. Also, the effect of NUV alone in transformation efficiency is greater than that of β–phenylpyruvic acid but considerably lower than the synergistic action of the two agents. This pattern is very similar to the one displayed in the induction of single-strand breaks by NUV in the presence and absence of this sensitiser.

The photosensitised modifications to the plasmid do not inhibit its replication. On the contrary, plasmid relaxation appears to increase the transformation efficiency. In addition, there is no apparent difference between the two *E. coli* strains, suggesting that transversion mutations do not affect survival of the plasmid. Actually, any

mutations on the plasmid would only affect survival of the cell if they occur at the sites encoding antibiotic resistance (a diagram of pBR322 is shown in Figure 5.4). Testing for double resistance decreases the chances of missing out any base misincorporations. It is possible that 8-oxo-dGuo lesions are not the common types of DNA damage that occur by photolysis of β–phenylpyruvic acid on naked DNA but rather single-strand breaks. This, however, would not exclude the occurrence of such lesions in the genome of a more complex cellular system (see section 5.3.5).

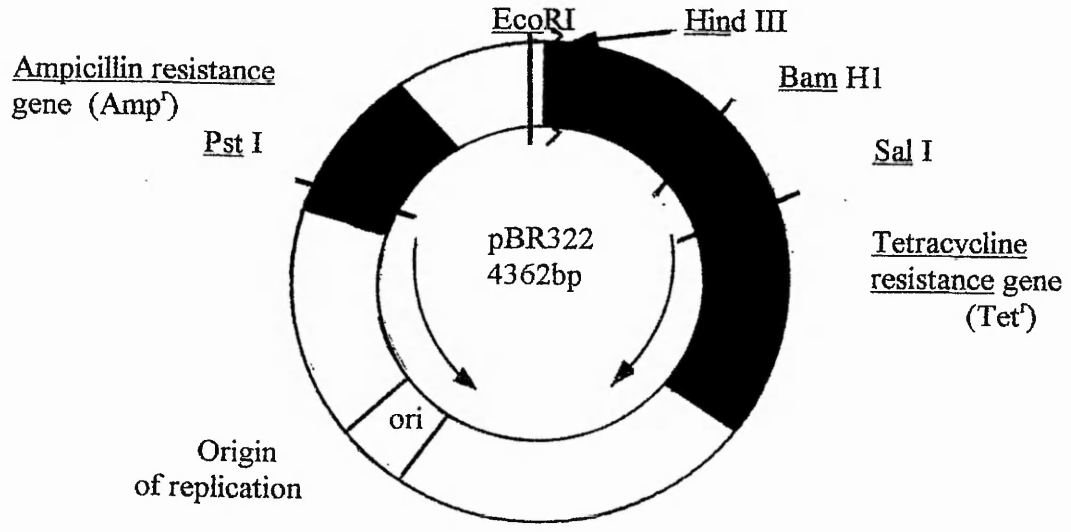

Figure 5.4: Diagram of plasmid pBR322 showing the areas of ampicillin and tetracycline resistance (Maniatis *et. al.*, 1982).

It is very likely that both *E. coli* strains are capable of repairing other types of damages that may occur to the plasmid. In a report by Padula *et. al.* (1996), wild type, *fpg-1* or *uvrA* mutant *E. coli* strains transformed with pBR322 were shown capable of repairing AP-sites and oxidised purines and pyrimidines, the principal lesions induced by $^1O_2$ to DNA. Only the *uvrA fpg-1* double mutant was unable to repair these damages. Another study that involved sensitised damage to pBR322 treated with psoralens and NUV and repair after transformation (Repanovici *et. al.*, 1997) concluded that cross-links between the two complementary strands hinder DNA replication, whereas formation of monoadducts does not block DNA replication. According to the results in Table 5.1, the type of plasmid modification due to the synergistic action of β–phenylpyruvic acid and NUV is such that it does not affect survival of the plasmid but increases its transformation efficiency. Because of the

similarity in the pattern of results between transformation experiments and induction of single-strand breaks by photosensitisation, it may be possible to conclude that the NUV photolysis of β–phenylpyruvic acid causes relaxation of pBR322 and consequently increased transformation efficiency. Following incorporation of the plasmid by the *E. coli* cells, single-strand breaks and other oxidative modifications are being repaired and the plasmid resumes its supercoiled form.

5.3.4 DNA Damage-Induced β–galactosidase Production in *E. coli* PQ37

This assay is based on the SOS responses of *E. coli* cells to DNA-damaging agents (Quillardet and Hofnung, 1985). The tester strain PQ37 has been constructed by an operon fusion that placed the structural gene for β–galactosidase (*lacZ*) under the control of a damage-inducible gene, *sfiA*, that is involved in the inhibition of cell division. Thus, β–galactosidase production is strictly dependent on *sfiA* expression. *E. coli* PQ37 is also deficient in excision repair (*uvrA* mutant) and lipopolysaccharide production (*rfa* mutant). These mutations render the strain sensitive to DNA-damaging agents and more permeable to certain chemicals.

The concentration of β–galactosidase was determined in an assay using *o*-nitrophenyl-β-D-galactopyranoside (ONPG) as the substrate (section 2.10). β–Galactosidase catalyses the hydrolysis of ONPG to the yellow *o*-nitrophenol that absorbs at 420 nm. If exposure of the tester strain to NUV plus L-histidine, L(+)mandelic acid, *p*-OH-phenylpyruvic acid or β–phenylpyruvic acid caused DNA damage, the *sfiA* gene, and subsequently the *lacZ* gene expression would lead to production of β–galactosidase. Indeed, as can be seen in Table 5.2, the effect of the NUV sensitisers on PQ37 resulted in an increased generation of β–galactosidase.

PRODUCTION OF β–GALACTOSIDASE (A_{420})							
Exp.	SA191	PQ37	PQ37 NUV	PQ37 NUV/His	PQ37 NUV/Mand	PQ37 NUV OH-PPA	PQ37 NUV β–PPA
1	2.315	0.312	0.500				0.532
2	2.280	0.202	0.242	0.641	0.620	0.394	0.452
3	2.321	0.373	0.561	0.836	0.692	0.590	0.664

Table 5.2: Production of β–galactosidase by *E. coli* PQ37 and SA191 (constitutive for β–galactosidase). The amount of β–galactosidase produced is expressed as the absorbance reading of *o*-nitrophenol at A_{420}. Before assaying, appropriate samples were exposed to 11.88 x 10^4 J m^{-2} NUV and 1 mM of the sensitiser at pH 7. The assay was terminated after five minutes.

E. coli SA191 produces β–galactosidase constitutively (Table 2.1) and was used as a positive control. The amount of *o*-nitrophenol generated by NUV in the presence and absence of the sensitiser is compared to that produced by unexposed PQ37 cells (third column). It is apparent that the unexposed *E. coli* PQ37 cells have some β–galactosidase activity. This is, however, much less than the positive control (*E. coli* SA191) and in agreement with the work of Quillardet and Hofnung (1985). An increase in absorbance readings caused by light scattering due to cell debris was avoided by including a centrifugation step before measuring the absorbance of the samples.

From Table 5.2, the units of enzyme activity has been calculated according to the formula suggested by Quillardet and Hofnung (1985):

Enzyme units = 1000 x A_{420} / t (min).

The results are shown in Table 5.3.

INCREASE IN β–GALACTOSIDASE ACTIVITY (enzyme units)					
Exp.	PQ37 NUV	PQ37 NUV/His	PQ37 NUV/Mand	PQ37 NUV OH-PPA	PQ37 NUV β–PPA
1	37.6				44.0
2	8.0	87.8	83.6	38.4	50.0
3	37.6	92.6	63.8	43.4	58.2

Table 5.3: Increased β–galactosidase production attributed to NUV plus sensitisers. Values represent the increase in units of enzyme activity, when that of the uninduced control was subtracted from each sample.

The variation in enzyme activities observed between experiments is probably due to a difference in the cell numbers involved, as the time of the assay was kept constant. Indeed, enzyme activity would depend on the initial number of bacteria and on the bacterial growth during the incubation time allowed (1 hour) for gene expression and protein synthesis (section 2.10). Despite these variations, a trend can be seen in both Tables (5.2 and 5.3), where NUV results in an increase in β–galactosidase production compared to the uninduced control, and the synergistic effect in the presence of the sensitisers is greater. The average effect of *p*-OH-phenylpyruvic acid is slightly greater than that of NUV alone, whereas photolysis of L(+)mandelic acid and L-histidine appear much more effective in inducing β–galactosidase generation. This result indicates that photolysis of these two sensitisers causes more extended DNA damage to the PQ37 genome. This is surprising since in section 5.3.2 L-histidine, and to a lesser extend L(+)mandelic acid, did not seem to cause significant strand breaking to plasmid DNA. The case may be that photolysis of the different sensitisers results in different types of DNA damage. Thus, whereas NUV exposure of β–phenylpyruvic acid and possibly *p*-OH-phenylpyruvic acid can result primarily in single-strand breaks, photolysis of L(+)mandelic acid and L-histidine may preferentially cause formation of 8-oxo-dGuo, FapyGua and/or other oxidation products, and generally cause DNA base modification depending on the ROS involved and the conditions of their generation. Any of these changes to the DNA may trigger an SOS response.

In addition, the rate of uptake of these sensitisers by PQ37 would affect the photosensitised effect. As mentioned earlier, this strain of *E. coli* is deficient in lipopolysacharide production and therefore more permeable to certain agents. HPLC experiments showed that increased concentrations of β–phenylpyruvic acid were present in bacterial cells (more in gram-positive than gram-negative ones) that were incubated with this agent (section 4.4). At the present, it is not clear to what extent the other sensitisers involved in this study can be incorporated in bacterial cells. If the uptake of L-histidine, for example, is more efficient than that of β–phenylpyruvic acid then the proximity of the former to the DNA may render it a more effective photosensitiser in inducing DNA damage. It is known that histidine is one of the essential amino acids for the survival of bacterial cells and that cells deficient in producing this amino acid (*E. coli* his$^-$ mutant strains) require media supplemented with histidine for growth. Thus, the uptake of histidine from the environment by *E. coli*, and possibly other bacterial species, is a natural process. Although β–phenylpyruvic acid absorbs more light in the NUV region and experimental work in this study leads to the suggestion that this sensitiser is the most effective among those tested in generating ROS at pH 7, the photolysis of L-hisidine at this pH may have a greater impact in causing a biological effect in some cases. The induction of β–galactosidase production as a result of DNA damage seems to be one of them.

Moreover, the NUV photolysis of β–phenylpyruvic acid was shown to cause a high level of inactivation of the *uvrA* mutant *E. coli* SA162 (DNA-repair deficient). *E. coli* PQ37 is also a *uvrA* mutant strain, and therefore, a similar effect would be expected on treatment with NUV plus β–phenylpyruvic acid. A low survival rate in the culture would explain the low production of β–galactosidase observed after the designated incubation period. Given the similarity in their structure, and the good absorption of *p*-OH-phenylpyruvic acid in the NUV region [Figure 3.3 (d)], a similar effect to that of β–phenylpyruvic acid would be expected in the experiments involving *E. coli* PQ37. As shown in Table 5.3, the photolysis of *p*-OH-phenylpyruvic acid resulted in an even smaller increase in β–galactosidase activity, over that of NUV alone, compared to the effect of the photolysis of β–phenylpyruvic acid, and this may also reflect increased cell death.

5.3.5 Mutagenesis and Rifampicin Resistance by NUV plus β–Phenylpyruvic Acid, L(+)Mandelic Acid or L-Histidine in *E. coli*

Whereas DNA strand breaks and cross-links may result in cell death, modification of DNA bases can lead to mutagenesis (Friedberg *et. al.*, 1995; Quillardet and Hofnung 1985; Stary and Sarasin, 2000). Mutations may arise directly upon ROS attack or indirectly during replication or repair of DNA damage (Kohen *et. al.*, 1995). Mutations resulting from oxidative damage to DNA depend on the repair efficiency of the cell, the nature of the mutagen involved, since different agents target different premutagenic lesions, and the site of attack on the DNA, since the local DNA environment determines the efficiency of a given mutagen. The determination of the mutagenic potential of a mutagen allows the identification and evaluation of the relative contribution toward deleterious biological end points of this compound as a source of DNA damage. Thus, the mutagenic potential of some of the sensitisers involved in this study was investigated.

INCREASE IN MUTAGENESIS AND RIFAMPICIN RESISTANCE				
	E. coli KL16		*E. coli mutT*⁻	
E (x 10^4 J m^{-2})	NUV	NUV/PPA	NUV	NUV/PPA
1.98	3.07 ± 1.80 (2)	1.91 ± 0.27 (4)		
3.96	1.81 ± 0.17 (5)		1.74 ± 0.39 (6)	2.57 ± 0.72 (7)
7.92	1.93 ± 0.45 (5)	2.10 ± 0.04 (2)	2.55 ± 0.07 (2)	4.69 ± 0.29 (3)
11.88	1.07 ± 0.21 (4)	3.60 ± 0.63 (4)	8.37 ± 0.79 (2)	65.3 ± 19.8 (2)
15.84	1.98 ± 0.39 (4)	4.13 ± 1.25 (9)		

Table 5.4: Increased mutagenesis and rifampicin resistance for *E. coli* KL16 and *E. coli mutT*⁻ treated with NUV alone or in the presence of β–phenylpyruvic acid (PPA). Values represent the average factor of increase in mutation frequency of the treated cultures over the spontaneous mutation frequency of the untreated control. Values are the average of the number of observations given in parenthesis ± the standard error of the mean.

ROS-induced 8-oxo-dGuo usually results in transversion mutations (Douki *et. al.*, 1999; Stary and Sarasin, 2000). Mutation spectra obtained in *E. coli* cells exposed

to $^1O_2$ showed that, $^1O_2$ induced predominately base substitutions (Stary and Sarasin, 2000). These point mutations were located at sites that could be oxidised specifically i.e. G : C base pairs. The predominant mutations found in this study were G•C → T•A transversions, suggesting that 8-oxodGuo could be the major premutagenic modification present in DNA damage by $^1O_2$ before replication. This is consistent with a role for 8-oxo-dGuo (pairs with either cytosine or adenine) and with the selectivity of $^1O_2$ for guanine (Pavlov *et. al.*, 1994; Ravanat and Cadet 1995).

To characterise the molecular nature of photosensitiser-induced mutations using β–phenylpyruvic acid, L-histidine and L(+)mandelic acid, experimental assays were carried out by the *in vivo* exposure of *E. coli* cells to NUV (as described in section 2.11). Induction of mutations was estimated as an increased number of resistant to rifampicin cells in the population. Also, in order to test the role of 8-oxo-dGuo type of DNA damage in induction of mutation in *E. coli*, the A•T → C•G transversions mutator strain (*E. coli mutT*$^-$) was used together with the wild type *E. coli* KL16.

In sections 3.5 and 4.2.2, photolysis of β–phenylpyruvic acid was proposed to generate $^1O_2$, amongst other species. The data in Table 5.4 supports these results. Whereas treatment with NUV alone resulted in an average of two orders of magnitude increase in mutagenesis for *E. coli* KL16, the same treatment caused a dose-depended increase in mutation frequency for *E. coli mutT*$^-$ up to nine times. The independence of the dose involved in mutagenisity for the wild type *E. coli* suggests that high irradiation doses may result in increased cell death rather than in mutations in these cells. On the other hand, the synergistic effect of NUV plus β–phenylpyruvic acid was greater than the effect of NUV alone, for both the wild type and mutant strains. However, on high energy exposure ($\geq 11.88 \times 10^4$ J m^{-2}), the wild type *E. coli* showed a mutation frequency about a four-fold higher than the control, whereas the *mutT*$^-$ strain showed an increase in mutation frequency by an average 65-fold. The synergistic effect for both strains was dose-depended.

Certain errors like the misincorporation of 8-oxo-dGou opposite adenine during replication are not corrected in *E. coli mutT*$^-$ (Pavlov *et. al.*, 1994). Thus, it

can be concluded from the results in Table 5.4 that the predominant mutations occurring on β–phenylpyruvic acid photosensitisation are A•T → C•G transversions, suggesting 8-oxodGuo as the major premutagenic lesion and the possible role of $^1O_2$ in the induction of mutations. Transversion mutations may, therefore, be one of the major types of ROS-mediated DNA damage that lead to induction of mutation in *E. coli* and possibly in other species. This type of damage can be repaired quite efficiently in wild type *E. coli*, but not completely, as an increase in mutagenesis is observed compared to the spontaneous mutation of the control (Table 5.4). Other types of DNA damage such as cross-links and strand-breaks may also occur as a result of sensitised damage in *E. coli*. These primary DNA lesions, although lethal when they persist until replication, could be converted by excision repair into a secondary lesion, which could be mutagenic rather than lethal. One can therefore conclude that β–phenylpyruvic acid can directly or indirectly induce mutations in E. coli when sensitised. This is clear when *E. coli* KL16 is treated with β–phenylpyruvic acid at an energy dose of 11.88 -15.84 x 10^4 J m^{-2}, and quite apparent from the data for the *mutT*⁻ strain. The mutagenic potential of β–phenylpyruvic acid, however, may be greater than that observed in these experiments, since mutations occurring to a different DNA locus would have an outcome other than rifampicin resistance.

When L(+)mandelic acid and L-histidine replaced β–phenylpyruvic acid, they didn't show as great an increase in mutation frequency as the latter, compared to the effect of NUV alone (Table 5.5). Photolysis of L(+)mandelic acid seemed to increase mutation *in E. coli* in a pH dependent manner. However, the NUV result for this set of experiment shows as high a mutation frequency. Given that the overall effect of NUV alone as shown in Tables 5.4 and 5.5 averages to less than a two-fold increase for *E. coli* KL16, it is likely that the near five-fold increase in mutation observed for NUV alone in Table 5.5 is not a representative set of data. Although the results are not conclusive, L-histidine and to a lesser extent L(+)mandelic acid do not have the mutagenic potential of β–phenylpyruvic acid. This observation is probably reflective of the low level of photolysis achieved at pH 7 and is consistent with the effect of these sensitisers in inducing single strand breaks in plasmid DNA (section 5.3.2), where the NUV photolysis of β–phenylpyruvic acid was considerably more effective than that of L(+)mandelic acid in causing DNA damage. The NUV pholysis of L-

histidine was also shown to be virtually ineffective in the formation of single-strand breaks.

INCREASED MUTATION IN *E. coli* KL16			
NUV	1.19 ± 0.35 (2)	4.82 ± 0.28 (2)	1.02 ± 0.02 (2)
NUV/Mandelate pH7	1.17 ± 0.08 (2)		
NUV/Mandelate pH8		4.62 ± 0.30 (2)	
NUV/Histidine pH9			1.91 ± 0.15 (2)

Table 5.5: Increased mutagenesis and rifampicin resistance for *E. coli* KL16 treated with NUV (11.88 x 10^4 J m^{-2}) in the presence or absence of L(+)mandelic acid or L-histidine. Values represent the average factor of increase in mutation frequency over the frequency of spontaneous mutation of the untreated control. Values are the average of the number of observations given in parenthesis ± the standard error of the mean.

Generally, it can be concluded that the photosensitised effects of the sensitisers involved in this study lie in causing inactivation rather than increased mutation. β–Phenylpyruvic acid, in particular, was shown to be of significant mutagenic potential mostly for cells deficient in DNA repair (Table 5.4), whereas it was found to cause, on NUV photolysis, similar increase of inactivation (above that attributed to NUV alone) to both wild type and DNA repair deficient *E. coli* cells (Figure 4.11).

5.4 Induction of Lipid Peroxidation by NUV and β–Phenylpyruvic Acid

ROS, such as ·OH and $^1O_2$, can readily attack polyunsaturated fatty acids, phospholipids and cholesterol causing lipid peroxidation (Paillous and Fery-Forgues, 1994). Due to the high content of phospholipids, cellular membranes are key targets for ROS-induced lipid peroxidation. This process results in the formation of highly reactive and unstable hydroperoxides (Schafer and Buettner, 1999). These products of lipid peroxidation can react further with membrane proteins and DNA as well as other lipids, threatening the function and integrity of the membrane and subsequently

the cell (Beer *et. al.*, 1993). Therefore, quantification of lipid peroxidation is essential to assess the role of sensitised oxidative injury to a living cell. Traditionally, lipid peroxidation was quantified by assays that measure malondialdehyde and 4-hydroxynonenal, the degradation products of polyunsaturated fatty acid hydroperoxides. However, these assays are non-specific, and since only hydroperoxides derived from polyunsaturated fatty acids give rise to these by-products, this often lead to an over- or under-estimation of lipid peroxidation (Pryor and Porter, 1990). For these reasons, an assay that measures hydroperoxide directly was chosen.

The ability of β–phenylpyruvic acid plus NUV to cause lipid peroxidation was studied *in vitro* using liposomes as a pure lipid system and *in vivo* using bacterial cells (section 2.12). The use of liposomes in suspension is a good system for the study of lipid peroxidation in model membranes and has been used previously to study the role of $^1O_2$ in membrane oxidation (Fukuzawa, 2000). The use of bacterial cells for the study of lipid peroxidation was included as a more realistic system to assess the role of lipid peroxidation in cell inactivation. Such a complicated system however, was proven harder to study.

When an aqueous suspension of liposomes was irradiated in the presence of β–phenylpyruvic acid, the concentration of lipid hydroperoxide was found to be around 14-15 nmoles ml^{-1} (Figures 5.5 and 5.6). This was significantly greater than the effect of NUV alone, which resulted in approximately 1.6-2.6 nmoles ml^{-1} hydroperoxide. As determined by the Mann-Whitney test for non-parametric distributions, the probability value (P) for the synergistic effect was less than 0.01 compared to the untreated samples and those treated with β–phenylpyruvic acid or NUV alone. The untreated samples shown in both Figures were also found to contain a very small amount of hydroperoxide (around 0.62-1.4 nmoles ml^{-1}).

From Figure 5.5, it can be seen that sensitised lipid peroxidation is dose-dependent. When one third of the total energy of exposure was applied (3.96×10^4 Jm^{-2}), the resulting hydroproxide was also one third of the total amount generated (4.6 nmoles ml^{-1}) ($P < 0.04$ compared to the untreated samples and those treated with

NUV alone). In addition, Figure 5.6 shows that β–phenylpyruvic acid alone did not cause lipid peroxidation, with only about 0.93 nmoles ml^{-1} hydroperoxide present.

In both Figures (5.5 and 5.6) addition of isopropyl alcohol (ISPA) in the liposome suspension resulted in some decrease in hydroperoxide formation (to around 10 nmoles ml^{-1}) ($P = 0.005$). Addition of mannitol had a similar protective effect, reducing hydroperoxide concentrations to approximately 7.3 nmoles ml^{-1} (Figure 5.6). As both chemicals are good scavengers of $^{\cdot}OH$, the contribution of this radical in inducing lipid peroxidation is evident. The increased reduction in hydroperoxide concentration observed on addition of mannitol compared to ISPA may reflect the higher affinity of the former for $^{\cdot}OH$ (the rate constant of reaction being 2.7×10^9 M^{-1} s^{-1} for mannitol and 1.5×10^9 M^{-1} s^{-1} for ISPA as shown in Table 2.2).

An incomplete reduction in lipid peroxidation, however, indicated that other ROS (e.g. $^1O_2$) might be involved in the peroxidation process. From the literature, it is known that $^{\cdot}OH$ is capable of initiating lipid peroxidation and, together with $^1O_2$, reacts with lipids and produces hydroperoxides (Paillous and Fery-Forgues, 1994). In Chapters 3 and 4, β–phenylpyruvic acid was shown to generate both $^{\cdot}OH$ (Table 3.5) and $^1O_2$ (Table 3.5 and Figure 4.8) on NUV photolysis, at pH 7. In fact, the actual amount of $^1O_2$ generated on NUV photolysis of β–phenylpyruvic acid may be greater than that shown by the NBT assay as the assay is specific for $O_2^{\cdot-}$ and only any $^1O_2$ involved in $O_2^{\cdot-}$ formation would be detected.

Generally, the concentration of hydroperoxides, and subsequently the extent of lipid peroxidation measured in this assay for liposomes, may be lower than that actually occurring. As mentioned in section 2.12.3, liposome stocks were initially dissolved in ethanol, which is known to scavenge $^{\cdot}OH$ (Halliwell and Gutteridge, 1999), thereby leading to an underestimation of lipid peroxidation induced on treatment with NUV plus β–phenylpyruvic acid.

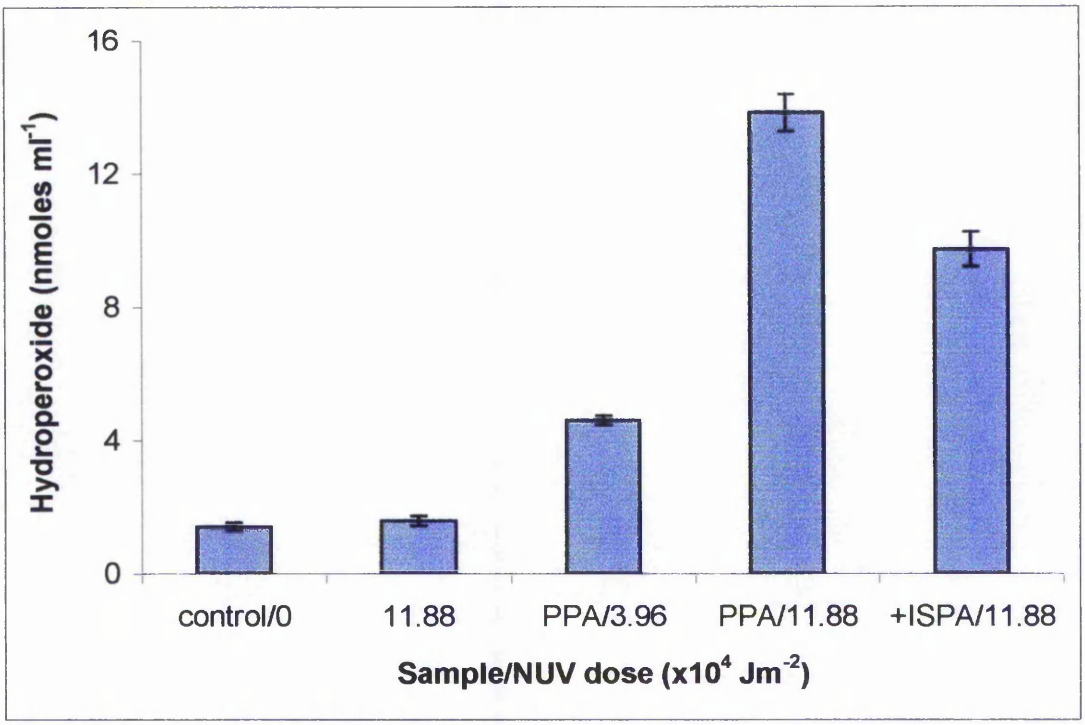

Figure 5.5: Peroxidation of pure liposomes (1.8 μmoles) treated with NUV plus 1 mM β–phenylpyruvic acid (PPA). The bars represent the concentration of hydroperoxide present in the samples as determined by the lipid hydroperoxide assay. All samples were irradiated with 11.88 x 10^4 Jm^{-2} NUV with the exception of the untreated control and the sample in bar three that was exposed to 3.96 x 10^4 Jm^{-2} NUV. The sample in the last bar was treated with 100 mM ISPA in addition to the 1 mM β–phenylpyruvic acid + NUV. The assay was carried out in triplicates and the average +/- the standard error of the mean is given.

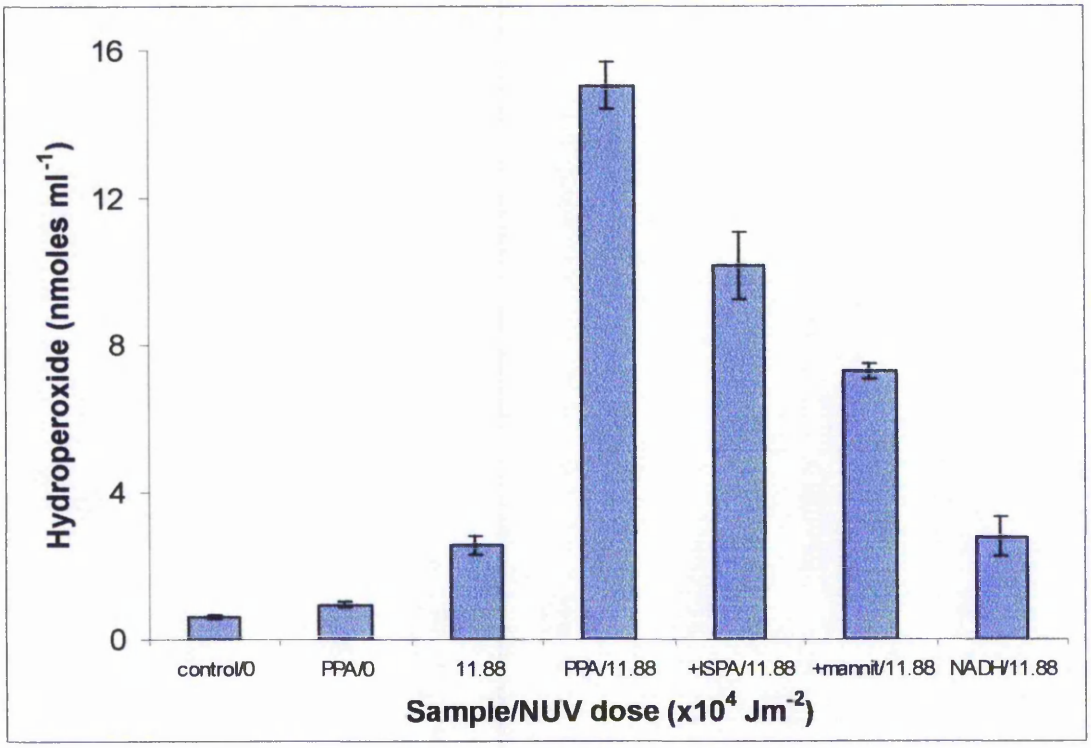

Figure 5.6: Peroxidation of pure liposomes (1.8 μmoles) treated with NUV plus sensitiser. The bars represent the concentration of hydroperoxide present in the samples as determined by the lipid hydroperoxide assay. The first bar represents the untreated control and the second bar a sample incubated with 1 mM β–phenylpyruvic acid in the dark. The rest of the samples were treated with NUV (11.88 x 10^4 Jm^{-2}) and 1 mM β–phenylpyruvic acid. For the sample in the last bar, β–phenylpyruvic acid was replaced with 1 mM NADH. 100 mM of ISPA or mannitol was also added to samples in bars five and six respectively. The assay was carried out in triplicates and the average +/- the standard error of the mean is given.

Even though the exact mechanism by which photolysis of β–phenylpyruvic acid would mediate lipid peroxidation is not known, a suggestion can be made based on the nature of the sensitiser and the liposome system studied. As mentioned earlier, since β–phenylpyruvic acid possesses both a hydrophilic and a hydrophobic group, it is expected to be partly integrated in the liposome cluster. In addition, β–phenylpyruvic acid in the ionic form carries a negative charge and can, therefore, react electrostatically with the positively charged liposome surface. This strong interaction between the sensitiser and the liposome target would result in site-specific generation of ROS. Furthermore, any $^1O_2$ produced will be highly localised in the core of the liposome as $^1O_2$ has higher solubility for this hydrophobic region, where it would react with the lipid molecules generating an elevated amount of lipid hydroperoxides and other peroxidation products.

In order to evaluate the effectiveness of β–phenylpyruvic acid in inducing lipid peroxidation in the presence of NUV, NADH was used as a known endogenous sensitiser of NUV for comparative studies. On NUV photolysis, NADH has been shown to induce single-strand breaks in plasmid DNA *via* production of ROS (Burchuladze and Fraikin, 1991). Its ability to cause lipid peroxidation was, therefore, examined. However, when β–phenylpyruvic acid was substituted with NADH, the amount of hydroperoxide produced on NUV irradiation (11.88×10^4 Jm^{-2}) was the same as that by NUV alone ($P = 0.037$ compared to the untreated control) (Figure 5.6). This result is in agreement with the knowledge that $O_2^{\cdot-}$, which is the primary ROS generated from the photolysis of NADH (Burchuladze and Fraikin, 1991; Cunningham *et. al.* 1985), is not as reactive towards lipids as $^1O_2$ and $^{\cdot}OH$ (Paillous and Fery-Forgues, 1994). Apparently, $^1O_2$ and $^{\cdot}OH$ are proposed to be generated indirectly from the spontaneous dismutation of $O_2^{\cdot-}$ during the NUV photolysis of NADH (Burchuladze and Fraikin, 1991). The photolysis of NADH was also shown to be less effective than that of β–phenylpyruvic acid in inducing phage T7 inactivation (Table 4.1 and Figure 4.9), suggesting that the later may produce $^1O_2$ and $^{\cdot}OH$, the most reactive ROS towards cell components, directly and in a greater quantity when the same energy dose is applied.

When whole cells (*E. coli* or *E. faecalis*) were exposed to NUV (11.88×10^4 Jm^{-2}) plus β–phenylpyruvic acid, the results obtained were more variable than with pure liposomes (Figures 5.7 and 5.8). Bacterial cells are more complex than liposomes, making the extraction of hydroperoxides more difficult and less accurate. The majority of lipids in bacteria are located in the cell membranes and are in more complicated forms than the components of liposomes. Also, besides lipids, bacterial membranes contain proteins and other substances that can quench ROS and lipid radicals, thus terminating peroxidation reactions (Kanofsky, 1991). In particular, enzymes and antioxidants such as catalase, peroxidase, glutatheone and carotenoids are present in cells with the role to protect against lipid peroxidation. As a result, the amount of hydroperoxide present in cell samples was less than that present in the pure lipid system making its accurate detection harder. Nevertheless, some conclusions can be drawn from the results in Figure 5.7.

As with liposomes, the irradiated *E. coli* samples contained more hydroperoxide (about 0.24 nmoles ml^{-1}) than the untreated control, showing around 0.14 nmoles ml^{-1} hydroperoxide (Figure 5.7). When β–phenylpyruvic acid was added to the cells before irradiation, the concentration of hydroperoxide increased to about 0.46 nmoles ml^{-1} ($P = 0.025$ compared to the untreated samples as determined by the Paired T test). Addition of mannitol to the culture treated with NUV and β–phenylpyruvic acid partially protected against lipid peroxidation, with the concentration of hydroperoxide dropped to approximately 0.3 nmoles ml^{-1}. The same was observed with inclusion of catalase, which also reduced the amount of hydroperoxide to around 0.3 nmoles ml^{-1}. Furthermore, the replacement of β–phenylpyruvic acid with NADH before irradiation did not resulted in a synergistic effect, with the concentration of hydroperoxide produced (about 0.23 nmoles ml^{-1}) being similar to that observed when the bacteria were treated with NUV alone.

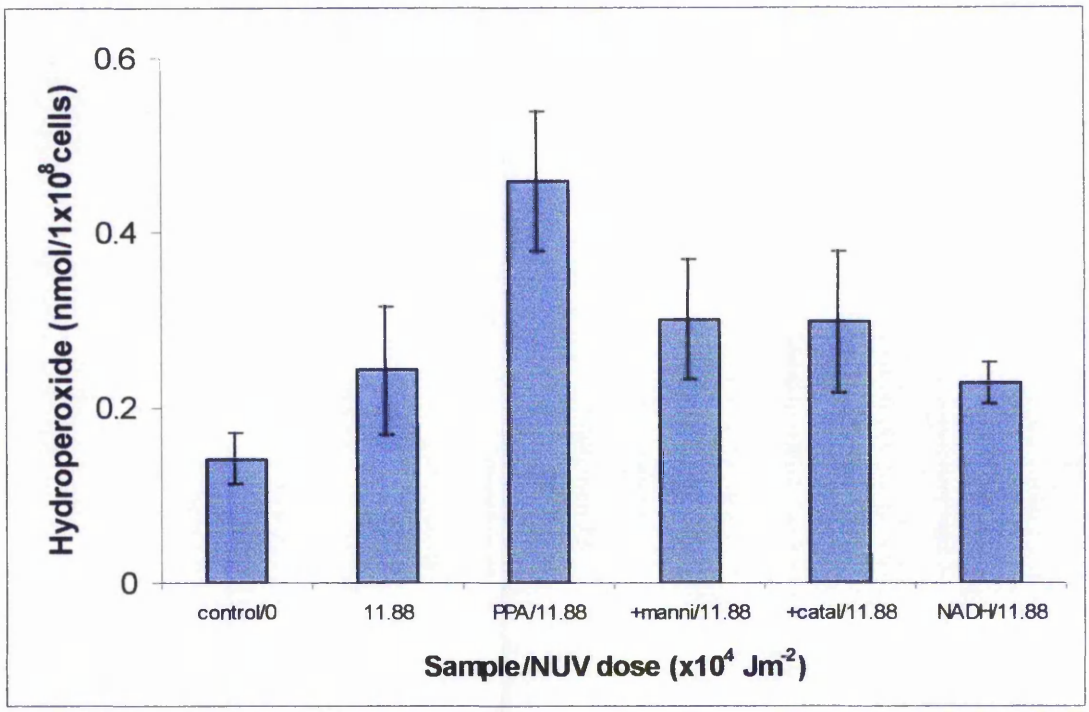

Figure 5.7: Lipid peroxidation of *E. coli* KL16. Cultures were irradiated with 11.88 x 10^4 Jm^{-2} in the presence and absence of 1 mM β–phenylpyruvic acid or NADH. In addition to NUV and β–phenylpyruvic acid, 100 mM mannitol or 1400 units ml^{-1} catalase were also included in two of the samples (columns 4 and 5 respectively). Bars represent the average concentration of hydroperoxide from three samples +/- the standard error of the mean.

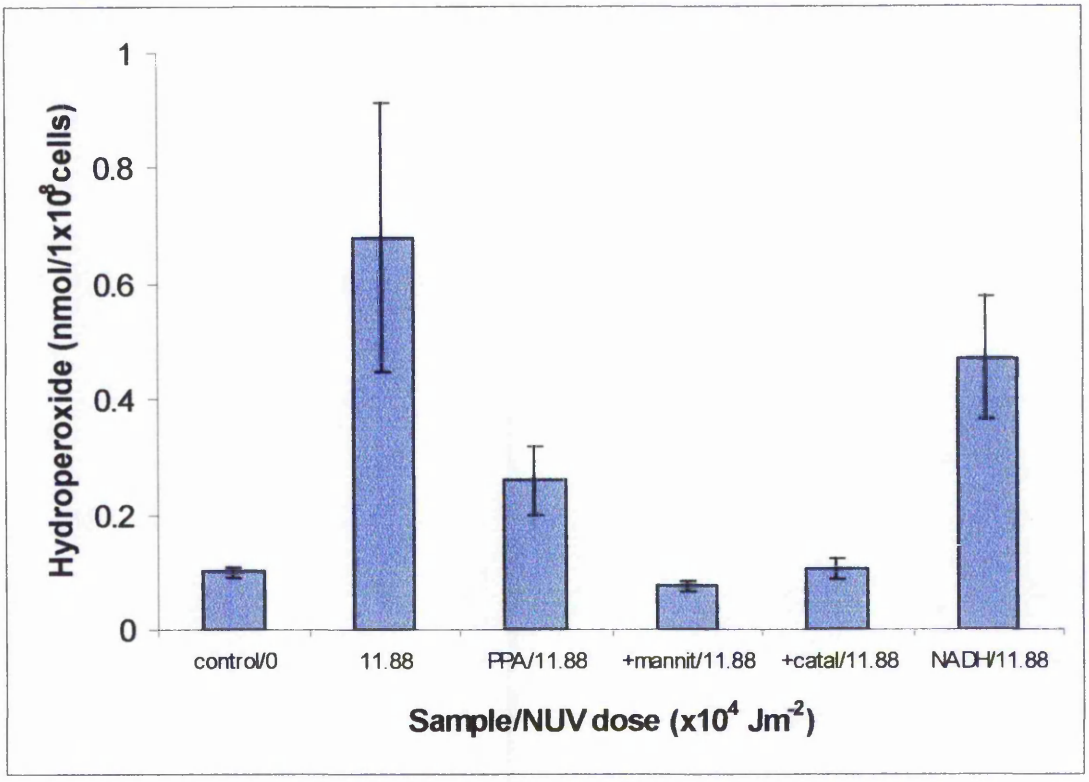

Figure 5.8: Lipid peroxidation of *E. faecalis*. Cultures were irradiated with 11.88 x 10^4 Jm^{-2} in the presence and absence of 1 mM β–phenylpyruvic acid or NADH. In addition to NUV and β–phenylpyruvic acid, 100 mM mannitol or 1400 units ml^{-1} catalase were also included in two of the samples (columns 4 and 5 respectively). Bars represent the average concentration of hydroperoxide from three samples +/- the standard error of the mean.

These results confirm the previous suggestion about the involvement of ·OH and $^1O_2$ in inducing lipid peroxidation. Moreover, the protective effect of catalase indicates that the ·OH radicals involved in the initiation of lipid peroxidation are probably generated *via* H_2O_2. Indeed, the long-lived, uncharged H_2O_2 species could cross cell membranes, and as a result ·OH can be generated inside as well as outside of the membranes and very close to lipids. In addition, the presence of metal ions (Fe^{2+}, Cu^{+}) in the cell environment would favour the occurrence of Fenton reactions, by which ·OH radicals can be produced from H_2O_2.

The results for lipid peroxidation for *E. faecalis* (Figure 5.8) were more erratic than the ones for *E. coli*. Thus, hydroperoxide concentrations seemed greater when the cells were treated with NUV alone (0.68 $\pm$ 0.23 nmoles ml^{-1}) compared to the synergistic effect on inclusion of β–phenylpyruvic acid (around 0.26 nmoles ml^{-1}) or NADH (about 0.47 nmoles ml^{-1}). Addition of both mannitol and catalase reduce the amount of hydroperoxide to about 0.07 nmoles ml^{-1} and 0.10 nmoles ml^{-1} respectively, whereas the untreated samples contained 0.1 nmoles ml^{-1} hydroperoxide. These results are not surprising as the quoted sensitivity of the assay is down to 0.25 nmoles of hydroperoxide, and most of the concentrations measured for *E. faecalis* are below that. The fact that the results for *E. faecalis* are very different from those for *E. coli* reflects the difference between gram-positive and gram-negative bacteria, in terms of lipid content. The majority of lipids in a cell are part of the cell membrane, and gram-positive bacteria, having one phospholipid membrane, contain considerably fewer lipids than the gram-negative ones, which have two. Therefore, although lipid peroxidation of both gram-positive and gram-negative bacteria can be equally destructive, it is harder to detect for the former with the available assay.

Unlike DNA damage, there are no repair mechanisms in the cell to deal with lipid peroxidation. Also, whereas DNA damage is very localised, lipid peroxidation is a chain reaction that results to the generation of highly reactive molecules that can, in turn, react with other cellular components and cause further damage (Figure 1.7). To avoid such destructive events for the cell, organisms are equipped with antioxidant molecules that quench ROS and hydroperoxides, and thus prevent the initiation and propagation of lipid peroxidation. This is why powerful antioxidants like

α–tocophenol and β–carotene, which are lipid-soluble, are associated with the cell membrane. Bearing this in mind, the low levels of hydroperoxide detected in the bacterial samples can be explained. Naturally occurring antioxidants in the cell keep the hydroperoxide levels low, even after irradiation and in the presence of sensitisers. This is not the case, however, when liposomes are used.

Additionally, another reason that would explain the difference in hydroperoxide concentrations, and therefore, the occurrence of lipid peroxidation between pure liposomes and cell membranes may be the different charges involved. As mentioned above, the liposomes used carried a positive charge that would enhance an interaction with β–phenylpyruvic acid. On the other hand, bacterial membranes carry different localised charges and an overall negative charge. Therefore, even though β–phenylpyruvic acid is still expected to integrate to the membrane before photolysis, this interaction may not be as favourable as in a pure lipid system that carries the 'right' charge.

Generally, as mentioned in section 4.4, β–phenylpyruvic acid is believed to be located in the cell membrane (outer for gram-negative cells), where, in the presence of NUV, ROS, such as $^1O_2$, $^{\cdot}OH$, and $HO_2^{\cdot}$ are generated and can readily react with lipids causing lipid peroxidation. The results when liposomes and to a lesser extend bacterial cells were treated with NUV plus β–phenylpyruvic acid confirm this suggestion.

5.5 NUV plus Sensitiser-Mediated Oxidative Modification to Proteins

Proteins are common targets of oxidative damage. They can undergo primary modification that involves direct oxidation of amino acid side chains or secondary modification by molecules generated by oxidation of other molecules (e.g. products of lipid peroxidation) (Stadtman, 1995). Enzymes and structural proteins may be attacked, in particular, whenever ROS are generated. Unlike nucleic acids, however, where small changes may affect the survival of the cell, proteins can withstand a considerable degree of oxidative modification before conformational or functional changes take place. Nevertheless, the damaging effect that ROS may have on a

protein may result in DNA-protein cross-links or formation of protein radicals that can damage DNA and lipids (Dean *et. al.*, 1993). For this reason, the potential effects that β–phenylpyruvic acid and its related *p*-OH-phenylpyruvic acid may have on the protein components of a cellular system were examined. The extent of protein damage that can be attributed to the NUV photolysis of these sensitisers was studied using samples of BSA and of total cell protein extracts. BSA, a 66 kDa protein with two identical subunits, was used as a model protein system.

Protein modification by ROS produced on photosensitisation reactions often has as a consequence the introduction of carbonyl groups into proteins. The appearance of such carbonyl groups is taken as evidence of oxidative modification (Levine *et. al.*, 1994). The method for the determination of carbonyl content used in this study was based on the reaction of carbonyl groups with 2,4-dinitrophenylhydrazine (DNPH) to form a 2,4-dinitrophenylhydrazone (section 2.13.4). Protein samples were derivatised with DNPH, and carbonyl containing protein bands were detected, after SDS-gel electrophoresis, with immunostaining using a monoclonal dinitriphenyl-IgE antibody (section 2.13.5). The total protein sample was visualised using Coomassie blue staining.

As seen from the untreated sample (lane 1) in Figure 5.9 (a), BSA appears in the gel as a single band of 66 kDa. Immunostaining of DNPH-reactive protein carbonyls after western blotting [Figures 5.9 (b)] indicated that a small amount of carbonyls is naturally present in BSA (lane 1). Treatment of the BSA samples with NUV alone (11.88×10^4 J m^{-2}) showed a slight increase in carbonyls over the untreated control (lane 2). However, exposure of BSA to NUV in the presence of 1 mM β–phenylpyruvic acid or *p*-OH-phenylpyruvic acid resulted in a marked increase in the content of protein carbonyls as demonstrated by the intensity of the bands (lanes 3 and 4 respectively).

Besides an increase in carbonyl content, oxidative modification of proteins may also result in aggregation, fragmentation or proteolytic fragmentation (Kohen *et. al.*, 1995). It can be observed in Figure 5.9 (a), that a combination of 1 mM β–phenylpyruvic acid and 11.88×10^4 J m^{-2} NUV resulted in fragmentation of the

protein, as indicated by the appearance of a second band of about 33 kDa (lane 3). Such a band was absent from samples treated with NUV alone or in the presence of *p*-OH-phenylpyruvic acid (lanes 2 and 4 respectively), suggesting that only the sensitised action of β–phenylpyruvic acid can cause fragmentation of BSA. From the western blot [Figure 5.9 (b)], it is apparent that the low molecular weight fragment is high in carbonyl content and therefore highly oxidised.

Similar experiments that involved a time-course assessment of photosensitised oxidative damage to BSA by β–phenylpyruvic acid showed that the sensitiser alone does not result in fragmentation of the protein or contribute to the concentration of carbonyls detected with this assay (Butler, unpublished results). These studies showed a dose-dependent increase in the carbonyl content of BSA samples when irradiated with NUV in the presence of a constant concentration of β–phenylpyruvic acid (1 mM). At this concentration, in the absence of NUV, there were no DNPH-reactive protein carbonyls detected by western blotting additional to that present in the untreated control. It is known that β–phenylpyruvic acid and the related *p*-OH-phenylpyruvic acid contain a carbonyl group in their molecule, so some interference with the assay was expected. However, the results mentioned above indicated that the carbonyl part of β–phenylpyruvic acid does not interfere with the assay. Apparently, the concentration of this sensitiser used in the experiments was sufficiently low, and any carbonyls attributed to β–phenylpyruvic acid were at much lower concentrations compared to that naturally present in BSA (a considerably larger and more complex molecule) to be detectable by this assay. Similar results would be expected for *p*-OH-phenylpyruvic acid, since the carbonyl content of this sensitiser is identical to that of β–phenylpyruvic acid at the same concentrations.

BSA is a peptide chain with a series of nine double loops formed by disulphide bonds between its thirty-four cystine residues (Peters, 1977). It is interesting to note that this protein is rich in phenylalanine, tyrosine and histidine residues, all of which are sensitive to ROS attack. In addition, the majority of these residues are located in the first three loops, whereas the last three loops contain the least. It is possible that upon photolysis, part of the oxidised protein undergoes fragmentation between loops six and seven. The highly oxidised fraction observed in

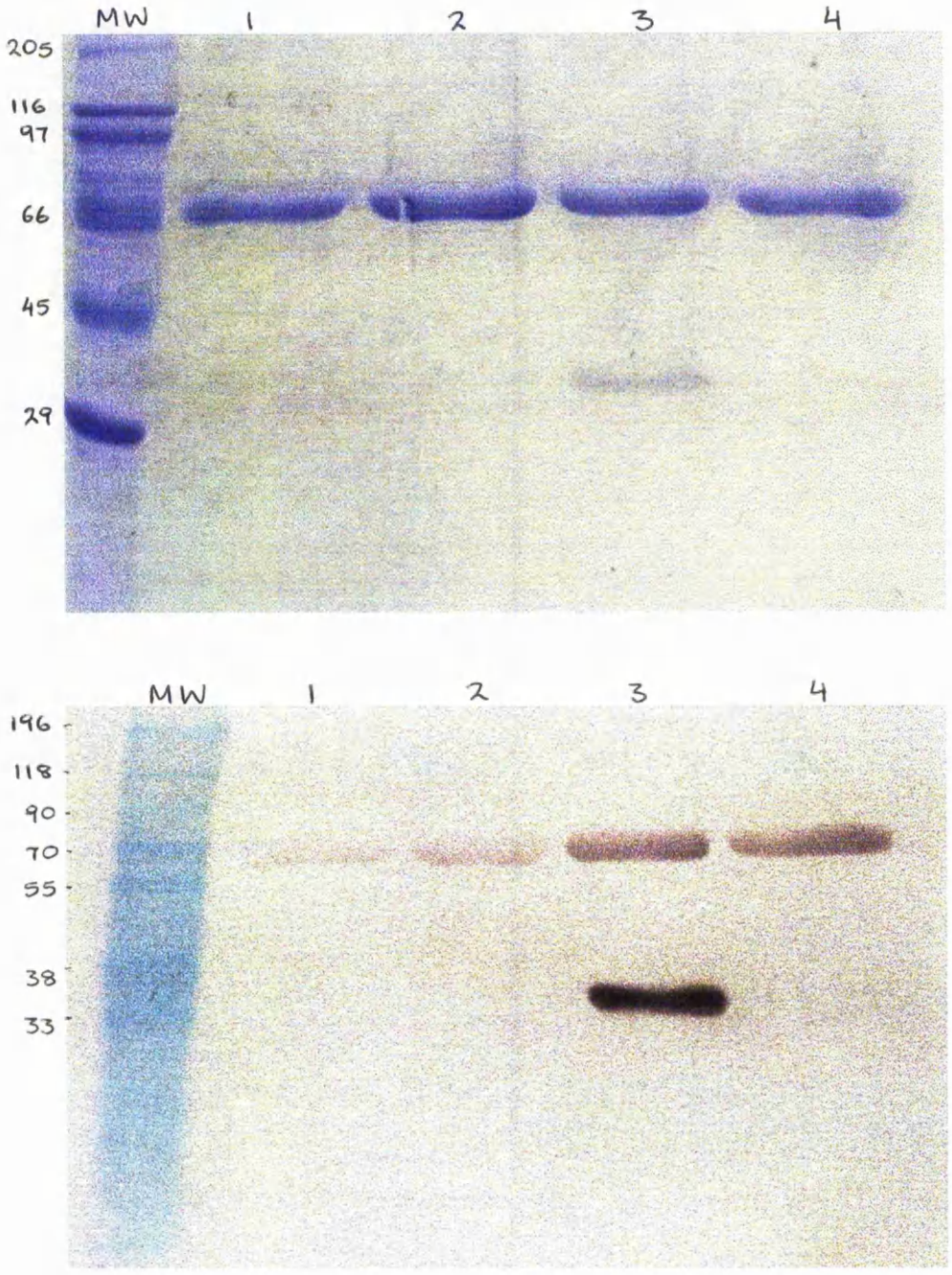

Figure 5.9: Modification of BSA (10 μg) by NUV radiation (11.88 x 10^4 J m^{-2}) in the presence of β–phenylpyruvic acid and OH- phenylpyruvic acid. (a) SDS-gel electrophoresis/ Coomassie staining; (b) Carbonyl-containing bands detected by western blotting; 1, untreated derivatised control; 2, NUV; 3, NUV and β–PPA (1 mM); 4, NUV and OH-PPA (1 mM).

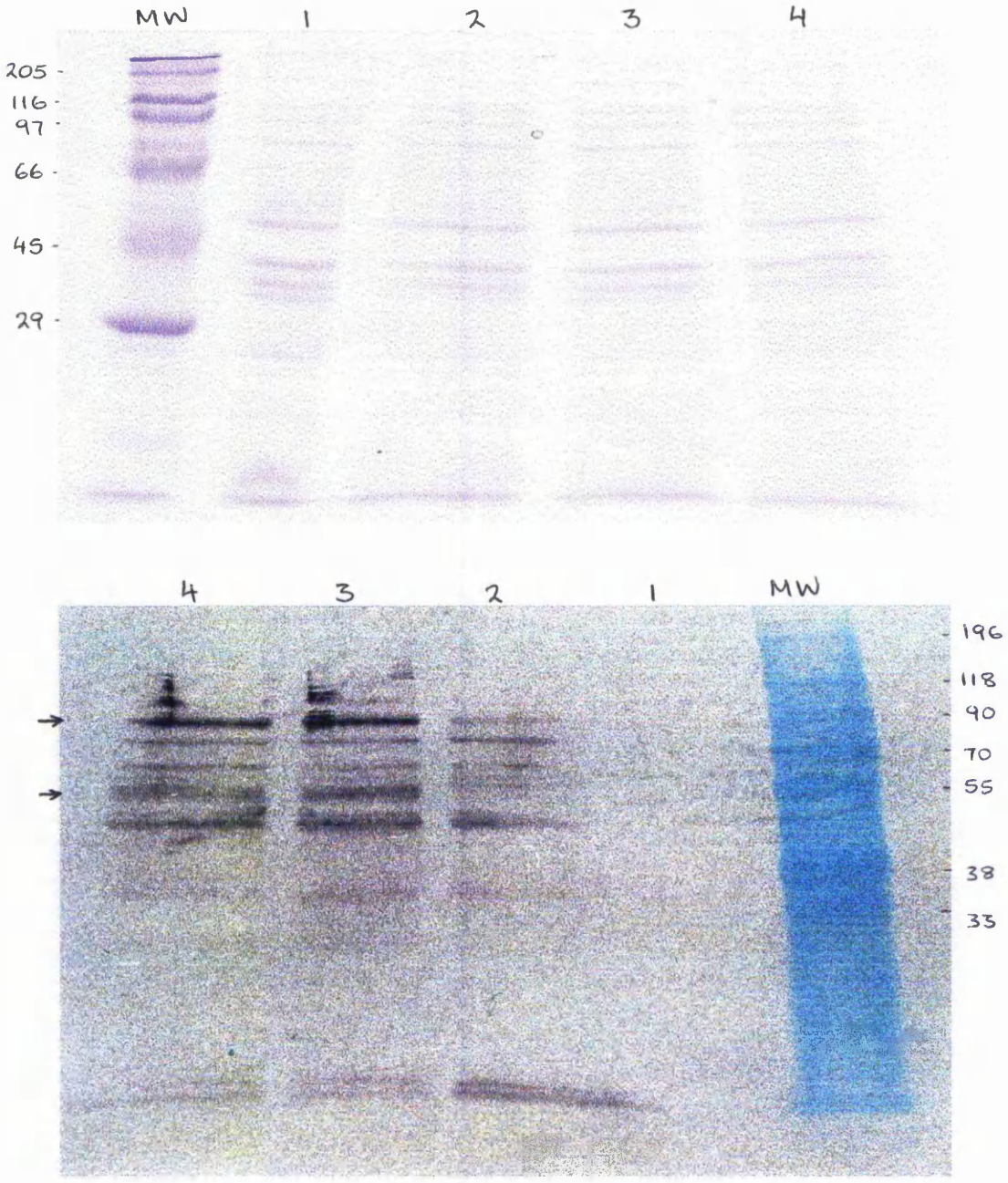

Figure 5.10: Modification of *E. coli* proteins (10 μg) by NUV radiation (11.88 x 10^4 J m^{-2}) in the presence of β–phenylpyruvic acid. (a) SDS-gel electrophoresis/ Coomassie staining; (b) Carbonyl-containing bands detected by western blotting; 1, non-derivatised control; 2, untreated control; 3, NUV; 4, NUV and β–PPA (1 mM).

Figure 5.9 (b) corresponds to the section containing loops one to six, whereas the second fragment is too small to see on the gel (its estimated MW is 12 kDa). Although this possibility needs to be confirmed, it is in agreement with the fragments presented previously on SDS-PAGE of peptic fragments of BSA (Peters, 1977).

In vitro experiments using BSA may give a good account of the oxidative modifications that proteins undergo when exposed to photosensitised generation of ROS, but the *in vivo* situation in a cell may be different. In the cell environment, some proteins may undergo preferential oxidation depending on their composition, location, and proximity to the source of ROS generation and antioxidant protection. To determine the effect of NUV plus β–phenylpyruvic acid in a more natural environment, total *E. coli* protein extracts (prepared as described in section 2.13.2) were used.

From the SDS gel electrophoresis [Figure 5.10 (a)], there are not any marked changes in protein patterns when the cell proteins were exposed to NUV in the presence or absence of β–phenylpyruvic acid (lanes 3 and 4) compared to the controls (lanes 1 and 2). The lack of high molecular aggregate and low molecular fragment formation indicates that these types or oxidation may not occur, or be significant, under the experimental conditions employed involving whole-cell extracts. However, functional cells contain a variety of proteins, which are at relatively low concentrations compared to the BSA samples used, and therefore any protein modifications would be harder to detect. Nevertheless, western blotting of the *E. coli* proteins showed that samples exposed to NUV irradiation (11.88×10^4 J m^{-2}) (lanes 3 and 4) contained more carbonyls than the non-irradiated control (lane 2). It can also be observe that this increase in the carbonyl content is selective of some protein bands, for example of 70 kDa and 118 kDa, whereas there is no apparent change in the carbonyl content of other bands such as those of 55 kDa and 90 kDa. Such selectivity in protein modification is suggestive of two possibilities. The case may be that some proteins (e.g. those that can interact electrostatically with the sensitiser) are more susceptible to ROS-mediated oxidative damage due to photosensitised reactions being localised. It is also possible that some proteins are more prone to ROS attack, depending on their amino acid composition and the presence of sulphur-containing

side chains (Kohen *et. al.*, 1995). For example, $^1O_2$ is known to react preferentially with histidine (Halliwell and Gutteridge, 1999), and therefore, proteins that contain this amino acid at sites exposed to ROS attack will be more susceptible to oxidative damage.

From Figure 5.10 (b), it can also be noted that addition of β–phenylpyruvic acid to the protein extracts before irradiation (lane 4) did not seem to have an additional effect to that of NUV alone (lane 3). This result, however, may reflect the difficulty in obtaining quantitative results with this assay, especially when low concentrations of individual proteins are involved, rather than the lack of a synergistic effect. Moreover, the protein samples used are expected to contain protein-bound chromophores such as tryptophan, histidine, tyrosine and phenylalanine that can act as sensitisers of NUV and cause additional protein damage to that attributed to NUV alone (Craggs *et. al.*, 1994; Ortwerth and Olesen 1994; Paretzoglou *et. al.*, 1998).

Although the method used in this study to assess protein damage caused by sensitised photolysis is accurate in measuring changes in the carbonyl content of protein samples, it does not specify the type of oxidative modification or ROS involved in carbonyl formation. Thus, whereas most of the oxidising pathways lead to carbonyl-containing products such as aldehydes and ketones that are detected by this assay, other products such as sulphoxides and amino acid derivatives (e.g. 4-hydroxy-phenylalanine and *N*-formylkynurenine) are not accounted for. In addition, other types of ROS-mediated damage to proteins such as decarboxylation, deamination, polypeptide-chain scission and crosslinking would go undetected.

5.6 Conclusion

A study of the effect of L-histidine, L(+)mandelic acid, *p*-OH-phenylpyruvic acid and β–phenylpyruvic acid in the induction of DNA and protein damage and lipid peroxidation, in the presence of NUV, indicated that these compounds can, in general, affect the integrity of such biomolecules. The photolysis of β–phenylpyruvic acid, in particular, was found to cause single-strand breaks on pBR322 DNA *in vitro*, in a concentration and dose-dependent manner. As a result, the transformation efficiency

of the plasmid was increased. In the presence of NUV, β–phenylpyruvic acid was also found able to induce mutations in *E. coli* that resulted in antibiotic resistance. This was particularly observed with *E. coli mutT*$^-$ and was an indication of the occurrence of transversion mutations upon photolysis of this compound. The ability of β–phenylpyruvic acid to cause DNA damage in the presence of NUV was further emphasised by the triggering of an SOS response in *E. coli* PQ37 (production of β–galactosidase). Such a response may be indicative of DNA oxidation, DNA base modification and similar types of DNA damage, which would be SOS inducing and mutagenic rather than lethal.

In vitro and *in vivo* studies of lipid peroxidation as the result of treatment with NUV plus β–phenylpyruvic acid indicated that ROS produced on photolysis of this sensitiser can readily attack lipids generating high concentrations of hydroperoxides. This result was more apparent for liposomes, probably due to the high content of lipids, lack of naturally present antioxidants and an electrostatic interaction with the negatively charged β–phenylpyruvic acid.

In addition to causing lipid peroxidation in the presence of NUV, β–phenylpyruvic acid was shown to be involved in protein damage. Thus photolysis of β–phenylpyruvic acid resulted in fragmentation of BSA and in elevated carbonyl contents in BSA and *E. coli* proteins, an indication of oxidative damage.

Besides β–phenylpyruvic acid, L-histidine, L(+)mandelic acid and *p*-OH-phenylpyruvic acid were also able to cause some DNA damage on NUV photolysis as indicated by the formation of single-strand breaks in pBR322 and DNA damage-induced production of β–galactosidase. In the presence of NUV, *p*-OH-phenylpyruvic acid was also shown to cause oxidative modification to BSA. These compounds were given a lower emphasis than β–phenylpyruvic acid, however, since their photolysis was shown to be most effective under alkaline conditions, and all of the experiments involving DNA, lipids and proteins were performed at near physiological pH (pH 7 – 7.5), as a better representation to natural processes.

CHAPTER SIX

DISCUSSION, CONCLUSIONS AND FURTHER WORK

6.1 Discussion

In this study, L-histidine, L(+)mandelic acid, β–phenylpyruvic acid, *p*-OH-phenylpyruvic acid and L-β–phenyllactic acid have been proposed to act as sensitisers of UVR and, when photolysed, to react with molecular oxygen in aqueous solution and produce a variety of reactive oxygen species such as H_2O_2, $^{\cdot}OH$, $O_2^{\cdot-}$ / $HO_2^{\cdot}$, and $^1O_2$. As demonstrated in this work, these compounds absorb in the UVR spectrum, are non-toxic to phages and bacteria, in themselves non-reactive, and dissolve rapidly in aqueous media at concentrations up to 10 mM. Their study was of interest as they are ubiquitous components of living organisms and part of the metabolic pathway of phenylalanine in humans. Moreover, these compounds have a structural similarity to phenylalanine, tyrosine and tryptophan, all of which have been shown previously to undergo photolysis in the presence of UVA radiation and generate ROS (Craggs *et. al.*, 1994; Kohen *et. al.*, 1995; Ortwerth and Olesen, 1994). L-histidine in particular, like tryptophan, has an indole ring, which is believed to be the functional group responsible for UVA absorption. It is likely that L-histidine is photolysed in a similar way (Paretzoglou *et. al.*, 1998).

All the compounds investigated absorb with varying intensities within the wavelength range of interest (290 – 400 nm). However, their ability to undergo photosensitised reactions to generate ROS and cause damage to biological systems do not necessarily correspond to their absorption pattern. The order of reactivity or induction of biological damage for all the different compounds and for all of the experiments performed is shown in Table 6.1. It is difficult to draw definite conclusions from these results, since in some experiments only one or two of the proposed sensitisers were used. However, some interesting observations can be made. The sensitising activities of β–phenylpyruvic acid and *p*-OH-phenylpyruvic acid reflect their absorption spectra. The strong absorption of UVA observed for these compounds seems to be responsible for their photolytic action. The formation

of ROS, however, from the photolysis of *p*-OH-phenylpyruvic acid was found to be strongly pH dependent. This pH dependence, which relates to $O_2^{\cdot-}$ generation, may have rendered this sensitiser less effective than β–phenylpyruvic acid in causing damage to cell components at near physiological pH. On the other hand, the pH of the solution had only a slight effect on the UVA photolysis of β–phenylpyruvic acid, suggesting a different mechanism of photolysis to *p*-OH-phenylpyruvic acid and generation of other ROS in addition to $O_2^{\cdot-}$. The ability of β–phenylpyruvic acid to cause, on photosensitised reactions, DNA and protein damage and lipid peroxidation, may be indicative of $^1O_2$ formation.

The use of a TL01 lamp and a filter to cut out the UVB wavelengths in the UV source made it possible to obtain separate results for the effect of UVA and UVB on the photolysis of β–phenylpyruvic acid. The results indicated that UVA had a greater effect in inducing photosensitised reactions than equal energy exposures of UVB. The extent of photolysis in the UVB region was lower than that expected from the absorption spectrum of β–phenylpyruvic acid. UVA seemed to be the primary wavelength range to induce a photosensitised reaction. Even though β–phenylpyruvic acid absorbs less in the UVA than in the UVB region, this absorption of photons appears sufficient to induce an enhanced photolytic effect. This, however, is in agreement with the suggestions that UVA is the predominant waveband to induce photosensitised reactions and not UVB.

In the case of L-histidine, the mode of photolytic action also corresponds to its absorption pattern. This compound exhibited lower UVA absorption that β–phenylpyruvic acid and to *p*-OH-phenylpyruvic acid and this reflects its reduced ability to cause DNA damage and phage T7 inactivation. It has been previously suggested that the weak light absorption in the long-wavelength tail of the amino acid spectra may initiate decomposition reactions and form products that can undergo further photolysis (Smith, 1989). However, the photosensitised action of L-histidine is not as strong as of other compounds investigated here.

EXPERIMENT	ORDER OF PHOTOLYSIS / BIOLOGICAL EFFECT
Absorption Spectra	OH-PPA > PPA > His > Mand ≥ PL
NBT Reaction	PPA > Mand > OH-PPA > His > PL
Deoxyribose Assay	Mand > His > OH-PPA > PPA > PL
T7 Inactivation	PPA > OH-PPA > His ≥ Mand
Bacterial Lethality	PPA
PBR322 Strand-breaks	PPA > Mand > His
β–Gal Production	His > Mand > PPA > OH-PPA
Induction of Mutation	PPA > Mand > His
Lipid Peroxidation	PPA
Damage to BSA	PPA > OH-PPA

Table 6.1: A summary of experiments performed in this study showing the order of effectiveness of photosensitised reactions by the compounds of interest. The overall effect of each compound for every experiment was considered irrespectively of the pH. These compounds were β–phenylpyruvic acid (PPA), *p*-OH-phenylpyruvic acid (OH-PPA), L-histidine (His), L(+)mandelic acid (Mand), and L-β–phenyllactic acid (PL).

L-β–phenyllactic acid was shown to exhibit very low absorption in the UVA and UVB wavebands and this was reflected in its ability to undergo photosensitised reactions. Chemical assays indicated that this compound can be photolysed in the presence of UV radiation and produce ROS like $O_2^{\cdot-}$ and $^{\cdot}OH$, but at very low concentrations. For this reason, L-β–phenyllactic acid was studied less extensively that the other sensitisers.

Of all the sensitisers studied, the behaviour of L(+)mandelic acid was unique. Although, like L-β–phenyllactic acid, it has a low UV absorption in the spectral region studied, it was shown by chemical assays to effectively produce a variety of ROS in the presence of UV radiation. In addition, the photolysis of this compound was quite effective in inducing DNA damage and inactivation on phage T7. Like with β–phenylpyruvic acid, the use of a TL01 lamp and a filter to cut out the UVB

wavelengths in the UV source made it possible to obtain results for the effect of UVB or UVA alone on the photolysis of this compound. The results indicated that equal energy exposures by UVA or UVB had the same effect. Although very little, the absorption of L(+)mandelic acid in the UVA and UVB wavebands is very similar and results in equal levels of photosensitised reactions. Generally, in both wavebands, the photosensitised potential of L(+)mandelic acid is much higher than that expected from the levels of UV absorption. From these observations, it can be concluded that either both UVB and UVA can equally induce photolysis and therefore generation of ROS, or that on low absorption of photons from UVB L(+)mandelic acid can become activated and directly react with a substrate (e.g. reduce NBT) by energy transfer and without the involvement of ROS.

During the UV photolysis of the sensitisers in this study, various ROS such as $^{\cdot}OH$, $O_2^{\cdot-}$, and $^1O_2$ are produced simultaneously and it is, therefore, difficult to assess the role of each species unambiguously in the resulting biological effects. However, looking at the different patterns in the behaviour of each compound and with the help of specific tools used in this study some suggestions can be made for the mechanism of action of these sensitisers. As mentioned previously, the weak pH dependence of the photolysis of β–phenylpyruvic acid suggests that $O_2^{\cdot-}$ is not the primary ROS generated from it. This is in agreement with the low reactivity of $O_2^{\cdot-}$ towards DNA and lipids and the high rate by which the UVA photolysis of this sensitiser causes damage to these components. Results from the deoxyribose assay also indicate the generation of low concentrations of $^{\cdot}OH$. From the damaging synergistic effect β–phenylpyruvic acid has on viruses, bacteria and their molecular components, the suggestion is that this sensitiser generates predominately $^1O_2$ and that this ROS is primarily responsible for the damage observed, since this ROS is very reactive towards DNA, proteins and lipids. Evidence for the involvement of $^1O_2$ in DNA damage, comes from the use of a transversion mutator strain of *E. coli* that is deficient in repairing 8-oxodGuo or the misincorporation of this modified base during DNA replication. An increased frequency of mutation (65-fold) of this strain compared to the wild type (4-fold) by the synergistic action of β–phenylpyruvic acid is indicative of high incidence of 8-oxodGuo modified bases. This suggests 8-oxodGuo as the major premutagenic modification present in DNA before replication and a possible

role for $^1O_2$ in DNA damage since this ROS modifies selectively the guanine residue (Ravanat and Cadet 1995; Stary and Sarasin, 2000).

The mechanism of action for *p*-OH-phenypyruvic acid and L-histidine appears to involve formation of $O_2^{\cdot-}$ and $^{\cdot}OH$ as indicated by the strong pH dependence of the photolysis of these compounds, as observed in the NBT assay and T7 inactivation experiments, and the results of the deoxyribose assay. Addition of selective scavengers in the experiments has also supported this suggestion, although the results are not very accurate due to the reactivity of such scavengers with other ROS. It is also not clear whether $^{\cdot}OH$ are generated directly on photolysis or indirectly *via* the decomposition of H_2O_2 and Fenton-like reactions. The high levels of phage T7 inactivation and protein oxidation observed on the photolysis of *p*-OH-phenypyruvic acid, support the involvement of $^{\cdot}OH$, which is highly reactive with both DNA and proteins. The same situation applies to the photolysis of L-histidine, and the lower lever of reactivity exhibited by this compound may just reflect its lower absorption in the UVA.

Like *p*-OH-phenypyruvic acid and L-histidine, the UVA photolysis of L(+)mandelic acid also resulted in the generation of $O_2^{\cdot-}$ and $^{\cdot}OH$. Evidence for this suggestion is the pH dependence of the photolysis of this sensitiser, as observed in the NBT assay and T7 inactivation experiments, and the results of the deoxyribose assay. The production of $^{\cdot}OH$ may, thus, be responsible for the strand-break formation observed on pBR322 and the inactivation of phage T7. The higher level of synergistic inactivation reported for *p*-OH-phenypyruvic acid compared to L(+)mandelic acid, and given that the latter appears to produce more $^{\cdot}OH$ species, is a suggestion that H_2O_2 may be a photoproduct of *p*-OH-phenypyruvic acid but not L(+)mandelic acid. In the presence of transition metal ions in the phage environment, H_2O_2 may result in the formation of $^{\cdot}OH$ very close to the DNA.

In order to assess the biological effect of the photolysis of β–phenylpyruvic acid, the most potent of the compounds studied, it was of interest to identify potential targets of ROS attack *in vivo*. Wild type and mutant strains of bacteria were, therefore, used for this purpose and some interesting observations were made. A nucleotide excision repair deficient strain of *E. coli* and the wild type exhibited

similar sensitivities to photosensitised damage. A similar rate of lethality in both strains suggested other than DNA damage as the cause of cell death. In addition, the increased susceptibility to photosensitised reactions of a gram-positive species compared to a gram-negative suggested the cell membrane as a potential target. It is believed that on sensitised formation, ROS attack on the cell membrane causes lipid peroxidation that may lead to cell lysis, and that cells with a thin cell membrane may be more susceptible to such attack. The determination of the effectiveness in the incorporation of the sensitiser in the cell, by measuring endogenous concentrations of the compound before irradiation, pointed to the importance of such incorporation on photosensitised damage. Thus, gram-positive cells that have thinner cell membranes were shown to be associated with a much higher concentration of the sensitiser and this believed to be responsible for the increase cell lethality observed, as ROS generation could take place near target macromolecules. The suggestion is that the hydrophilic, ionic group of β–phenylpyruvic acid (the carboxylate) remains on the outer region of the cell membrane, whilst the hydrophobic, phenyl group penetrates further to the inner part of the membrane. The carbonyl group, which is believed to be the chromophore, and therefore the locus of ROS generation, is located mid-way between the carboxylate and phenyl groups on the molecule. This suggestion was supported by results showing gram-positive bacteria to be more prone to synergistic inactivation. The difference between the gram-positive and negative species is suspected to be due to the double phospholipid membrane of gram-negative bacteria. The outermost of these membranes can act as a trap leading to the preferential location of the sensitiser in an area where its effects will be less lethal. In the case of gram-positive species no such barrier is available.

The ability of the UV photolysis of β–phenylpyruvic acid to cause lipid peroxidation was investigated using liposomes, as a pure lipid system, together with bacterial extracts. Liposomes have the advantage of lacking any of the antioxidants that are normally present in cells or other potential targets for ROS (e.g. proteins), which would interfere with the determination of the actual oxidative damage to lipids. They are also positively charged which ensures favourable ionic interaction with the negatively charged sensitiser and thus ROS generation near potential lipid targets. The high levels of lipid peroxidation to liposomes and bacterial cells

indicated that ROS produced on photolysis of this compound could readily attack lipids generating high concentrations of hydroperoxides. As expected, this result was more apparent for liposomes. The results of lipid peroxidation in bacteria indicated that both gram-positive and gram-negative cells are prone to sensitised peroxidation of membrane lipids, but the occurrence of higher hydroperoxide concentrations in the gram-negative cells may reflect the increased lipid content in the membranes of these species. The use of $^{\cdot}OH$ radical scavengers made apparent the contribution of this radical in inducing lipid peroxidation, whereas addition of catalase suggested that $^{\cdot}OH$ was generated *via* H_2O_2.

Lipids are not the only targets of ROS generated by photosensitised reactions since rapid inactivation of phage T7 was observed with a number of the photosensitisers reported in this study. Inactivation of the phage could be the result of DNA and / or protein damage. The use of pBR322 as a model system to study oxidative DNA damage revealed that photosensitised reactions were responsible for single-strand break formation. However, single-strand breaks were formed in a concentration and dose-dependent manner and, with the exception of β–phenylpyruvic acid, were quite apparent only at higher than 1 mM concentration of the sensitiser. If this is the situation with naked DNA, then in a more complex system such as the phage, DNA would be a more inaccessible target. It is, therefore, believed that ROS generated on photolysis of the compounds of interest target phage proteins rather than DNA. It has been previously reported that single-strand DNA breaks did not account for phage inactivation, but DNA-protein crosslinks prevent normal injection of phage DNA (Hartman *et. al.*, 1979). In addition, whereas it is possible for DNA lesions to be repaired by the DNA-repair machinery of the host, protein damage that occurs before injection can not be corrected.

Although the suggestion is that damage to the phage proteins is primarily responsible for inactivation, the photosensitised effect of the compounds studied in causing DNA damage is indisputable. However, all types of DNA damage that were observed in this study and were the result of the synergistic action of the sensitiser were oxidative modifications. There was no apparent double strand-break formation on pBR322 (as this would have led to linearisation of the plasmid). Also,

photosensitised reactions induced the triggering of an SOS response in *E. coli* PQ37 (production of β–galactosidase). Such a response might be indicative of DNA oxidation, DNA base modification and similar types of DNA damage, which would be SOS inducing and mutagenic rather than lethal. β–phenylpyruvic acid was also shown able to induce transversion mutations in *E. coli* that were predominantly a result of guanine oxidation. The ability to cause oxidative modification of DNA is consistent with the role of UVA-induced sensitised damage. However high levels of cell inactivation rather than mutations to bacterial cells were observed, and this may be mainly due to photosensitised reactions taking place far from the bacterial genome or due to the effect of the 1.2 % of UVB that was emitted from the UV source.

In vitro studies of the sensitised action of β–phenylpyruvic acid and *p*-OH-phenylpyruvic acid on proteins revealed that the UV photolysis of these compounds can cause oxidative modification to proteins as demonstrated by immunostaining of DNPH-reactive protein carbonyls. Such modifications to BSA were expressed as an increase in the carbonyl content and fragmentation of the protein. The use of *E. coli* proteins, allowed for the study of preferential protein oxidation. A selective increase in the carbonyl content of some *E. coli* protein bands indicated that proteins might have undergone preferential oxidation. This is not surprising, as the susceptibility of a protein to oxidative damage would depend on its conformation and amino acid composition. Thus, ROS would preferentially attack proteins with sulphur-containing side chains and a high content of exposed aromatic amino acids. Similar studies that involved the assessment of the relative susceptibility of the major plasma proteins to $^{\cdot}OH$ induced oxidative modification, concluded that fibrinogen was much more susceptible to oxidative damage compared to albumin, immunoglobulins and transferrin (Shacter *et. al.*, 1994).

In order to evaluate the biological relevance of the data presented here, it is important to compare the concentrations of the compounds used to that expected to be present in human skin. 1 mM of each senstitiser was used for all the experiments with the exception of concentration dependence studies where 1 – 8 mM was used. At this concentration, all of the compounds investigated exhibited significant biological damage in the presence of UVR. The concentrations of these sensitisers in

real life are expected to be considerably lower. However, cells like skin fibroblasts are also expected to be more susceptible to synergistic damage than bacterial cells, since eukaryotic cells have thinner cell membranes than bacteria and UV can induce cell cycle arrest and apoptosis to these cells. In addition, even small amounts of cellular damage (less than that detectable by the methods used) may have considerable health consequences. In addition, the indirect effects of UVR in humans can have an accumulative effect with repeated exposures. For these reasons, any information on endogenous photosensistisers is of interest and may help in the understanding and prevention of the hazardous effects of UV exposure.

Furthermore, the biological relevance of the photosensitised reactions investigated is better understood if the irradiation energies applied in this study are put in context with that present in the environment. Thus, the energy required to achieve the photosensitised effects detailed in this study by L-histidine, L(+)mandelic acid, β–phenylpyruvic acid, *p*-OH-phenylpyruvic acid and β–L-phenyllactic acid are comparable to global radiation (the sum of direct solar radiation and diffused scattered radiation from the sky which hit an area per time unit). The maximum ultraviolet radiation (UVR) at noontime at sea level and a cloudless sky for a zenith angle of 90° is 6.3 mW cm^{-2} UVA and 0.5 mW cm^{-2} UVB (Hader and Tevini, 1987). This equals to 2.4 x 10^5 Jm^{-2} UVR per hour. For solar zenith angles less than 30° under the same conditions the maximum UVA irradiance is 5 mW cm^{-2} or 1.8 x 10^5 Jm^{-2} per hour (Parrish *et. al.*, 1978). Since UVB wavelengths reaching the earth are more strongly dependent on the solar zenith angle than are UVA wavelengths, the UVB irradiance would be much less than the above mentioned. Similarly, Central Europe receives approximately 4.2 x 10^9 Jm^{-2} in a year (4.8 x 10^5 Jm^{-2} per hour) of UVR (Hader and Tevini, 1987). In comparison, the irradiance emitted by the UV lamps used in this work was 6.03 mW cm^{-2} UVA and 0.07 mW cm^{-2} UVB by the NUV source, and 1.13 mW cm^{-2} UVB by the TL01 lamp. Also, the irradiation doses used throughout this work were lower than 1.2 x 10^5 Jm^{-2} with one exception where 1.8 x 10^5 Jm^{-2} was used. This means that many individuals are exposed daily to energy levels as high as those used in the laboratory. This, together with the probability that these individuals contain small but significant amounts of

the endogenous sensitisers proposed, may contribute to the occurrence of photoageing and maybe other sun related illnesses.

6.2 Biological Relevance of the Compounds Studied

From all of the compounds investigated in this study as potential phtosensitisers, L-histidine is believed to be the most abundant in humans. Being one of the most common amino acids, histidine is a major building block of proteins and is frequently found within the active sites of enzymes. The significance of this compound to undergo photolysis is, therefore, apparent. In addition, the pH dependent generation of ROS on histidine-driven photosensitised reactions may be of particular importance as damage can occur at localised environments within the cell.

The keto acids phenylpyruvic acid and OH-phenylpyruvic acid are also believed to play an important role in human biology. OH-phenylpyruvic acid is a product of tyrosine metabolism and a metabolite of 3,4-dihydroxy-phenylalanine (DOPA), a precursor of melanin. Phenylpyruvic acid is a metabolite of phenylalanine and plays an important role in catabolic reactions of endogenous amino acids in the cell. Studies showed phenylpyruvic acid to be located on the cell membrane of rat hepatocytes and from there to participate in the intracellular protein degradation (Kadowaki *et. al.*, 1992). The role of phenylpyruvic acid in proteolysis is to increase transamination reactions by triggering the release of insulin (Malaisse *et. al.*, 1983). Although all these studies were performed in rats, a similar situation is believed to occur in human cells. Also, even though liver cells are expected to have higher concentrations of this compound than the cells of the skin, the presence of phenylpyruvic acid in skin may contribute to the hazardous effects of UVR.

Elevated amounts of L(+)mandelic acid are found in the serum after exposure to styrene or ingestion of drugs (e.g. methenamine mandelate, a urinary antibacterial) of which L(+)mandelic acid is a major component (Chalmers and Lawson, 1982; Roesel *et. al.*, 1980). L(+)mandelic acid, together with phenylpyruvic acid, is also present in persons with a defect in phenylalanine metabolism (e.g. phenylketonuria). Persons with such a disorder are known to have reduced pigmentation, and this can

indirectly increase their UV sensitivity. Such cases however are quite rare and there is not sufficient data available.

From the biological effects observed by the UV photolysis of the compounds investigated in this study, it can be generally concluded that their potentially harmful effects on living cells lie in the induction of lipid peroxidation and protein oxidation rather than damage to the genome. It is therefore unlikely that the photosensitised action of these compounds may result in sun related health conditions such as skin cancer, but could play an important role in the event of photoageing and contribute in sun induced ocular damage.

6.3 Future Work

For most of the experiments in this study, an R-UVA solarium lamp was used as the irradiation source. The damaging effects on the skin from using such a source to obtain a tan have been addressed in a history of studies including those on damage induced from the direct absorption of UVB by cellular components and from indirect photosensitisation reactions of UVA (de Fabo and Noonan 1983; Ibbotson *et. al.*, 1999; Lowe *et. al.*, 1995; Morliere *et. al.*, 1995). The use of this source has generated data that provides additional evidence for the role of endogenous sensitisers on UVA mediated cellular damage. However, this source has proven inefficient in obtaining quantitative results, since the 1.2 % of UVB emitted by the source is sufficient to produce damage to biological systems as indicated by some experiments, therefore making it very difficult to determine the contribution of UVA in inducing a biological effect. The importance of separating contaminating UVB wavelengths from the irradiation source was further emphasised by the results obtained using a filter, cutting out UVB, and a TL01 narrow-band UVB lamp. The use of specific narrow-band lamps or near monochromatic sources, in addition to filters, is a good way of obtaining reliable data on the individual wavelengths responsible for phtosensitised biological damage. Such studies are necessary for the determination of the action spectrum for a specific type of UVR-mediated damage, such as lipid peroxidation, protein oxidation or DNA damage. In addition, performing experiments using a solar simulator is a better representation of the actual effect of solar radiation in inducing damage to cells and their components.

Most photosensitisers instigate their damaging effect on biological molecules *via* the generation of ROS. It is therefore important to identify the types of ROS involved in a given photosensitised reaction in order to understand the mechanism of the reaction and evaluate the relative contribution of each ROS in the resulting biological damage. The use of specific scavengers and quenchers that exhibit high affinity for a given ROS have been used extensively in the past by many investigators and were also used in this study. The use of such a system, however, was not very efficient as these compounds can also react non-selectively with other ROS and lead to an overestimation of the contribution of a specific ROS in a given biological effect. It was also observed that compounds such as β–carotene showed absorption in the UVA and UVB wavebands, thus acting as a filter of UVR. For these reasons, the exact mechanism of the formation of ROS on photolysis of the compounds studied and the relative contribution of each ROS on the resulting biological damage cannot be clarified without further experiments. A good way of identifying ROS generated on a photosensitised reaction is using electron spin resonance (ESR), since each type of ROS produces a unique ESR spectrum. In cases were the ROS of interest has a very short half-life as in the case of $^{\cdot}OH$, a spin-trap can be used prior to ESR. For example, 5,5-dimethylpyrroline-N-oxide added in the reaction mixture will react with both $^{\cdot}OH$ and $O_2^{\cdot-}$ to form products with different ESR spectra allowing for the detection of both ROS. D_2O has also been used in the past instead of H_2O as another approach to the effective detection of ROS in solution, since this medium enhances the half-life of ROS such as $^1O_2$. In addition, the use of degassed solvents to remove the dissolved oxygen in the reaction mixtures is an easy way of assessing the role of ROS in photosensitised damage to macromolecules. On photolysis of the sensitiser molecule, oxygen acts as the substrate for energy or electron transfer, with ROS being the products of this reaction. Purging nitrogen into the solution and performing irradiation in an anaerobic environment eliminates any reactions that involve oxygen. In this way, the contribution of ROS in biological damage can be evaluated. In the past, researchers have studied the involvement of $^1O_2$ in the inactivation of bacterial cells by physically separating the $^1O_2$ generating system from the substrate (Dahl *et. al.*, 1989). In their studies they immobilised the irradiated sensitiser on a glass plate placed a short distance above bacteria collected on membrane filters. In this way it was ensured that only $^1O_2$ could diffuse through

and react with the cell components. The application of similar methods using the compounds identified in this study as sensitisers of UVA will clarify further the types of ROS generated on their photolysis and the involvement of such ROS in specific biological effects.

Although the data presented in this work sheds some light on the mechanism of action of the photosensitisers studied, the exact mode of action still remains to be confirmed. It is not yet clear as to what is the contribution of photolysis to ROS generation and whether other reactions independent of ROS take place. This particularly applies to the reactions of L(+)mandelic acid on UV irradiation. It would therefore be of interest to perform experiments to obtain the absorption spectra of the compounds after irradiation and to look for possible changes in the absorption spectrum of the sensitiser in the presence of other reagents (e.g. NBT). In the event of alteration of the absorption spectrum, HPLC or GC can be used to identify the products of photolysis.

In this study, experiments were performed using bacteria deficient in nucleotide excision repair, nucleoside triphosphatase activity and lipopolysaccharide production to investigate the role of the sensitiser molecules in inducing DNA damage and mutations in the presence of UV. These studies can be carried further, with an emphasis on the involvement of ROS in the induced damage, by using bacterial species deficient in endogenous antioxidants. Moreover, since the contribution of the compounds identified as photosensitisers here in enhancing the damaging effects of UVR on skin is of particular interest, further studies should be focussed on the determination of the endogenous concentrations of these compounds in skin fibroblasts and keratinocytes.

6.4 Conclusion

In this study it was demonstrated that certain endogenous compounds that are part of human metabolism have the potential to act as sensitisers of UVR, and when photolysed, to produce ROS. In turn, these ROS were shown to be responsible for increased phage and bacterial inactivation. An investigation of the photosensitised damage to individual cell components revealed that DNA, proteins and lipids are

major targets for ROS-mediated oxidative modification. It is, therefore, believed that all the compounds studied may contribute, to different extents, to some of the effects of solar radiation on skin, such as in photoageing.

REFERENCES

Adam, W., S. Marquardt and C. R. Saha-Moller (1999) Oxidative DNA damage in the photolysis of N-hydroxy-2-pyridone, a specific hydroxyl-radical source. *Photochem. Photobiol.* **70:** 287-291.

Ahmad, S. I. (1981) Synergistic action of near ultraviolet radiation and hydrogen peroxide on the killing of coliphage T7: possible role of superoxide radical. *Photobiochemistry and Photobiophysics* **2:** 173:180.

Aikens, J. and T. A. Dix (1991) Perhydroxyl radical ($HOO^{\cdot}$) initiated lipid peroxidation. The role of fatty acid hydroperoxides. *J. Biol. Chem.* **266:** 15091-15098.

Ambrosone, C. B., J. L. Freudenheim, P. A. Thompson, E. Bowman, J. E. Vena, J. R. Marshall, S. Graham, R. Laughlin, T. Nemoto and P. G. Shields (1999) Manganese superoxide dismutase (MnSOD) genetic polymorphisms, dietary antioxidants and risk of breast cancer. *Canc. Res.* **59:** 602-606.

Arai, S., Y. H. Nakanishi and M. Hayashi (1997) Effect of UVA on RNA synthesis in isolated chicken liver nuclei. *J. Radiat. Res.* **38:** 5-14.

Banwell, C. N. (1983) *Fundamentals of Molecular Spectroscopy*. Third edition, McGraw-Hill Book Company (UK) Ltd, London.

Batty, D. P. and R. D. Wood (2000) Damage recognition in nucleotide excision repair of DNA. *Gene* **241:** 193-204.

Beer, J. Z., K. M. Olvey, S. A. Miller, D. P. Thomas and D. E. Godar (1993) Non-nuclear damage and cell lysis are induced by UVA, but not UVB or UVC, radiation in three strains of L5178Y cells. *Photochem. Photobiol.* **58:** 676-681.

Beutner, S., B. Bloedorn, T. Hoffmann and H. D. Martin (2000) Synthetic singlet oxygen quenchers *Methods in Enzymology* **319:** 226-241.

Berlett, B. and E. R. Stadtman (1997) Protein oxidation in ageing, disease, and oxidative stress. *J. Biol. Chem.* **272:** 20313-20316.

Berneburg, M., S. Grether-Beck, V. Kurten, T. Ruzicka, K. Briviba, H. Sies and J. Krutmann (1999) Singlet oxygen mediates the UVA-induced generation of the photoaging-associated mitochondrial common deletion. *J. Biological Chemistry* 274: 15345-15349.

Blau, K. (1970) Aromatic acid excretion in phenylketonuria. Analysis of the unconjugated aromatic acids derived from phenylalanine. *Clinica Chimica Acta* **27:** 5-18.

Breen, A. P. and J. A. Murphy (1995) Reactions of oxyl radicals with DNA. *Free Radic. Biol. Med.* **18:** 1033-1077.

Bruls, W. A. G., H. Slaper, J. C. Van der Leun and L. Berrens (1984) Transmission of human epidermis and stratum corneum as a function of thickness in the ultraviolet and visible wavelengths. *Photochem. Photobiol.* **40:** 485-494.

Burchuladze T. G. and G. Y. Fraikin (1991) A study of the mechanism of the NADH-sensitized formation of breaks in DNA during irradiation with near-UV light. *Molec. Biol.* **25:** 748-752.

Butler, J. (1999) Unpublished results. The Nottingham Trent University.

Cadet, J., C. Anselmino, T. Douki and L. Voituriez (1992) Photochemistry of nucleic acids in cells. *J. Photochem. Photobiol. B: Biol.* **15:** 277-298.

Cadet, J., T. Delatour, T. Douki, D. Gasparutto, J. P. Pouget, J. L. Ravanat and S. Sauvaigo (1999) Hydroxyl radicals and DNA base damage. *Mutation Research* **424:** 9-21.

Cadet, J., T. Douki, D. Gasparutto, J. P. Pouget and J. L. Ravanat (2000) Singlet oxygen DNA damage products: formation and measurement. *Methods in Enzymology* **319:** 143-153.

Carbonare, M. D. and M. A. Pathak (1992) Skin photosensitizing agents and the role of reactive oxygen species in photoaging. *J. Photochem. Photobiol. B: Biol.* **14:** 105-124.

Ceburkov, O. and H. Gollnick (2000) Photodynamic therapy in dermatology. *Europ. J. Dermatol.* **10:** 568-575.

Chalmers, R. A. and A. M. Lawson (1982) Disorders of aromatic amino and organic acid metabolism. In *Organic Acids in Man.* Chapman and Hall, pp. 420-428.

Chaudhary, A. K., M. Nokubo, G. R. Reddy, S. N. Yeola, J. D. Morrow, I. A. Blair and L. J. Marnett (1994) Detection of endogenous malondialdehyde-degoxyguanosine adducts in human liver. *Science* **265:** 1580-1582.

Cheng, K. C, D. S. Cahill, H. Kasai, S. Nushimura and L. A. Loeb (1992) 8-Hydroxyguanine, an abundant form of oxidative damage, causes G $\rightarrow$ T and A $\rightarrow$ C substitutions. *J. Biol. Chem.* **267:** 166-171.

Clark, J. M. and G. P. Beardsley (1987) Functional effects of cis-thymine glycol lesions on DNA synthesis *in vitro*. *Biochemistry* **26:** 5398-5403.

Craggs, J. S. H. Kirk and S. I. Ahmad (1994) Synergistic action of near-UV and phenylalanine, tyrosine or tryptophan on the inactivation of phage T7: role of superoxide radicals and hydrogen peroxide. *J. Photochem. Photobiol. B: Biol.* **24:** 123-128.

Cunningham, M. L., J. S. Johnson, S. M. Giovanazzi and M. J. Peak (1985) Photosensitized production of superoxide anion by monochromatic (290-405 nm) ultraviolet irradiation of NADH and NADPH co-enzymes. *Photochem. Photobiol.* **42:** 125-128.

Dahl, T. A., W. R. Midden and P. E. Hartman (1987) Pure singlet oxygen cytotoxicity for bacteria. *Photochem. Photobiol.* **46:** 345-352.

Dahl, T. A., W. R. Midden and P. E. Hartman (1989) Comparison of killing of gram-negative and gram-positive bacteria by pure singlet oxygen. *J. Bacteriol.* **171:** 2188-2194.

Dean, R. T., S. Gieseg and M. J. Davies (1993) Reactive species and their accumulation on radical-damaged proteins. *TIBS* **18:** 437-441.

Dizdaroglu, M. (1993) Chemistry of free radical damage to DNA and nucleoproteins. In: *DNA and Free Radicals*. B. Halliwell and O. I. Aruoma, eds. Ellis Horwood Ltd., England.

Douki T. and J. Cadet (1999) Modification of DNA bases by photosensitized one-electron oxidation. *Int. J. Radiat. Biol.* **75:** 571-581.

Douki T., D. Perdiz, P. Grof, Z. Kuluncsics, E. Moustacchi, J. Cadet and E. Sage (1999) Oxidation of guanine in cellular DNA by solar UV radiation: biological role. *Photochem. Photobiol.* **70:** 184-190.

Dumaz, N., H. J. Van Kranen, A. de Vries, R. J. W. Berg, P. W. Wester, C. F. Van Kreijl, A. Sarasin, L. Daya-Grosjean and F. R. de Gruijl (1997) The role of UVB radiation in skin carcinogenesis through the analysis of *p53* gene mutations in squamous cell carcinomas of hairless mice. *Carcinogenesis* **18:** 897-904.

Dunn, J. J. and F. W. Studier (1983) Complete nucleotide sequence of bacteriophage T7 DNA and the location of T7 genetic elements. *J. Mol. Biol.* **166:** 477-535.

Esterbauer H., and P. Ramos (1996) Chemistry and pathophysiology of oxidation of LDL. *Physiol. Biochem. Pharmacol.* **127:** 31-64.

Evans, J., M. Maccabee, Z. Hatahet, J. Courcelle, R. Bockrath, H. Ide and S. Wallace (1993) Thymine ring saturation and fragmentation products: lesion bypass, misinsertion and implications for mutagenesis. *Mutation Research* **299:** 147-156.

de Fabo, E. C. and F. P. Noonan (1983) Mechanism of immune suppression by ultraviolet irradiation *in vivo*. Evidence for the existence of a unique photoreceptor in skin and its role in photoimmunology. *J. Exp. Med.* **157:** 84-98.

Farmer, K. C. and M. F. Naylor (1996) Sun exposure, sunscreens, and skin cancer prevention: a year-round concern. *The Annals of Pharmacotherapy* **30:** 662-673.

Fekete, A., A. A. Vink, S. Gaspar, A. Berces, K. Modos, G. Ronto and L. Roza (1998) Assessment of the effects of various UV sources on inactivation and photproduct induction in phage T7 dosimeter. *Photochem. Photobiol.* **68:** 527-531.

Fekete, A., A. A. Vink, S. Gaspar, K. Modos, A. Berces, G. Ronto and L. Roza (1999) Influence of phage proteins on formation of specific UV DNA photproducts in phage T7. *Photochem. Photobiol.* **69:** 545-552.

Fernandez, J. M., M. D. Bilgin and L. I. Grossweiner (1997) Singlet oxygen generation by photodynamic agents. *J. Photochem. Photobiol. B: Biol.* **37:** 131-140.

Flindt-Hansen, H., N. McFadden, T. Eeg-Larsen and P. Thune (1991) Effect of a new narrow-band UVB lamp on photocarcinogenesis in mice. *Acta Derm. Venereol.* **71:** 245-248.

Flint, D. H. and R. M. Allen (1996) Iron-sulfur proteins with non-redox functions. *Chem. Rev.* **96:** 2315-2334.

Frei, B., R. Stocker and B. N. Ames (1992) Small molecule antioxidant defenses in human extracellular fluids. In: *Molecular Biology of Free Radical Scavenging Systems*. J. G. Scandalios, ed., Cold Spring Harbor Laboratory Press, pp. 23-43.

Gardner, P. R. (1997) Superoxide-driven aconitase FE-S center cycling. *Biosci. Rep.* **17:** 33-42.

Friedberg, E. C., G. C. Walker and W. Siede (1995) *DNA Repair and Mutagenesis*. ASM Press, Washington, D.C.

Fukuzawa, K. (2000) Singlet oxygen scavenging in phospholipid membranes. *Methods in Enzymology* **319:** 101-110.

Garssen, J., M. Norval, A. El-Ghorr, N. K. Gibbs, C. D. Jones, D. Cerimele, C. de Simone, S. Caffieri, F. Dall' Acqua, F. R. de Gruijl, Y. Sontag and H. Van Loveren (1998) Estimation of the effect of increasing UVB exposure on the human immune system and related resistance to infectious diseases and tumours. *J. Photochem. Photobiol. B: Biol.* **42:** 167-179.

Gieseg, S. P., J. A. Simpson, T. S. Charlton, M. W. Duncan and R. T. Dean (1993) Protein-bound 3,4-dihydroxyphenylalanine is a major reductant formed during hydroxyl radical damage to proteins. *Biochemistry* **32:** 4780-4786.

Girard P. M. and S. Boiteux (1997) Repair of oxidized DNA bases in the yeast *Saccharomyces cerevisiae*. *Biochimie* **79:** 559-566.

Greenwood N. N. and A. Earnshaw (1984) *Chemistry of the Elements*. Pergamon Press Plc., Oxford.

de Gruijl, F. R. and J. C. Van der Leun (1997) Estimate of the wavelength dependency of ultraviolet carcinogenesis in humans and its relevance to risk assessment of stratospheric ozone depletion. *Health Phys.* **67:** 319-325.

de Gruijl, F. R. (1997) Health effects from solar UV radiation. *Radiation Protection Dosimetry* **72:** 177-196.

de Gruijl, F. R., H. J. C. M. Sterenborg, P. D. Forbes (1993) Wavelength dependence of skin cancer induction by ultraviolet irradiation of albino hairless mice. *Cancer Res.* **53:** 53-60.

Hader, D. P. and M. Tevini (1987) *General photobiology*. Chapter Two, Natural radiation. Pergamon Press, pp. 20-26.

Halliwell, B. and J. M. C. Gutteridge (1981) Formation of a thiobarbituric-acid-reactive substance from deoxyribose in the presence of iron salts. *FEBS Letters* **128:** 347-352.

Halliwell, B. and J. M. C. Gutteridge (1999) *Free Radicals in Biology and Medicine*. Third edition. Oxford University Press Inc., New York.

Hanawalt, P. C., P. Gee, L. Ho, R. K. Hsu and C. J. Kane (1992) Genomic heterogeneity of DNA repair. Role in aging? *Annals New York Acad. Sciences* **663:** 17-25.

Hansson, J. (1992) Inherited defects in DNA repair and susceptibility to DNA-damaging agents. *Toxicology Letters* **64-65:** 141-148.

Hartman, P. S., A. Eisenstark and P. G. Pauw (1979) Inactivation of phage T7 by near-ultraviolet radiation plus hydrogen preoxide: DNA-protein crosslinks prrevent DNA injection. *Proc. Natl. Acad. Sci. USA* **76:** 3228-3232.

Hartman, P. S. and A. Eisenstark (1978) Synergistic killing of *Escherichia coli* by near-UV radiation and hydrogen peroxide: distinction between *recA*-repairable and *recA*-nonrepairable damage. *J. Bacteriology* **133:** 769-774.

Hill, A, G. N. Hoag and W. A. Zaleski (1972) The investigation of aromatic acids in phenylketonuria, alkaptonuria and tyrosineosis using gas-liquid chromatography. *Clinica Chimica Acta* **37:** 455-462.

Hirata, T., M. Kai, K. Kohashi and Y. Ohkura (1981) Determination of phenylpyruvic acid in urine and serum by high-performance liquid chromatography with fluorescence detection. *J. Chromatography* **226:** 25-31.

Hoeijmakers, J. H. J. (2001) Genome maintenance mechanisms for preventing cancer. *Nature* **411:** 366-374.

Hodgson, E. K. and I. Fridovich (1975) The interaction of bovine erythrocyte superoxide dismutase with hydrogen peroxide: inactivation of the enzyme. *Biochemistry* **14:** 5294-5298.

Hogg, N. (1998) Free radicals in disease. *Seminars in Reproductive Endocrinology* **16:** 241-248.

Hurks, H. M., C. Out-Luiting, B. J. Vermeer, E. H. Claas and A. M. Mommaas (1997) *In situ* action spectra suggest that DNA damage is involved in ultraviolet radiation-induced immunosuppression in humans. *Photochem. Photobiol.* **66:** 76-81.

Ibbotson, S. H. M. N. Moran, J. F. Nash and I. E. Kochevar (1999) The effects of radicals compared with UVB as initiating species for the induction of chronic cutaneous photodamage. *J Investig. Dermatol.* 112: 933-938.

Ito, K., S. Inoue, K. Yamamoto and S. Kawanishi (1993) 8-Hydroxydeoxyguanosine formation at the 5′ site of 5′-GG-3′ sequences in double-stranded DNA by UV radiation with riboflavin. *J. Biol. Chem.* **268:** 13221-13227.

Jekler, J, I. M. Bergbrant, J. Faergemann and O. Larko (1992) The *in vivo* effect of UVB radiation on skin bacteria in patients with atopic dermatitis. *Acta Dermato-Venereologica* **72:** 33-36.

Jones, C. D., M. Guckian, A. A. El-Ghorr, N. K. Gibbs and M. Norval (1996) Effects of phototherapy on the production of cytokines by peripheral blood mononuclear cells and on systemic antibody responses in patients with psoriasis. *Photodermatol. Photoimmunol. Photomed.* **125:** 204-210.

Jose, J. L. and D. G. Pitts (1985) Wavelength dependence of cataracts in albino mice following chronic exposure. *Exp. Eye Res.* **41:** 545-563.

Kanofsky, J. R. (1989) Singlet oxygen production by biological systems. *Cem.-Biol. Interactions* **70:** 1-28.

Kanofsky, J. R. (1991) Quenching of singlet oxygen by human red cell ghosts. *Photochem. Photobiol.* **53:** 93-99.

Kawaguchi, Y., H. Tanaka, T. Okada, H. Konishi, M. Takahashi, M. Ito and J. Asai (1997) Effect of reactive oxygen species on the elastin mRNA expression in cultured human dermal fibroblasts. *Free Radical Biology and Medicine* **23:** 162-165.

Kawaguchi, Y., H. Tanaka, T. Okada, H. Konishi, M. Takahashi, M. Ito and J. Asai (1996) The effects of ultraviolet A and reactive oxygen species on the mRNA expression of 72-kDa type IV collagenase and its tissue inhibitor in cultured human dermal fibroblasts. *Arch. Dermatol. Res.* **288:** 39-44.

Kelfkens, G., F. R. de Gruijl and J. C. Van der Leun (1990) Ozone depletion and increase in annual carcinogenic ultraviolet dose. *Photochem. Photobiol.* **52:** 819-823.

Keyer, K., A. Strohmeier Gort and J. A. Imlay (1995) Superoxide and the production of oxidative DNA damage. *J. Bacteriology* **177:** 6782-6790.

Klug, D., J. Rabani and I. Fridovich (1972) A direct demonstration of the catalytic action of superoxide dismutase through the use of pulse radiolysis. *J. Biol. Chem.* **247:** 4839-4842.

Kohen, E., R. Santus and J. G. Hirschberg, eds. (1995) *Photobiology*. Academic Press, New York.

Koppenol, W. H., W. A. Pryor, J. J. Moreno, H. Ischiropoulos and J. S. Bechman (1992) Peroxynitrite, a cloaked oxidant formed by nitric oxide and superoxide. *Chem. Res. Toxicol.* **6:** 834-842.

Kress, S., C. Sutter, P. T. Strickland, H. Mukhtar, J. Schweizer and M. Schwarz (1992) Carcinogen-specific mutational pattern in the *p53* gene in ultraviolet-B radiaiton-induced squamous cell carcinomas of mouse skin. *Cancer Res.* **52:** 6400-6403.

de Laat, A., J. Van der Leun, and F. R. de Gruijl (1997) Carcinogenesis induced by UVA (365-nm) radiation: the dose-time dependence of tumor formation in hairless mice. *Carcinogenesis* **18:** 1013-1020.

Lao, Y., X. V. Gomes, Y. Ren, J. S. Taylor and M. S. Wood (2000) Replication protein A interactions with DNA. III. Molecular basis of recognition of damaged DNA. *Biochemistry* **39:** 850-859.

Le Page, F., A. Guy, J. Cadet, A. Sarasin and A. Gentil (1998) Repair and mutagenic potency of 8-oxoG:A and 8-oxoG:C pairs in mammalian cells. *Nucleic Acids Research* **26:** 1276-1281.

Levine, R. L., J. A. Williams, E. R. Stadtman and E. Shacter (1994) Carbonyl assays for determination of oxidatively modified proteins. *Methods in Enzymology* **233:** 346-357.

Ley, R. D. (1997) Ultraviolet radiation A-induced precursors of cutaneous melanoma in *Mondelphis domestica*. *Cancer Res.* **57:** 3682-3684.

Li, W. and H. Z. Hill (1997) Induced melanin reduces mutations and cell killing in mouse melanoma. *Photochem. Photobiol.* **65:** 480-485.

Linetsky, M. and B. J. Ortwerth (1997) Quantitation of the singlet oxygen produced by UVA irradiation of human lens proteins. *Photochem. Photobiol.* **65:** 522-529.

Linetsky, M., H. L. James and B. J. Ortwerth (1996) The generation of superoxide anion by the UVA irradiation of human lens proteins. *Exp. Eye Res.* **63:** 67-74.

Lledias, F. and W. Hansberg (2000) Catalase modification as a marker for singlet oxygen. *Methods in Enzymology* **319:** 110-119.

Longstreth, J., F. R. de Gruijl, M. L. Kripke, S. Abseck, F. Arnold, H. I. Slaper, G. Velders, Y. Takizawa and J. C. Van der Leun (1998) Health risks. *J. Photochem. Photobiol. B: Biol.* **46:** 20-39.

Lowe, N. J., D. P. Meyers, J. M. Wieder, D. Luftman, T. Borget, M. D. Lehman, A. W. Johnson and I. R. Scott (1995) Low doses of repetitive ultraviolet A induce morphologic changes in human skin. *J. Invist. Dermatol.* **105:** 739-743.

Lyras, L., N. J. Cairns, A. Jenner, P. Jenner and B. Halliwell (1997) An assessment of oxidative damage to proteins, lipids, and DNA in brain from patients with Alzheimer's disease. *J. Neurochem.* **68:** 2061-2069.

Maniatis, T., E. F. Fritsch and J. Sambrook (1982) *Molecular Cloning*. Cold Spring Harbour Publications, USA.

March, J (1985) *Advanced Organic Chemistry*. Third edition, Wiley-Interscience Publication, New York.

Martinez, L. and C. F. Chignell (1998) Photocleavage of DNA by the fluoroquinolone antibacterials. *J. Photochem. Photobiol. B: Biol.* **45:** 51-59.

Masaki, H., N. Okamoto, S. Sakaki and H. Sakurai (1997) Protective effects of hydroxybenzoic acids and their esters on cell damage induced by hydroxyl radicals and hydrogen peroxides. *Biol. Pharm. Bull.* **20:** 304-308.

Masaki, H., Y. Okano and H. Sakurai (1997) Generation of active oxygen species from advanced glycation end-products (AGE) under ultraviolet light A (UVA) irradiation. *Biochemical and Biophysical Research Communications* **235:** 306-310.

McCord, J. M. and I. Fridovich (1969) Superoxide dismutase. An enzymic function for erythrocuprein (hemocuprein). *J. Biol. Chem.* **244:** 6049-6055.

McCormick, J. P., J. R. Fisher, J. P. Pachlatko and a. Eisenstark (1976) Characterisation of a cell-lethal tryptophan photo-oxidation product: hydrogen peroxide. *Science* **191:** 468-469.

Menon, I. A., P. K. Basu, S. D. Persad, A. Das and J. D. Wiltshire (1992) Reactive oxygen species in the photosensitization of retinal pigment epithelium cells by rose bengal. *J. Toxicol.–Cut. & Ocular Toxicol.* **11:** 269-283.

Morales-Ducret, C. R., M. Van der Rijn, D. P. Le Brun and B. R. Smoller (1995) Bcl-2 expression in privacy malignancies of the skin. *Arch. Dermatol.* **131:** 909-912.

Morliere, P., A. Moysan and I. Tirache (1995) Action spectrum for UV-induced lipid peroxidation in cultured human skin fibroblasts. *Free Radical Biology and Medicine* **19:** 365-371.

Moustacchi, E. (2000) DNA damage and repair: Consequences on dose-responses. *Mutation Research* **464:** 35-40.

Nackerdien, Z., G. Rao, M. A. Cacciuttolo, E. Gajewski and M. Dizdaroglu (1991) Chemical nature of DNA-protein cross-links produced in mammalian chromatin by hydrogen peroxide in the presence of iron or copper ions. *Biochemistry* **30:** 4873-4879.

Nixon, R. A. and A. M. Cataldo (1994) Free radicals, proteolysis and the degeneration of neutrons in Alzheimer disease: how essential is the β–amyloid link? *Neurobiol. Aging* **15:** 463-469.

Noonan, F. P. and E. C. de Fabo (1992) Immunosuppression by ultraviolet B radiation: initiation by urocanic acid. *Immunol. Today* **13:** 250-254.

Ohara, Y., T. E. Peterson and D. G. Harrison (1993) Hypercholesterolemia increases endothelia superoxide anion production. *J. Clin. Invest.* **91:** 2546-2551.

Okada, K., Y. Takahashi, K. Ohnishi, O. Ishikawa and Y. Miyachi (1994) Time-dependent effect of chronic UV irradiation on superoxide dismutase and catalase activity in hairless mice skin. *J. Dermatological Science* **8:** 182-186.

Oroskar, A. A., C. Lambert and M. J. Peak (1996) Effects of hydroxyl radical scavengers on relaxation of supercoiled DNA by aminomethyl-trimethyl-psoralen and monochromatic UVA photons. *Free Radical Biology and Medicine* **20:** 751-756.

Ortwerth, B. J. and P. R. Olesen (1994) UVA photolysis using the protein-bound sensitizers present in human lens. *Photochem. Photobiol.* **60:** 53-60.

Ortwerth, B. J., M. Prabhakaram, R. H. Nagaraj and M. Linetsky (1997) The relative UV sensitizer activity of purified advanced glycation endproducts. *Photochem. Photobiol.* **65:** 666-672.

Padula, M., S. Boiteux, I. Felzenszwalb and S. Menezes (1996) Photodynamic action of phycocyanin: damage and repair. *J. Photochem. Photobiol. B: Biol.* **32:** 19-26.

Paillous, N. and S. Fery-Forgues (1994) Interest of photochemical methods for induction of lipid peroxidation. *Biochimie* 76: 355-368.

Palozza, P. and N. I. Krinsky (1992) Antioxidant effects of caretenoids *in vivo* and *in vitro*: an overview. *Methods in Enzymology* **213:** 403-439.

Paretzoglou, A., C. Stockenhuber, S. H. Kirk and S. I. Ahmad (1998) Generation of reactive oxygen species from the photolysis of histidine by near-ultraviolet light: effects on T7 as a model biological system. *J. Photochem. Photobiol. B: Biol.* **43:** 101-105.

Parrish, J. A., R. R. Anderson, F. Urbach and D. Pitts (1978) *UVA: Biological Effects of Ultraviolet Radiation with Emphasis on Human Responses to Longwave Ultraviolet*. Plenum Press, New York.

Pavlov, Y. I., D. T. Minnick, S. Izuta and T. A. Kunkel (1994) DNA replication fidelity with 8-oxodeoxyguanosine triphosphate. *Biochemistry* **33:** 4695-4701.

Peak, M. J. and J. G. Peak (1989) Solar-ultraviolet-induced damage to DNA. *Photodermatology* **6:** 1-15.

Pellieux, C., A. Dewilde, C. Pierlot and J. M. Aubry (2000) Bactericidal and virucidal activities of singlet oxygen generated by thermolysis of naphthalene endoperoxides. *Methods in Enzymology* **319:** 101-110.

Petersen, M., T. Hamilton and H. L. Li (1995) Regulation and inhibition of collagenase expression by long-wavelength ultraviolet radiation in cultured human skin fibroblasts. *Photochem. Photobiol.* **62:** 444-448.

Peters, T. (1977) Serum albumin: recent progress in the understanding of its structure and biosynthesis. *Clin. Chem.* **23:** 5-12.

Pourzand, C. and R. M. Tyrrell (1999) Apoptosis, the role of oxidative stress and the example of solar UV radiation. *Photochem. Photobiol.* **70:** 380-390.

Pourzand, C., G. Rossier, O. Reelfs C. Borner and R. M. Tyrrell (1997) The overexpression of Bcl-2 inhibits UVA-mediated immediate apoptosis in rat 6

fibroblasts: evidence for the involvement of Bcl-2 as an antioxidant. *Cancer Res.* **57:** 1405-1411.

Pryor, W. A. and N. A. Porter (1990) Suggested mechanisms for the production of 4-hydroxynonenal, malonaldehyde and related aldehydes. *Free Rad. Biol. and Med.* **11:** 81-128.

Punnonen, K., A. Puntala and M. Ahotupa (1991) Effects of ultraviolet A and B irradiation on lipid peroxidation and activity of the antioxidant enzymes in keratinocytes. *Photodermatol. Photoimmunol. Rhotomed.* **8:** 3-6.

Quillardet, P. and M. Hofnung (1985) The SOS chromotest, a colorimetric bacterial assay for genotoxins: procedures. *Mutation Research* **147:** 65-78.

Rauk, A, D. Yu and D. A. Armstrong (1997) Towards site specificity of oxidative damage in proteins: C-H and C-C bond dissociation energies and reduction potentials of the radicals of alanine, serine, and threonine residues – an *ab initio* study. *J. Am. Chem. Soc.* **119:** 208-217.

Ravanat, J. L. and J. Cadet (1995) Reaction of singlet oxygen with 2'-deoxyguanosine and DNA. Isolation and characterization of the main oxidation products. *Chemical Research in Toxicology* **8:** 379-388.

Redmond R. W. and J. N. Gamlin (1999) A compilation of singlet oxygen yields from biologically relevant molecules *Photochem. Photobiol.* **70:** 391-475.

Reinheckel, T., M. Bohne, W. Halangk, W. Augustin and H. Gollnick (1999) Evaluation of UVA-mediated oxidative damage to proteins and lipids in extracorporeal photoimmunotherapy. *Photochem. Photobiol.* **69:** 566-570.

Reiter, R. J., D. Tan, S. J. Kim and W. Qi (1998) Melatonin as a pharmacological agent against oxidative damage to lipids and DNA. *Proc. West. Pharmacol. Soc.* **41:** 229-236.

Repanovici, R. A. Plesa and G. Anton (1997) Trasformation of *Escherichia coli* cells by pH 2.3 plasmid DNA treated with psoralens plus near-UV light. *J. Photochem. Photobiol. B: Biol.* **37:** 26-30.

Roesel, R. A., M. E. Coryell, P. R. Blankenship, T. G. Thevaos, and W. K. Hall (1980) Interference by methenamine mandelate in screening for organic and amino acid disorders. *Clinica Chimica Acta* **100:** 55-58.

Ronto, G., S. Gaspar and A. Berces (1992) Phage T7 in biological UV dose measurement. *J. Photochem. Photobiol. B: Biol.* **12:** 285-294.

Rosen, J. E., A. K. Prahalad and G. M. Williams (1996) 8-oxodeoxyguanosine formation in the DNA of cultured cells after exposure to H_2O_2 alone or with UVB or UVA irradiation. *Photochem. Photobiol.* **64:** 117-122.

Rosenstein, B. S. and D. L. Mitchell (1987) Action spectra for the induction of pyrimidine photoproducts and cyclobutane pyrimidine dimers in normal human skin fibroblasts. *Photochem. Photobiol.* **45:** 775-780.

Sage, E. (1993) Distribution and repair of photolesions in DNA: genetic consequences and the role of sequence context. *Photochem. Photobiol.* **57:** 163-174.

Santanam, N., S. Ramachandran and S. Parthasarathy (1998) Oxygen radicals, antioxidants and lipid peroxidation. *Seminars in Reproductive Endocrinology* **16:** 275-280.

Schafer, F. Q. and G. R. Buettner (1999) Singlet oxygen toxicity is cell line-dependent: a study of lipid peroxidation in nine leukemia cell lines. *Photochem. Photobiol.* **70:** 858-867.

Schmutte, C. (1999) Genomic instability: First step to carcinogenesis. *Anticancer Research* **19:** 4665-4696.

Schwarz, M. D., J. E. Repine and E. Abraham (1995) Xanthine oxidase-derived oxygen radicals increases lung cytokine expression in mice subjected to hemorrhagic shock. *Am. J. Respir. Cell Mol. Biol.* **12:** 434-440.

Schwarz, T. (1998) UV light affects cell membrane and cytoplasmic targets. *J. Photochem. Photobiol. B: Biol.* **44:** 91-96.

Selvaag, E., H. Anholt, J. Moan and P. Thune (1997) Inhibiting effects of antioxidants on drug-induced phototoxicity in cell cultures. Investigations with sulphonamide-derived oral antidiabetics and diuretics. *J. Photochem. Photobiol. B: Biol.* **38:** 88-93.

Selverstone Valentine, J., D. L. Wertz, T. J. Lyons, L. L. Liou, J. J. Goto and E. Butler Gralla (1998) The dark side of dioxygen biochemistry. *Current Opinion in Chemical Biology* **2:** 253-262.

Setlow, R. B., E. Grist, K. Thompson and A. D. Woodhead (1993) Wavelengths effective in induction of malignant melanoma. *Proc. Natl. Acad. Sci. USA* **90:** 6660-6670.

Shennan, M. G., C. M. Palmer and H. E. Schellhorn (1996) Role of fapy glycosylase and uvrABC excinuclease in the repair of UVA (320-400 nm)-mediated DNA damage in *Escherichia coli*. *Photochem. Photobiol.* **63:** 68-73.

Shindo, Y. and T. Hashimoto (1997) Time course of changes in antioxidant enzymes in human skin fibroblasts after UVA irradiation. *J. Dermatological Science* **14:** 225-232.

Shindo, Y., E. Witt and L. Packer (1993) Antioxidant defence mechanism in murine epidermis and dermis and their response to ultraviolet light. *J. Invest. Dermatol.* **100:** 260-265.

Smith, K. C. ed. (1989) *The Science of Photobiology*. Second edition, Plenum Press, New York.

Sodum, R. S. and F. L. Chung (1988) 1,*N*-Ethenodeoxyguanosine as a potentiol marker for DNA adduct formation By *trans*-4-hydroxy-2-nonenal. *Cancer Res.* **48:** 320-323.

Spikes, J. D., H. R. Shen, P. Kopeckova and J. Kopecek (1999) Photodynamic crosslinking of proteins. III. Kinetics of the FMN- and rose bengal-sensitized photooxidation and intermolecular crosslinking of model tyrosine-containing *N*-(2-hydroxypropyl)methacrylamide copolymers. *Photochem. Photobiol.* **70:** 130-137.

Stadtman, E. R. (1995) Role of oxidized amino acids in protein breakdown and stability. *Methods in Enzymology* **258:** 379-393.

Stary, A. and A. Sarasin (2000) Ultraviolet A and singlet oxygen-induced mutation spectra. *Methods in Enzymology* **319:** 153 –165.

Tebbe, B., S. Wu, C. C. Geilen, J. Eberle, V. Kodeljia and C. E. Orfanos (1997) L-ascorbic acid inhibits UVA-induced lipid peroxidation and secretion of IL-1α and IL-6 in cultured human keratinocytes *in vitro*. *J. Invest. Dermatol.* **108:** 302-306.

Toyokuni, S. (1999) Reactive oxygen species-induced molecular damage and its application in pathology. *Pathology International* **49:** 91-102.

Tyrrell, R. M. (1990) The interaction of UVA radiation with cultured cells. *J. Photochem. Photobiol. B: Biol.* **4:** 349-361.

Tyrrell, R. M. (1995) Ultraviolet radiation and free radical damage to skin. *Biochem. Soc. Symp.* **61:** 47-53.

Van Houten, B. (1990) Nucleotide Excision Repair in *Escherichia coli*. *Microbiol. Rev.* **54:** 18:51.

Vargas, F., I. M. Volkmar, J. Sequera, H. Mendez, J. Rojas, G. Fraile, M. Velasquez and R. Medina (1998) Photodegradation and phototoxicity studies of furosemide.

Involvement of singlet oxygen in the photoinduced hemolysis and lipid peroxidation. *J. Photochem. Photobiol. B: Biol.* **42:** 219-225.

Verweij, H. and J. Van Steveninck (1982) Model studies on photodynamic cross-linking. *Photochem. Photobiol.* **35:** 265-267.

Walter, S. D., L. D. Marrett, L. From, C. Hertyman, H. S. Shannon and P. Roy (1990) The association of cutaneous malignant melanoma with the use of sunbeds and sunlamps. *Amer. J. Epidemiol.* **131:** 232-243.

Wang, J. Y. J. (1998) Cellular responses to DNA damage. *Current Opinion in Cell Biology* **10:** 240-247.

Yasui, H and H. Sakurai (2000) Chemiluminescent detection and imaging of reactive oxigen species in live mouse skin exposed to UVA. *Biochemical Biophysical Research Communications* 269: 131-136.

Yoshimura, M., S. Namura, H. Akamatsu, and T. Horio (1996) Antimicrobial effects of phototherapy and photochemotherapy *in vivo* and *in vitro*. *British J. of Dermatology* **135:** 528-532.

Zhang, X., B. S. Rosenstein, Y. Wang, M. Lebwohl, D. M. Mitchell and H. Wei (1997) Induction of 8-oxo-7,8-dihydro-2-deoxyguanosine by ultraviolet radiation in calf thymus DNA and HeLa Cells. *Photochem. Photobiol.* **65:** 119-124.

Zheng, P. S. and L. H. Kligman (1993) UVA-induced structural changes in hairless mouse skin – a comparison to UVB-induced damage. *J. Invest. Dermatol.* **100:** 194-199.

Zigman, S., T. Paxia, T. McDaniel, M. F. Lou and N. T. Yu (1991) Effect of chronic near-ultraviolet radiation on the grey squirrel lens *in vivo*. *Invest. Ophthalmol. Vis. Sci.* **32:** 1723-1732.

Ziegler, A., A. S. Jonason, D. J. Leffel, A. Simon, H. W. Sharma, J. Kimmelman, L. Remington, T. Jacks and D. E. Brash (1994) Sunburn and *p53* in the onset of skin cancer. *Nature* **372:** 773-776.